5

VIBRATIONAL RELAXATION IN GASES

A Thesis submitted for the Degree of

Doctor of Philosophy

in the

University of London

and for the

Diploma of Imperial College

by

BRIAN JAMES LAVERCOMBE, A.R.C.S.

March 1966

ABSTRACT

This thesis is concerned with the use of the optic-acoustic effect for the measurement of vibrational relaxation times in gases.

A brief review is given of the theoretical background to vibrational relaxation and vibrational energy transfer during collisions, followed by a survey of experimental techniques used in the investigation of this phenomenon.

A theoretical analysis is presented of the physical process occurring in the spectrophone, extending earlier work to consider spatial variation of the radiation input to the gas, and the case of a 'two-step' relaxing vibration.

Details are given of the re-designed apparatus, together with the experimental procedure adopted for measuring relaxation phase shifts, and hence calculating vibrational relaxation times. The results are given of tests and precautions taken to eliminate or evaluate instrumental phase shifts, including the use of a calibrating gas.

Measurements have been made on the infra-red active modes of carbon dioxide and nitrous oxide. Results trongly suggest that the asymmetric valence modes of these molecules relax by a complex process involving the bending modes. Measurements on carbon dioxide-inert gas mixtures show that inert gas molecules are relatively inefficient at de-exciting both the carbon dioxide vibrations. The results indicate that for these mixtures, the transition probability depends in a regular way upon the collision reduced mass, the dependence being close to that postulated by current theory.

CONTENTS

Page No.

ACKNOWLEDGEMENTS

The author wishes to express his sincere thanks to Dr. R. W. B. Stephens for the continual encouragement and advice given to him during his period of postgraduate study at Imperial College, and to his colleagues in the Acoustics Group for many stimulating discussions.

Thanks are also due to members of the technical staff of the Physics Department, notably Mr. A. E. Davis, Mr. T. Shand and Mr. O. Millbank for valuable help during the design and construction of apparatus, and to Fiona Hunt and Mr. A. J. Rowe, for typing and photographic services respectively, during the preparation of this thesis.

Finally the author acknowledges his debt to the Department of Scientific and Industrial Research for providing a maintenance grant.

CHAPTER 1

VIBRATIONAL RELAXATION AND VIBRATIONAL ENERGY TRANSFER

A. Introduction

A polyatomic gas molecule with n atoms has in general 3n-6 independent normal vibrations (3n-5 for linear molecules). The energy possessed by these vibrations is quantised, so that each vibration is in one of a discrete set of energy states. Molecules also possess other degrees of freedom, translational, rotational, electronic, etc.

In a gas maintained under steady external conditions, the various degrees of freedom will be in equilibrium with each other, i.e. the mean energy in each is associated with an identical temperature - the translational temperature. This equilibrium implies a mechanism of energy transfer between the various degrees of freedom. This mechanism may be the absorption and emission of electromagnetic quanta or the consequence of strong intermolecular forces - in gases these only occur during collisions. For vibrational modes in most polyatomic gases (except at very low pressures), collision induced transfer is the main energy exchange process. In the collision, the vibrational mode may gain or lose energy to a) translation, b) other vibrational modes of the same molecule or of the collision partner, c) rotational (and even electronic modes) of either molecule. However, since internal energy levels are discrete, some energy is usually needed from translation to balance the interaction. Collision induced

vibrational energy transfer is a comparatively inefficient process. At room temperatures for many molecules at least 10^5 collisions are needed on average before an 'inelastic' collision occurs. This is important in the occurrance of vibrational relaxation phenomena. Although the probability of any particular collision inducing a particular energy exchange is obviously a complicated problem involving the internal molecular parameters, it should intuitively depend upon the ratio of the available collision energy to the internal energy to be transferred. Thus modes with small energy quanta should be more easily excited and de-excited than modes with large quanta, and the number of transitions occurring in unit time in a gas should vary with the translational temperature.

If the equilibrium conditions in the gas are suddenly disturbed, e.g. by changing the translational temperature, or injecting energy into a vibrational mode by means of radiation, then equilibrium may only be restored by means of the slow collisional energy exchange described above, and thus will take a finite time, which will depend upon the efficiency of the exchange process for that particular system. These considerations were first discussed by Herzfeld and Rice [1].

Consider the simple case of a molecule with one vibration (i.e. diatomic) in which the other internal modes may be ignored. The energy exchange process will be between vibration and translation. The mechanics of the exchange will depend upon the form assumed for the vibration. Here we consider the case of a 'two-state' vibration, where it is assumed that the only appreciably populated states are a ground state and a first excited state at an energy $h\nu$ above it. This approximation holds good for many vibrational modes at room

temperatures. If N_o and N_1 are the populations of the ground and excited states in a given volume of gas at a translational temperature T in which equilibrium between vibration and translation is not established, then we may write the rate equation:-

$$\frac{dN_1}{dt} = -f_{10} N_1 + f_{01} N_0 \qquad 1.1$$

where f_{10} and f_{01} are rate constants, the probabilities/unit time that a molecule will undergo the collisionally-induced transition $1 \longrightarrow 0$ or $0 \longrightarrow 1$ respectively.

Since at equilibrium $\frac{dN_1}{dt} = 0$

$f_{10} N_1^o = f_{01} N_0^o$ where N_1^o and N_0^o represent the equilibrium values of N_1 and N_0 at the translational temperature. From statistical thermodynamics

$$\frac{N_1^o}{N_0^o} = e^{-h\nu/kT}$$

therefore:- $$\frac{f_{01}}{f_{10}} = e^{-h\nu/kT} \qquad 1.2$$

Thus (1) becomes:-

$$\frac{dN_1}{dt} = -(f_{10} + f_{01})\left[N_1 - N_1^0\right] \qquad 1.3$$

Multiplying this by $h\nu$, the energy of the excited state, gives:-

$$\frac{dE}{dt} = \frac{1}{\tau}(E - E_o) \qquad 1.4$$

where we write $\frac{1}{\tau} = (f_{10} + f_{01})$

and E and E_o represent the vibrational energy actually in the gas and that which there would be for equilibrium with translation. Equation (4) was first derived by Kneser [2]. Landau and Teller [3] treated the case of a gas with one vibration whose energy levels are those of an harmonic oscillator. This simply leads to (4) where for this case $\frac{1}{\tau} = (k_{10} - k_{01})$ and k_{10} and k_{01} are the rate constants for exchange between the two lowest energy levels of the oscillator.

Equation (4) is the typical differential equation describing a relaxation process. It describes the approach of the internal energy E to the equilibrium value, and shows that the rate of approach is directly proportional to the difference in energy from this equilibrium. Suppose the equilibrium value of the internal energy were suddenly changed at time t = 0 from E_0 to E_1 for a gas in equilibrium. The translational energy will come into equilibrium with the new conditions practically instantaneously, since the translational relaxation time (the time taken for a Maxwellian velocity distribution to be established in a gas) is extremely short. (See, for example, Herzfeld and Litovitz [4], page 231). Equation (4) may thus be solved to yield:-

$$E = E_1 + (E_0 - E_1)\, e^{-t/\tau} \qquad 1.5$$

so that E 'relaxes' to the new equilibrium value with a time constant τ, called the relaxation time.

If the translational conditions are made to vary harmonically with time, so that $E_0 = E_0\, e^{i\omega t}$, then the steady state solution of (4) is:-

$$E = \frac{E_0}{(1 + i\omega\tau)} = \frac{E_0 e^{-i\theta}}{\sqrt{1 + (\omega\tau)^2}} \qquad 1.6$$

where $\tan\theta = \omega\tau$

Thus E never achieves its equilibrium value and lags behind the changes in equilibrium with a phase lag θ. As the frequency ω increases and $\omega\tau$ becomes $\gg 1$, so E becomes more and more unable to follow the changes in E_0 and lags further and further behind until as $\omega \to \infty$ the varying amplitude $\to 0$ and the phase lag $\to \pi/2$. On the other hand, at low frequencies where $\omega\tau < 1$, E will follow the changes in E_0 almost completely, and instantly.

These simple considerations can only approximately apply to real molecules. The above analysis takes no account of radiative transfer, and energy exchange between different internal modes. However, for most gases, the vibrational radiative lifetime is so long that radiative energy transfer does not compete with collisional transfer. Electronic modes are usually of such high energy that they do not interact readily with other modes or exchange energy during collisions, however there are exceptions. Rotational states in general have small quanta

which exchange energy very readily with translation. From a vibrational point of view they may usually be lumped with translation as external energy, since they are usually in equilibrium with translation unless the changes in equilibrium are very rapid. This does not apply to hydrogen and certain halide molecules where rotational energy may be very important in vibrational energy transfer.. Thus (4) may describe vibrational relaxation satisfactorily for many diatomic molecules. For molecules with more than one vibration the relaxation will depend upon the mechanism of energy exchange between the various modes. If the various vibrations only exchange energy with translation then they will relax separately and there will be a relaxation equation of type (4) for each mode. If energy is exchanged between the vibrations themselves then 'complex' collisions occur in which some modes exchange energy with translation via other lower energy modes. This vibration-vibration energy exchange is still a collision induced process, and will be described by a rate equation similar to (1). However, the simple equation (4) will only apply to the overall relaxation of a mode if one of the complex steps in the exchange of energy with translation is much slower than the others or 'rate determining'. In this case the relaxation will be described approximately by equation (4) with the relaxation time equal to the inverse of this slowest rate constant. If this approximation does not hold then the relaxation equation is complicated in form, containing two or more different relaxation times. Such cases have been dealt with comprehensively by Herzfeld and Litovitz [4] and Bauer [5].

Mixtures of two gases may usually be simply treated. Consider a diatomic gas A diluted with a monatomic gas B. The relaxation time of a given mixture at a given pressure will be:-

$$\frac{1}{\tau} = \frac{x}{\tau_{AA}} + \frac{(1-x)}{\tau_{AB}} \qquad 1.7$$

where τ_{AA} and τ_{AB} are the relaxation times respectively of a) pure diatomic gas at the pressure of the mixture, b) one diatomic molecule of A in the monatomic gas, also at the pressure of the mixture. x is the mole fraction of A in the mixture. Equation (7) will give the relaxation time for any vibration in a binary mixture provided that complex collisions do not take place. If τ_{AB} is much shorter than τ_{AA}, then the presence of even tiny amounts of impurity gas can very significantly alter the apparent relaxation time as given by equation (7). This is an obvious experimental difficulty in the measurement of long relaxation times.

The importance of relaxation, i.e. the slow adjustment through collisions, of equilibrium between the various degrees of freedom of molecules, lies in its effect upon the bulk properties of the gas. To see how relaxation effects these bulk properties it must be remembered that thermodynamically a substance is characterised by its specific heat. Since any energy given to a gas is ultimately distributed through all its degrees of freedom, the specific heat of a polyatomic gas may be written:-

$$C = C_{\text{translational}} + C_{\text{vibrational}} + C_{\text{rotational}} + C_{\text{electronic}}$$

For slow disturbances, equilibrium is established between all the degrees of freedom, and the gas appears to have its total specific heat C. However, if the changes in equilibrium are too rapid, then as seen above one or more of the internal modes may not be in equilibrium with translation. To consider this case, consider the simple system leading to equation (4), i. e. a gas with one internal mode, exchanging energy with translation. If we write $C = C_e + C_i$ where C_e and C_i represent the translational or external, and internal parts of the specific heat respectively, then for harmonic changes, equation (6) can be written in terms of the varying amplitudes, as:-

$$\Delta E = \frac{\Delta E_o}{1 + i\omega\tau} \qquad 1.6a$$

$$C_i \Delta T_i = \frac{C_i \Delta T_{tr.}}{1 + i\omega\tau} \qquad 1.8$$

where T_i is the temperature associated with the instantaneous energy in the internal mode, and $T_{tr.}$ is the actual translational temperature. Now from the point of view of the internal modes, (8) may be written:-

$$C_i \Delta T_i = C_i \left(\frac{\Delta T_{tr.}}{1 + i\omega\tau} \right) \qquad 1.8a$$

i. e. the varying internal temperature amplitude is smaller than the corresponding translational amplitude and lags behind it in phase. However, from the point of view of the bulk properties of the gas, (8)

may be written:-

$$C_i \Delta T_i = \left(\frac{C_i}{1 + i\omega\tau} \right) \Delta T_{tr.} \qquad 1.8b$$

i.e. the gas behaves to changes in translational temperature as if its specific heat were $C_e + \frac{C_i}{1 + i\omega\tau}$. The apparent specific heat of the gas will depend upon the rapidity of changes in the external conditions, leading to the concept of a relaxing specific heat.

This relaxation may have an important effect upon the physical phenomena which result in a rapid disturbance of the equilibrium between the degrees of freedom of a molecule. Obvious examples are the passage of a sound wave through a fluid or in various aerodynamical flows, such as nozzle expansions, etc. Relaxation effects depend in each case upon the ratio τ/τ_p where τ_p is the period associated with the physical process. Vibrational relaxation is the most important relaxation process because the range of τ's means that many cases occur where $\tau/\tau_p \sim 1$, and relaxation effects will occur. Rotational relaxation times are usually too short to effect most physical phenomena, except for example, very high frequency sound waves. Vibrational and rotational relaxation effects do not usually overlap, since at frequencies where the former is important rotation will be in equilibrium with translation, and at frequencies where rotational effects occur, the vibrations are probably in the range $\omega\tau \gg 1$ where they do not take part in the thermodynamic process at all. In this work, rotational modes are of interest only in so far as they may influence vibration energy

transfer.

The study of vibrational relaxation is of obvious importance in itself since it can have an important influence on certain phenomena in acoustics and aerodynamics. Its main interest, however, lies in the information it yields on the problems of molecular structure as outlined in part B of this chapter. Vibrational energy transfer is important in chemical kinetics as determining the rate of unimolecular reactions and in molecular spectroscopy as determining the form and characteristics of electronic as well as vibrational spectra. Vibrational relaxation investigations should give useful information in both these fields of study.

B Calculation of vibrational energy transfer probabilities and relaxation times

The relaxation time of a simple harmonic oscillator, ignoring other internal modes, is:-

$$\tau = \frac{1}{f_{10}(1 - e^{-h\nu/kT})} \qquad 1.9$$

as given above. A similar expression will hold for any 'single' relaxation process, given the appropriate rate constant. Equation (9) may be written:-

$$\tau = \frac{1}{Z\bar{P}_{10}(1 - e^{-h\nu/kT})} \qquad 1.10$$

where Z is the number of collisions a molecule makes per second and $\bar{P}_{10}$ is the average probability of collisional de-excitation per collision. Z can be easily calculated from simple kinetic considerations, although its exact value depends on the molecular 'collision diameter', a size parameter which can only be estimated from indirect experimental evidence - usually viscosity data. (See, for example, reference (6)).

$\overline{P_{10}}$ will be obtained from a knowledge of P_{10} for a particular collision by a straightforward averaging over the molecules, assuming a Boltzmann distribution of molecular energies. The main problem therefore, in the theoretical calculation of τ is the evaluation of P_{10} for a particular collision where the initial and final internal states are specified and the translational motion is known energetically and geometrically before collision. There has been considerable work on the theoretical calculation of molecular collision dynamics, and vibrational relaxation measurements provide useful experimental evidence to check with theory. There are a number of recent reviews of the theoretical development, references (7), (8), (9), (10), (32), and here is discussed the more important results of theory with a view of interpreting the experimental results.

Both theory, and the experimental fact that τ varies inversely with pressure, shows that vibrational energy transfer occurs almost entirely during binary collisions. The probability of energy transfer occurring during a collision will depend upon the magnitude of the perturbation given to the molecular forces controlling the vibration. Thus qualitatively it may be said, following Landau and Teller [3], that P_{10} will depend upon the ratio of the period of the vibration to

the duration of the collisions (i. e. the period during which appreciable intermolecular forces act). If this ratio is small, then the perturbation will be small, for the internal coordinates of the molecule will be able to adjust themselves to the slowly changing force-field. On the other hand, if the vibration period is comparable with the collision period, the perturbing forces on the oscillating atoms will be large, giving a considerable vibrational transition probability. From this simple argument, knowing the average thermal velocities of gas molecules and typical frequencies of molecular vibrations, we can say that the probability of a vibrational energy transfer in any average collision at room temperatures should be very small for the majority of molecules.

The quantitative study of molecular collisions presents formidable problems. For all but the simplest systems it is not possible to work out the intramolecular forces controlling the vibrations, or the intermolecular forces which come into play during collisions. Consequently empirical models for these forces must be used, based upon experimental evidence such as viscosity or molecular beam scattering data. Such evidence suggests a strong short range repulsive force and a weak long range cohesive force, and models such as the Morse potential:-

$$V = \varepsilon\left[\exp.\left\{-\alpha(r - r_o)\right\} - 2\exp.\left\{-\frac{\alpha}{2}(r - r_o)\right\}\right] \qquad 1.11$$

the Lennard-Jones potential:-

$$V = 4\varepsilon\left[\left(\frac{r_o}{r}\right)^{12} - \left(\frac{r_o}{r}\right)^{6}\right] \qquad 1.12$$

and the "28-7" potential have been tried:-

$$V = A\left[\left(\frac{r_o}{r}\right)^{28} - \left(\frac{r_o}{r}\right)^{7}\right] \qquad 1.13$$

Such models may be good approximations for some molecules, but spherical symmetry will fail badly in the case of long chain or strongly polar molecules.

Secondly, even for quite simple intermolecular potentials, the exact solution of the appropriate equations governing the collision is very difficult mathematically, for all but the simplest idealised collisions. Consideration of 'complex' collisions involving energy exchange by more than one internal mode, and between various internal modes themselves, necessitates extensive approximation. Thus theory must attempt to find the most important factors governing the collision, using simple models, and test the results against experiment. In this way a semi-empirical theory of molecular collisions has been built up.

Since low energy molecular collisions are not so obviously a quantum mechanical problem as other higher energy scattering processes, both classical and quantum mechanical approaches have been made. Classically, one has to solve the equations of motion for the collision system and the vibrating molecules, but the most popular method known as the semi-classical method, treats the relative motion of the two molecules classically, and the effect upon the vibration by means of quantum time-dependent perturbation theory. This has the advantage of giving individual transition probabilities for

various internal transitions, although Takayanagi [8] has shown that to first order approximation at least, the results are identical with those using the wholly classical method. Most quantum mechanical treatments have employed stationary state perturbation theory, using an approximation first used by Zener [11] called the method of distorted waves (D.W.A.). All these methods assume that the interaction between the molecules is small, i.e. all probabilities will be small.

The first model to be considered was that of the 'head-on' collision between an atom A and a non-rotating diatomic molecule B. The potential adopted was that of a repulsive exponential, usually taken as:-

$$V(xr) = C \exp. \left[-\alpha (r - \lambda x) \right] \qquad 1.14$$

where r is the distance between the two centres of gravity of the colliding pair. x is an internal coordinate of the molecule and $\lambda = \frac{m_1}{m_1 + m_2}$ where m_1 and m_2 are respectively the masses of the atoms of B nearer and farther from A. It is usually assumed that $r \gg x$ so that the dependence of V on x can be simplified still further in the interests of mathematical convenience. The quantum mechanical solution for this collision was first given by Jackson and Mott [12], and the semi-classical by Zener [13] and Landau and Teller [3]. Both solutions are practically identical, except at threshold where the semi-classical breaks down, and are of the form:-

$$\bar{P}_{10} = K(m, M, \theta', \theta, T) \exp. \left[-\frac{3}{2} \left(\frac{\theta'}{T} \right)^{1/3} + \frac{\theta}{2T} \right] \qquad 1.15$$

where m and M are the reduced masses of the diatomic molecule and the colliding pair respectively.

$$\theta = \frac{h\nu}{k}$$

$$\theta' = \frac{16 \pi^4 M \nu^2}{\alpha^2 k}$$

where k is Boltzmann's constant. $h\nu$ is the energy quantum separating the ground and first excited states.

The predicted temperature dependence of $\bar{P}_{10}$ in equation (1.15) ($\exp\left(-\frac{A}{T}^{1/3}\right)$ is the dominant term), has been found to hold for many collision systems [14]. But equation (15) has not proved very successful in calculating absolute values of relaxation times. This is hardly surprising in view of the simplicity of the model.

The extension of the quantum mechanical treatment to more realistic collision models has been mainly due to Takayanagi, and to Herzfeld and co-workers. The two most necessary modifications to the simple model leading to equation (15) are the removal of the head-on collision restriction and the consideration of a better interaction potential. A complete transformation to 3-dimensions is difficult since it involves consideration of interchange between orbital angular momentum and rotational states, and consideration of the orientation of molecules for non-spherical potentials.

As stated above, more realistic, although still empirical, intermolecular potential functions than (14) are given by equations (11), (12), (13). The Lennard-Jones potential has been much used in interpreting other experimental data such as transport phenomena measurements, and hence the constants ε and r_o are well known for many gases. Unfortunately the direct use of this potential prevents the analytical solution of the collision problem in closed form.

Slawsky, Schwartz and Herzfeld [15] presented a theory for molecular collisions in which an approximate attempt was made to improve on these two limitations of the original theory. Their treatment, the S. S. H. theory, and its modifications, have been the most commonly used calculations for comparison with experiment. In their first paper, they considered the diatomic molecule-atom collision, removed the head-on collision restriction but considered a non-rotating molecule with a spherically symmetric potential. This leads merely to an extra centrifugal energy term which is made a constant depending upon the initial orbital angular momentum. Herzfeld et al. decided to use the known Lennard-Jones constants, but unable to use the actual potential in their equations, they fitted it to the negative exponential repulsive function actually used. The attractive part was regarded as merely causing a constant 'accelerating' effect which increased the mean kinetic energy of collision and hence the transition probability, but did not directly cause transitions. Using this model, the expression for the averaged transition probability is:-

$$\bar{P}_{10} = \left(\frac{r_c}{r_o}\right)^2 \left(\frac{2\pi}{3}\right)^{1/2} \left(\frac{\theta'}{\theta}\right) \left(\frac{\theta'}{T}\right)^{1/6} \frac{M}{m} \left(1 - 2\lambda + 2\lambda^2\right) \times$$

$$\exp.\left[- \frac{3}{2}\left(\frac{\theta'}{T}\right)^{1/3} + \frac{\theta}{2T} + \frac{\varepsilon}{kT} \right] \qquad 1.16$$

where the last term in the exponent represents the correction due to the accelerating cohesive potential. r_c is defined as the distance of closest approach. Cottrell et al. [16], [9] obtained a very similar expression for the same model but using the semi-classical method. In order to take account of orientations of the molecules, Herzfeld divided the expression above by a 'steric factor', Z_o which has been given various forms depending upon the assumptions made in evaluating it. A simple geometric averaging over all possible orientations leads to a value of $Z_o = 3$.

The S.S.H. formula has been compared with experiment by many workers. (For comprehensive comparisons see references (4), (9), (17), (14)). For diatomic molecules agreement is generally very good, both in temperature dependence and for the calculation of absolute transition probabilities using molecular constants derived from viscosity data. However, if the experimental temperature dependence of $\bar{P}$ is used to find α, this is consistently $\alpha_{\text{viscosity}}$ by a factor not greater than ten. It has been suggested that adjustment of the steric factor may account for this discrepancy [17], [9] since its exact calculation is difficult without a detailed knowledge of the intermolecular potentials. Z_o has thus become a kind of arbitrary adjustable

parameter. Certain collision systems disagree markedly from theory, but these may often be caused by near resonant vibration-vibration transfer (for example CO - O_2), or other complex process.

The extension of the S. S. H. theory to collisions involving polyatomic molecules was made by Tanczos[18]. He considered vibration-vibration as well as vibration-translation energy transfer. Since equation (16) consists essentially of the product of vibrational and translational matrix elements, the polyatomic case merely has the product of two or more vibrational matrix elements, corresponding to the normal vibrations exchanging energy. However, the procedure is quite difficult because one has to obtain the motion of individual atoms in terms of the normal coordinates describing the vibrations, and then average the probability over all the surface atoms of the molecule. Cottrell and Ream[16] and Parker[19] similarly extended the semi-classical treatment. These polyatomic formulae have been tested against experiment for several molecular systems, see references (18), (16), (17), (20). Agreement is satisfactory in most cases but not so consistently good as for the simpler molecules.

The chief criticism which may be levelled at the S. S. H. theory and its equivalents is that it still uses the simple repulsive exponential intermolecular potential in the analytical solution of the translational matrix elements, with the addition of a plausible, but empirical accelerating factor, $\exp.\left(\frac{\varepsilon}{kT}\right)$, to take account of the attractive forces. That attractive forces may be important in causing vibrational transitions is shown by the CO_2 - H_2O system. Widom and Bauer[33] have shown that the high value and negative temperature

coefficient of $\bar{P}$ for this system can be explained by the large attractive potential well. Besides the accelerating effect, the attractive potential determines the slope of the repulsive potential well which is the critical factor in determining inelastic collision probabilities, and hence should be considered in its complete form.

A major contribution to the clarification of this problem has been made by Widom [21]. He has used a method originally developed by Landau and Lifshitz [22], [23]. Relying on the nearly classical nature of the translational motion, he employs a semi-classical method, but using the so-called W.K.B. wave functions, instead of perturbed oscillator functions. The matrix elements, taken to the classical limit, are solvable for more complex potentials than is possible with the distorted wave quantum method. The most important terms determining the magnitude of $\bar{P}$ are the exponential terms which arise from the translational matrix elements. Widom shows that these terms are only important if they are independent of h (Planck's constant) or remain large as $h \to 0$. Thus the W.K.B. method, although valid only near the classical limit, will yield all the important expoential terms, which chiefly determine $\bar{P}$. In particular the Morse potential has been studied by Widom and Shin [24] and the Lennard-Jones potential by Shin [25]. In both cases the three terms of the exponent given by the S.S.H. equation, are obtained, but the main attractive term is now of the form:-

$$\exp. \quad \frac{4\varepsilon^{1/2}\chi^{1/2}}{kT} \qquad 1.17$$

$$\text{where } \chi = \left[\left(\frac{M}{2}\right)^{1/2} \pi r_o EkT \right]^{2/3}$$

This term, which is larger than $\frac{\varepsilon}{kT}$ cannot be obtained by the S. S. H. method. Other potentials give other important terms and the conclusion to be drawn is that serious errors could result in using an empirical procedure such as leads to equation (16). In these cases an exact analysis using the proper potential interaction would be needed. However, as the application of functions such as the Lennard-Jones to intermolecular potentials is quite arbitrary there seems little point in using such a potential function in very detailed calculations when the actual form of the intermolecular potential is unknown. The fact that the S. S. H. equation is adequate in so many cases indicates that its simple approximations hold fairly well for most small molecules.

There are other obvious limitations of the theory. All perturbation methods fail at sufficiently high energies because the transition probabilities become too large. Less approximate calculations have been made using electronic computers.[26][27][28] Also, in some complex collisions, the quantum numbers of low energy vibrations should change by more than one. This means that the dependence of V(x,r) upon the intramolecular coordinate x, has to be more accurately considered than the 'dipole' approximation usually adopted. A more serious failing is the non-consideration of vibrational-rotational energy exchange. Although the effect of rotation-

translation exchange upon vibrational transitions can be readily examined - Herzfeld considers this in deriving a form of the steric factor Z_o - the obviously more important vibration-rotation exchange process is difficult to handle. Takayanagi [8] and Curtis and Adler [29] have been obtained the general equations, but these are difficult to evaluate since the rotational transition probabilities are too large to treat by perturbation methods. There is strong evidence that the anomalous behaviour of hydrides (see Cottrell and Matheson [30]) and the difference in $\bar{P}$ between O_2 - O_2, and O_2 - A, collisions (see Nikitin [35]), may be due to rotation-vibration transfer. A recent paper by Moore [62] has shown that a simple semi-classical theory of vibration-rotational energy transfer derived from that of Cottrell and Ream [16] for vibration-translational transfer, is very successful in predicting values of relaxation times in a whole range of collisions involving molecules with high rotational energies. His calculations are far more in agreement with experimental results than any vibration-translation energy exchange calculations for this type of collision, despite the obvious simplicity of the model adopted - namely, neglecting translational energy, and the quantisation of the rotational energy. Vibrational-electronic energy transfer may also be important in a few cases at low temperatures; for example, Nikitin [31] suggests it as a cause of the very rapid vibrational de-excitation of NO in self-collisions.

To sum up, the calculation of vibrational transition probabilities, and hence vibrational relaxation times, by theories such as the quantum-mechanical S. S. H., is successful in obtaining values in agreement with experiment for a large number of collision systems involving simple

molecules. This would seem to be quite satisfactory in view of the limited available knowledge about actual intermolecular forces. In general, the types of collision where the theory fails more or less to agree with experiment include, collisions involving large polyatomic molecules, collisions where one molecule is much lighter than the other, collisions involving molecules containing hydrogen atoms, and collisions involving some polyatomic molecules and the inert gases. Some cases of failure may be readily explained; collisions involving polar molecules, and where there is chemical affinity between the colliding pair would be expected to deviate from simple collision models.

Theoretical Relaxation Times for carbon dioxide and nitrous oxide

In the present work, vibrational relaxation measurements have been made on the infra-red active bands of carbon dioxide and nitrous oxide. These are both linear tri-tratomic molecules with fundamental vibration frequencies given by:-

CO_2

$\nu_1 = 1351\ cm^{-1}$	Symmetric valence vibration (NOT INFRA-RED ACTIVE)
$\nu_2 = 672\ cm^{-1}$	2-degenerate bending vibration
$\nu_3 = 2396\ cm^{-1}$	Asymmetric valence vibration

N_2O

$\nu_1 = 1285\ cm^{-1}$	Non-totally symmetric valence vibration
$\nu_2 = 589\ cm^{-1}$	2-degenerate bending vibration
$\nu_3 = 2223.5\ cm^{-1}$	Asymmetric valence vibration

The bending modes, being the lowest energy modes in each molecule, should decay via direct interchange with translation. The straightforward S. S. H. calculations have been applied to these modes [34].

For $Z_{10} = \frac{1}{P_{10}}$

$$= \tau Z \left[1 - \exp. \left(- h\nu_2/kT \right) \right]$$

At 300°K the results are,

for CO_2, $Z_{10} = 16,300$

and for N_2O, $Z_{10} = 11,000$,

corresponding to relaxation times at 1 atmosphere of about 1.8 μsec and 1.2 μsec respectively.

The symmetric valence vibration of carbon dioxide has a fundamental frequency almost exactly double that of the bending mode, thus resonant exchange $\nu_1 \longrightarrow 2\nu_2$ should be very fast (S. S. H. theory gives $Z \sim 500$ at room temperature), and the relaxation time of ν_1 should be very similar to that of ν_2, since the $h\nu_2 \longrightarrow$ translation will be the rate determining step.

For the ν_3 mode of CO_2 the possible decay modes for excitation to the first excited state are

a) $h\nu_3 \longrightarrow$ kinetic energy (3380. k)

b) $h\nu_3 \longrightarrow h\nu_2$ + kinetic energy (2420. k)

c) $h\nu_3 \longrightarrow h\nu_1$ + kinetic energy (1460. k)

d) $h\nu_3 \longrightarrow 2h\nu_2$ + kinetic energy (1460. k)

e) $h\nu_3 \longrightarrow h\nu_2 + h\nu_1$ + kinetic energy (500. k)

f) $h\nu_3 \longrightarrow 3h\nu_2$ + kinetic energy (500. k)

Here the kinetic energies which have to be exchanged with translation in each process are given in terms of kT (k = Boltzmann's constant, T = absolute temperature).

Using the S. S. H. technique as extended by Tanczos, Herzfeld [34] has worked out the Z_{10} numbers for each of these processes. He inserted a steric factor of 3 in the direct de-activation but left this out of the complex processes. His results, taking into account the multiplicity of decay paths, for the complex de-activations, were:-

Process	$Z_{10}(300^{\circ}K)$
a)	4.7×10^{13}
b)	4.4×10^{11}
c)	88×10^{8}
d)	10^{9}
e)	1.9×10^{5}
f)	4.0×10^{5}

From this it would seem that e) and f) are the only processes which will effectively occur. Since $\nu_1 \rightarrow 2\nu_2$ should be very rapid, then an effective Z_{10} can be estaimated for these two processes together. Giving

$$Z_{10} \ (\nu_3 \rightarrow 3\nu_2) \ = \ 1.3 \times 10^5$$

This corresponds to a relaxation time for this process of $\sim$ 15 μsec.

Witteman [36] has also made calculations based on S. S. H. theory for the three carbon dioxide vibrations. Instead of using a simple symmetric potential he used one of the form

$V = \sum_{\text{all}}^{i} \sum_{\text{atoms}}^{j} V(r_{ij})$, where $V(r_{ij})$ are exponential functions representing the potential between the i^{th} and j^{th} atoms of the two molecules. This leads to matrix elements of the form $\left| V_{in}(r) \right|^2 \left| x_{in} \right|^2 \left| w_{in} \right|^2$ where w_{in} is a function of the orientation of the colliding molecules. x_{in} and w_{in}, are calculated individually for each vibration, and then integrated over all possible orientations of the molecules. Thus in effect Witteman. calculates individual steric factors for each vibration. Witteman finds that process e) is dominant in the energy transfer from the ν_3 vibration, and ignores the others. His values for the transition probabilities for both the bending and asymmetric valence modes are much smaller than those given by Herzfeld. At 300°K he obtains:-

$$Z_{10}\ (\nu_2) \simeq 1.6 \times 10^{6}$$

$$Z_{10}\ (\nu_3) \simeq 3.0 \times 10^{8}$$

No calculations have been made for the valence modes of nitrous oxide. Although the resonance between two bending mode quanta and one quantum of the 1285 cm^{-1} mode is not so exact as for carbon dioxide, the energy difference is only 154k so that this process should be relatively efficient. For the 2223 cm^{-1} band, similar decay processes can be written as for the corresponding CO_2 band. Again the $\nu_3 \rightarrow \nu_2 + \nu_1$ decay should be the most efficient, and peculiar orientation effects excluded, this will have approximately the same probability as the carbon dioxide case.

Laidler [37] from observations on unimolecular dissociation processes, has suggested that transfer of energy between symmetric and antisymmetric modes of a molecule is an inefficient process in cases where high vibrational levels are involved; however, there seems no reason why this effect should occur in the low energy states involved in room temperature collisions.

CHAPTER 2

SURVEY OF EXPERIMENTAL TECHNIQUES FOR VIBRATIONAL RELAXATION MEASUREMENT

In this chapter a brief review is given of the various methods by which vibrational relaxation times have been measured, indicating the range and any special advantages or limitations of each.

I Measurement of dispersion and absorption of sound

a) Theory As explained in the previous chapter, the passage of a high frequency sound wave through a gas is a good example of a periodic disturbance of the equilibrium between internal and translational degrees of freedom, which leads to relaxation. If the frequency of the sound wave is large enough, there is insufficient time in each cycle for the internal modes to obtain the energy necessary for equilibrium with the translational temperature changes caused by the sound wave, and it can be readily shown that this leads both to dispersion and absorption of the sound. The theory has been extensively examined by many authors, notably Herzfeld and Litovitz [4].

As shown in Chapter 1, the specific heat (at constant volume), of a gas possessing one vibrational excited state, for slow changes of temperature normally consists of two contributions $C = C_{\text{translational}} + C_{\text{vibrational}}$, which we write as:-

$$C_o = C_\infty + C_i \qquad 2.1$$

In Chapter 1 (equation 1.8b) it was shown that the effective vibrational specific heat for harmonic changes at a frequency ω, took the form:-

$$C_i(\omega) = \frac{C_i}{(1 + i\omega\tau)} \qquad 2.2$$

Thus the total effective specific heat of the gas will be:-

$$C = C_\infty + \frac{C_i}{(1 + i\omega\tau)} \qquad 2.3$$

which approaches C_o as $\omega \to 0$ and C_∞ as $\omega \to \infty$. This immediately leads to dispersion for the velocity of sound in a gas (assumed perfect) is given by $c^2 = \gamma \frac{RT}{M}$ where R is the molar gas constant and M = molecular weight.

$$c^2 = \gamma \frac{RT}{M} \left(1 + \frac{R}{C}\right) \qquad 2.4$$

and from (4):-

$$c^2 = \frac{RT}{M} + \frac{R^2T}{M} \frac{(1 + i\omega\tau)}{(C_o + i\omega\tau C_\infty)} \qquad 2.5$$

From this by rearrangement we get:-

$$\omega^2\tau^2 = \frac{C_o^2}{C_\infty^2} \left[\frac{c(\omega)^2 - c_o^2}{c_\infty^2 - c(\omega)^2} \right] \qquad 2.6$$

The relaxation also leads to absorption because the wave equation for plane waves:-

$$\frac{\partial^2 \xi}{\partial t^2} = c^2 \frac{\partial^2 \xi}{\partial x^2}$$

where ξ = particle displacement, now has a complex velocity

$c^2 = (c_{Real})^2 + i(c_{Imaginary})^2$ and thus has a solution of the form:-

$$\xi = ae^{-\alpha x} e^{i\omega(t - x/c')}$$

where the absorption per wavelength

$$2\alpha\lambda = \frac{2\pi\omega\tau RC_i}{C_o(R + C_o) + \omega^2\tau^2(R + C_\infty)C_\infty} \qquad 2.7$$

Before expressions (6) and (7) may be used to find τ from measurements of $c(\omega)$ and $\alpha(\omega)$ the gas must be corrected for non-ideality and allowance made for the 'classical' absorption due to thermal conductivity and shear viscosity. Figure 1(a)* shows the variation of $c(\omega)$ and $2\alpha\lambda$ with frequency together with a typical classical absorption-frequency curve. Actually both classical absorptions are true relaxation processes. However, their relaxation times are extremely short so that measurements are usually made far below the relaxation frequencies, and the classical absorption is usually taken to vary with the square of the frequency. Classical dispersion is usually very small.

* Page 115

b) Experimental It is difficult to get acoustic energy from a solid transducer into gases which have low characteristic impedances. Hence standing wave systems have proved most successful in practice.

At low frequencies a resonance, or Kundt's, tube has been used, with a movable vibrating piston or loudspeaker at one end and a fixed microphone at the other. By plotting the Q's of the various gas resonances, it is possible to obtain the absorption coefficient. Non-relaxation losses, due mainly to wall effects, may be substracted by calibration with a monatomic gas. The tube length is usually not known with sufficient accuracy for velocity measurements, unless each measurement is duplicated, using a gas of known velocity. The method has proved successful for gases with long relaxation times such as nitrogen and oxygen (see, for example, reference (38)).

The method which has been most extensively used in gas relaxation time measurements is undoubtedly the ultrasonic interferometer. This also employs a standing plane wave system, set up between the quartz crystal transducer and the movable reflector. However, here the transducer surface, radiating into the gas, is many times greater than the acoustic wavelength, so that the waves may only be assumed plane if the source-reflector distance is kept within the Fresnel region. Typical interferometers are described in the papers by Pielmayer [39] and Stewart [40]. Resonance is detected by the reaction of the radiation impedance of the gas column upon the driving crystal. This will cause a minimum displacement amplitude at the crystal at resonance, and hence a minimum in the crystal current and other electrical quantities in the circuit driving the crystal. In some interferometers the reflector is replaced by a separate receiving crystal.

Velocity is the most straightforward measurement in the interferometer. Successive resonances will occur $\lambda/2$ apart and this, together with a measurement of the frequency, will give the velocity. Absorption measurements are not so straightforward in a standing wave system. The technique as developed by Hubbard et al.[41] is to plot the shape and height of successive resonances. From these data, making approximations depending upon the exact conditions, the absorption coefficient may be calculated. Care must be taken in measurements to avoid errors due to non-parallel crystal and reflector surfaces, and diffraction effects. Also at high frequencies where absorption is usually large, the effective path length may only be a few wavelengths so that great precision is needed in measuring reflector displacements.

Measurements on progressive waves have not been greatly used with gases. More refined techniques are needed to attain accuracy comparable with standing wave set-ups, since the relative absorption in gases is high and the source and detector cannot be too close together if standing waves are to be avoided. Also reflections from the walls and diffraction effects must be eliminated. In such measurements the use of pulsed instead of continuous sound has advantages, allowing accurate velocity as well as absorption determinations. With pulse methods in which difficulties with standing waves, diffraction and gas heating are alleviated, the working frequency has been pushed up to over 50 Mc/s.

One further technique used to measure sound absorption is that of reverberation. In this, the decay of diffuse sound in an enclosure is measured. For such a decay we have the well-known formulae:-

$$I_t = I_o \exp.\left[- \frac{t}{T} \right] \qquad 2.8$$

where I is the sound intensity and $T = \frac{4V}{\alpha' c}$ where α' is the total absorption coefficient and V is the volume of the enclosure. α' will be partly due to absorption by the walls, so two enclosures are used of different surface area to volume ratios, to extract the true volume absorption. Usually the sound source is a transducer mounted flush with the walls, the microphone being similarly mounted. This is essentially a low frequency method but has been used up to 130 kc/s [42].

Since both the dispersion and absorption $\propto \frac{\omega}{P}$, where P is the total pressure, the range of measurements may be extended by varying P as well as ω. By this means relaxation times in the wide range 10^{-2} - 10^{-9} sec. have been measured ultrasonically. Because of the difficulties in working at high frequency, various methods such as introducing known amounts of impurity, or working on the low slopes of the absorption curve, have been used for very short relaxation times. Such techniques inevitably mean a loss of accuracy. In the case of polyatomic molecules with more than one vibration the ultrasonic method is limited. Although multiple relaxation times can be theoretically detected, giving double absorption and dispersion curves, unless the relaxation times are quite widely separated and give rise to roughly equal effects, it is difficult to separate the various processes from the curves. Furthermore, vibrations with frequencies much greater than 1500 cm^{-1} are difficult to examine acoustically, since they contribute such a

small vibrational specific heat at room temperatures that the dispersion and absorption in a sound wave of small intensity will be negligible. Nevertheless, a large number of gases and mixtures have been examined by this method and, allowing for the fact that in early work the effect of small traces of catalytic impurities was not appreciated, reliable results were obtained. It seems likely that the results obtained from sound measurements will remain the basis upon which more versatile methods, allowing for examination of individual relaxation processes in polyatomic gases, will compare and establish their measurements.

II Shock wave studies

a) Theory Shock waves are propagated at velocities greater than the normal speed of small amplitude sound, and in a shock wave ideally, there is a finite discontinuity in the gas variables at the shock front. Theoretical considerations of shock wave propagation are based upon the conservation of mass, momentum and energy across the shock front. Thus for unit cross-section of shock front:-

$$\rho_1 u_1 = \rho_2 u_2 \qquad 2.9a$$

$$P_1 + \rho_1 u_1^2 = P_2 + \rho_2 u_2^2 \qquad 2.9b$$

$$E_1 + \frac{P_1}{\rho_1} + \frac{u_1^2}{2} = E_2 + \frac{P_2}{\rho_2} + \frac{u_2^2}{2} \qquad 2.9c$$

where the suffixes 2 and 1 refer to the shocked and unshocked gas respectively, E is the internal energy/gm. and u the velocity relative

to the shock front. These equations, together with the appropriate equation of state for the gas, will determine the various shock wave parameters.

In practice, the shock front is not a finite discontinuity. Even in monatomic gases, the front has some thickness due to the 'classical' viscous and heat conductivity processes. In a polyatomic gas there will be an additional and usually much larger thickening of the front due to vibrational and rotational relaxation. Upon the passage of a shock front the translational temperature of the shocked gas is raised almost instantaneously to a high value, say T_1, whilst the vibrational temperature remains at T_o. Then as energy 'leaks' into the internal modes bringing them into equilibrium with translation, the translational temperature will fall from T_1 to a final shocked temperature of T_2. From the general relaxation conditions of Chapter 1 it is easy to show that for one internal mode having a relaxation time τ, the external temperature will approach T_2 exponentially during the latter part of its fall to equilibrium with a time constant τ, i.e.

$$T_1 - T_2 = (T' - T_2)\ e^{-\left(\frac{t}{\tau}\ \frac{C_{po}}{C_{p\infty}}\right)} \qquad 2.10$$

where T' is not equal to T_1 but is some intermediate temperature from which the temperature change may be taken approximately as exponential. C_{po} and $C_{p\infty}$ have the same meaning as C_o and C_∞, but for referring to the specific heat at constant pressure. The rotational modes will in general relax much faster than the vibrational

modes; a typical variation in translational and vibrational temperatures behind the shock front is shown in Figure 1(b)*. Similarly the density will approach its final shocked value ρ_2 at approximately the same rate:-

$$\rho_2 - \rho_1 = (\rho_2 - \rho') \quad \exp. \quad \left(-\frac{t}{\bar{\tau}} \quad \frac{C_{po}}{C_{p\infty}} \right) \qquad 2.11$$

Thus measurement of either the shock front temperature or the density profiles should enable the relaxation time to be calculated. As remarked in Chapter 1, τ is a function of temperature, but as equations (11) and (12) apply only at the end of the relaxation, the mean temperature may be taken as that between T' and T_2, over which range τ may be considered constant. Since T_2 is usually $> 1000^{\circ}K$ shock waves yield information of high temperature relaxation times.

b) Experimental A large number of different techniques have been used to obtain information regarding relaxation from shock wave experiments, although the design of the basic shock tube is fairly standard. These are dealt with in detail in various specialised texts, see, for example, reference (43), and are briefly mentioned here.

The measurement of temperature by conventional thermometric methods or of pressure using transducers is of little use in detecting the rapid changes of condition across a shock front. This is because of poor transient response and the impracticability of sufficiently small units. Consequently the optical techniques have been mainly used. These apply themselves especially to density profile studies.

*Page 115.

The Mach-Zehnder interferometer, in which the shift in fringes is observed when the shock front intersects one of the two light beams, provides an excellent method for fairly long relaxation times. Less satisfactory is the well-known Schlieren technique. Although this shows up the form of the density profile well, quantitative measurements are difficult. For short relaxation times, < 1 μsec where the shock front is too narrow for the interferometric method, Hornig [44] has used a reflection technique, utilising the fact that the reflectivity of the shock front depends upon the variation of refractive index, and hence upon the density profile. For low density shocks, however, all these methods are rather insensitive, and the varying attenuation in a beam of X-rays or electrons, shot normally across the shock tube, has provided density profiles for shocks in gases with ambient pressure as low as 5×10^{-2} torr.

Gaydon and his co-workers [45] have shown that electronic excitation temperatures of metals such as sodium and chromium in a relaxing gas tend to follow the effective vibrational temperature and not the translational temperature. Thus by introducing a trace of metallic vapour into the shock tube and measuring the excitation temperature in the shocked gas by their line reversal method, the vibrational temperature profile in the shock front may be directly observed. For infra-red active molecules such as carbon monoxide, it is possible directly to observe the growth of infra-red emission behind the shock front as the vibrational temperature rises, however, for strong spectral lines there are serious difficulties arising from self-absorption.

Many of the above techniques are somewhat uncertain as far as quantitative measurements are concerned. In obtaining measurements on a transient phenomenon like a shock wave, the recording and display system is as vital as the actual measuring apparatus in obtaining accurate results. The range of measurable τ's is rather limited. Times below 1 μsec call for very precise technique, and for times longer than a few hundred μsec, it is impractical to obtain sufficient duration of flow. For most techniques detection of multiple relaxation times, or the study of particular relaxation processes in polyatomic molecules, is impossible; however, this does not apply to spectroscopic methods. Shock wave studies take the place of sound dispersion and absorption as the basic method for high temperatures; however, the two do not overlap as shock wave temperatures much below 1000^{o}K are not easily attainable.

III Impact Tube Method

In this method, first developed by Kantrowitz [46] the disturbance in internal-translational equilibrium is caused by bringing an aerodynamic jet flow of gas quickly to rest by means of an impact (or Pitot) tube. If the time of compression in front of the impact tube is small compared with τ, then the vibrational states will not be able to follow the translational changes, and relaxation will occur. The whole procedure may be looked on as having three separate stages. At first gas in a reservoir at a pressure P_o is allowed to expand through a nozzle to form a jet. This expansion will be adiabatic and slow enough for the vibrational modes to remain in

equilibrium. Thus this stage is isentropic. The second stage is the rapid adiabatic compression of the gas in the jet in front of the impact tube. This will also be isentropic, but the vibrational modes are frozen at the jet temperature, while the translational temperature rises suddenly to a new value. In the third stage, energy leaks into the vibrational modes, bringing them into equilibrium with translation. The translational temperature falls to that of the original gas in the reservoir, while the pressure remains essentially constant. This last stage is an irreversible redistribution of energy and results in a rise in entropy. This entropy increase for a perfect gas is given by

$$\Delta S = R \log_e \frac{P_o}{P} \qquad 2.12$$

where P is the stagnation pressure measured by the impact tube, which will be $< P_o$.

The entropy rise may also be computed if the temperature history of the gas in the jet flow is known. This will depend upon the velocity and geometrical parameters of the jet flow and impact tube, and the relaxation time. By making reasonable approximations and using numerical computational methods, the parameters of the jet flow may be accurately worked out for simple geometrical systems, thus giving an expression for the entropy rise, which, when compared with ΔS above, yields an expression connecting τ with the pressure defect $(P_o - P)$ as measured by the impact tube.

The method has given results in good agreement with sound absorption and dispersion measurements, for a number of gases. Experimentally it is a very simple method, although care must be taken in calculating the exact aerodynamic flow. The range of relaxation times which can be measured is large, since the 'time constant' of the method, i.e. the time of compr ession of the gas at the impact tube, can be varied widely and quite precisely using different expansion nozzles,impact tubes and flow geometry, thus 10^{-8} - 10^{-2} sec. seems practical. Impact tube me asurements have the same limitations with regard to polyatomic molecules as with sound measurements, but have one important advantage in that the impact tube may be used at higher temperatures, thus bridging the gap to shock wave measurements. A disadvantage as Cottrell points out is that the method needs a large quantity of gas, which is impractical in many cases.

IV Spectroscopic Methods

An apparently simple and direct method of investigating vibrational relaxation would be the observation of the infra-red fluorescence produced when, say, the population of the excited vibrational state was increased by a pulse of resonant resonance radiation. Fluorescence and collisional de-excitation will be competing processes. The rate of loss of vibrational energy being given by a rate equation of the form (in the absence of irradiation);-

$$\frac{dN_1}{dt} = -N_1 f_{10} - N_{ff} + N_o f_{01} \qquad 2.13$$

where N_1 and N_o are the excited and ground state populations and f_{01}, f_{10} and f_f are the rate constants for collisional excitation, collision de-excitation and fluorescence respectively. By measuring the changes in fluorescence intensity or decay rate induced by changes in pressure or inert gas dilution, it should be possible to calculate the rate constants and evaluate the vibrational relaxation time, provided that the radiational lifetime τ_R is known.

However, for nearly all molecules, this is difficult because for vibrational excitation the radiative lifetime is much greater than the collisional lifetime, except at very low pressures, so that effectively no vibrational energy is radiated. An exception to this is carbon monoxide. The extremely long relaxation time ($\sim$1 sec. at one atmosphere), of this gas was first measured successfully by Millikan [47] by a method similar to that outlined above.

For electronic radiational transitions on the other hand, τ_R is much shorter - typically 10^{-7} sec. and electronic fluorescence may be readily observed. This has been utilised to investigate vibrational energy transfer in collisions. Basically all spectroscopic studies rely upon the fact that molecular electronic transitions depend upon the vibrational state of the molecule, and electronic spectra have well-defined band structure due to the variable vibrational state of the molecule before and after the electronic transition. From a knowledge of the vibrational energies the various vibrational species may be identified. Thus by observing the changes in intensity of a particular line, population changes in the vibrational state of the initial electronic state may be followed, and

hence the collisional lifetime calculated. The vibrational energy in electronically excited molecules is often very high, thus spectroscopic studies give information concerning energy transfer in high as well as the low energy states investigated in the above methods. States with quantum number as high as 30 can be involved.

Experimentally, spectroscopic techniques fall into two main groups, depending upon whether the electronic emission or absorption spectra is observed. In the former (see, for example, references (48) and (49)) fluorescence is recorded after the selective excitation of the required electronic states by a suitable source. The fluorescence may be observed in the steady state or as a decay, and by adding varying amounts of inert gas, the efficiency of the diluent gas molecules in de-exciting the vibrations of the electronically excited molecules can be measured. A knowledge of the true radiative lifetime of the electronic state enables quantitative measurements to be made. A variation on fluorescence measurements is that of 'fluorescence stabilization', where the primary effect of vibrational relaxation by the diluent molecules is to suppress radiationless transitions and thus enhance the fluorescence [50]. Fluorescence measurements give information of vibrational de-excitation in electronically excited molecules and these may have different collision parameters from those in the ground electronic state.

Vibrational de-excitations in the ground electronic state may be studied by absorption studies, see, for example, references (51) and (52) A particularly interesting technique is that of flash spectroscopy [53]. In this the gas is first irradiated by a flash from a high intensity light source such as a krypton discharge tube. The electronically

excited molecules (they may be the original gas molecules or products or photolysis), decay rapidly in a time 10^{-6} - 10^{-8} sec. to the ground electronic state and to a variety of vibrationally excited states. Then a second, usually weaker, flash is sent through this vibrationally hot gas and the absorption spectra observed. By means of high speed photography the variation in the intensity of the various vibrational species with time may be recorded. The techniques and results of flash spectroscopy, with respect to vibrational relaxation, have recently been reviewed by Callear (54).

The extraction of vibration energy transfer probabilities from spectroscopic experiments needs carefully planned experimentation and there are many difficulties. For example, the radiational lifetime for many electronic states cannot be simply calculated from the theoretical Einstein coefficients because of appreciable radiationless self-quenching processes. Usually a separate experiment or experiments are needed to measure this. Trouble may be experienced with self-absorption and since the permissable pressure of the electronically active molecule is usually small, the gas must be diluted with some electronically inert gas. This sometimes leads to pressure broadening difficulties. In some experiments it is necessary to use more than one diluent and in flash spectroscopy there are often two or more photolytic products. In these cases the collisional de-excitation process is complex, and again several different experiments may be needed to determine the various rate constants. Finally the time resolution of the spectroscopic techniques is basically rather small. Fluorescence measurements depend upon the radiational lifetime of the electronic states $\sim 10^{-7}$ sec., making

direct examination of slow vibrational de-excitation impossible. Flash spectroscopy is limited by recording technique to minimum time intervals of about 10 μsec.

Despite these difficulties, spectroscopic measurements have certain basic advantages over the methods previously discussed. The first point to note is that they do not measure the time constant for an energy transfer process between a vibrational mode and translation. Spectroscopic studies essentially determine the rate constant for the decay of a particular vibrational state; irrespective of whether energy transfer is vibration-vibration, vibration-translation, etc. Thus not only do they allow particular modes to be examined in polyatomic molecules, but in cases where the decay is complex, i.e. where the energy transfers to translation via one or more lower energy states, then theoretically the rate constants for separate steps of the chain could be determined.

V The Optic-acoustic effect

This method was first suggested independently by Gorélik [55] and by Cottrell [61]. The optical-acoustic effect, discovered originally by Tyndall [56] is a direct acoustical method of demonstrating the existence of vibrational modes and vibrational relaxation. If a gas with infra-red active vibrations is irradiated with resonant infra-red radiation, then the vibrational energy will be increased and by means of inelastic collisions, this energy is eventually transferred to translation. Thus if the amplitude of the incident radiation is chopped or modulated, there will be similarly

modulated translational temperature changes in the gas. These temperature changes will give rise to pressure fluctuations, and, in a large volume of gas, a sound wave is generated with a fundamental frequency equal to that of the radiation modulation. If the gas is contained in a small chamber, with dimensions much smaller than the appropriate acoustic wavelength, there will be approximately identical pressure changes throughout the volume. These pressure changes may be detected by a pressure transducer, and the chamber in which such pressure measurements can be made is called a 'spectrophone'.

Because of the slow collisional energy exchange between vibrational and translational energy, the fundamental temperature amplitude (and hence the pressure amplitude) will lag behind the corresponding radiation amplitude - a typical relaxation effect. Although the theory will be treated in detail in the next chapter, it may be said here that we should expect, for a sinusoidally modulated radiation input $I_o e^{i\omega t}$, translational temperature changes of the form:-

$$\Delta T_{tr.} = \frac{K I_o e^{i(\omega t - \theta)}}{\sqrt{1 + \omega^2 \tau^2}} \qquad 2.14$$

where K is a function of the apparatus, ω is the chopping pulsatence and τ the vibrational relaxation time. $\tan \theta = \omega\tau$. Thus both the phase lag and the amplitude of the pressure fluctuations should be a function of τ, and measurement of both these quantities has provided a means of evaluating it.

The spectrophone has, in theory, considerable advantages over mechanical methods of investigating vibrational relaxation. Infra-red active vibrations may be excited individually so that the relaxation time of a particular vibrational mode may be measured. This is especially useful for modes with a large quantum, which are difficult to excite mechanically. Unlike spectroscopic methods, vibrational-vibrational energy transfer cannot be directly studied, but as the spectrophone requires generally simpler and more straightforward experimental techniques, it should provide, if the theory may be adequately solved, the best method for investigating individual mode relaxation in polyatomic gases.

The optical-acoustic method does not seem to have been established as one of the standard techniques despite the appearance of results from time to time, see references (57), (58) and (59). This may well arise from the inconsistent results obtained by different observers for carbon monoxide. A good deal of the work published, deals with this gas, since it appears to be ideal for spectrophone study. However, as discussed in Section IV (above), CO constitutes an exceptional case with its extremely long relaxation time, making severe demands on the maintenance of gas purity throughout an experiment. For other gases there seems no reason why spectrophone results should not be accepted, and one of the main aims of the present research is to try and confirm earlier work and prove the consistency of the results.

The method has been reviewed by Delany [60] and Cottrell [9].

CHAPTER 3

SPECTROPHONE THEORY

A Introduction

(i) Defining the system

In the spectrophone the gas is contained in a chamber incorporating an infra-red window, and a pressure sensitive device, i.e. a microphone. Infra-red radiation entering by the window is absorbed and through optic-acoustic effect, pressure changes occur in the gas which are detected by the microphone. The amplitude of the varying pressure will follow the amplitude of the incident radiation. In order to calculate vibrational relaxation times it is necessary to connect theoretically the phases of the infra-red radiation input and the varying component of the gas pressure.

The solution of the most general problem with, for example, no restrictions on size or geometry of spectrophone, or on the spatial and temporal distribution of the incident radiation, is extremely difficult. Many assumptions must be made, some fully justified with regard to the experimental set up, others only approximated in experiment, before the physical process in the spectrophone may be analysed. It is important before applying spectrophone theory to the analysis of experimental results that all approximations be shown to be valid for the range of conditions covering the measurements.

The following geometrical boundary conditions are assumed:

a) Cylindrical spectrophone cavity

b) Optically transparent window forming one complete end-face

c) Microphone set in wall - diaphragm flush with wall

d) Cell axis mounted horizontally

e) Walls of spectrophone absolutely rigid

f) Radiation incident along axis of cell and of uniform intensity over window

g) Amplitude of incident radiation is sinusoidally modulated with respect to time.

It is convenient to describe the above system by cylindrical-polar coordinates with the origin at the mid-point of the optical window and z-axis pointing along the axis of the spectrophone, as shown in Figure 2.

Fig 2

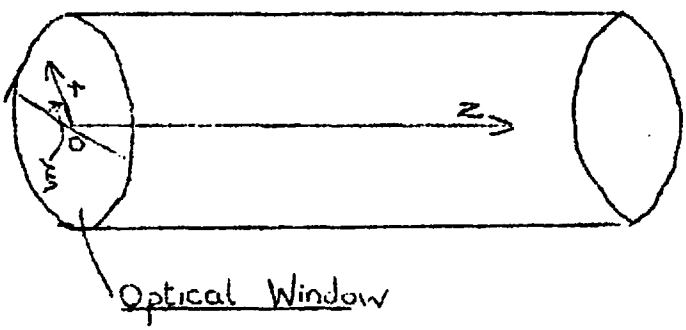

From the assumed symmetry and uniformity of radiation over the end-face the physical parameters should be independent of ϕ, the azimuthal angle.

(ii) Equations governing the spectrophone process

The spectrophone process may be divided into two main parts; the absorption of radiation by the gas molecules and the conversion of

this energy via the internal modes into translational energy (molecular kinetic energy), and secondly, the effect of the latter in producing pressure fluctuations in the gas volume. The first of these processes will depend upon infra-red absorption theory and the theory of inelastic molecular collisions. The second part demands essentially the solution of the equation of heat transfer for a gas with a time-dependent volume heat source and having given boundary conditions. The solution of this equation, giving the temperature distribution in the gas, together with a knowledge of the acoustic boundary conditions and the equation of state for the gas, will yield the pressure and density distributions inside the cell.

Before considering an explicit form for the heat transfer equation various factors must be considered.

Firstly, since a cylindrical cell with horizontal axis is assumed with uniform irradiation over one end-face, convection may be neglected.

Secondly, since the gases used in the spectrophone are strong absorbers, the intensity of the resonant radiation will fall off along the axis of the cell. This means in effect that the density of excited molecules will vary along the length of the cell, and some redistribution will occur due to normal diffusion. Montan [63] has considered the effect in his analysis. Its importance depends upon the ratio of the acoustic wave-length to the "diffusional length", $(D\tau)^{\frac{1}{2}}$ where D is the coefficient of diffusion and τ is the relaxation time. In the present experiment the chopping frequency is such that such diffusion may be neglected, as was concluded by Montan.

The third factor to be considered is that of the spatial distribution of the varying pressure amplitude. If the acoustic wavelength, determined by the modulation frequency of the radiation, is much greater than the dimensions of the chamber, then the pressure amplitude should be identical throughout the cell. If this assumption is not made, or cannot be justified then the full equations for an acoustic system, i.e. equation of motion, equation of continuity, must be applied. Terms allowing for viscous drag within the gas and at the walls are needed in the heat transfer equation, and the average pressure immediately in front of the microphone diaphragm would have to be found. The solution of such a generalised problem would be a formidable task. However, as Arnold and Crandall [64], and Ballantine [65] showed in the original theories of the thermophone, no matter how localised the area of heat input, a uniform pressure variation will result in a volume of gas provided $\lambda_{acoust.} \gg L_{chamber}$ holds. Every worker on the spectrophone has made the same assumption which should hold in the present experiment.

In the light of the above considerations and assumptions, the equation of heat transfer governing the spectrophone process will be

$$C_v \rho \frac{\partial T}{\partial t} = K\nabla^2 T + H + q' \qquad 3.1$$

which is essentially the equation of heat conduction in a compressible fluid,

where H = external heat energy input/unit vol/sec.

q' = compressional heat input/unit vol/sec.

The energy term H constitutes the energy obtained from the radiation via the internal mode relaxation process. It will in general be f(r, z, ξ, t). H will be obtained, following Delany, from a molecular viewpoint by finding an expression for the equilibrium number of molecules de-exciting/sec. for a given radiation intensity. However, the number of molecules de-exciting/sec. does depend upon the translational temperature of the gas and hence H is not a strictly independent quantity determined from the internal parameters of the particular gas and the given radiation intensity, but is also a function of T. This can be seen from the relaxation equation

$$H = \frac{1}{\tau}(E - E_o - C_v v)$$

where E is the internal energy of the gas at its instantaneous vibrational temperature and E_o is the equilibrium internal energy at the external ambient temperature. However, since in the spectrophone process the excess temperature v is small it seems reasonable to neglect the term $C_v v$ and avoid the considerable complication of having H a function of T. This procedure has been followed in all previous work, except that of Jones.

The term q' arises from the first law of thermodynamics for compressible fluids:

$$dQ = dE + PdV \qquad \text{in the usual notation.}$$

The general equation of heat trasnfer for a static compressible, conducting fluid with no external heat sources, can be shown to be[66]

$$\rho T \frac{\partial s}{\partial t} = \text{div (K grad T.)} \qquad \text{where s = specific entropy}$$

which gives

$$q' = \frac{d}{dt} (PdV) \tag{3.2}$$

It should be noted that from the nature of the spectrophone process, if the external energy input is identical throughout the cell then the term q' must be zero for a rigid walled chamber. When, as is generally the case, H is spatially dependent, then q' will not be zero. In some work on the spectrophone the factor q' has been neglected in which case the equation of heat transfer becomes

$$\rho C_v \frac{\partial T}{\partial t} = K \nabla^2 T + \cdot H \tag{3.3}$$

which is identical with that for an incompressible fluid or an isotropic solid.

The second important equation determining the spectrophone process is the equation of state for the gas. $F(T, \rho, P) = 0$

Since the experimental work is largely carried out at low pressure, the ideal gas equation will be assumed, i. e.

$$P = mR\rho T \tag{3.4}$$

Finally it remains to consider the basic acoustic boundary condition. This is made simple by the assumption of identical pressure throughout the cell.

The volume rate of change throughout

$$\left(\frac{dV}{dt}\right)_{\text{chamber}} = \frac{p}{Z}$$

where Z is the impedance offered by the walls and microphone to the pressure fluctuations.

Therefore for an assumption of rigid walls

$$\left(\frac{dV}{dt}\right)_{\text{chamber}} = 0 \qquad 3.5$$

(iii) Survey of previous work and scope of present analysis

Previous theoretical treatments of the spectrophone fall into two main categories, depending on whether equations (1) or (3) are assumed for the equation of heat transfer. It is difficult to decide a priori on the importance of the factor q'. It should depend upon the rate of fall off of absorption of energy along the cell axis.

In view of the complexity of the problem and the number of approximations which have to be made, it is to be expected that the main practical use of spectrophone theory is to establish the range of experimental conditions suitable for relaxation measurements, i.e. where the relaxation phase shift is much greater than others due to heat conduction, etc., so that these may be neglected or allowed for by small correction terms. The theory must also show under what conditions the calibrating gas procedure is valid. Even with these limited aims in view, it is important to consider the problem as rigorously as possible. In particular it would seem useful to compare differences in the solutions obtained using the compressible and incompressible heat transfer equations for the system outlined in section (i). However, in previous work several different and generally simpler systems have been considered.

Jones [67] and Delany [68] have both considered the incompressible equation (1).

Jones attempted to keep his treatment strictly therodynamical and avoided molecular conditions in obtaining his expression for the heat input from the internal modes. He complicated his equations with second-order terms, in particular the dependence of the heat input term H on the translational temperature, as discussed in section (ii). Thus he was forced to look for an approximate harmonic solution.

Delany considered an infinitely long cylindrical cell, neglecting fall-off radiation intensity along the length of the cell, and solving the equation exactly for this simpler system.

Stephanov and Girin [69] and other Russian workers have considered the complete heat transfer equation for an infinitely long spectrophone - again neglecting radiation 'fall-off' along the cell axis.

Montan [63] endeavoured to consider the most general problem, i.e. without initially assuming identical cell pressure, and also taking diffusion into account. The complexity, this introduced, forced him to treat the problem in one dimension.

In the present analysis therefore, it is proposed to solve both equations 1 and 3 applied to the spectrophone system as defined in section (i). Equation 1 may be readily solved exactly using transform methods. The exact solution of 3 is possible but very laborious to obtain. As any important difference with the above solution will be contained in the harmonic terms, an harmonic solution will be impressed on the equation, as attempted by previous workers but for

the more complete system outlined above.

Prior to attempting these solutions, H the heat input to the gas from relaxation will be examined, following Delany, from the molecular viewpoint with the additional problem of determining the radiation attenuation factor.

Finally the amplitudes and phases of the varying pressure components obtained for the two different heat transfer equations will be compared with a view to their use in determining vibrational relaxation times and the experimental conditions necessary for the validity of the calibration method.

B Energy Input Theory

(i) The excited state population in a two-state gas

In the present work the relaxation times of the fundamental modes of the infra-red active vibrations of carbon dioxide and nitrous oxide have been measured. Spectroscopically, the excitation of these fundamental modes gives rise to vibration-rotation bands at 4.3μ and 15μ for carbon dioxide, and at 4.4μ, 7.7μ and 16μ for nitrous oxide.

These bands correspond to vibrational transitions between the n^{th} and $(n + 1)^{th}$ states. The probabilities of such transitions may be approximately equal for all initial states (see Stull et al. [70]), giving rise to a harmonic oscillator model. However, the importance of any particular transition in the series will depend upon the equilibrium population of the lower state, given approximately by the well known statistical relation:

$$\frac{N_n}{N_o} = \frac{g_n}{g_o} e^{-nh\nu/kT}$$

where N_n and N_o are the equlibrium number of molecules in the n^{th} excited and ground states at absolute temperature T, and g_n and g_o are degeneracy weighting factors. At room temperature for carbon dioxide, the populations of all states except the ground state are negligible for the 4.3 μ band, and small, except for about 10 per cent in the first excited state, for the 15 μ band. For nitrous oxide, likewise the populations above the ground state are negligible except for the 16 μ band which has a small first excited state population. Thus approximately the bands correspond vibrationally to a two-state process from ground state to first excited state.

The complex structure of the bands is due to the simultaneous rotational transitions, each different rotational transition producing a separate rotational line, contributing to the band and having slightly different energies so that the band is spread over a considerable frequency range. The widths of the individual rotational lines themselves is determined by the various line broadening processes - under spectrophone conditions essentially collision (or impact) broadening.

The absorption of radiation by the gases in the spectrophone and the resulting equilibrium population of vibrationally excited molecules may now be treated quantum-mechanically closely following the work of Delany. Initially it is assumed that we have a two-state gas which absorbs radiation at a resonant frequency ν. Consider unit volume of gas where the incident radiation density at frequency ν is

$\rho(\nu)$ f(z), where $\rho(\nu) = \rho_o(\nu) + \rho_1(\nu) \cos \omega t$, is the radiation density just inside the window, and f(z) is a function of z the axial coordinate of the spectrophone as defined in the system of section A(ii). f(z) will be 1 at z = 0.

Let N_1 = the number of excited molecules (in vibrational state 1) per cc.

Let N_o = the number of molecules in the ground state (vibrational state 0) per cc.

Then according to the quantum theory of radiation absorption we may write the rate equation:-

$$\frac{dN_1}{dt} = - N_1(f_{10} + B_{10} \rho(\nu) f(z) + A) + N_o (f_{01} + B_{01} \rho(\nu) f(z)) \qquad 3.6$$

where f_{10} = number of collisional de-excitations/sec/molecule

f_{01} = number of collisional excitations/sec/molecule.

B_{01} and B_{10} are the induced Einstein probability coefficients defined such that $B_{01}\rho(\nu)$ $\left[B_{10}\rho(\nu)\right]$ is the probability/sec)molecule of a radiational transition from state $0 \rightarrow 1$ $\left[\text{state } 1 \rightarrow 0\right]$ induced by a radiation field of density $\rho(\nu)$ where ν is resonant with the transition. Statistical thermodynamics shows that

$$\frac{B_{01}}{B_{10}} = \frac{g_1}{g_0} = g$$ where g_o and g_1 are the weighting factors of the two states.

A is the spontaneous Einstein probability coefficient defined as:- the probability/sec/molecule of a spontaneous radiational transition, state 1 $\longrightarrow$ 0. Again theory shows that

$$A = \frac{8 \pi h \nu^3 B_{10}}{c^3}$$

where c = velocity of light in vacuo.

Writing $N = N_1 + N_o$, the total number of molecules/unit volume gives

$$\frac{dN_1}{dt} = - N_1(f_{10} + f_{01} + A + (B_{10} + B_{01}) \rho(\nu) f(z)) + N(f_{01} + \rho(\nu) f(z) B_{01}) \qquad 3.7$$

Writing $\rho(\nu) = \rho_o(\nu) + \rho_1(\nu) \cos \omega t$

gives

$$\frac{dN_1}{dt} = -N_1 \left[C + (B_{10} + B_{01}) \rho_1(\nu) f(z) \cos \omega t \right] + N(D + \rho_1(\nu) f(z) B_{01} \cos \omega t \qquad 3.8$$

where

$$\left.\begin{aligned} C &= f_{10} + f_{01} + A + (B_{01} + B_{10}) \rho_o(\nu) \ f(z) \\ D &= f_{01} + \rho_o(\nu) B_{01} \ f(z) \end{aligned}\right\} \qquad 3.8a$$

Delany has solved equation (8) exactly, his solution being

$$N_1 = K\, e^{-C(t - (\eta/\omega)\sin\omega t)} + N\frac{D}{C}\left[\frac{\delta}{\eta} - \left(\frac{\delta-\eta}{\eta}\right)\sum_{m=-\infty}^{\infty}\sum_{n=-\infty}^{\infty}(-1)^m i^{(m+n)} I_m\left(\frac{\eta C}{\omega}\right) I_n\left(\frac{\eta C}{\omega}\right)\frac{e^{i(m+n)\omega t}}{\left(1+i\frac{m\omega}{C}\right)}\right] \qquad 3.9$$

where K = a constant, $I_m\left(\frac{\eta C}{\omega}\right)$, $I_n\left(\frac{\eta C}{\omega}\right)$ are modified Bessel functions of the first kind,

$$\eta = \frac{\rho(\nu)\, f(z)\,(B_{01} + B_{10})}{C} \qquad 3.9a$$

and

$$\delta = \frac{\rho(\nu)\, B_{01}\, f(z)}{D} \qquad 3.9b$$

Delany shows that providing $\frac{\eta\omega}{C} \ll 1$ this simplifies to

$$N_1 = N\frac{D}{C}\left[1 - \frac{\eta(\delta-\eta)}{2\left[1+\frac{\omega}{C}\right]^2}\right] + N\frac{D}{C}\frac{(\delta-\eta)\cos(\omega t - \gamma)}{\left[1+\left(\frac{\omega}{C}\right)^2\right]^{1/2}} \qquad 3.10$$

where the transient term has been omitted and $\tan\gamma = \frac{\omega}{C}$

The validity of the assumption $\frac{\eta\omega}{C} \ll 1$ will be discussed later.

For the valence modes of CO_2 and N_2O the weighting factors g_o and g_1 are both equal to 1, thus $B_{10} = B_{01}$. For the doubly degenerate bending modes however, the excited state with one vibrational quantum of energy has a weighting factor of 2. Thus for these modes, $g_o = 1$, $g_1 = 2$, and $B_{01} = 2B_{10}$. In thermal equlibrium, the bending mode

population of molecules with one vibrational quantum (n_{01}), is related to the ground state population n_{00} by $\frac{n_{10}}{n_{00}} = 2\,e^{-h\nu_2/kT}$, thus f_{10} and f_{01} as defined, are related for this mode by $\frac{f_{01}}{f_{10}} = 2\,e^{h\nu/kT}$.

(ii) The Einstein probability coefficients for a vibration-rotation band

Equation (10) thus gives the steady state expression for the number of excited molecules/cc. for a two-state gas, the excited state having an energy $h\nu$ greater than the ground state. Can this expression be applied to the actual transitions occurring in the spectrophone? For the vibrations under consideration, "two-state" conditions exist to an excellent approximation for all except the 15μ carbon dioxide and 15μ nitrous oxide bands, and even for these the discrepancy is small. More important however, the theory presented above takes no account of even the finite width of a single rotational line, let alone the large band-width of a complete rotation-vibration band.

Now the rotational energy of a vibrationally excited molecule of carbon dioxide or nitrous oxide is very small compared with the vibrational energy and should play little part in determining the dynamics of vibrational relaxation.* Many workers have ignored

---

* Recently there has been evidence that rotational-vibrational interaction can be of importance in vibrational relaxation, see Chapter 1 or R. C. Millikan [71]. However, this involves the collisional de-excitation of vibrations, and should not affect the above argument concerning the total amount of energy liberated in the gas.

the rotational states altogether in treating the vibrational colli sional de-excitation process, lumping them with translation as external degrees of freedom. By this model it is unimportant which rotational state a molecule is in for determining the vibrational de-excitation probability. Whether this is justified or not, as far as the spectrophone process is concerned, the energy entering the gas from radiation, via the internal modes, depends to a good approximation only upon the vibrational energy. Thus all the transitions in a vibration-rotation band, corresponding to a single vibrational transition, are equally important in the spectrophone process. In other words the entire integrated vibration-rotation band determines the number of excited molecules produced and hence the energy liberated in the gas. The Einstein coefficients are defined as probabilities of absorption and emission of quanta: therefore it seems reasonable that as long as they can be defined as probabilities of transitions throughout the whole of the vibration-rotation band, and not at some theoretical and non-existent resonant radiation frequency, and provided that the incident radiation intensity is approximately constant over the spectral width of the band, then equation (10) will hold without modification for the number of excited molecules/cc. produced by the entire vibration-rotation band.

It is obviously important to be able to at least estimate the numerical values of the coefficients A and B_{01}. Their magnitude will determine the truth or otherwise of the inequality upon which the validity of equation (10) dea ends. The phase shift, γ, between

the modulated radiation and the harmonic component of the excited molecule population, which determines the relaxation time, also depends on A and B_{01}. A direct quantum-mechanical calculation of A and B_{01} is difficult since it demands a precise knowledge of molecular constants and has led to errors in the past. It seems preferable to relate the coefficients if possible directly to measured spectroscopic data. The most accurately measured parameter of a band is the integrated absorption coefficient α_{ν_n} as defined below.

The spectral absorption coefficient $P_{\bar{\nu}}$ is defined as:-
$P_{\bar{\nu}}$ = fraction of intensity absorbed /unit path length/unit pressure, at a wave number $\bar{\nu}$. The usual units are cm^{-1} $atmos^{-1}$. Analogous spectral absorption coefficients P_ν and P_λ may be defined with respect to frequency and wavelength. Thus the fraction of incident radiation intensity absorbed in the narrow wave number range $\bar{\nu}$ to $\bar{\nu} + d\bar{\nu}$ will be $P_{\bar{\nu}} \cdot d\bar{\nu}$.

For a whole line or band, the integrated or total absorption coefficient is defined as $S = \int_{\bar{\nu}_1}^{\bar{\nu}_2} P_{\bar{\nu}} \, d\bar{\nu}$ where the integration limits are such that the band or line has negligible intensity outside them. A distinction must be made between the absorption coefficient for a single spectral line, e.g. for a single rotational-vibrational transition, usually denoted by $S_{JJ'}$ (where J and J' refer to the initial and final rotational quantum numbers), and that for a complete band, usually denoted by $\alpha_{\substack{\nu_n \\ 0 \to 1}}$ etc.

Obviously

$$\alpha_{\substack{\nu_n \\ 0 \to 1}} = \sum S_{JJ'}$$

summed over all the lines comprising the band.

S is thus the average fraction of intensity absorbed throughout the band/cm/atmos. multiplied by the bandwidth. Its units are therefore cm^{-2} $atmos^{-1}$.

Consider unit volume of gas, irradiated by radiation of intensity I_ν. The amount of energy absorbed per second by the gas in frequency range $\nu \rightarrow \nu + d\nu$

$$dE = I_\nu P_{\bar{\nu}} P \, d\nu$$

where P is the partial pressure of the absorbing gas in atmospheres. Alternatively

$$dE = c \rho(\nu) P_{\bar{\nu}} P \, d\nu$$

This is equivalent to a number of quanta absorbed/sec

$$dN = c \rho(\nu) P_{\bar{\nu}} P \, d\nu / h\nu$$

and which will equal the number of transitions from the ground vibrational state to the excited state. Hence the number of transitions occurring in unit volume per sec for the whole line or band will be

$$N_{transitions} = \frac{Pc}{h} \int_{\Delta\nu} \frac{\rho(\nu) P_{\bar{\nu}} \, d\nu}{\nu}$$

where $\Delta\nu$ is again the effective bandwidth. If now $\rho(\nu)$ may be considered constant over this bandwidth and we neglect the variation of ν over the band (or can put some average value of ν for the band) we obtain:-

$$N_{transitions} = \frac{Pc^2}{h\nu}\,\rho(\nu)\int_{\Delta\bar{\nu}} P_{\bar{\nu}}\, d\bar{\nu}$$

$$= \frac{Pc^2}{h\nu}\,\rho(\nu)S \qquad 3.11$$

But from the definitions of the Einstein Coefficients, number of transitions/unit vol/ sec induced by radiation density $\rho(\nu)$ equals $N_{transitions}$ where

$$N_{transitions} = N_0 B_{01} \rho(\nu) - N_1 B_{10} \rho(\nu)$$

$$= B_{01} \rho(\nu) \left[N_0 - \frac{1}{g} N_1 \right] \qquad 3.12$$

Therefore from (11) and (12)

$$S = \frac{h\nu B_{01}}{Pc^2} \left(N_0 - \frac{1}{g} N_1\right) \qquad 3.13$$

or

$$S = \frac{N_0 h\nu B_{01}}{Pc^2} \left(1 - e^{h\nu/kT}\right) \qquad 3.14$$

Since N_0, the number of molecules/cc. in the ground state, is connected with N, the total number of molecules/cc. by the relation

$$N_0 = \frac{N}{Q} \quad g_o \, e^{-E/kT} \qquad 3.14a$$

where E is the internal energy of the molecule in the ground state and Q is the particle function, then (14) becomes

$$S = \frac{Nh\nu B_{01}}{c^2 P} \quad (1 - e^{-h\nu/kT}) \, \frac{g_o}{Q} \quad e^{-E/kT} \qquad 3.15$$

Equation 14 connects the Einstein Coefficients with the integrated absorption coefficient.

At first sight it might seem a more justifiable procedure to apply equation (14) not to a whole band but to a single rotational line, so that S becomes $S_{JJ'}$, and not α_{ν_n}. Obviously the approximations involved in assuming $\rho(\nu)$ and ν constant over a line width are much less than similar approximations over a whole band. In this case equation (10) for N_1 would refer not to the total number of excited molecules in a band, but to the number contributed by the J^{th} rotational transition. N_1 would then be obtained by summing $N_1 = \sum_{JJ'} N_J$. However, this procedure, besides being more complicated, has the following disadvantage. Individual $S_{JJ'}$, are not accurately known for most vibration-rotation bands, owing to experimental difficulties caused by overlapping of lines and inadequate instrumental resolution. In fact a general procedure has been to obtain $S_{JJ'}$ from the measured α_{ν_n} using some theoretical band model. Thus a straightforward application of (14) to a whole band seems more practical.

The problem has indirectly received a good deal of attention from various spectroscopists (for references see Penner [72], page 138). Most work has been primarily concerned with comparing the experimental integrated absorption coefficients and theoretically calculated matrix elements, but since the Einstein coefficients are simply related to the matrix elements for the transitions, then this work has relevance. In particular carbon dioxide has been studied by Dennison et al.[73]. The method basically consists of initially applying equation (14) to a single rotational line in the band and then summing the individual line intensities to give the total band intensity, using quantum-mechanical summation rules together with the modifications based on experimental evidence for the molecule in question.

(iii) Estimation of Einstein coefficients for carbon dioxide

For carbon dioxide, equation (15) may be used to calculate B_{01}, B_{10} and A, for the two infra-red active vibrations using the results of Dennison and Penner.

For the parallel 4.3μ band (ν_3)

$$B_{01} = \frac{\alpha_{\nu_3}}{Nh\bar{\nu}_3 \left[1 - \exp.(-hc\bar{\nu}/kT)\right]} cp \frac{Q_V}{\exp.\left(-\frac{E(\nu_3)}{kT}\right)} \qquad 3.16a$$

where $E(\nu_3)$ is the energy of a molecule in the ground state of ν_3 vibration. α_{ν_3} is the integrated absorption coefficient for this mode. Q_V is the vibrational partition function.

Similarly for the 2-degenerate perpendicular 15μ band (ν_2)

$$B_{01} = \frac{2\alpha_{\nu_2} cP\, Q_V \exp.\,(E(\nu_2))/kT}{Nh\bar{\nu}_2\left[1 - \exp.(-hc\bar{\nu}_2/kT)\right]} \qquad 3.16b$$

For the values of ν_2 and ν_3 Penner takes the so called band origins, values for transitions for which the rotational quantum numbers do not change. These are forbidden transitions in the 4.3 μ band and correspond to the Q branch in the 15μ band.

The values are

$$= 667.3 \text{ cm}^{-1}$$
$$= 2349.3 \text{ cm}^{-1}$$

The values of α_{ν_2} and α_{ν_3} used are

α_{ν_2} = 241 cm^{-2} atmos^{-1} (after Birch et al.)[74]

α_{ν_3} = 2500 cm^{-2} atmos^{-1} (after Birch et al.)[74]

Using these values and values for the other parameters given by Dennison

4.3μ band

B_{01} = 1.79 x 10^{17} erg^{-1}sec^{-2}cm^3

B_{10} = 0.89 x 10^{17} erg^{-1}sec^{-2}cm^3

A = 9.0 sec^{-1}

15μ band

B_{01} = 1.4 x 10^{17}erg^{-1}sec^{-2}cm^3

B_{10} = 0.7 x 10^{17} erg^{-1}sec^{-2}cm^3

A = 3.5 sec^{-1}

(iv) Einstein Coefficients for Nitrous Oxide

Values for the integrated absorption coefficients of the three fundamental modes of nitrous oxide, reported by Burch and Williams[75] are $1\ \alpha_{\nu_1} = 12\ cm^{-2}\ atmos^{-1}$

$2\ \alpha_{\nu_2} = 35\ cm^{-2}\ atmos^{-1}$

$3\ \alpha_{\nu_3} = 1850\ cm^{-2}\ atmos^{-1}$

Using these values an approximate calculation similar to that for carbon dioxide gives for the three bands, values of B_{01}:-

for ν_1, $B_{01} = 0.015 \times 10^{17}\ erg^{-1} sec^{-2} cm^3$

ν_2, $B_{01} = 0.2 \times 10^{17}$ " " "

ν_3, $B_{01} = 1.3 \times 10^{17}$ " " "

(v) Estimation of radiation attenuation factor

Equation (10) contains the factor f(z) allowing for the absorption of radiation and hence the attenuation of the amplitude as it passes through the cell. It is obvious that no simple factor f(z) will correctly account for the fall off of intensity with distance along the cell for a whole band. f(z) will vary widely with ν, from almost unity at the edges of the band, where absorption is low, to a factor which rapidly brings the intensity to zero at wavelengths near the centre of the band. Attempts to allow for the variation in spectral absorption coefficient by treating the absorption at some fixed wavelength and then integrating over the bandwidth are hardly practical without assuming some unrealistically simple model of the band structure, as admitted by Montan in his analysis[63]. However, remembering that it is the total number of vibrational transitions which is significant in the spectrophone

process, irrespective of their precise spectral origins, it should be possible to determine an empirical factof f(z) which corresponds to the actual total energy absorption profile in the chamber.

The following definitions are useful for finite optical pathlengths.

a) transmissivity $T(\bar{\nu})$ defined as

$$T(\bar{\nu}) = \frac{I_o(\bar{\nu})\, e^{-P_{\bar{\nu}} X}}{I_o(\bar{\nu})}$$

where $I_o(\bar{\nu})$ is the incident intensity at wavenumber $\bar{\nu}$, X is the optical density or pathlength (also called absorber concentration) in units of atmosphere-cm. and $P_{\bar{\nu}}$ is as previously defined.

b) absorptivity $A(\bar{\nu})$ defined as

$$A(\bar{\nu}) = \frac{I_o(\bar{\nu})(1 - e^{-P_{\bar{\nu}} X})}{I_o(\bar{\nu})}$$

Thus $T(\bar{\nu})$ and $A(\bar{\nu})$ represent the fraction of incident intensity transmitted and absorbed respectively, at wave number $\bar{\nu}$ after travelling a pathlength X cm.

For whole lines or bands may be defined the integrated transmissivity $\int_{\bar{\nu}_1}^{\bar{\nu}_2} T_{\bar{\nu}}\, d\bar{\nu}$ and integrated absorptivity $\int_{\bar{\nu}_1}^{\bar{\nu}_2} A_{\bar{\nu}}\, d\bar{\nu}$, where the limits of $\bar{\nu}$ encompass the whole line or band.

There is also "fractional transmissivity" T_R

$$T_R = \frac{\int_{\bar{\nu}_1}^{\bar{\nu}_2} I_o(\bar{\nu})\, e^{-P_{\bar{\nu}} X}\, d\bar{\nu}}{\int_{\bar{\nu}_1}^{\bar{\nu}_2} d\bar{\nu}}$$

Thus T_R is the mean fractional intensity transmitted throughout the band for a given optical density. If the incident radiation intensity is constant over the bandwidth, $T_R(\bar{\nu}_2 - \bar{\nu}_1)$ = integrated transmissivity.

In mixtures the absorption depends upon the total pressure as well as the partial pressure (P) of the absorbing gas.

From the point of view of the spectrophone process, the important quantity is the heat energy input/unit volume/sec. This is obviously proportional to the number of molecules de-exciting/sec/unit volume, which in turn will be proportional to the total energy absorbed from radiation/sec in that unit volume. From the definitions above for a unit cross section along the length of the cell:-

the energy absorbed/sec after traversing an optical path-length X at wave number $\bar{\nu}$ is $\propto I_o(\nu)\, A(\bar{\nu})\, d\bar{\nu}$

Therefore the total energy absorbed in the band after traversing an optical path length X will be

$$W \propto \int_{\bar{\nu}_1}^{\bar{\nu}_2} I_o(\nu)\, A(\bar{\nu})\, d\bar{\nu}$$

Further, assuming I_o constant over the bandwidth

$$W \propto I_o \int_{\bar{\nu}_1}^{\bar{\nu}_2} A(\bar{\nu})\, d\bar{\nu}$$

i.e. $\propto$ Integrated absorptivity for optical path-length.

The energy released in any interval $(z_1 - z_2)$, corresponding to $\frac{X_1}{P} - \frac{X_2}{P}$, is thus from the above reasoning proportional to the difference in integrated absorptivities for these two optical path lengths.

It would seem, therefore, that using spectroscopic data of integrated absorptivities it should be possible to investigate how radiation absorption varies along the axis of the spectrophone for actual optical densities and pressures encountered experimentally. Such a study has been made using data for carbon dioxide published by Stull et al.[70].

Figure 3 shows the absorptivity frequency profiles for the 4.3μ and 15μ CO_2 bands for various optical densities and equivalent total pressures (P_E). Figure 4 and Figure 5 show the variation of integrated absorptivity with the distance travelled along the chamber axis, for typical experimental conditions. From these graphs, Figures 6, 7, 8, 9, 10 have been prepared, giving histograms for the energy absorbed in 0.25 cm intervals along the spectrophone axis. These give an approximate indication of the energy absorption profile in the spectrophone under varying experimental conditions. Figures 11 and 12 show plots of $\log_e$ (energy absorbed/unit length) against z, as taken from the previous graphs for the 4.3 and 15μ bands respectively. The energy absorbed/unit length is expressed as a fraction of that absorbed just inside the window. As can be seen the plots are not linear, as would be expected from the previous discussion. However, for simplicity the factor f(z) will be made an exponential $e^{-\alpha z}$, where α is not directly connected with the spectroscopic absorption coefficient but determined from the best fit straight lines to the Figure 11 and 12 data.

FIG. 3. ABSORPTION — WAVENUMBER ($\bar{\nu}$) PROFILES
4·3μ & 15μ bands of CO_2

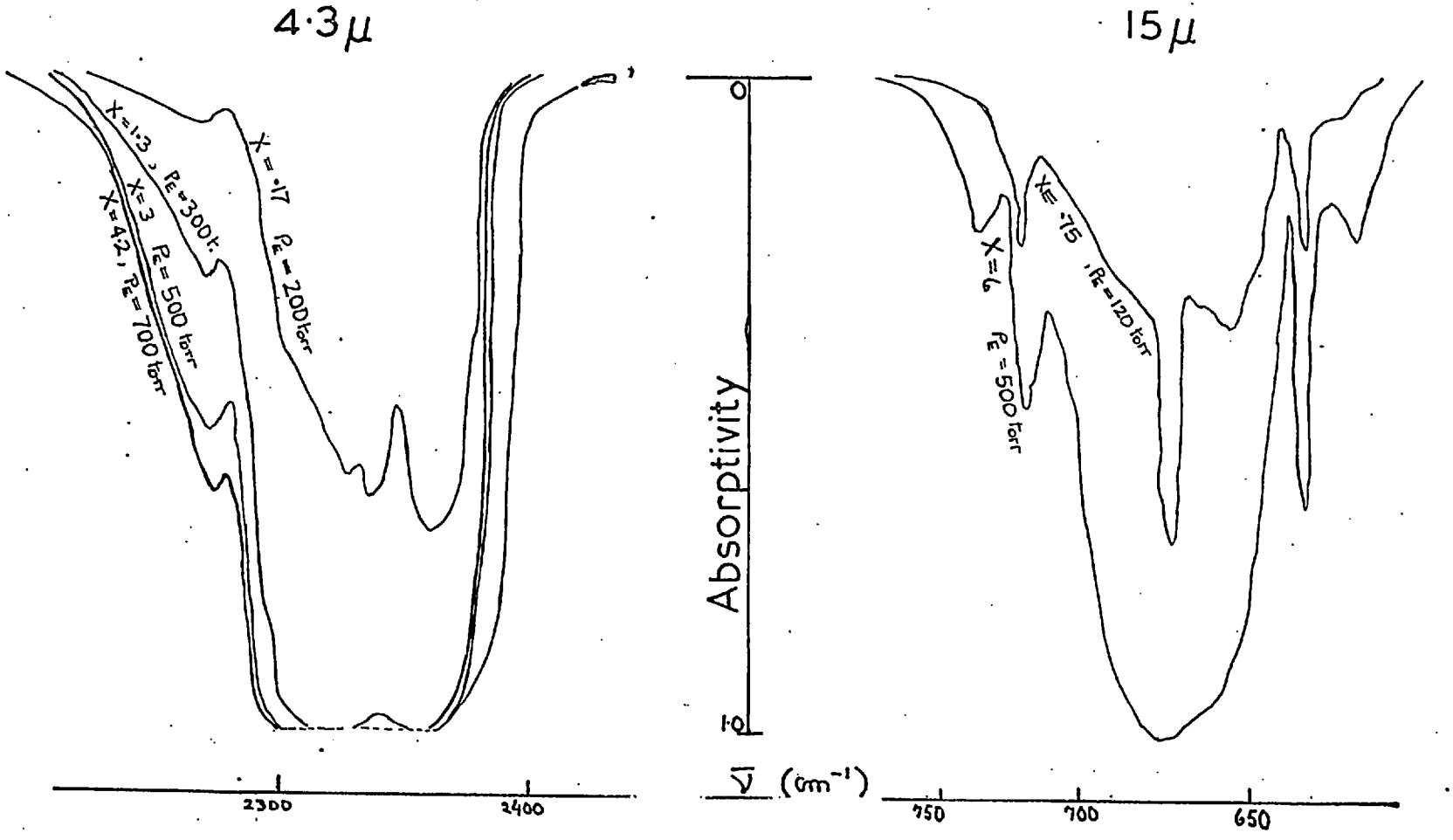

FIG 4

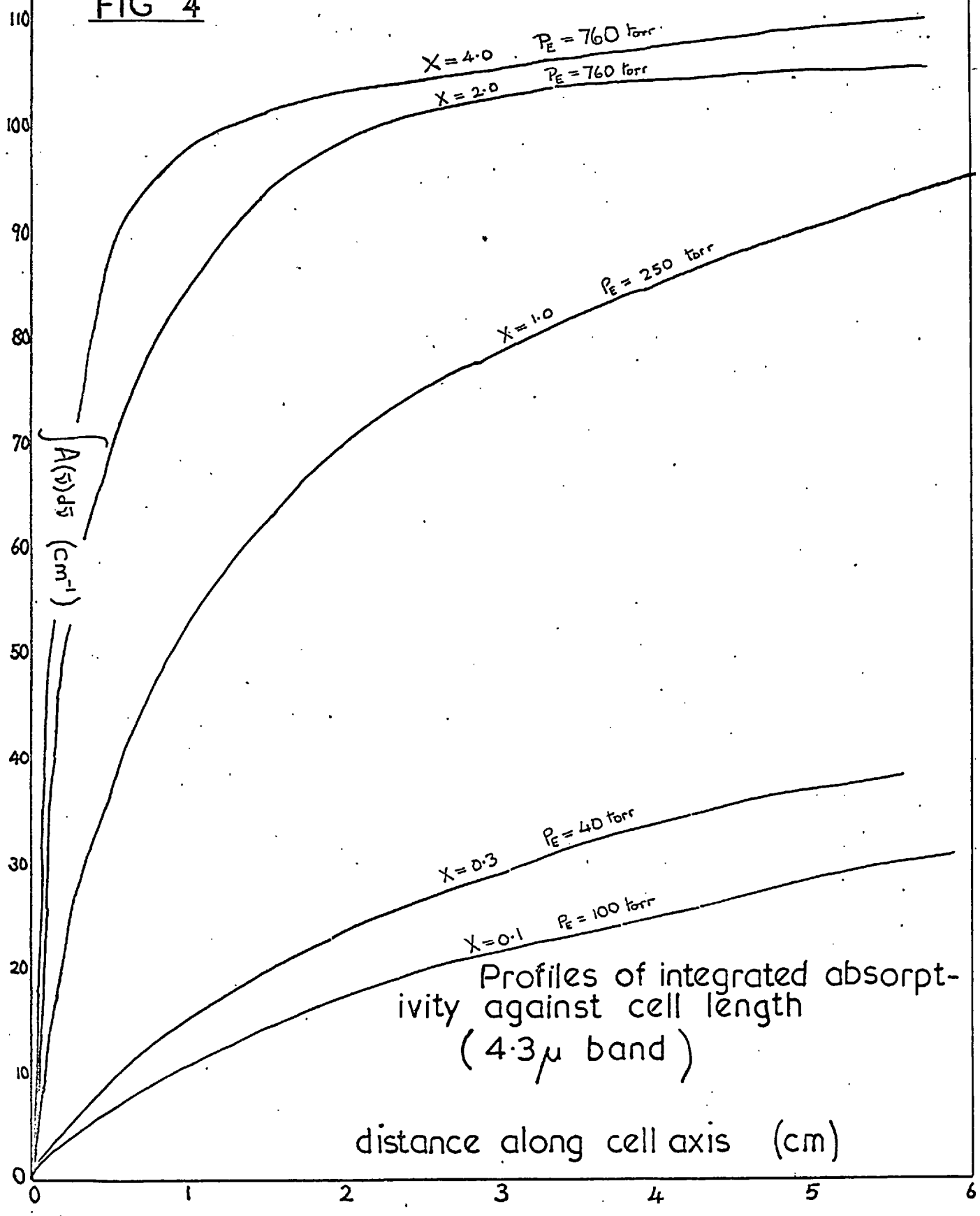

Profiles of integrated absorptivity against cell length
(4·3μ band)

FIG. 5. Profiles of integrated absorptivity against cell length. (15μ band)

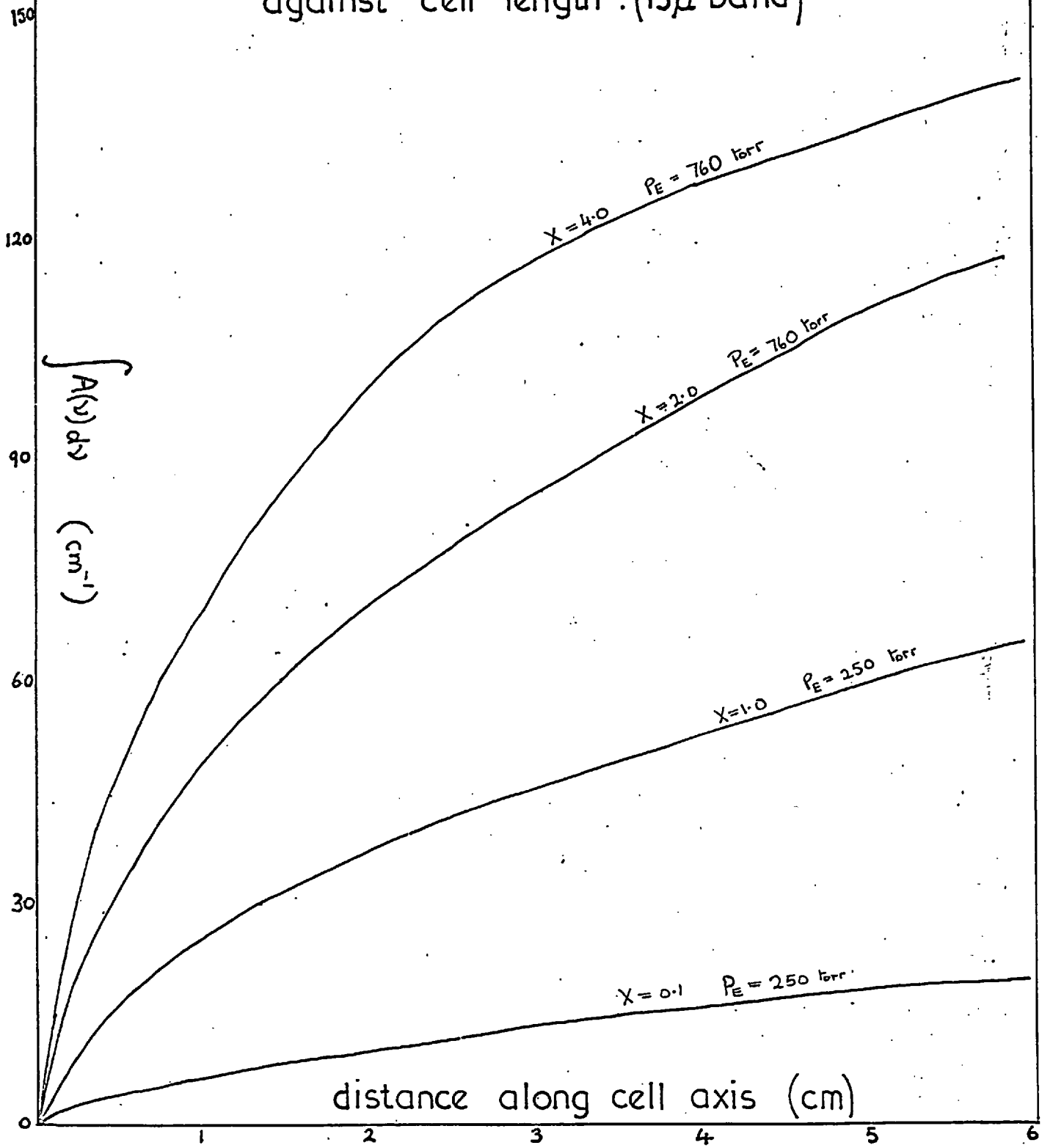

FIG 6. Histograms showing absorption of radiation along the cell. ($4{\cdot}3\mu$ band of CO_2) (differences in integrated absorptivities at 0·25 cm intervals)

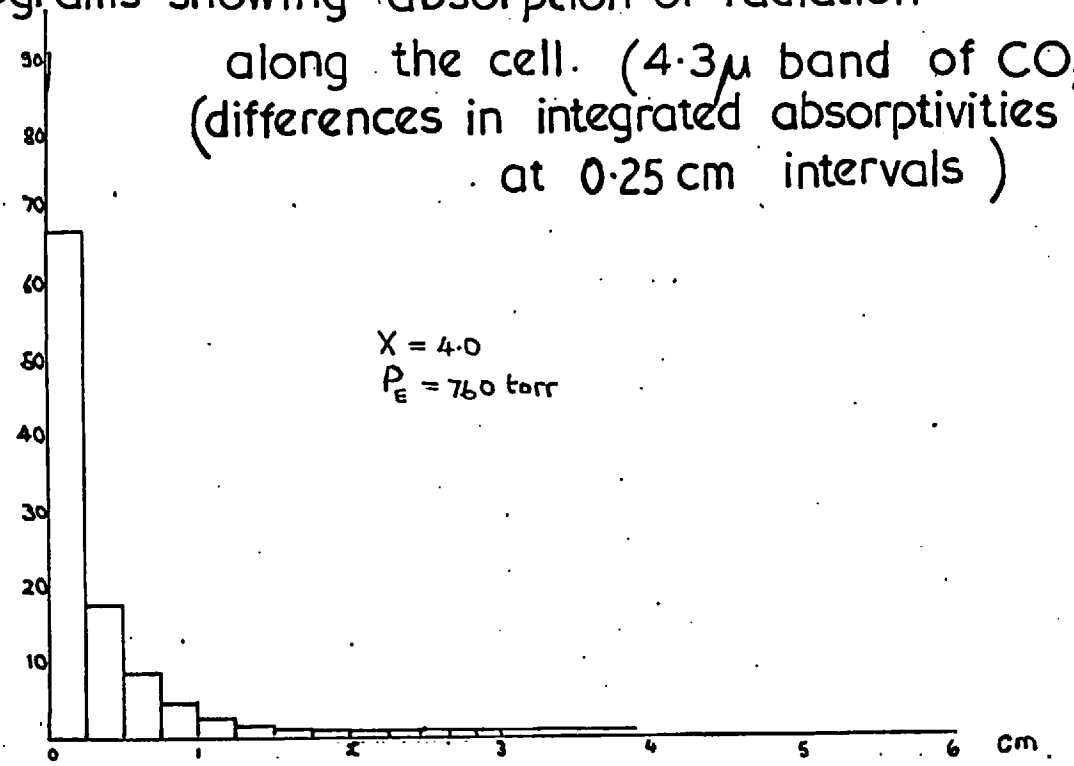

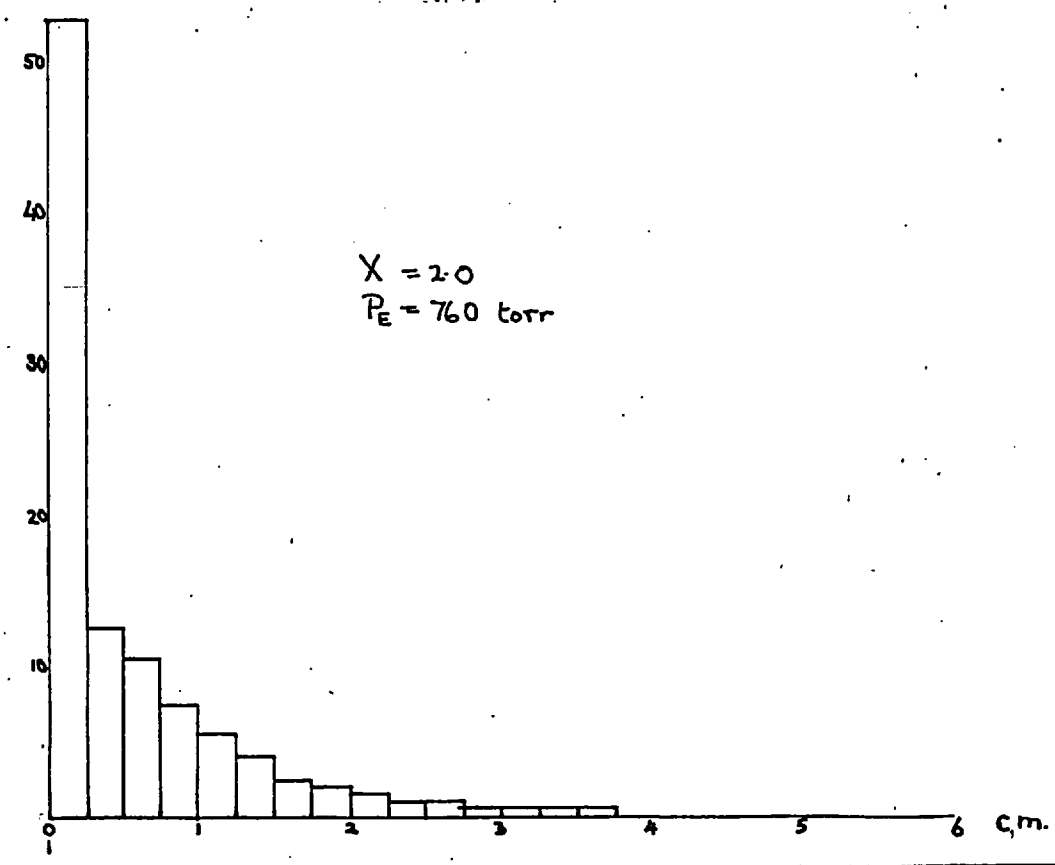

FIG. 7

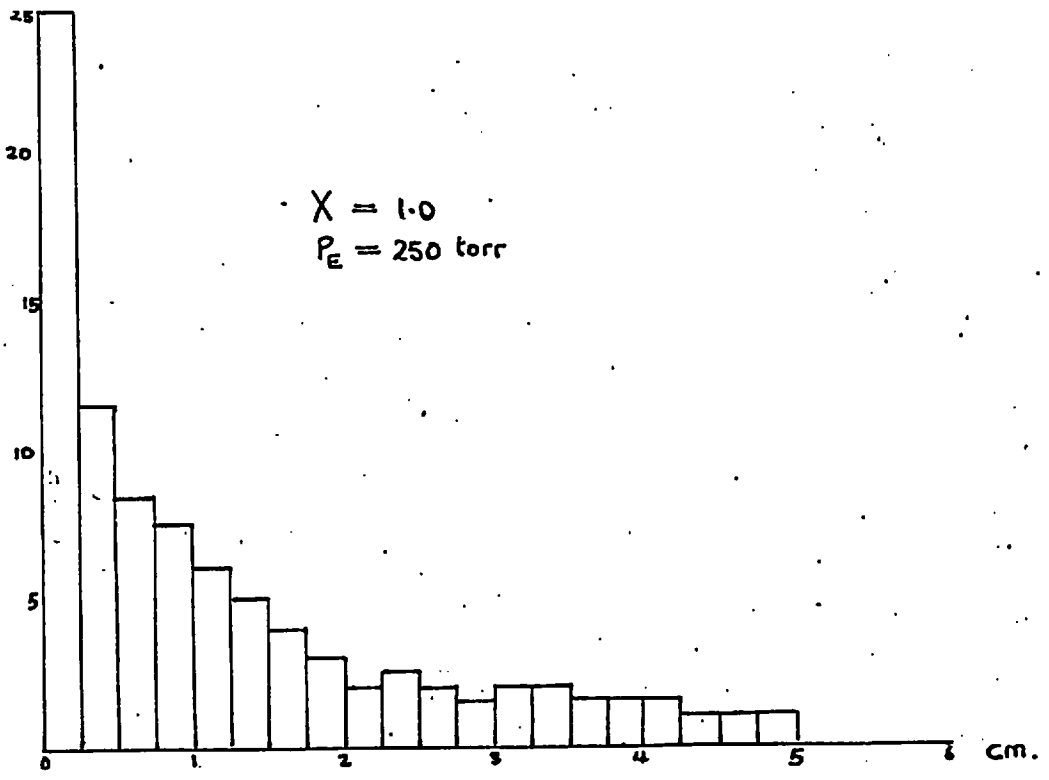
25
20
15
10
5
0
1
2
3
4
5
6
cm.
X = 1·0
P_E = 250 torr

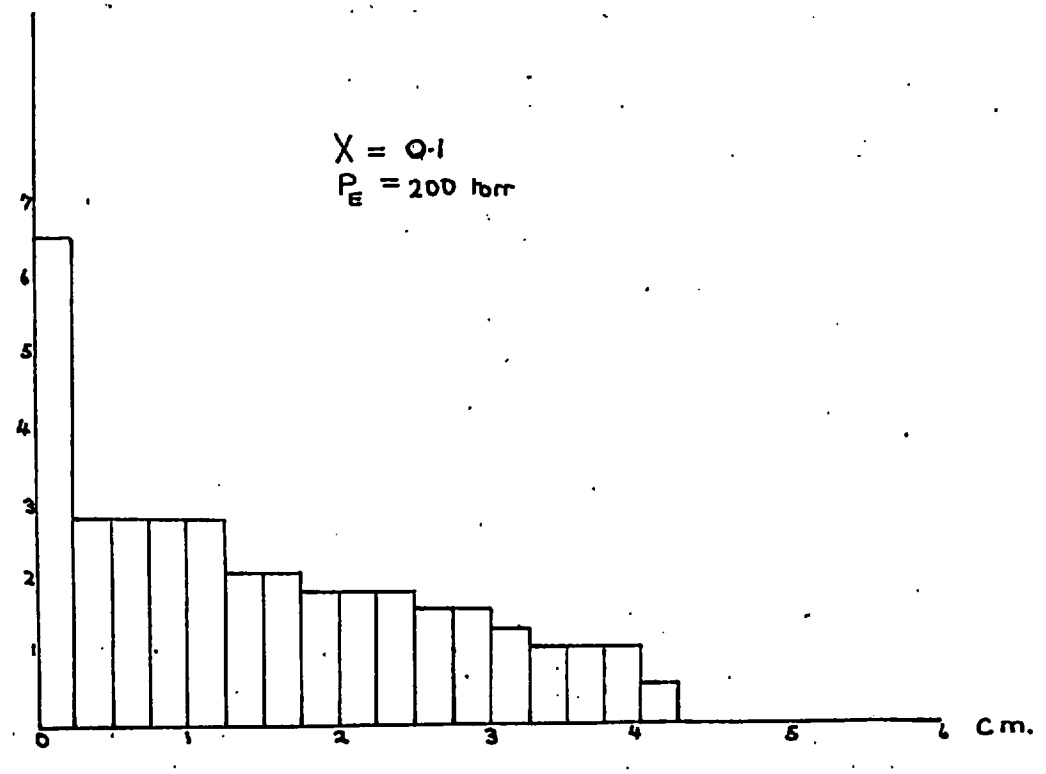
7
6
5
4
3
2
1
0
1
2
3
4
5
6
cm.
X = 0·1
P_E = 200 torr

FIG 8

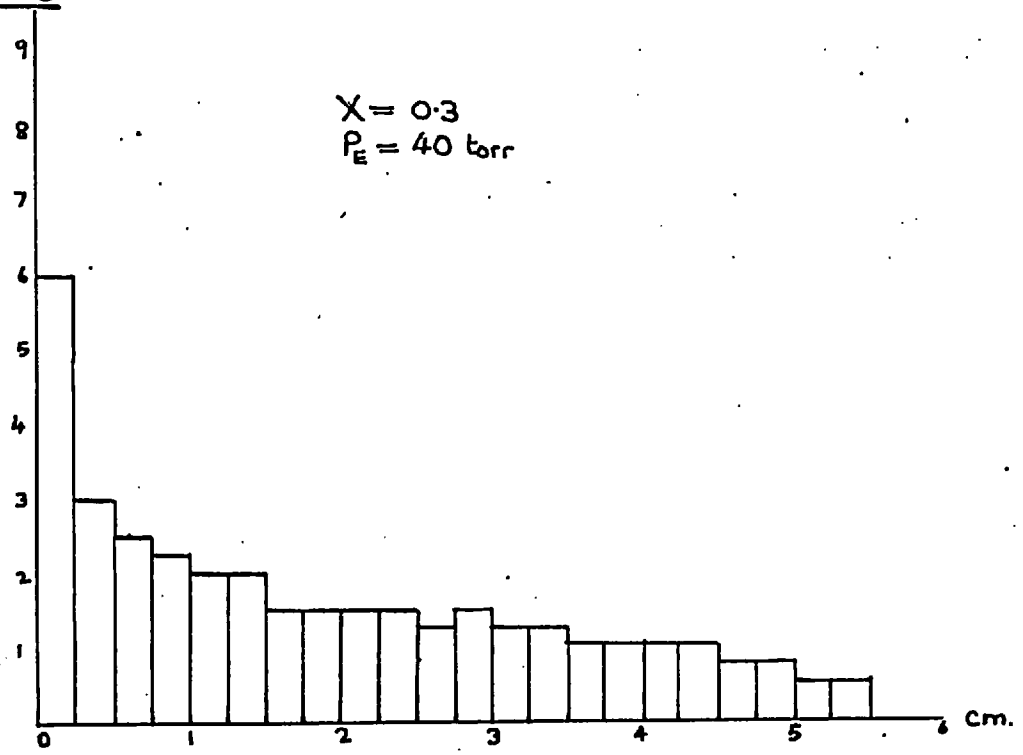
X = 0·3
P_E = 40 torr
9
8
7
6
5
4
3
2
1
0
1
2
3
4
5
6
cm.

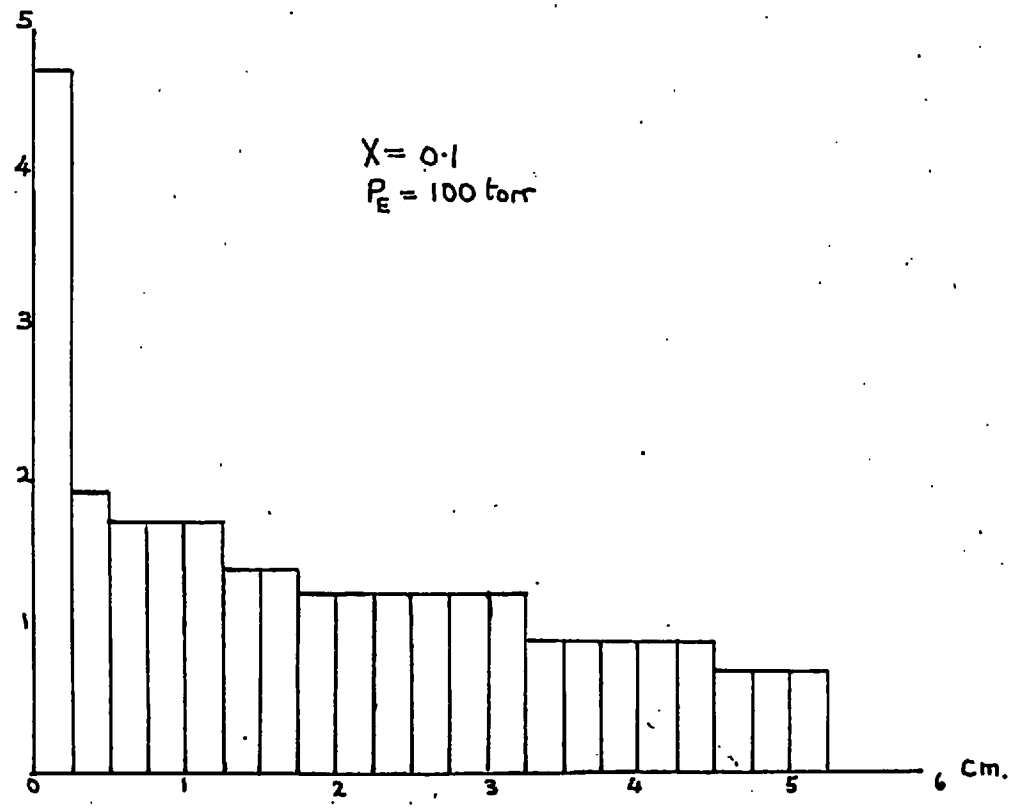
X = 0·1
P_E = 100 torr
5
4
3
2
1
0
1
2
3
4
5
6
cm.

FIG 9 Histograms showing absorption of radiation along length of cell (15μ CO_2 band)

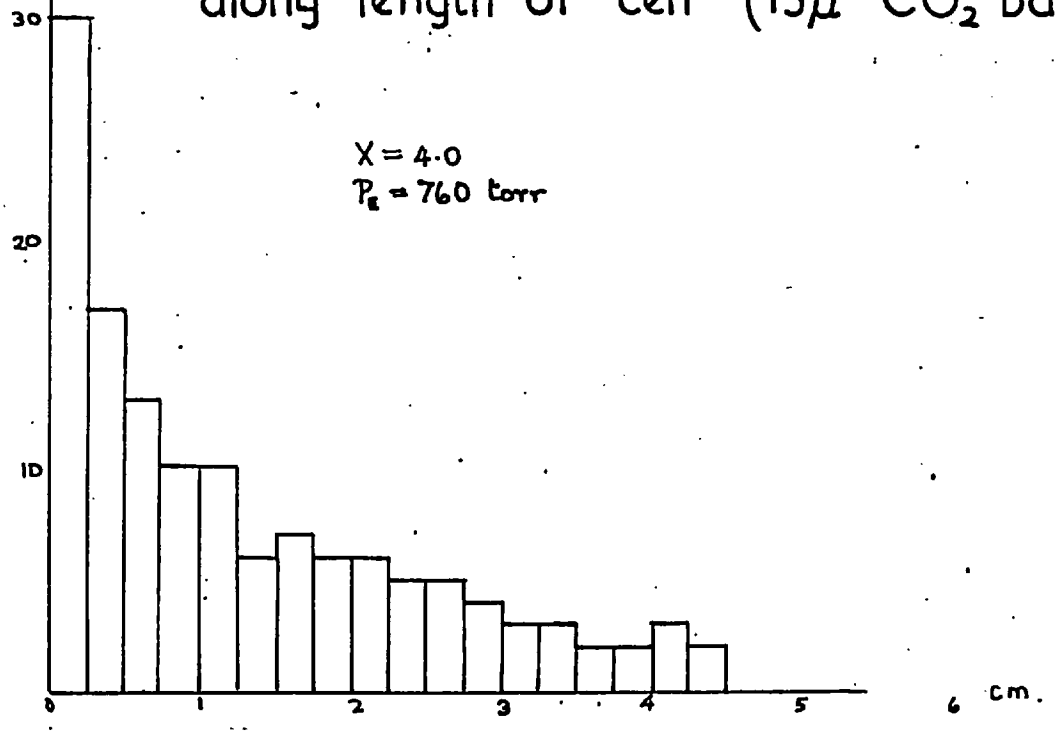

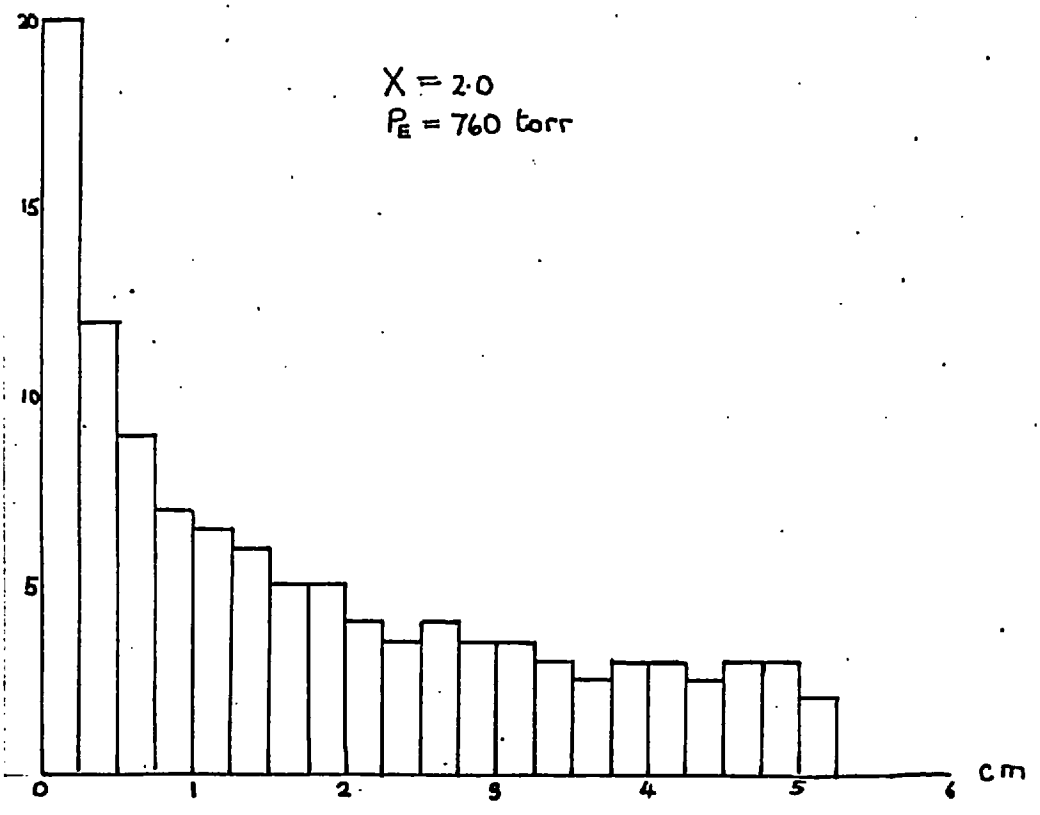

FIG 10

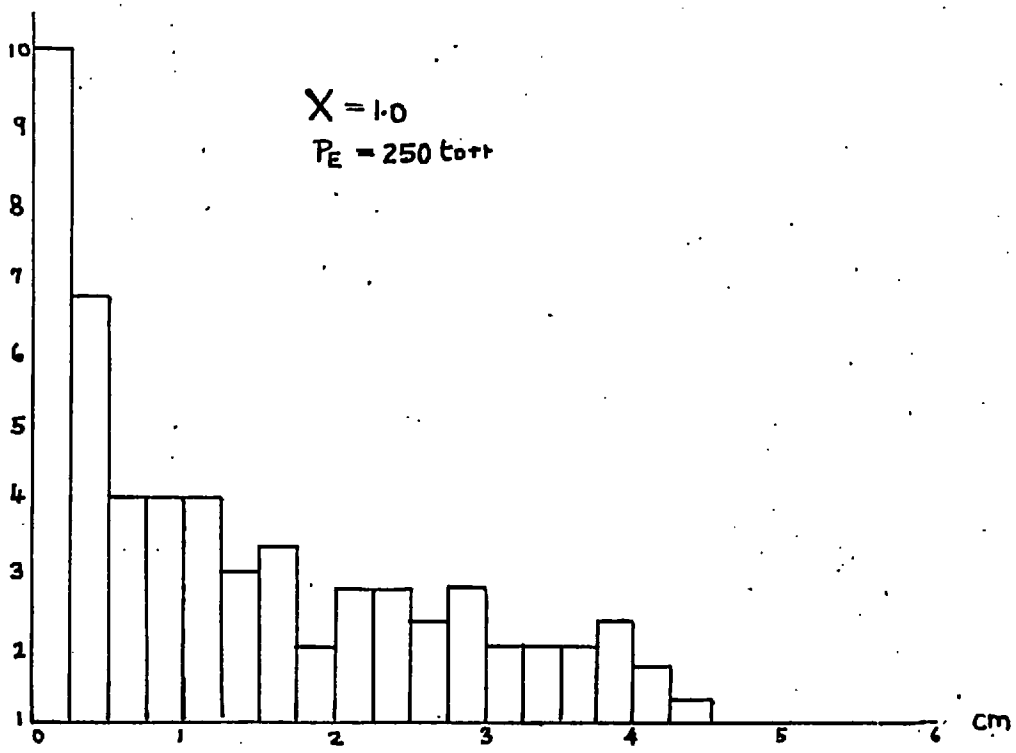
X = 1·0
P_E = 250 torr
10
9
8
7
6
5
4
3
2
1
0
1
2
3
4
5
6
cm

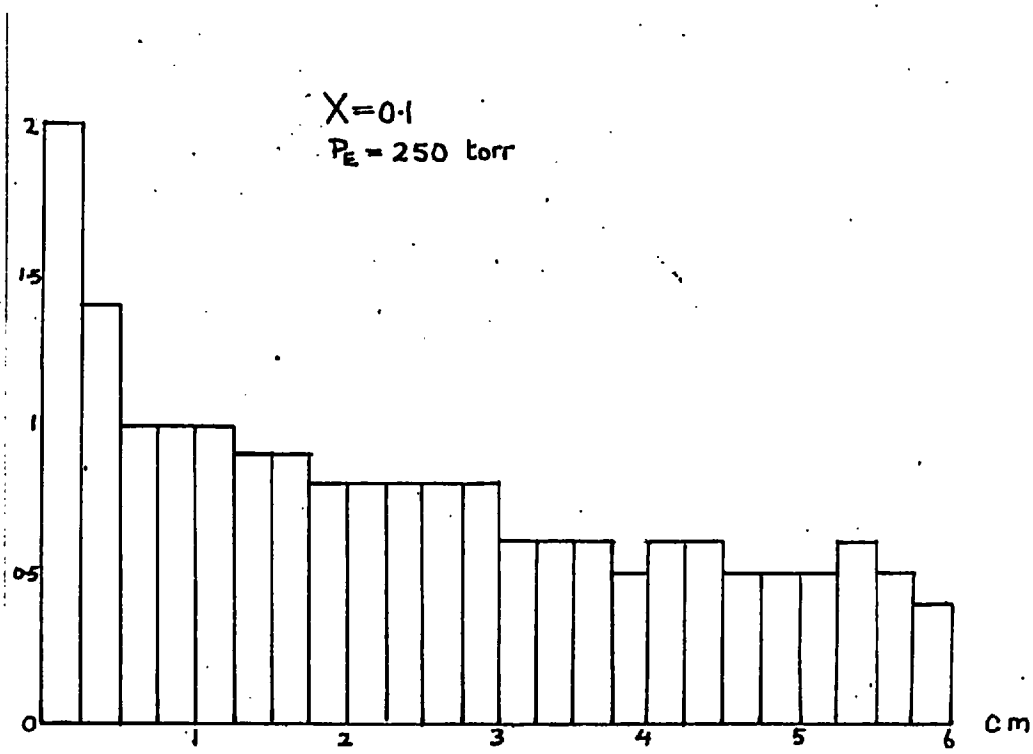
X=0·1
P_E = 250 torr
2
1·5
1
0·5
0
1
2
3
4
5
6
cm.

FIG. 11.

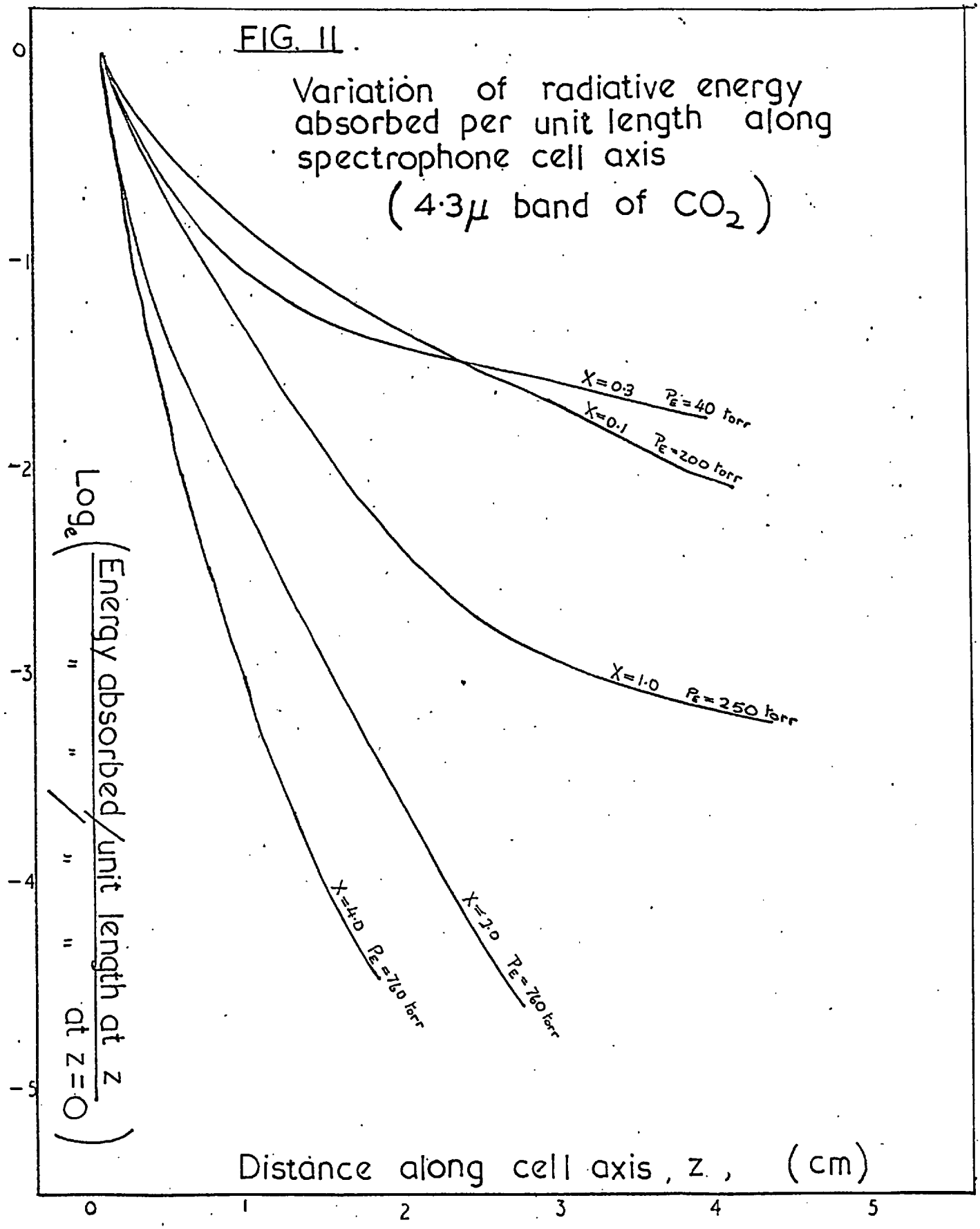
Variation of radiative energy absorbed per unit length along spectrophone cell axis
(4·3μ band of CO_2)
X=0·3 P_E=40 torr
X=0·1 P_E=200 torr
X=1·0 P_E=250 torr
X=4·0 P_E=760 torr
X=2·0 P_E=760 torr
$\log_e\left(\frac{\text{Energy absorbed/unit length at } z}{\text{" " " " at } z=0}\right)$
Distance along cell axis, z, (cm)
0
-1
-2
-3
-4
-5
0
1
2
3
4
5

FIG 12

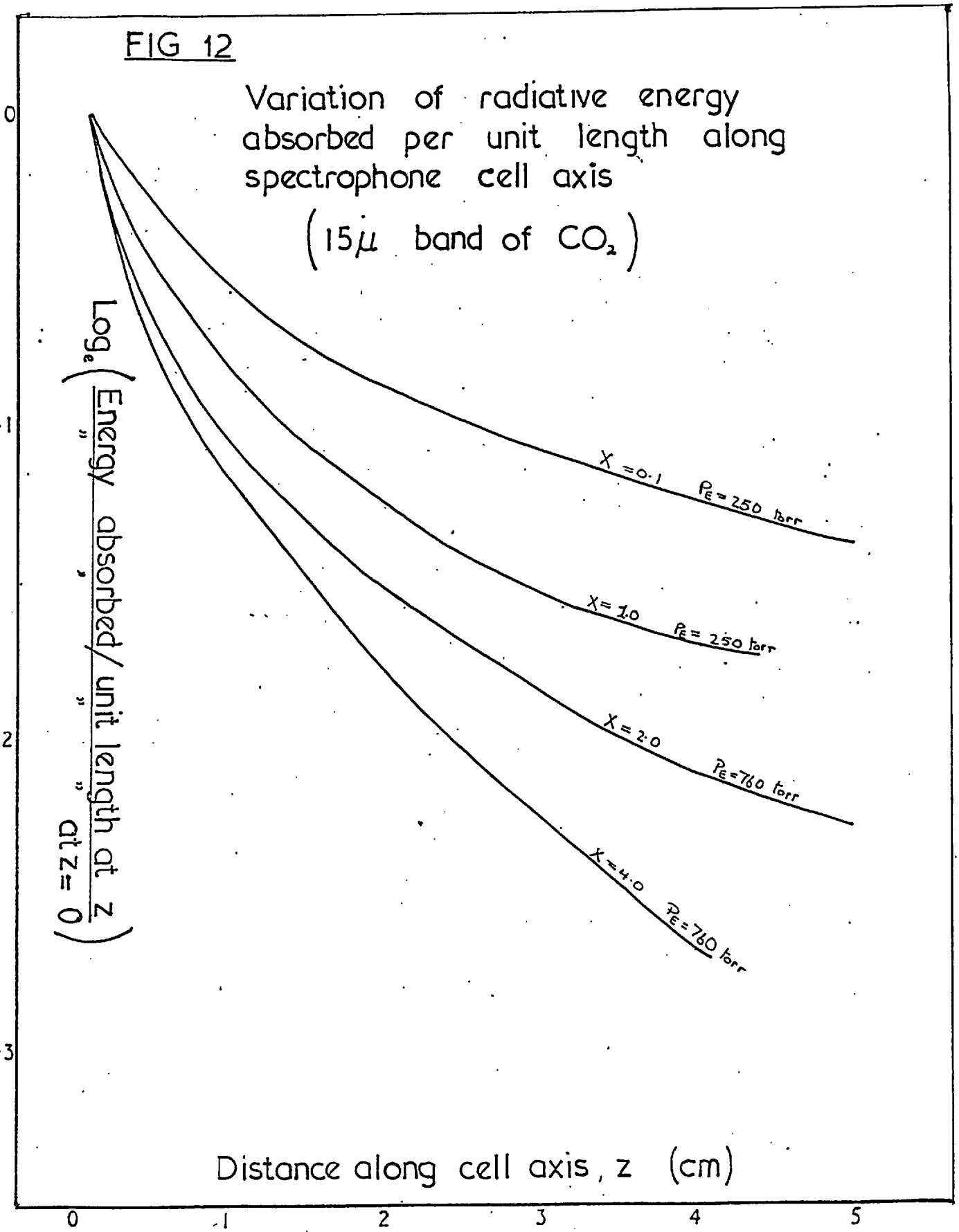
Variation of radiative energy absorbed per unit length along spectrophone cell axis
(15μ band of CO_2)
$\log_e\left(\frac{\text{Energy absorbed/unit length at } z}{\text{" " " at } z=0}\right)$
X = 0·1 P_E = 250 torr
X = 1·0 P_E = 250 torr
X = 2·0 P_E = 760 torr
X = 4·0 P_E = 760 torr
0
-1
-2
-3
Distance along cell axis, z (cm)
0
1
2
3
4
5

These are given in Table 3.1 This will at least allow an estimation of the importance of the fall off of energy absorption (and hence translational heat input along the spectrophone axis without undue mathematical difficulties.

For nitrous oxide, the 4.5 μ band should give very similar values of to the 4.3 μ CO_2 band. The 7.8 μ and 16 μ bands which are both comparatively weak should have smaller values of α than given in Table 3.1 for the 15 μ CO_2 band.

TABLE 3.1

Values of for varying spectrophone conditions

	Optical density (atmos. cm.)	Equivalent Pressure (torr)	α
4.3 μ CO_2 band	4.0	760	3.3
	2.0	760	2.1
	1.0	250	1.1
	0.3	40	0.5
	0.1	100	0.4
15 μ CO_2 band	4.0	760	0.7
	2.0	760	0.4
	1.0	250	0.38
	0.1	250	0.3

(vi) The heat input/cc./sec in the spectrophone

Equation 10 gives the steady state population of excited molecules in the spectrophone, for a gas with a single two-state vibration, with the various parameters defined by equations 9 and 8a. The Einstein coefficients are as defined in section (iii), and the factor f(z) is to be written as $e^{-\alpha z}$ as discussed in section (v).

The net translational energy input to the gas/cc./sec will be

$$H = h\nu(N_1 f_{10} - N_0 f_{01})$$
$$= h\nu(f_{10} + f_{01}) \left[N_1 - N \frac{f_{01}}{f_{10} + f_{01}} \right] \qquad 3.17$$

Substituting from (10) yields

$$H = N h \nu (f_{01} + f_{10}) \left[\frac{D}{C} - \frac{D}{2C} \frac{\eta(\delta - \eta)}{(1 + \frac{\omega}{C})^2} - \frac{f_{01}}{f_{10} + f_{01}} \right]$$

$$+ N h \nu (f_{01} + f_{10}) \frac{D}{C} \frac{(\delta - \eta) \cos(\omega t - \chi)}{\left[1 + (\frac{\omega}{C})^2 \right]^{1/2}} \qquad 3.18$$

It is useful at this stage to evaluate the order of magnitude of the two parameters in equation (18) which have not previously been considered, namely, the radiation densities $\rho_1(\nu)$ and $\rho_0(\nu)$ assumed constant over the width of the band. These will now be estimated numerically. $\rho_0(\nu)$ will be mainly due to the radiation from the surroundings at 300°K; $\rho_1(\nu)$ will be radiation from the Nernst filament source.

a) Assuming the cell cavity to contain blackbody radiation at 300°K. Then

$$\rho_o(\nu) = 8\pi h \bar{\nu}^3 \left[\exp \frac{(h\nu)}{(kT)} - 1 \right]^{-1} \qquad 3.19$$

For a band at 4μ

$$\rho_o(\nu) \simeq 2 \times 10^{-18} \text{ erg. cm.}^3 \text{ sec.}$$

For a band at 15

$$\rho_o(\nu) \simeq 2 \times 10^{-20} \text{ erg. cm.}^3 \text{ sec.}$$

b) Assuming the Nernst filament is a blackbody radiator at 2000°K.

The energy emitted/unit area of surface/sec into a solid angle 2π in the wave number range $\bar{\nu} \rightarrow \bar{\nu} + d\bar{\nu}$ by a black body at a temperature T°K is given by Planck's law as

$$E_{\bar{\nu}}\, d\bar{\nu} = \frac{2\pi hc^2 \bar{\nu}^3\, d\bar{\nu}}{\left[\exp. \left({}^{hc\bar{\nu}}/_{kT} \right) - 1 \right]} \qquad 3.20$$

Thus the energy density $\rho_1(\bar{\nu})$ just inside the window due to modulated infra-red radiation from the Nernst filament will be

$$\rho_1(\nu) = \frac{\Omega}{2\pi} \frac{a}{S} \frac{E_{\bar{\nu}}}{c} \cdot \frac{1}{2} \text{ (erg. cm.}^{-3} \text{cm.)} \qquad 3.21$$

where

Ω = solid angle subtended at the filament by the optical mirror system.

a = effective area of Nernst filament

S = area of infra-red window

c = velocity of light

1 = fractional loss factor.

Taking the values for the constants from the present experiment (this should be a typical set up), estimated values for $\rho_1(\nu)$ are:- for a band at 15μ

$$\rho_1(\bar{\nu}) \simeq 10^{-9} \text{ erg. cm.}^{-3}\text{cm.}$$

or $$\rho_1(\nu) \simeq 3 \times 10^{-20} \text{ erg. cm.}^{-3}\text{sec.}$$

For a band at 4μ

$$\rho_1(\bar{\nu}) \simeq 5 \times 10^{-9} \text{ erg. cm.}^{-3}\text{cm. or}$$

$$\rho_1(\nu) \simeq 2 \times 10^{-19} \text{ erg. cm.}^{-3}\text{sec.}$$

We note from this that the induced transition factors $B_{01}\ \rho_0(\nu)$, $B_{10}\ \rho_0(\nu)$, $B_{01}\ \rho_1(\nu)$, $B_{10}\ \rho_1(\nu)$ are all generally smaller than the spontaneous transition factor A for all practical frequencies. This is to be expected if saturation of the excited state never occurs.

Recalling that the expression for C in equation (18) is given by (equation 8a):-

$$C = f_{10} + f_{01} + A + (B_{10} + B_{01})\, f(z).\ \rho_0(\nu)$$

we now assume that

$$(f_{10} + f_{01}) \gg A + (B_{10} + B_{01})\, f(z).\ \rho_0(\nu)$$

Since $(f_{10} + f_{01})$ is the inverse of the relaxation time for the two-state model assumed, this assumption is equivalent to assuming that the collisional lifetimes of the excited molecules are much smaller than the radiational lifetimes. This assumption should be valid for all the

bands studied in the present work, but in any case, the validity of equation (22) as it stands is doubtful in cases where this assumption cannot be made. Thus, providing that all re-radiated energy escapes from the gas (22) should hold for all cases (providing that $\frac{\omega\eta}{C} \ll 1$). In actual cases where the collisional de-excitation is inefficient compared with re-radiation however, self-absorption will usually render equation (22) invalid. This arises from the highly unsaturated nature of the N_1 population for all practical radiation intensities. Consider a highly absorbing gas whose collisional lifetime is longer (?) than its radiational lifetime. Although most of the incident absorbed energy will be re-radiated, provided that the gas density is not extremely low - most of this energy will be re-absorbed by neighbouring molecules. Thus a quantum of radiation may be re-radiated and re-absorbed several times until either a) it escapes to the walls of the chamber, or b) it is finally converted into translational energy through an inelastic collision. The proportions of the absorbed energy going direct to the walls and absorbed translationally by the gas will depend upon gas absorbitivity, density, spectrophone size, etc. In the extreme case where all the energy finds its way by process b) into the gas and not by a) to the walls; then equation (10) can be immediately seen not to hold. For the energy transfer rate from vibrational energy to translational energy must depend essentially on the collisional transition probabilities f_{01} and f_{10}, not on C as given by equation (10), the radiational transitions merely acting in a cycle to keep the energy available for the eventual collisional transition. Thus a given N_1 population will decay

not as given by (10) but by simple vibrational relaxation as if $f_{01} + f_{10} > A + \rho B$ and not as is actually the case, viz. $f_{01} + f_{10} < A + \rho B$. In order to correct the analysis so as to apply to the case now considered, it would be necessary to write the radiation density as $\rho(\nu) + \rho(\nu)^*$ where $\rho(\nu)^*$ is the contribution due to scattered radiation. Although neglected in the above treatment, in this case $\rho(\nu)^*$ will be highly significant for it will persist after the cut-off of $\rho(\nu)$ maintaining the N_1 population until all the energy has gone to translation. Such an analysis is relevant in the case of carbon monoxide where the relaxation time has been found to be extremely long.

Returning to equation (18), making the assumption

$$C \doteq f_{01} + f_{10} = \frac{1}{\tau}$$

and noting that since for all relevant vibrations $f_{10} \gg f_{01}$, then $C \gg D$, it follows from (18) that

$$H = N h\nu \left[\rho_0(\nu) B_{01} f(z) - \tfrac{1}{2} \left(\rho_1(\nu) B_{01} f(z) \right)^2 \frac{\tau}{(1+\omega\tau)^2} \right]$$

$$+ N h\nu \rho_1(\nu) B_{01} f(z) \tau \left[\frac{1}{\tau} - (1+g) \left(f_{01} + \rho_0(\nu) B_{01} f(z) \right) \right] \frac{\cos(\omega t - \gamma)}{\sqrt{1+(\omega\tau)^2}}$$

3.18a

And as a further approximation it is generally permissible to neglect the second constant and harmonic terms, as being small compared with the first. Giving

$$H \simeq N h\nu \left[\rho_o(\nu) B_{01} f(z) + \frac{\rho_1(\nu) B_{01} f(z) \cos(\omega t - \gamma)}{(1 + (\omega\tau)^2)^{\frac{1}{2}}} \right] \qquad 3.22$$

where $\tan \gamma = \dfrac{\omega}{f_{01} + f_{10}} = \omega\tau$

and $f(z) = e^{-\alpha z}$.

It should be noted that since the unmodulated radiation density $\rho_o(\nu)$ comes mostly from equilibrium black-body radiation inside the cell, it will not be attenuated down the length of the cell by the factor $e^{-\alpha z}$. However, equation (22) above is used in the subsequent analysis of the spectrophone. The adjustment to the constant terms is easily performed and no correction is necessary to the more important harmonic terms.

(vii) Heat input for a two-stage relaxation

In the previous sections it has been assumed that the gas in the spectrophone has only one vibration, or that only one vibration was concerned in the optic-acoustic process. This should be true for the 15 μ CO_2 band and the bending mode of N_2O. These will decay straight to translation and the above equations will apply. However, as discussed in Chapter 1, the asymmetric value modes probably de-excite through a complex process.

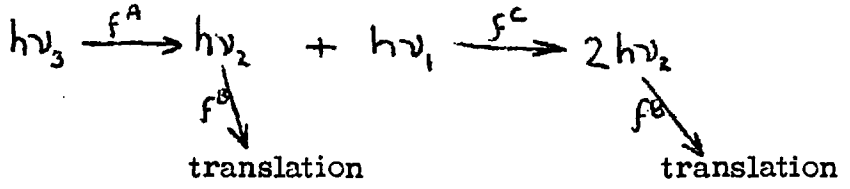

In this process, the rate constant f^C should be very large compared with f^A and f^B because of the near resonant exchange. Thus effectively the de-excitation may be described as

$$h\nu_3 \xrightarrow{f^A} 3h\nu_2 \xrightarrow{f^B} \text{kinetic energy}$$

Although some energy is released to translation during the first stage of the process, much more is released in the second stage so that to a good approximation the ν_3 vibration only exchanges energy with translation via the bending modes.

For such a decay equation (10) and hence equation (22) is not valid, and expressions for the excited state populations of both the ν_3 and ν_2 vibrations must be obtained.

Defining

f^A = rate constant (number of de-excitations per molecule per sec.) for collisional de-excitation of $\nu_3 \rightarrow 3\nu_2$.

f^B_{10} = rate constant for collisional de-excitation of $\nu_2 \rightarrow$ translation.

f^B_{01} = rate constant (no. of excitations per molecule per sec.) for collisional excitation of ν_2 from translation.

Rate equations for the asymmetric valence and bending modes may be written as follows:

$$\frac{dN_3}{dt} = -f^A N_3 - (A + B\rho)N_3 + B\rho(N - N_3)$$

$$= -N_3(f^A + A + 2B\rho) + B\rho N$$

3.23

$$\frac{dN_2}{dt} = 3f^A N_3 - f_{10}^B N_2 + f_{01}^B (N - N_2)$$

$$= -\left(f_{10}^B + f_{01}^B\right) N_2 + 3f^A N_3 - f_{01}^B N \qquad 3.24$$

Here ν_3 may safely be regarded as a two-state vibration and N_3 thus represent the number of molecules in the first excited state of the vibration per unit volume. The interpretation of N_2, however, is more difficult. ν_2 is a doubly degenerate vibration, and unlike a direct optic-acoustic excitation of the mode (for which the analysis of section (i) would apply) the present energy transfer process makes it probable that both degenerate vibrations will be excited, or in other words, that one molecule will acquire a vibrational energy of 2 $h\nu_2$. However, it is far more probable for the vibrational energy to reach translation by two successive de-excitations of $h\nu_2$ rather than by one of $2h\nu_2$, and the transition probability for a decay $2h\nu_2 \rightarrow h\nu_2$ should not be largely different from that of $h\nu_2 \rightarrow$ ground. Furthermore, it seems likely that the vibrational energy in the ν_2 vibration is rapidly redistributed amongst the molecules by vibration-vibration energy transfer before vibration-translation exchange occurs, reducing the number of molecules with $2h\nu_2$ energy to its normal small proportion. Therefore, to a good degree of approximation N_2 may be written as the 'effective' or 'equivalent' number of excited molecules with vibrational energy $h\nu_2$, or the number of ν_2 vibrational quanta per unit volume, and f_{01}^B and f_{10}^B refer to collisional transitions between the ground and first excited states of the ν_2 vibration.

Another factor which has been neglected is the possible difference in probability of transitions between the valence and bending modes of the same molecule, and transitions involving the bending modes of the collision partner. Finally the excitation of the ν_3 mode collisionally by the process $2\nu_2 \longrightarrow \nu_1 + \nu_2 \longrightarrow \nu_3$ or $3\nu_2 \longrightarrow \nu_3$, and the spontaneous radiational de-excitation of ν_2 have both been ignored as small compared with other terms. As before N refers to the total number of molecules/cc. The incident radiation is taken as $\rho_0 + \rho_1 e^{i\omega t}$.

Proceeding to the solution of equation (23), this may be solved exactly as previously, but here we shall impose a harmonic solution.

Let $N_3 = \bar{N}_3 + \Delta N_3 e^{i\omega t}$.

Therefore

$$i\omega \Delta N_3 e^{i\omega t} + \left\{ \left(f^A + A + 2B\rho_0 \right) + 2B\rho_1 e^{i\omega t} \right\} \left(\bar{N}_3 + \Delta N_3 e^{i\omega t} \right) \qquad 3.23a$$
$$= B\rho_0 N + B\rho_1 e^{i\omega t} N$$

Since $2B\rho_1$ should be considerably smaller than $\left(f^A + A + 2B\rho_0 \right)$ and (see discussion, page) $\Delta N_3 < \bar{N}_3$ we may neglect the term in $e^{2i\omega t}$ giving

$$i\omega \Delta N_3 e^{i\omega t} + \bar{N}_3 \left(f^A + A + 2B\rho_0 \right) + \bar{N}_3 2B\rho_1 e^{i\omega t}$$
$$+ \left(f^A + A + 2B\rho_0 \right) \Delta N_3 e^{i\omega t} = B\rho_0 N + B\rho_1 N e^{i\omega t}.$$

Equating coefficients of $e^{n i\omega t}$ $\quad n = 0, 1$

$$\bar{N}_3 = \frac{B\rho_0 N}{(f^A + A + 2B\rho_0)}$$

3.25a

$$\Delta N_3 = \frac{NB\rho_1 \left[1 - \frac{2B\rho_0}{(f^A + A + 2B\rho_0)}\right]}{\left[(f^A + A + 2B\rho_0) + i\omega\right]}$$

3.25b

Considering now equation (24)

$$\frac{dN_2}{dt} = -\left(f_{10}^B + f_{01}^B\right) N_2 + 3f^A N_3 + f_{01}^B N.$$

3.24

Substituting for N_3

$$N_3 = \bar{N}_3 + \Delta N_3 e^{i\omega t}$$

3.23a

$$N_2 = \bar{N}_2 + \Delta N_2 e^{i\omega t}$$

3.24a

$$i\omega \Delta N_2 e^{i\omega t} + \left(f_{10}^B + f_{01}^B\right)\left(\bar{N}_2 + \Delta N_2 e^{i\omega t}\right) =$$
$$= 3f^A\left(\bar{N}_3 + \Delta N_3 e^{i\omega t}\right) + f_{01}^B N.$$

$$i\omega \Delta N_2 e^{i\omega t} + \left(f_{10}^B + f_{01}^B\right)\bar{N}_2 + \left(f_{01}^B + f_{10}^B\right)\Delta N_2 e^{i\omega t}$$
$$= 3f^A \Delta N_3 e^{i\omega t} + f_{01}^B N + 3f^A \bar{N}_3$$

Equating coefficients of $e^{n_1 i\omega t}$ $n_1 = 0, 1$.

$$\bar{N}_2 = \frac{3f^A N_3 + f_{01}^B N}{\left(f_{01}^B + f_{10}^B\right)} \qquad 3.26a$$

$$\Delta N_2 = \frac{3f^A \Delta N_3}{\left[\left(f_{10}^B + f_{01}^B\right) + i\omega\right]} \qquad 3.26b$$

Or

$$\bar{N}_2 = \frac{N\left[f_{01}^B + \dfrac{3f^A B\rho_0}{(f^A + A + 2B\rho_0)}\right]}{\left(f_{01}^B + f_{10}^B\right)} \qquad 3.27a$$

$$\Delta N_2 = \frac{3 f^A N B \rho_1 \left[1 - \frac{2B\rho_0}{(f^A + A + 2B\rho_0)}\right]}{\left[(f^A + A + 2B\rho_0) + i\omega\right]\left[(f_{10}^B + f_{01}^B) + i\omega\right]} \qquad 3.27b$$

Now the translational energy entering the gas per sec will be approximately

$$H = h\nu_2 \left[f_{10}^B N_2 - f_{01}^B N_0\right]$$

$$H = h\nu_2 \left[(f_{10}^B + f_{01}^B) N_2 - f_{01}^B N\right]$$

$$H = 3h\nu_2 N \left\{\frac{f^A B \rho_0}{(f^A + A + 2B\rho_0)}\right\} +$$

$$+ 3h\nu_2 N \left\{\frac{(f_{01}^B + f_{10}^B) f^A B \rho_1 \left[1 - \frac{2B\rho_0}{(f^A + A + 2B\rho_0)}\right]}{\left[(f^A + A + 2B\rho_0) + i\omega\right]\left[(f_{01}^B + f_{10}^B) + i\omega\right]}\right\} e^{i\omega t}$$

3.28

$$H = 3h\nu_2 f^A B\left[\frac{\rho_0}{(f^A + A + 2B\rho_0)} + \frac{(f_{10}^B + f_{01}^B)\rho_1\left[1 - \frac{2B\rho_0}{(f^A + A + 2B\rho_0)}\right] e^{i(\omega t - \gamma_1 - \gamma_2)}}{\sqrt{\left[(f^A + A + 2B\rho_0)^2 + \omega^2\right]\left[(f_{01}^B + f_{10}^B)^2 + \omega^2\right]}}\right]$$

3.29

Where here

$$\tan\gamma_1 = \frac{\omega}{(f^A + A + 2B\rho_0)} \quad , \quad \tan\gamma_2 = \frac{\omega}{(f_{10}^B + f_{01}^B)}$$

3.29a

Approximately since $f^A \gg A + 2B\rho_0$ and $f_{10}^B \gg f_{01}^B$.

$$\tan\gamma_1 \simeq \frac{\omega}{f^A} = \omega\tau_3 \qquad \tan\gamma_2 \simeq \frac{\omega}{f_{10}^B} \simeq \omega\tau_2$$

where τ_2 and τ_3 are relaxation times associated with the collisional de-excitation of the ν_2 and ν_3 vibrations.

Thus we see that the phase lag of the heat energy input behind the incident radiation consists of two parts arising from the two stages of the process. If the de-excitation of ν_3 is a much slower process than that of ν_2, then the effective relaxation time will be τ_3; conversely if the de-excitation time of ν_2 is the rate determining step, then the effective relaxation time will be τ_2.

If both γ_1 and γ_2 are significant, then

$$\gamma = \gamma_1 + \gamma_2 \qquad = \tan^{-1}\omega\tau_2 + \tan^{-1}\omega\tau_3 \qquad 3.30$$

and

$$\tan\gamma \quad = \tan(\gamma_1+\gamma_2) = \frac{\omega(\tau_2+\tau_3)}{(1-\omega^2\tau_2\tau_3)} \qquad 3.31$$

Thus $\tan\gamma = \infty$ or $\gamma = \frac{\pi}{2}$ when $\omega = \frac{1}{\sqrt{\tau_1\tau_2}}$

Experimentally, it should be possible to distinguish a double relaxation process obeying equation (31) from a single one in which $\tan\gamma = \omega\tau$ from the pressure dependence of $\tan\gamma$. This is considered again in Chapter 5, in discussing the experimental results.

C Solution of the Equation of heat conduction in the spectrophone for an incompressible fluid

As stated in Part A, if the gas in the spectrophone is considered incompressible the equation of heat conduction becomes

$$\frac{1}{\beta}\frac{\partial v}{\partial t} = \nabla^2 v + \frac{H}{K} \qquad 3.3$$

This is to be solved for the system outlined in Part A, section (i). Therefore the equation may be written in cylindrical polar coordinates as

$$\frac{\partial^2 v}{\partial r^2} + \frac{1}{r}\frac{\partial v}{\partial r} + \frac{\partial^2 v}{\partial z^2} - \frac{1}{\beta}\frac{\partial v}{\partial t} = -\left[Q_0 + Q_1 \cos(\omega t - \gamma)\right] e^{-\alpha z} \qquad 3.32$$

where $Q_0 = \frac{H_0}{K}$ and $Q_1 = \frac{H_1}{K}$ and H_0 and H_1 correspond to the constant and time varying terms of the heat input/cc./sec as derived in the last section (equation 22) just inside the window.

The boundary conditions are

$v = 0$ at $t = 0$ at all points in the spectrophone

$v = 0$ at $r = a$ and finite when $r = 0$

$v = 0$ $\left.\begin{matrix} z = 0 \\ z = 1 \end{matrix}\right\}$ for all time

Applying a Laplace transform to (32) to eliminate the time variable.

Writing $$v' = \int_0^\infty v e^{-yt} dt$$

(32) becomes

$$\frac{\partial^2 v'}{\partial r^2} + \frac{1}{r}\frac{\partial v'}{\partial r} + \frac{\partial^2 v'}{\partial z^2} - \frac{y}{\beta} v' = \left[-\frac{Q_0}{y} - \int_0^\infty Q_1 \cos(\omega t - \gamma) e^{-yt} dt\right] e^{-\alpha z}$$

Integrating by parts

$$\int_0^\infty Q_1 \cos(\omega t - \gamma) e^{-yt} dt = Q_1 \left[\frac{y\cos\gamma + \omega \sin\gamma}{(y^2 + \omega^2)}\right]$$

Giving

$$\frac{\partial^2 v'}{\partial r^2} + \frac{1}{r}\frac{\partial v'}{\partial r} + \frac{\partial^2 v'}{\partial z^2} - \frac{y v'}{\beta} = -\left\{\frac{Q_0}{y} + Q_1\left[\frac{y\cos\gamma + \omega\sin\gamma}{(y^2+\omega^2)}\right]\right\} e^{-\alpha z} \qquad 3.33$$

The boundary conditions are now

$v' = 0$ r = a and finite at r = 0

$v' = 0$ $\begin{cases} z = 0 \\ z = 1 \end{cases}$

Now apply a finite Fourier sine transform for the interval $0 \leqslant z \leqslant \ell$.

Writing

$$v'' = \int_0^{\ell} v' \sin\frac{m\pi}{\ell} z\, dz$$

(33) becomes

$$\frac{\partial^2 v''}{\partial r^2} + \frac{1}{r}\frac{\partial v''}{\partial r} + \left(-\frac{m^2\pi^2}{\ell^2} - \frac{y}{\beta}\right)v'' = -Q\int_0^{\ell} e^{-\alpha z}\sin\frac{m\pi}{\ell} z\, dz.$$

where $Q = \left[\frac{Q_0}{y} + Q_1\left(\frac{y\cos\gamma + \omega\sin\gamma}{y^2+\omega^2}\right)\right]$

Integrating by parts.

$$\int_0^{\ell} e^{-\alpha z}\sin\frac{m\pi}{\ell} z\, dz = \frac{m\pi}{\ell}\cdot\frac{1}{\left(\alpha^2 + \left(\frac{m\pi}{\ell}\right)^2\right)}\left[1 - (-1)^m e^{-\alpha\ell}\right]$$

Giving

$$\frac{\partial^2 v''}{\partial r^2} + \frac{1}{r}\frac{\partial v''}{\partial r} - \left(\frac{m^2\pi^2}{\rho^2} + \frac{y}{\beta}\right)v'' = -Q\frac{m\pi}{\ell}\left(\alpha^2 + \frac{m^2\pi^2}{\rho^2}\right)^{-1}\left[1 - (-1)^m e^{-\alpha\rho}\right]$$

3.34

With boundary conditions.

$v'' = 0$ at $r = a$, and finite when $r \longrightarrow 0$.

Introducing the following notation

$$\sigma = \frac{m\pi}{\ell}$$

$$q_m^2 = \left[\left(\frac{m\pi}{\ell}\right)^2 + \frac{y}{\beta}\right] \equiv \left(\sigma^2 + \frac{y}{\beta}\right)$$

$$-B = Q\left(\frac{m\pi}{\ell}\right)\left(\alpha^2 + \left(\frac{m\pi}{\ell}\right)^2\right)^{-1}\left[1 - (-1)^m e^{-\alpha\rho}\right]$$

$$\frac{\partial^2 v''}{\partial r^2} + \frac{1}{r}\frac{\partial^2 v''}{\partial r} - q_m^2 v'' = B$$

Let $u = v'' + \frac{B}{q_m^2}$ and substitute in above we get

$$\frac{\partial^2 u}{\partial r^2} + \frac{1}{r}\frac{\partial u}{\partial r} - q_m^2 u = 0$$

This is Bessel's modified equation of order zero with general solution

$$u = X\ I_0(q_m r) + Y K_0(q_m r)$$

where X and Y are constants.

Since u = finite as r $\rightarrow$ 0 then Y = 0.

Therefore

$$u = X I_0(q_m r)$$

Therefore

$$v'' = X I_0(q_m r) - \frac{B}{q_m^2}$$

Using Boundary condition, r = a , $v'' = 0$

$$X = \frac{B}{q_m^2}\frac{1}{I_0(q_m a)}$$

Therefore $$v'' = \frac{B}{q_m^2}\frac{I_0(q_m r)}{I_0(q_m a)} - \frac{B}{q_m^2} \qquad 3.35$$

Applying the inverse transform equation for the finite Fourier sine transform:-

$$v' = \frac{2}{\ell}\sum_{m=1}^{\infty}\left[\frac{B}{q_m^2}\left(\frac{I_0(q_m r)}{I_0(q_m a)} - 1\right)\right]\sin\frac{m\pi}{\ell}z$$

and applying the Inversion Theorem for Laplace transforms

$$v = \frac{1}{\pi \rho i} \int_{\zeta - i\infty}^{\zeta + i\infty} e^{yt} \sum_{m=1}^{\infty} \left(\frac{B}{q_m^2} \frac{I_0(q_m r)}{I_0(q_m a)} - \frac{B}{q_m^2} \right) \sin \frac{m\pi}{\rho} z \, dy$$

or, more correctly, since the variables must now be considered complex and the functions of the integrand to be functions of the complex variable, write λ (complex variable) for y and $\mu = \left(\sigma^2 + \frac{\lambda}{\beta}\right)^{\frac{1}{2}}$ for q_m.

With this notation and reversing the order of integration and summation we have

$$v = \frac{1}{\rho \pi i} \sum_{m=1}^{\infty} \sin \frac{m\pi}{\rho} z \int_{\zeta - i\infty}^{\zeta + i\infty} e^{\lambda t} \left[\frac{B}{\mu^2} \frac{I_0(\mu r)}{I_0(\mu a)} - \frac{B}{\mu^2} \right] d\lambda \qquad 3.36$$

where ζ is so large that all singularities of the intergrand lie to the left of the line ($\zeta + i\infty$, $\zeta - i\infty$).

The solution of the integral

$$I = \int_{\zeta - i\infty}^{\zeta + i\infty} e^{\lambda t} \frac{B}{\mu^2} \left(\frac{I_0(\mu r)}{I_0(\mu a)} - 1 \right) d\lambda$$

is found by contour integration in the complex plane and the calculus of residues.

Since the integrand of I has only poles and no branch points it is possible to complete the contour by a large circle, of radius R, the line integral along which is zero in the limit as $R \to \infty$ and thus enabling Cauchy's residue theorem to be applied to I.

So $I \to \oint = 2\pi i \sum$ Residues of the poles of the integrand.

We proceed as follows, introducing notation

$$B = \frac{m\pi}{\ell}\left(\alpha^2+\left(\frac{n\pi}{\ell}\right)^2\right)^{-1}\left[(-1)^m e^{-\alpha\ell}-1\right]\left\{\frac{Q_0}{\lambda}+Q_1\left[\frac{\lambda\cos\gamma+\omega\sin\gamma}{\omega^2+\lambda^2}\right]\right\}$$

$$=\frac{\sigma}{\alpha^2+\sigma^2}\left[(-1)^m e^{-\alpha\ell}-1\right]\left[\frac{Q_0}{\lambda}+Q_1\left[\frac{\lambda\cos\gamma+\omega\sin\gamma}{\omega^2+\lambda^2}\right]\right]$$

$$=\frac{G_0}{\lambda}+G_1\left\{\frac{\lambda\cos\gamma+\omega\sin\gamma}{\lambda^2+\omega^2}\right\}$$

where $G_0 = \dfrac{Q_0\sigma}{(\alpha^2+\sigma^2)}\left[(-1)^m e^{-\alpha\ell}-1\right]$

$$G_1 = \frac{Q_1\sigma}{(\alpha^2+\sigma^2)}\left[(-1)^m e^{-\alpha\ell}-1\right]$$

Therefore $I = \displaystyle\int_{\xi-i\infty}^{\xi+i\infty}\frac{e^{\lambda t}}{\mu^2}\frac{G_0}{\lambda}\frac{I_0(\mu r)}{I_0(\mu a)}\,d\lambda \quad +$

$$+\int_{\xi-i\infty}^{\xi+i\infty}\frac{e^{\lambda t}}{\mu^2}\frac{I_0(\mu r)}{I_0(\mu a)}G_1\left\{\frac{\lambda\cos\gamma+\omega\sin\gamma}{\lambda^2+\omega^2}\right\} - \int_{\xi-i\infty}^{\xi+i\infty}\frac{e^{\lambda t}}{\mu^2}\frac{G_0}{\lambda}\,d\lambda \; -$$

$$-\int_{\xi-i\infty}^{\xi+i\infty}\frac{e^{\lambda t}}{\mu^2}G_1\left\{\frac{\lambda\cos\gamma+\omega\sin\gamma}{(\lambda^2+\omega^2)}\right\} \qquad 3.37$$

Names these four integrals (A) (B) (C) (D)

Consider (A)

$$q_0 \int_{\zeta-i\infty}^{\zeta+i\infty} \frac{e^{\lambda t}}{\mu^2} \frac{1}{\lambda} \frac{I_0(\mu r)}{I_0(\mu a)} \, d\lambda \quad = \quad 2\pi i \, q_0 \sum \text{Residues}$$

(A) has simple poles at $\lambda = 0$

$\lambda = -\beta\sigma^2$

and the zeros of $I_0(\mu a)$ which are at $\lambda = -\beta(\alpha_n^2 + \sigma^2)$

where α_n are roots of $J_0(\alpha a) = 0$

a) Residue of simple pole, $\lambda = 0$

$$R = \lim_{\lambda \to 0} \left[\lambda F(\lambda) \right]$$

$$= \lim_{\lambda \to 0} \left[\frac{\lambda e^{\lambda t} \; I_0\left(\sqrt{\frac{\lambda}{\beta} + \sigma^2}\right) r}{\left(\frac{\lambda}{\beta} + \sigma^2\right) \lambda \; I_0\left(\sqrt{\frac{\lambda}{\beta} + \sigma^2}\right) a} \right]$$

$$= \lim_{\lambda \to 0} \left[\frac{e^{\lambda t} \; I_0\left(\sqrt{\frac{\lambda}{\beta} + \sigma^2}\right) r}{\left(\frac{\lambda}{\beta} + \sigma^2\right) I_0\left(\sqrt{\frac{\lambda}{\beta} + \sigma^2}\right) a} \right]$$

$$= \frac{I_0(\sigma r)}{\sigma^2 I_0(\sigma a)}$$

b) Residue of simple pole, $\lambda = -\beta\sigma^2$.

$$R = \lim_{\lambda \to -\beta\sigma^2} \left[\frac{\beta\left(\frac{\lambda}{\beta}+\sigma^2\right) e^{\lambda t}\, I_0\left(\sqrt{\frac{\lambda}{\beta}+\sigma^2}\, r\right)}{\left(\frac{\lambda}{\beta}+\sigma^2\right).\lambda \cdot I_0\left(\sqrt{\frac{\lambda}{\beta}+\sigma^2}\, a\right)} \right]$$

$$= \lim_{\lambda \to -\beta\sigma^2} \left[\frac{\beta\, e^{\lambda t}\, I_0\left(\sqrt{\frac{\lambda}{\beta}+\sigma^2}\, r\right)}{\lambda\, I_0\left(\sqrt{\frac{\lambda}{\beta}+\sigma^2}\, a\right)} \right]$$

$$= -\frac{e^{-\beta\sigma^2 t}}{\sigma^2}$$

c) Residue at simple poles, $\lambda = -\beta(\sigma^2+\alpha_n^2)$ (α_n roots of $J(\alpha a) = 0$)

n = 1, 2, 3, ...

To evaluate the residues at these poles write

$$F(\lambda) = \frac{f(\lambda)}{g(\lambda)} = \frac{e^{\lambda t}\, I_0\left(\sqrt{\frac{\lambda}{\beta}+\sigma^2}\, r\right)}{I_0\left(\sqrt{\frac{\lambda}{\beta}+\sigma^2}\, a\right)}$$

Therefore $R = \lim_{\lambda \to a_m} \left[\frac{(\lambda - a_m) f(\lambda)}{\lambda\left(\frac{\lambda}{\beta}+\sigma^2\right) g(\lambda)} \right]$ for any of the zeros of $I_0(\mu a)$, $\lambda = a_m$

Therefore by Cauchy's Rule,

$$R = \left[\frac{\frac{\partial}{\partial\lambda}(\text{Numerator})}{\frac{\partial}{\partial\lambda}(\text{Denominator})} \right]_{\lambda=a_m}$$

$$= \frac{f(a_m)}{a_m\left(\frac{a_m}{\beta}+\sigma^2\right) g'(a_m)}$$ since other terms vanish.

Therefore for $a_m = -\beta(\sigma^2+\alpha_n^2)$

$$R = \frac{e^{-\beta(\sigma^2+\alpha_n^2)t}\ I_0(i\alpha_n r)}{-\alpha_n^2\left[-\beta(\sigma^2+\alpha_n^2)\left[\frac{d}{d\lambda}(I_0(\mu a)\right]\right]_{\lambda=-\beta(\sigma^2+\alpha_n^2)}}$$

Now when

$$\lambda = -\beta(\sigma^2+\alpha_n^2)$$
$$\mu = i\alpha_n$$

Therefore

$$\frac{d}{d\lambda} I_0(\mu a) = \frac{a}{2i\beta\alpha_n} I_1(i\alpha_n a)$$

Therefore $$R = \frac{2e^{-\beta(\sigma^2+\alpha_n^2)t}\ J_0(\alpha_n r)}{\alpha_n(\sigma^2+\alpha_n^2)a\ J_1(\alpha_n a)}$$

Therefore sum of residues for poles of $I_0(\mu a)$ are

$$\frac{2}{a}\sum_{n=1}^{\infty} \frac{e^{-\beta(\sigma^2+\alpha_n^2)t}\ J_0(\alpha_n r)}{\alpha_n(\alpha_n^2+\sigma^2)\ J_1(\alpha_n a)}$$

Therefore integral (A)

$$I_A = 2\pi i\, q_0\left\{ \frac{I_0(\sigma r)}{\sigma^2 I_0(\sigma a)} - \frac{e^{-\beta\sigma^2 t}}{\sigma^2} + 2\frac{e^{-\beta\sigma^2 t}}{a}\sum_{n=1} \frac{e^{-\beta\alpha_n^2 t}\ J_0(\alpha_n r)}{\alpha_n(\sigma^2+\alpha_n^2)\ J_1(\alpha_n a)} \right.$$

Now consider integral (C)

$$\int_{\zeta-i\infty}^{\zeta+i\infty} \frac{e^{\lambda t}}{\mu^2} \frac{\varsigma_0}{\lambda} d\lambda = 2\pi i \varsigma_0 \sum \text{Residues}$$

(C) has simple poles at $\lambda = 0$

$$\lambda = -\beta\sigma^2$$

a) Residue of simple pole at $\lambda = 0$.

$$R = \lim_{\lambda \to 0} \left[\lambda F(\lambda)\right]$$

$$= \lim_{\lambda \to 0} \left[\frac{e^{\lambda t}}{(\sigma^2 + \frac{\lambda}{\beta})}\right] = \frac{1}{\sigma^2}$$

b) Residue of simple pole at $\lambda = -\beta\sigma^2$.

$$= \lim_{\lambda \to \beta\sigma^2} \left[\frac{\beta e^{\lambda t}}{\lambda}\right]$$

$$= -\frac{e^{-\beta\sigma^2 t}}{\sigma^2}$$

Therefore integral (C)

$$I_C = 2\pi i \varsigma_0 \frac{1}{\sigma^2}\left(1 - e^{-\beta\sigma^2 t}\right) \qquad 3.39$$

Now consider integral (B)

$$\frac{1}{2\pi i}\int_{\xi-i\infty}^{\xi+i\infty} \frac{e^{\lambda t}}{(\sigma^2+\frac{\lambda}{\beta})}\cdot\frac{I_0(\mu r)}{I_0(\mu a)}\cdot\frac{\lambda\cos\gamma+\omega\sin\gamma}{\lambda^2+\omega^2}\,d\lambda = 2\pi i \sum \text{Residues}$$

This has poles at

$$\lambda = -\sigma^2\beta$$

$$\lambda = \pm i\omega$$

$$\lambda = -\beta(\alpha_n^2+\sigma^2)$$

where $\pm\alpha_n$ are roots of

$$J_0(\alpha_n a) = 0$$

a) Simple pole at $\lambda = -\beta\sigma^2$

$$R = \lim_{\lambda\to-\beta\sigma^2}\left[\frac{\beta(\frac{\lambda}{\beta}+\sigma^2)\,e^{\lambda t}\,I_0(\mu r)(\lambda\cos\gamma+\omega\sin\gamma)}{(\frac{\lambda}{\beta}+\sigma^2)(\lambda^2+\omega^2)\,I_0(\mu a)}\right]$$

$$= \lim_{\lambda\to-\beta\sigma^2}\left[\frac{\beta e^{\lambda t}\,I_0(\mu r)(\lambda\cos\gamma+\omega\sin\gamma)}{(\lambda^2+\omega^2)\,I_0(\mu a)}\right]$$

$$= \beta e^{-\beta\sigma^2 t}\left[\frac{-\beta\sigma^2\cos\gamma+\omega\sin\gamma}{(\beta^2\sigma^4+\omega^2)}\right]$$

b) Pole at $\lambda = i\omega$

$$R = \lim_{\lambda \to i\omega} \left[\frac{(\lambda - i\omega) e^{\lambda t} I_0(\mu r) [\lambda \cos\gamma + \omega \sin\gamma]}{(\sigma^2 + \frac{\lambda}{\beta})(\lambda - i\omega)(\lambda + i\omega) I_0(\mu a)} \right]$$

$$= \lim_{\lambda \to i\omega} \left[\frac{e^{\lambda t} I_0(\mu r) [\lambda \cos\gamma + \omega \sin\gamma]}{(\sigma^2 + \frac{\lambda}{\beta})(\lambda + i\omega) I_0(\mu a)} \right]$$

$$= \frac{e^{i\omega t} I_0\left(\sqrt{i\frac{\omega}{\beta} + \sigma^2}\right) r [i\omega \cos\gamma + \omega \sin\gamma]}{2(\sigma^2 + i\frac{\omega}{\beta}) i\omega \; I_0\left(\sqrt{i\frac{\omega}{\beta} + \sigma^2}\right) a}$$

c) Pole at $\lambda = -i\omega$

This is obviously the complex conjugate of the above expression.

$$R = \frac{e^{-i\omega t} I_0\left(\sqrt{-i\frac{\omega}{\beta} + \sigma^2} \cdot r\right) [-i\omega \cos\gamma + \omega \sin\gamma]}{2(\sigma^2 - i\frac{\omega}{\beta})(-i\omega) \; I_0\left(\sqrt{-i\frac{\omega}{\beta} + \sigma^2}\right) a}$$

d) Poles at zeros of $I_0(\mu a)$, i.e. $\lambda = -\beta(\alpha_n^2 + \sigma^2)$ where $\pm\alpha_n$ are roots of $J_0(\alpha_n a) = 0$

We have as before, using Cauchy's Rule

$$R = \left[\frac{f(\lambda)}{(\lambda^2+\omega^2)\left(\frac{\lambda}{\beta}+\sigma^2\right) g'(\lambda)}\right]_{\lambda=a_m}$$

where $f(\lambda) = e^{\lambda t} I_0(\mu r)(\lambda\cos\gamma + \omega\sin\gamma)$

$$g(\lambda) = I_0(\mu a)$$

$$a_m = -\beta(\alpha_n^2+\sigma^2)$$

$$= \frac{e^{-\beta(\sigma^2+\alpha_n^2)t}\, J_0(\alpha_n r)\left[-\beta(\sigma^2+\alpha_n^2)\cos\gamma + \omega\sin\gamma\right]}{\left[\beta^2(\sigma^2+\alpha_n^2)^2+\omega^2\right] - \alpha_n^2 \frac{a}{2i\beta\alpha_n} \cdot i \cdot J_1(\alpha_n a)}$$

$$= \frac{2\beta\, e^{-\beta(\sigma^2+\alpha_n^2)t}\, J_0(\alpha_n r)\left[\beta(\sigma^2+\alpha_n^2)\cos\gamma - \omega\sin\gamma\right]}{\left[\beta^2(\sigma^2+\alpha_n^2)^2+\omega^2\right]\alpha_n a \cdot J_1(\alpha_n a)}$$

Thus the sum of the residues of all the poles due to $I_0(\mu a)$ is

$$\sum_{n=1}^{\infty} \frac{2\beta\, e^{-\beta(\sigma^2+\alpha_n^2)t}\, J_0(\alpha_n r)\left[\beta(\sigma^2+\alpha_n^2)\cos\gamma - \omega\sin\gamma\right]}{\left[\beta^2(\sigma^2+\alpha_n^2)^2+\omega^2\right]\alpha_n a \cdot J_1(\alpha_n a)}$$

Therefore integral (B)

FIG. Ia

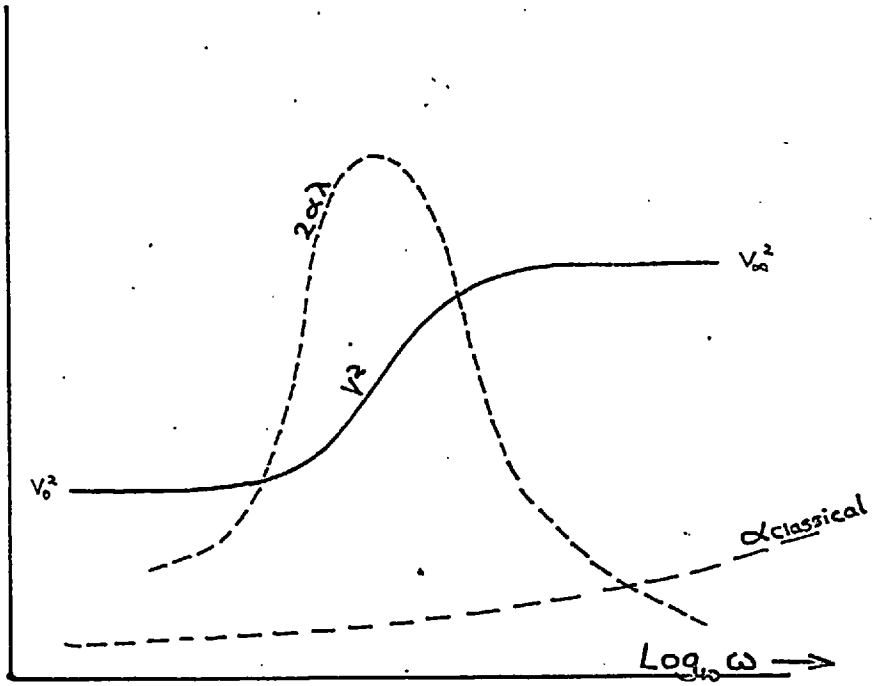

Variation of sound absorption and dispersion with frequency for a singly relaxing gas.

FIG. Ib

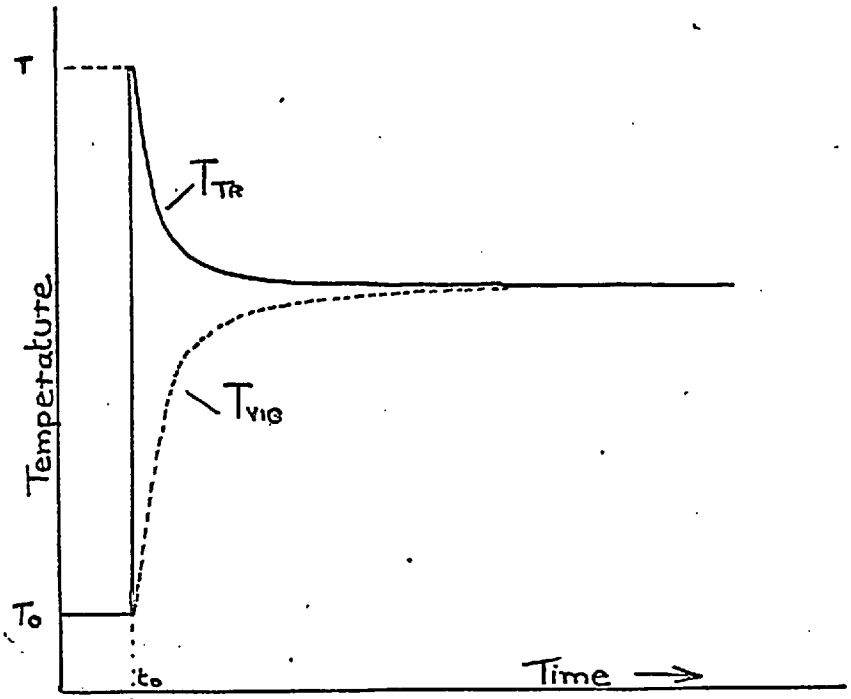

Variation of vibrational & translational temperatures with time, behind a shock front in a polyatomic gas

$$I_B = 2\pi i G_1 \left\{ \beta \frac{e^{-\sigma^2\beta t}(-\beta\sigma^2\cos\gamma + \omega\sin\gamma)}{(\beta^2\sigma^4 + \omega^2)} \right.$$

$$+ \frac{e^{i\omega t} I_0\left(\sqrt{i\frac{\omega}{\beta}+\sigma^2}\right)\tau \left(i\omega\cos\gamma + \omega\sin\gamma\right)}{2\left(\sigma^2 + i\frac{\omega}{\beta}\right) i\omega \; I_0\left(\sqrt{i\frac{\omega}{\beta}+\sigma^2}\right)a}$$

$$+ \frac{e^{-i\omega t} I_0\left(\sqrt{-i\frac{\omega}{\beta}+\sigma^2}\right)\tau \left(-i\omega\cos\gamma + \omega\sin\gamma\right)}{2\left(\sigma^2 - i\frac{\omega}{\beta}\right)(-i\omega)\, I_0\left(\sqrt{-i\frac{\omega}{\beta}+\sigma^2}\right)a}$$

$$\left. + \frac{2\beta}{a} e^{-\beta\sigma^2 t} \sum_{n=1}^{\infty} \frac{e^{-\beta\alpha_n^2 t} J_0(\alpha_n r)\left[\beta(\sigma^2+\alpha_n^2)\cos\gamma - \omega\sin\gamma\right]}{\left[\beta^2(\sigma^2+\alpha_n^2)^2 + \omega^2\right]\alpha_n \; J_1(\alpha_n a)} \right\}$$

3.40

Finally consider integral (D)

$$I_D = G_1 \int_{\zeta - i\infty}^{\zeta + i\infty} \frac{e^{\lambda t}}{\left(\frac{\lambda}{\beta} + \sigma^2\right)} \frac{(\lambda\cos\gamma + \omega\sin\gamma)}{(\omega^2 + \lambda^2)} d\lambda = 2\pi i \sum \text{Residues}$$

(D) has simple poles at $\lambda = -\beta\sigma^2$
$\lambda = \pm i\omega$

a) Pole at

$$\lambda = -\beta\sigma^2$$

$$R = \lim_{\lambda \to -\beta\sigma^2} \left[\frac{\beta\left(\frac{\lambda}{\beta} + \sigma^2\right) e^{\lambda t} \left[\lambda \cos\gamma + \omega \sin\gamma\right]}{\left(\frac{\lambda}{\beta} + \sigma^2\right)\left(\lambda^2 + \omega^2\right)} \right]$$

$$= \lim_{\lambda \to -\beta\sigma^2} \left[\frac{\beta e^{\lambda t} \left(\lambda \cos\gamma + \omega \sin\gamma\right)}{\left(\lambda^2 + \omega^2\right)} \right]$$

$$= \frac{\beta e^{-\beta\sigma^2 t} \left(-\beta\sigma^2 \cos\gamma + \omega \sin\gamma\right)}{\left(\beta^2\sigma^4 + \omega^2\right)}$$

b) Pole at $\lambda = i\omega$

$$R = \lim_{\lambda \to i\omega} \left[\frac{(\lambda - i\omega) e^{\lambda t} \left[\lambda \cos\gamma + \omega \sin\gamma\right]}{\left(\frac{\lambda^2}{\beta} + \sigma^2\right)(\lambda + i\omega)(\lambda - i\omega)} \right]$$

$$= \lim_{\lambda \to i\omega} \left[\frac{\left(\lambda \cos\gamma + \omega \sin\gamma\right) e^{\lambda t}}{\left(\frac{\lambda}{\beta} + \sigma^2\right)(\lambda + i\omega)} \right]$$

$$= \frac{e^{i\omega t} \left[i\omega \cos\gamma + \omega \sin\gamma\right]}{2\left(\frac{i\omega}{\beta} + \sigma^2\right) i\omega}$$

c) The pole at $\lambda = -i\omega$ will give the complex conjugate of the pole at $\lambda = i\omega$ and therefore has residue

$$R = \frac{e^{-i\omega t}\left[-i\omega\cos\gamma + \omega\sin\gamma\right]}{2\left(\sigma^2 - i\frac{\omega}{\beta}\right)(-i\omega)}$$

Thus integral (D) has value

$$I_D = 2\pi i\, g_i \left\{ \frac{\beta\, e^{-\beta\sigma^2 t}\left(-\beta\sigma^2\cos\gamma + \omega\sin\gamma\right)}{\left(\beta^2\sigma^4 + \omega^2\right)} \right.$$

$$\left. + \frac{e^{i\omega t}\left(i\omega\cos\gamma + \omega\sin\gamma\right)}{2\left(\sigma^2 + i\frac{\omega}{\beta}\right)i\omega} + \frac{e^{-i\omega t}\left(-i\omega\cos\gamma + \omega\sin\gamma\right)}{2(-i\omega)\left(\sigma^2 - i\frac{\omega}{\beta}\right)} \right.$$

3.41

Therefore the solution of (37) is

$$I = I_A + I_B + I_C + I_D.$$

$$I = 2\pi i\, g_0 \left\{ \frac{I_0(\sigma r)}{\sigma^2 I_0(\sigma a)} - \frac{e^{-\beta\sigma^2 t}}{\sigma^2} + \frac{2}{a} e^{-\beta\sigma^2 t} \sum_{n=1}^{\infty} \frac{e^{-\beta\alpha_n^2 t}\, J_0(\alpha_n r)}{\alpha_n\left(\sigma^2 + \alpha_n^2\right) J_1(\alpha_n a)} \right.$$

$$\left. + \frac{e^{-\beta\sigma^2 t}}{\sigma^2} - \frac{1}{\sigma^2} \right\} + 2\pi i\, C_1 \left\{ \frac{\beta e^{-\beta\sigma^2 t}\left(-\beta\sigma^2\cos\gamma + \omega\sin\gamma\right)}{\left(\beta^2\sigma^4 + \omega^2\right)} \right.$$

$$\left. + \frac{e^{i\omega t}\, I_0\left(\sqrt{i\frac{\omega}{\beta} + \sigma^2}\, r\right)\left(i\omega\cos\gamma + \omega\sin\gamma\right)}{2\left(\sigma^2 + i\frac{\omega}{\beta}\right)i\omega\; I_0\left(\sqrt{i\frac{\omega}{\beta} + \sigma^2}\, a\right)} + \right.$$

$$+\frac{e^{-i\omega t}\, I_0\!\left(\sqrt{-\frac{i\omega}{\beta}+\sigma^2}\right)r\,(-i\omega\cos\gamma+\omega\sin\gamma)}{2\left(\sigma^2-\frac{i\omega}{\beta}\right) I_0\!\left(\sqrt{-\frac{i\omega}{\beta}+\sigma^2}\right)a\,.\,(-i\omega)} \;-\; \beta\,\frac{e^{-\beta\sigma^2 t}\left(-\beta\sigma^2\cos\gamma+\omega\sin\gamma\right)}{\left(\beta^2\sigma^4+\omega^2\right)}$$

$$+\;\frac{2\beta}{a}\,e^{-\beta\sigma^2 t}\sum_{n=1}^{\infty}\frac{e^{-\beta\alpha_n^2 t}\,J_0(\alpha_n r)\left[\beta(\sigma^2+\alpha_n^2)\cos\gamma-\omega\sin\gamma\right)}{\left[\beta^2(\sigma^2+\alpha_n^2)^2+\omega^2\right]\alpha_n\,J_1(\alpha_n a)}$$

$$-\frac{e^{i\omega t}(i\omega\cos\gamma+\omega\sin\gamma)}{2\left(\sigma^2+\frac{i\omega}{\beta}\right)i\omega}\;-\;\frac{e^{-i\omega t}\left(-i\omega\cos\gamma+\omega\sin\gamma\right)}{2(-i\omega)\left(\sigma^2-\frac{i\omega}{\beta}\right)} \qquad 3.42$$

Collecting terms from 3.42 yields

(i) Constant terms

$$\frac{2\pi i\, q_0}{\sigma^2}\left[\frac{I_0(\sigma r)}{I_0(\sigma a)}-1\right] \qquad 3.42a$$

(ii) Transient terms

$$2\pi i\, q_0\,\frac{2}{a}\,e^{-\beta\sigma^2 t}\sum_{n=1}^{\infty}\frac{e^{-\beta\alpha_n^2 t}J_0(\alpha_n r)}{\alpha_n(\sigma^2+\alpha_n^2)\,J_1(\alpha_n a)} + 2\pi i\, q_1.\frac{2\beta}{a}\,e^{-\beta\sigma^2 t}\sum\frac{e^{-\beta\alpha_n^2 t}\,J_0(\alpha_n r)\left[\beta(\sigma^2+\alpha_n^2)\cos\gamma-\omega\sin\gamma\right]}{\left[\beta^2(\sigma^2+\alpha_n^2)^2+\omega^2\right]\alpha_n\,J_1(\alpha_n a)}$$

which is written

$$4\pi i\,\frac{\beta}{a}\,e^{-\beta\sigma^2 t}\sum_{n=1}^{\infty}\frac{e^{-\beta\alpha_n^2 t}}{\alpha_n}\,\frac{J_0(\alpha_n r)}{J_1(\alpha_n a)}\left[\frac{q_0}{\beta\left(\sigma^2+\alpha_n^2\right)}+\right.$$

$$\left.+\;\frac{q_1\cos(\gamma-\theta_1)}{\sqrt{\beta^2\left(\sigma^2+\alpha_n^2\right)^2+\omega^2}}\right] \qquad 3.42b$$

where $\tan\theta_1 = \dfrac{\omega}{\beta(\sigma^2+\alpha_n^2)}$

(iii) Harmonic terms

$$2\pi i \, S_1\left[\frac{e^{i(\omega t-\gamma)}}{2(\sigma^2+i\frac{\omega}{\beta})}\left\{\frac{I_0\left(\sqrt{i\frac{\omega}{\beta}+\sigma^2}\right)r}{I_0\left(\sqrt{i\frac{\omega}{\beta}+\sigma^2}\right)a} - 1\right\} \quad + \text{Complex Conjugate}\right] \qquad 3.42c$$

The transient terms (42b) are interesting in giving the time constant for the system to take up equilibrium. However, they may be neglected in finding the phase and amplitude of the excess pressure component in the cell.

Thus the expression for the excess temperature in the spectrophone $v(r,z)$ becomes, in the steady state,

$$v(r,z) = \frac{1}{\ell\pi i}\sum_{m=1}^{\infty}\sin\frac{m\pi}{\ell}z \;(\text{Constant terms + harmonic terms})$$

$$v(r,z) = \frac{2}{\ell}Q_0\sum_{m=1}^{\infty}\sin\frac{m\pi}{\ell}z\,\frac{\sigma}{\sigma^2+\alpha}\left[1-(-1)^m e^{-\alpha\ell}\right]\frac{1}{\sigma^2}\left\{1-\frac{I_0(\sigma r)}{I_0(\sigma a)}\right\}$$

$$+\frac{1}{\ell}Q_1\left\{\sum_{m=1}^{\infty}\sin\frac{m\pi}{\ell}z\,\frac{\sigma}{(\sigma^2+\alpha^2)}\left[1-(-1)^m e^{-\alpha\ell}\right]\frac{e^{i(\omega t-\gamma)}}{(\sigma^2+i\frac{\omega}{\beta})}\left\{1-\frac{I_0\left(\sqrt{\sigma^2+i\frac{\omega}{\beta}}\right)r}{I_0\left(\sqrt{\sigma^2+i\frac{\omega}{\beta}}\right)a}\right\}\right.$$

$$\left. + \text{Complex conjugate}\right\} \qquad 3.43$$

The acoustic boundary conditions, as discussed in section A(ii), above, are:-

1. **Pressure** is constant in phase and amplitude throughout the cell.
2. Ideal gas.
3. Rigid walls.

Thus from the equation of state

$$\frac{p}{P_0} = \frac{\Delta\rho}{\rho_0} + \frac{\tau}{T_0}$$

Integrating this over the volume of the cell, V_0

$$\frac{p}{P_0} V_0 = 0 + \int_{V_0} \frac{\tau \, dV}{T_0} \qquad 3.44$$

$$p = \frac{P_0}{V_0 T_0} \int_{V_0} \tau \, dV \qquad 3.44a$$

or $p = \frac{P_0}{T_0} \bar{\tau}$ where $\bar{\tau}$ is the spatially averaged excess temperature amplitude in the spectrophone.

To obtain $\bar{\tau}$, $\tau(rz)$ is integrated over the cell volume.

$$\bar{\tau} = \frac{1}{V_0} \int_0^l \int_0^a \int_0^{2\pi} \tau(rz) \, d\xi \, r \, dr \, dz$$

$$= \frac{2\pi}{V_0} \int_0^l \int_0^a \tau(rz) \, r \, dr \, dz \qquad \text{since } \tau \neq f(\xi)$$

Integrate next w.r.t. r. This is valid as long as the convergence of the series over m is not affected.

$$v(z) = \frac{4\pi}{\ell} Q_0 \sum_m \sin\frac{m\pi}{\ell} z \cdot \frac{\sigma}{\sigma^2+\alpha^2}\left(1-(-1)^m e^{-\alpha\ell}\right)\frac{1}{\sigma^2}\int_0^a \left(r - r\,\frac{I_0(\sigma r)}{I_0(\sigma a)}\right)dr$$

$$+ \frac{2\pi Q_1}{\ell}\left\{ e^{i(\omega t-\gamma)} \sum_m \sin\frac{m\pi}{\ell} z \,\frac{\sigma}{(\sigma^2+\alpha^2)}\left(1-(-1)^m e^{-\alpha\ell}\right)\frac{1}{\left(\sigma^2+i\frac{\omega}{\beta}\right)} \times \right.$$

$$\int_0^a \left(r - r\,\frac{I_0\sqrt{\left(i\frac{\omega}{\beta}+\sigma^2\right)}r}{I_0\sqrt{\left(i\frac{\omega}{\beta}+\sigma^2\right)}a}\right)dr. \; +$$

$$\left. + \text{Complex conjugate} \right\}$$

Which gives

$$v(z) = \frac{4\pi Q_0}{\ell} \sum_m \frac{\sigma}{\sigma^2+\alpha^2} \cdot \frac{1}{\sigma^2}\left(1-(-1)^m e^{-\alpha\ell}\right) \sin\frac{m\pi}{\ell} z \left[\frac{a^2}{2} - \frac{a}{\sigma}\frac{I_1(\sigma a)}{I_0(\sigma a)}\right]$$

$$+ \frac{2\pi Q_1}{\ell}\left\{ e^{i(\omega t-\gamma)} \sum_m \sin\frac{m\pi}{\ell} z \cdot \frac{\sigma}{\sigma^2+\alpha^2} \frac{\left[1-(-1)^m e^{-\alpha\ell}\right]}{\sigma^2+i\frac{\omega}{\beta}} \left[\frac{a^2}{2} - \frac{a}{\sqrt{\sigma^2+i\frac{\omega}{\beta}}} \cdot \frac{I_1\sqrt{\left(\sigma^2+i\frac{\omega}{\beta}\right)}a}{I_0\sqrt{\left(\sigma^2+i\frac{\omega}{\beta}\right)}a}\right.\right.$$

$$\left.\left. + \text{Complex Conjugate} \right\}\right. \qquad 3.45$$

Now integrate w.r.t. z between limits 0 and l. This is again valid providing the series over m converge.

$$\bar{v} = \frac{4\pi Q_0}{V_0 l} \sum_m \frac{\sigma}{\alpha^2+\sigma^2} \frac{1}{\sigma^2} \left(1-(-1)^m e^{-\alpha l}\right)\left[\frac{a^2}{2} - \frac{a}{\sigma}\frac{I_1(\sigma a)}{I_0(\sigma a)}\right] \int_0^l \sin \frac{m\pi}{l} z \, dz$$

$$+ \frac{2\pi Q_1}{V_0 l} \left\{ e^{i(\omega t-\gamma)} \sum_m \frac{\sigma}{(\alpha^2+\sigma^2)} \left[1-(-1)^m e^{-\alpha l}\right] \frac{1}{(\sigma^2+i\frac{\omega}{\beta})} \left[\frac{a^2}{2} - \frac{a}{\sqrt{\sigma^2+i\frac{\omega}{\beta}}} \times \right.\right.$$

$$\left. \times \frac{I_1\left(\sqrt{i\frac{\omega}{\beta}+\sigma^2}\right)a}{I_0\left(\sqrt{i\frac{\omega}{\beta}+\sigma^2}\right)a}\right] \int_0^l \sin \frac{m\pi}{l} z \, dz \quad +$$

$$\left. + \text{Complex Conjugate} \right\}$$

Yielding

$$\bar{v} = \frac{4Q_0}{l^2 a^2}\left[1+e^{-\alpha l}\right] \sum_m \frac{1}{\sigma^2} \frac{1}{(\alpha^2+\sigma^2)} \left[1-(-1)^m\right] \left[\frac{a^2}{2} - \frac{a}{\sigma}\frac{I_1(\sigma a)}{I_0(\sigma a)}\right]$$

$$+ \frac{2Q_1}{l^2 a^2} \left\{ e^{i(\omega t-\gamma)} \left[1+e^{-\alpha l}\right] \sum_m \frac{\left[1-(-1)^m\right]}{(\alpha^2+\sigma^2)(\sigma^2+i\frac{\omega}{\beta})} \left[\frac{a^2}{2} - \frac{a}{\sqrt{\sigma^2+i\frac{\omega}{\beta}}} \frac{I_1\left(\sqrt{\sigma^2+i\frac{\omega}{\beta}}\right)a}{I_0\left(\sqrt{\sigma^2+i\frac{\omega}{\beta}}\right)a}\right] \right.$$

$$\left. + \text{Complex Conjugate} \right\} \qquad 3.46$$

The next task is to evaluate the sum over m. Consider first the constant terms.

$$\frac{4Q_0}{\rho^2 a^2}\left[1+e^{-\alpha\ell}\right]\sum_{m=1}^{\infty}\frac{\rho^2}{m^2\pi^2}\,\frac{1}{\left(\alpha^2+\frac{m^2\pi^2}{\ell^2}\right)}\left[1-(-1)^m\right]$$

$$\times\left[\frac{a^2}{2}-\frac{a\rho}{m\pi}\,\frac{I_1\left(\frac{m\pi}{\ell}a\right)}{I_0\left(\frac{m\pi}{\ell}a\right)}\right].$$

Introducing the notation

$$w=\frac{\pi}{\ell}$$

$$u^2=\frac{\alpha^2}{w^2}=\frac{\alpha^2\ell^2}{\pi^2}$$

gives

$$\frac{8Q_0}{w^4\rho^2a^2}\left[1+e^{-\alpha\ell}\right]\sum_{\substack{m=1\\(m\ odd)}}^{\infty}\frac{1}{m^2(m^2+u^2)}\left[\frac{a^2}{2}-\frac{a}{mw}\,\frac{I_1(mwa)}{I_0(mwa)}\right]$$

Provided all resultant series are absolutely convergent this expression may be manipulated as follows:-

$$\frac{8Q_0}{w^4\rho^2a^2}\left[1+e^{-\alpha\ell}\right]\left\{\sum_{\substack{m=1\\(m\ odd)}}^{\infty}\frac{a^2}{2}\,\frac{1}{m^2(m^2+u^2)}-\sum_{\substack{m=1\\(m\ odd)}}^{\infty}\frac{a}{w}\,\frac{I_1(mwa)}{I_0(mwa)}\,\frac{1}{m^3(m^2+u^2)}\right\}$$

$$\frac{8Q_0}{w^4\rho^2a^2}\left[1+e^{-\alpha\ell}\right]\left\{\frac{a^2}{2u^2}\sum_{(m\ odd)}'\frac{1}{m^2}-\frac{a^2}{2u^2}\sum_{(m\ odd)}'\frac{1}{(m^2+u^2)}-\frac{a}{w}\sum_{(m\ odd)}'\frac{I_1(mwa)}{I_0(mwa)}\,\frac{1}{m^3(m^2+u^2)}\right\}$$

The first two series in (47) may be summed to analytical expressions.

$$\sum_{\substack{m=1 \\ (m\ \text{odd})}}^{\infty} \frac{1}{m^2} = \frac{\pi^2}{8}$$

$$\sum_{\substack{m=1 \\ (m\ \text{odd})}}^{\infty} \frac{1}{(m^2+u^2)} \quad \frac{\pi}{4u} \tanh \frac{u\pi}{2}$$

The third series $\sum \frac{I_1(mwa)}{I_0(mwa)} \frac{1}{m^3(m^2+u^2)}$ converges very rapidly and can be conveniently enumerated for given values of a, l, and α to any required accuracy. Thus the constant part of becomes:-

$$\frac{8Q_0 l^2}{\pi^4}\frac{l^2}{a^2}\left[1+e^{-\alpha l}\right]\left\{\frac{a\pi^4}{16\alpha^2 l^2} - \frac{a^2\pi^4}{8\alpha^3 l^3}\tanh\frac{\alpha l}{2} - \frac{al}{\pi}\sum_{\substack{m=1 \\ (m\ \text{odd})}}^{\infty}\frac{I_1\left(\frac{m\pi a}{l}\right)}{I_0\left(\frac{m\pi a}{l}\right)}\frac{1}{m^3(m^2+u^2)}\right\} \quad 3.48$$

or

$$Q_0 l^2\left[1+e^{-\alpha l}\right]\left\{\frac{1}{2(\alpha l)^2} - \frac{\tanh\alpha l}{(\alpha l)^3}\frac{}{2} - \frac{8}{\pi^5}\frac{l}{a}\sum_{\substack{m=1 \\ (m\ \text{odd})}}^{\infty}\frac{I_1\left(\frac{m\pi a}{l}\right)}{I_0\left(\frac{m\pi a}{l}\right)}\frac{1}{m^3\left(m^2+\left(\frac{\alpha l}{\pi}\right)^2\right)}\right\}$$

$$Q_0 \ell^2 \left[1+e^{-\alpha\ell}\right]\left\{\frac{1}{2(\alpha\ell)^2}-\frac{1}{(\alpha\ell)^3}\tanh\frac{\alpha\ell}{2}-\frac{8}{\pi^5}\frac{\ell}{a}\sum_{(m\,odd)}^{\infty}\frac{I_1\left(\frac{m\pi}{a}\right)}{I_0\left(\frac{m\pi a}{\ell}\right)}\times\right.$$

$$\left.\times\frac{1}{m^3\left(m^2+\left(\frac{\alpha\ell}{\pi}\right)^2\right)}\right.$$

3.48a

Consider now the harmonic terms, and first the term in $e^{+i\omega t}$.

$$\frac{2Q_1}{\ell^2 a^2}e^{i(\omega t-\gamma)}\left[1+e^{-\alpha\ell}\right]\sum_{m=1}^{\infty}\frac{(1-(-1)^m)}{(\alpha^2+\sigma^2)\left(\sigma^2+i\frac{\omega}{\beta}\right)}\left[\frac{a^2}{2}-\frac{a}{\sqrt{\frac{m^2\pi^2}{\ell^2}+i\frac{\omega}{\beta}}}\frac{I_1\sqrt{\left(\sigma^2+i\frac{\omega}{\beta}\right)}a}{I_0\sqrt{\left(\sigma^2+i\frac{\omega}{\beta}\right)}a}\right]$$

Using notation

$$W=\frac{\pi}{\ell}\quad,\quad u^2=\frac{\alpha^2}{W^2}\quad,\quad x^2=\frac{i\omega}{\beta W^2}=\frac{i\omega\ell^2}{\beta\pi^2}$$

yields

$$\frac{4Q_1}{\ell^2a^2}\frac{e^{i(\omega t-\gamma)}}{W^4}\left[1+e^{-\alpha\ell}\right]\sum_{(m\,odd)}^{m=1,\infty}\frac{1}{(m^2+u^2)}\frac{1}{(m^2+x^2)}\left[\frac{a^2}{2}-\frac{a}{W\sqrt{m^2+x^2}}\times\right.$$

$$\left.\times\frac{I_1\left(\sqrt{m^2+x^2}\,Wa\right)}{I_0\left(\sqrt{m^2+x^2}\,Wa\right)}\right]$$

3.49

Splitting up the series as before, again on condition of convergence of each resulting series, yields

$$\frac{4Q_1}{\rho^2 a^2}\frac{e^{i(\omega t-\gamma)}}{W^4}\left[1+e^{-\alpha\ell}\right]\left\{\sum_{1\,(m\,odd)}^{\infty}\frac{a^2}{2}\frac{1}{(m^2+u^2)(m^2+x^2)}-\sum_{1\,(m\,odd)}^{\infty}\frac{a}{W}\frac{I_1\left((m^2+x^2)^{\frac{1}{2}}Wa\right)}{I_0\left(m^2+x^2\right)^{\frac{1}{2}}Wa)}\times\right.$$

$$\left.\times\frac{1}{(m^2+u^2)(m^2+x^2)^{3/2}}\right\}$$

The first series may be further split up by partial fractions into two convergent series and summed

$$\frac{4Q_1}{\rho^2 a^2}\frac{e^{i(\omega t-\gamma)}}{W^4}\frac{\left[1+e^{-\alpha\rho}\right]}{(u^2-x^2)}\left\{\frac{a^2}{2}\sum_{1\,(m\,odd)}^{\infty}\frac{1}{(m^2+x^2)}-\frac{a^2}{2}\sum_{1\,(m\,odd)}^{\infty}\frac{1}{(m^2+u^2)}-\right.$$

$$\left.-(u^2-x^2)\frac{a}{W}\sum_{1\,(m\,odd)}^{\infty}\frac{I_1\left((m^2+x^2)^{\frac{1}{2}}Wa\right)}{I_0\left((m^2+x^2)^{\frac{1}{2}}Wa\right)}\cdot\frac{1}{(m^2+u^2)(m^2+x^2)^{3/2}}\right\}$$

$$\frac{4Q_1}{\rho^2 a^2}\frac{e^{i(\omega t-\gamma)}}{W^4}\frac{\left[1-e^{-\alpha\ell}\right]}{(u^2-x^2)}\left\{\frac{a^2}{8}\frac{\pi}{x}\tanh\frac{x\pi}{2}-\frac{a^2}{8}\frac{\pi}{u}\tanh\frac{u\pi}{2}-\sum\left(3^{rd}\text{ series}\right)\right\}$$

3.50

The third series $\sum\frac{I_1\left\{(m^2+x^2)^{\frac{1}{2}}Wa\right\}}{I_0\left\{(m^2+x^2)^{\frac{1}{2}}Wa\right\}}\frac{1}{(m^2+x^2)^{\frac{3}{2}}(m^2+u^2)}$

is difficult to evaluate exactly, but is highly convergent.

Thus (50) becomes

$$\frac{Q_1}{2\pi}\left[1+e^{-\alpha\ell}\right]\frac{e^{i(\omega t-\gamma)}}{(\alpha^2-i\frac{\omega}{\beta})}\left[\frac{1}{x}\tanh\frac{x\pi}{2}-\frac{1}{u}\tanh\frac{u\pi}{2}-\right.$$

$$\left.-(u^2-x^2)\frac{a}{w}\sum_{(m\,odd)}^{\infty}\frac{I_1\{(m^2+x^2)^{\frac{1}{2}}wa\}}{I_0\{(m^2+x^2)^{\frac{1}{2}}wa\}}\frac{1}{(m^2+u^2)(m^2+x^2)^{3/2}}\right] \qquad 3.51$$

A similar analysis on the terms in $e^{-i\omega t}$ yields the complex conjugate of (51).

In order to go further with this expression we must approximate. Assume that the chopping frequency is high enough so that $\sqrt{\frac{\omega}{\beta}} \gg 1$.

If this is so, then the following approximations are valid:-

a) $$\frac{I_1\{(m^2+x^2)^{\frac{1}{2}}wa\}}{I_0\{(m^2+x^2)^{\frac{1}{2}}wa\}} \simeq 1$$

b) since $\left|\frac{aw}{2}(m^2+x^2)^{\frac{1}{2}}\right| \gg 1$ for all m. Then the third term in (51) above (and its complex conjugate), is much smaller than the other two terms and may be neglected.

c)

$$\frac{1}{x}\tanh\frac{x\pi}{2} = \frac{1}{\sqrt{\frac{\omega}{2\beta w^2}}(1+i)}\tanh\sqrt{\frac{\omega}{2\beta w^2}}\cdot\frac{\pi}{2}(1+i$$

$$\simeq \frac{\pi}{2}\sqrt{\frac{2\beta}{\omega}}(1-i)$$

Thus in this case, (51) becomes

$$\frac{Q_1}{2\pi}\frac{[1+e^{-\alpha\ell}]}{(\alpha^2-i\frac{\omega}{\beta})}e^{i(\omega t-\gamma)}\left[\frac{2\pi}{4\ell\sqrt{\frac{2\beta}{\omega}}}(1-i)-\frac{\pi}{\ell\alpha}\tanh\frac{\alpha\ell}{2}\right]$$

$$=\frac{Q_1}{2\ell}[1+e^{-\alpha\ell}]\frac{e^{i(\omega t-\gamma)}}{(\alpha^2-i\omega/\beta)}\left[\sqrt{\frac{\beta}{2\omega}}-\frac{1}{\alpha}\tanh\left(\frac{\alpha\ell}{2}\right)-i\sqrt{\frac{\beta}{2\omega}}\right] \qquad 3.52$$

Similarly, the term $me^{-i\omega t}$ becomes

$$\frac{Q_1}{2\ell}[1+e^{-\alpha\ell}]\frac{e^{i(\omega t-\gamma)}}{\alpha^2+i\frac{\omega}{\beta}}\left[\left(\sqrt{\frac{\beta}{2\omega}}-\frac{1}{\alpha}\tanh\frac{\alpha\ell}{2}\right)+i\sqrt{\frac{\beta}{2\omega}}\right] \qquad 3.52a$$

Thus the harmonic terms of $\overline{T}$ become

$$\frac{Q_1}{\ell}[1+e^{-\alpha\ell}]\frac{\left[\left\{\left(\frac{\beta}{2\omega}\right)^{\frac{1}{2}}-\frac{1}{\alpha}\tanh\frac{\alpha\ell}{2}\right\}^2+\frac{\beta}{2\omega}\right]^{\frac{1}{2}}}{\left(\alpha^4+\frac{\omega^2}{\beta^2}\right)^{\frac{1}{2}}}\cos.\left(\omega t-\gamma+\theta'-\phi'\right) \qquad 3.53$$

where

$$\tan\theta'=\frac{\omega}{\beta\alpha^2}\ ,\ \tan\phi'=\frac{1}{\left(1-\frac{1}{\alpha}\sqrt{\frac{2\omega}{\beta}}\tanh\frac{\alpha\ell}{2}\right)} \qquad 3.53a$$

Also, since we have assumed that $\sqrt{\frac{\omega}{\beta}} \gg 1$. The spectrophone phase shifts θ' and ϕ' will approximate to a lead of 90° and a lag of 180° respectively.

For conditions encountered in the spectrophone the thermal diffusivity varies from about 0.1 to 1. Thus the approximations leading to (53) will hold for chopping frequencies greater than about 20 c.p.s. For lower frequencies the approximation does not hold and the full equation (51) and its complex conjugate must be used.

Finally from equations (44a), (48) and (53), the varying pressure amplitude in a spectrophone for which equation (3) holds will be:-

$$P = \frac{P_0}{T_0}\left[1+e^{-\alpha l}\right]\left\{Q_0 l^2\left[\frac{1}{2(\alpha l)^2} - \frac{1}{(\alpha l)^3}\tanh\frac{\alpha l}{2} - \right.\right.$$

$$\left.\left. - \frac{8}{\pi^5}\frac{l}{a}\sum_{\substack{1\\(m\ odd)}}^{\infty}\frac{I_1\left(\frac{m\pi}{l}a\right)}{I_0\left(\frac{m\pi}{l}a\right)}\frac{1}{m^3\left(m^2+\left(\frac{\alpha l}{\pi}\right)^2\right)}\right]\right.$$

$$+\frac{Q_1}{l}\left[\left(\sqrt{\frac{\beta}{2\omega}} - \frac{1}{\alpha}\tanh\frac{\alpha l}{2}\right)^2 + \frac{\beta}{2\omega}\right]^{\frac{1}{2}}\frac{1}{\left(\alpha^4 + \frac{\omega^2}{\beta^2}\right)^{\frac{1}{2}}}\cos\left(\omega t - \gamma + \theta' - \phi'\right)$$

3.54

D <u>Solution of the equation of heat conduction in the spectrophone, treating the gas as compressible</u>

Here the equation to be solved is

$$\rho_0\frac{C_v}{K}\frac{\partial v}{\partial t} = \nabla^2 v + \frac{H}{K} + q'$$

(equation (1))

for the same system and boundary conditions as those used in the solution of the incompressible fluid equation in Part C (above).

To find q', the compressional energy released/sec., consider a small mass of gas with volume δV.

$$q' = \frac{\partial}{\partial t}(P\delta V)$$

but since varying pressure amplitude is small, i.e. $\frac{p}{P_0} \ll 1$

$$q' \simeq P_0\frac{\partial(\delta V)}{\partial t}$$

Now for any given mass of gas $\rho\delta V$ = constant

Therefore $q' = \frac{P_o}{\rho} \frac{\partial \rho}{\partial t} . \delta V$

and again assuming the density change is small compared with the equilibrium density, the above relation becomes

$$q' = \frac{P_o}{\rho_o} \frac{\partial \rho}{\partial t} \delta V$$

and for unit volume

$$q' = \frac{P_o}{\rho_o} \frac{\partial \rho}{\partial t} \qquad 3.55$$

This expression (3.55) is a definite approximation since in the steady state process the mean values of density and pressure will not be P_o and ρ_o.

Now from the equation of state of the gas

$$P = \rho RT$$

$$\frac{\partial P}{\partial t} = RT \frac{\partial \rho}{\partial t} + R\rho \frac{\partial T}{\partial t}$$

from which we get, using the same approximation as above and putting $P = P_o$, $\rho = \rho_o$ and $T = T_o$, it follows that

$$\frac{\partial p'}{\partial t} = \frac{P_o}{\rho_o} \frac{\partial \rho}{\partial t} + \frac{P_o}{T_o} \frac{\partial T}{\partial t}$$

Therefore $q' = \left[\frac{\partial p}{\partial t} - \frac{P_o}{T_o} \frac{\partial T}{\partial t} \right]$ 3.56

Thus (1) becomes

$$\nabla^2 T - \frac{1}{K}\left[\rho_o C_v + \frac{P_o}{T_o}\right] \frac{\partial T}{\partial t} + \frac{1}{K} \frac{\partial P}{\partial t} + \frac{H}{K} = 0 \qquad 3.57$$

Impressing a harmonic solution for the varying amplitudes of pressure and temperature

$$p = \rho e^{i\omega t}$$
$$v = v e^{i\omega t}$$

Giving

$$\nabla^2 v - \frac{i\omega \rho_0 C_p}{K} v + \frac{i\omega}{K} p + \frac{H}{K} e^{-\alpha z} = 0 \qquad 3.58$$

Alao recalling that from the acoustic boundary conditions in the cell

$$p = \frac{P_0}{V_0 T_0} \int_{V_0} v \, dV \qquad 3.44$$

$$\nabla^2 v - \frac{i\omega \rho_0 C_p}{K} v + \frac{i\omega P_0}{K V_0 T_0} \int_{V_0} v \, dV + Q' e^{-\alpha z} \qquad 3.59$$

where the heat input from internal modes Q' is

$$Q' = Q_i e^{i(\omega t - \gamma)} \qquad 3.60$$

Introducing notation

$$A = \frac{i\omega}{K} \frac{P_0}{T_0 V_0}$$

$$k^2 = \frac{i\omega \rho_0 C_p}{K} \qquad 3.59a$$

(50) becomes in polar cylindrical coordinates

$$\frac{\partial^2 v'}{\partial r^2} + \frac{1}{r}\frac{\partial v'}{\partial r} - \kappa_m^2 v' + \frac{A}{\sigma}(1-(-1)^m)\int_{V_0} v\,dV + \frac{Q'\sigma}{\alpha^2+\sigma^2}\left[1-(-1)^m e^{-\alpha\rho}\right] = 0 \qquad 3.63$$

where $\sigma = \frac{m\pi}{\rho}$

$$\kappa_m^2 = (\kappa^2+\sigma^2)$$

Now introducing notation

$$\frac{i\omega}{K}\frac{P_0}{T_0 V_0}\frac{(1-(-1)^m)}{\sigma} = \frac{A}{\sigma}(1-(-1)^m) \equiv U \qquad \therefore$$

and $$\frac{Q'\sigma}{\sigma^2+\alpha^2}(1-(-1)^m e^{-\alpha\rho}) \equiv B \qquad 3.63a$$

Equation (63) reduces to

$$\frac{\partial^2 v'}{\partial r^2} + \frac{1}{r}\frac{\partial v'}{\partial r} - \kappa_m^2 v' + B + U\int_{V_0} v\,dV = 0$$

which is written as

$$\frac{\partial^2 v}{\partial r^2} + \frac{1}{r}\frac{\partial v'}{\partial r} - \kappa_m^2 v' = -F \qquad 3.64$$

where

$$\frac{\partial^2 v}{\partial r^2} + \frac{1}{r}\frac{\partial v}{\partial r} + \frac{\partial^2 v}{\partial z^2} - k^2 v + A\int_{V_0} v\,dV + Q' e^{-\alpha z} = 0$$

3.61

The boundary conditions are as before.

$v = 0$ at $z = 0$, $z = l$

$v = 0$ at $r = a$ and finite when $r \to 0$

} for all time

Applying a finite Fourier sine transform for the z variable in the interval z(0 to l)

If $v = v' = \int_0^l v \sin\frac{m\pi}{l} z \cdot dz$. we obtain

$$\frac{\partial^2 v'}{\partial r^2} + \frac{1}{r}\frac{\partial v'}{\partial r} - \left(\frac{m^2\pi^2}{l^2} + k^2\right) v' + \int_0^l \left[A\int_{V_0} v\,dV\right] \sin\frac{m\pi}{l} z \cdot dz$$

$$+ Q' \frac{m\pi}{l}\left(1 - (-1)^m e^{-\alpha l}\right) \frac{1}{\alpha^2 + \left(\frac{m\pi}{l}\right)^2} = 0$$

3.62

Although v is a function of z, $\int_{V_0} v\,dV$ is not

hence

$$\int_0^l A\int_{V_0} v\,dV \sin\frac{m\pi}{l} z\,dz = A\int_{V_0} v\,dV \int_0^l \sin\frac{m\pi}{l}\,dz$$

$$= A\frac{l}{m\pi}\left(1 - (-1)^m\right)\int_{V_0} v\,dV$$

giving

$$F = \left[U \int_{V_0} v \, dV + B \right]$$

Equation (64) is Bessel's modified equation of order zero which has solution (for given boundary conditions)

$$v' = \frac{F}{\kappa_m^2} - \frac{F}{\kappa_m^2} \frac{I_0(\kappa_m r)}{I_0(\kappa_m a)} \qquad 3.65$$

Applying the inverse Fourier transform gives

$$v = \frac{2}{\ell} \sum_{m=1}^{\infty} \frac{F}{\kappa_m^2} \left(1 - \frac{I_0(\kappa_m r)}{I_0(\kappa_m a)} \right) \sin \frac{m\pi}{\ell} z. \qquad 3.66$$

Consider next $\int_{V_0} v \, dV$

$$\int_{V_0} v \, dV = \int_0^{2\pi} \int_0^{a} \int_0^{\ell} v \cdot r \, dr \, dz \, d\xi = 2\pi \int_0^{a} \int_0^{\ell} v \cdot r \, dr \, dz \equiv I$$

Therefore from (66)

$$I = \frac{4\pi}{\ell} \int_0^{a} \int_0^{\ell} \sum_{m=1}^{\infty} \left(\frac{U \cdot I + B}{\kappa_m^2} \right) \left[1 - \frac{I_0(\kappa_m r)}{I_0(\kappa_m a)} \right] \sin \frac{m\pi}{\ell} z \cdot r \, dr \, dz.$$

Assuming the series is convergent and may be integrated term by term, the order of integration and summation may be reversed, giving

$$I = \frac{4\pi}{\ell} \sum_{m=1}^{\infty} \left\{ \int_0^a \int_0^{\ell} \frac{(UI+B)}{\kappa_m^2} \left(1 - \frac{I_0(\kappa_m r)}{I_0(\kappa_m a)}\right) \sin \frac{m\pi}{\ell} z \; r \, dr \, dz \right\}$$

3.67

Integrating with respect to r.

$$I = \frac{4\pi}{\ell} \sum_{m=1}^{\infty} \left\{ \int_0^{\ell} \frac{(UI+B)}{\kappa_m^2} \left[\frac{a^2}{2} - \frac{a}{\kappa_m} \frac{I_1(\kappa_m a)}{I_0(\kappa_m a)}\right] \sin \frac{m\pi}{\ell} z \, dz \right.$$

Integrating with respect to z.

$$I = \frac{4\pi}{\ell} \sum_{m=1}^{\infty} \frac{(UI+B)}{\kappa_m^2} \left[\frac{a^2}{2} - \frac{a}{\kappa_m} \frac{I_1(\kappa_m a)}{I_0(\kappa_m a)}\right] \frac{1}{\sigma} \left(1 - (-1)^m\right)$$

3.68

Provided that each constituent series is absolutely convergent it is possible to break (68) up into two parts.

$$I = \frac{4\pi}{\ell} \sum_{m=1}^{\infty} \frac{UI}{\kappa_m^2} \left[\frac{a^2}{2} - \frac{a}{\kappa_m} \frac{I_1(\kappa_m a)}{I_0(\kappa_m a)}\right] \frac{1}{\sigma} \left(1 - (-1)^m\right)$$

$$+ \frac{4\pi}{\ell} \sum_{m=1}^{\infty} \frac{B}{\kappa_m^2} \left[\frac{a^2}{2} - \frac{a}{\kappa_m} \frac{I_1(\kappa_m a)}{I_0(\kappa_m a)}\right] \frac{1}{\sigma} \left(1 - (-1)^m\right)$$

3.69

Furthermore I itself, provided the sums are finite, is not a function of m,

and may be taken outside the summation sign of the first term in (69) above.

$$I = \frac{4\pi}{\rho} I \sum_{m=1}^{\infty} \frac{U}{\kappa_m^2}\left[\frac{a^2}{2} - \frac{a}{\kappa_m}\frac{I_1(\kappa_m a)}{I_0(\kappa_m a)}\right]\frac{1}{\sigma}\left(1-(-1)^m\right)$$

$$+ \frac{4\pi}{\rho}\sum_{m=1}^{m} \frac{B}{\kappa_m^2}\left[\frac{a^2}{2} - \frac{a}{\kappa_m}\frac{I_1(\kappa_m a)}{I_0(\kappa_m a)}\right]\frac{1}{\sigma}\left(1-(-1)^m\right)$$

so that

$$I = \frac{4\pi}{\rho}\sum_{m} \frac{B}{\kappa_m^2}\left[\frac{a^2}{2} - \frac{a}{\kappa_m}\frac{I_1(\kappa_m a)}{I_0(\kappa_m a)}\right]\frac{\left(1-(-1)^m\right)}{\sigma} \quad \div$$

$$\div \left\{1 - \frac{a}{\sqrt{\kappa^2 + \frac{m^2\pi^2}{\rho^2}}}\frac{4\pi}{\rho}\sum_{m} \frac{U}{\kappa_m^2}\left[\frac{a^2}{2} - \frac{a}{\kappa_m}\frac{I_1(\kappa_m a)}{I_0(\kappa_m a)}\right]\frac{\left(1-(-1)^m\right)}{\sigma}\right\} \qquad 3.70$$

or

$$I = \frac{4\pi Q'}{l}\left(1+e^{-\alpha\rho}\right)\sum_{m=1}^{\infty}\frac{\left(1-(-1)^m\right)}{\left(\alpha^2 + \frac{m^2\pi^2}{\rho^2}\right)}\frac{1}{\left(\kappa^2 + \frac{m^2\pi^2}{\rho^2}\right)} \times$$

$$\times\left[\frac{a^2}{2} - \frac{a}{\sqrt{\kappa^2 + \frac{m^2\pi^2}{\rho^2}}}\frac{I_1(\kappa_m a)}{I_0(\kappa_m a)}\right]$$

$$\div$$

$$\left[1 - \frac{8\pi}{\rho} A \sum_{m=1}^{\infty} (1-(-1)^m) \frac{\rho^2}{m^2\pi^2 \left(\kappa^2 + \frac{m^2\pi^2}{\rho^2}\right)} \left[\frac{a^2}{2} - \frac{a}{\sqrt{\kappa^2 + \frac{m^2\pi^2}{\rho^2}}} \frac{I_1(\kappa_m a)}{I_0(\kappa_m a)}\right]\right]$$

3.71

Comparing this equation with (3.50) in Part C, it will be seen that the expression for I above is identical with the harmonic part of $V_{\overline{r}}$ given in (50) (provided that $\kappa^2 \equiv \frac{i\omega}{\beta}$) except for the extra term in the denominator which is obviously a correction factor arising from consideration of compressional effects in the gas.

Thus the numerator in (71) may be treated exactly as for the harmonic terms in the last part. The complete expression being (cf. (51))

$$\text{Numerator} = \frac{Q\ell a^2[1+e^{-\alpha\ell}]}{(\alpha^2 - \kappa^2)} \left[\frac{1}{x} \tanh\frac{x\pi}{2} - \frac{1}{u}\tanh\frac{u\pi}{2} - \frac{a\rho}{\pi}(u^2-x^2) \sum_{\substack{m=1 \\ (m\,\text{odd})}}^{\infty} \frac{I_1(\kappa_m a)}{I_0(\kappa_m a)} \times \frac{1}{\left[m^2+u^2\right]\left[m^2+x^2\right]^{3/2}}\right]$$

3.71a

where $x^2 = \frac{\kappa^2\rho^2}{\pi^2}$

$u^2 = \frac{\alpha^2\rho^2}{\pi^2}$

On approximating as before, so that the frequency of chopping is high enough so that the last term may be neglected, the numerator of (71) becomes

$$\text{Numerator} = \frac{Q'\pi a^2\left[1+e^{-\alpha\ell}\right]}{\sqrt{\alpha^4+\kappa^4}}\left[\left(\sqrt{\frac{1}{2|\kappa^2|}}-\frac{\tanh\left(\frac{\alpha\ell}{2}\right)}{\alpha}\right)^2+\frac{1}{2|\kappa^2|}\right]^{\frac{1}{2}} e^{i(\theta'-\phi')}$$

3.61b

where $\tan\theta' = \frac{|\kappa^2|}{\alpha^2} = \frac{\omega\rho_0 C_\rho}{K\alpha^2}$

$$\tan\phi' = \frac{1}{\left(1-\frac{1}{\alpha}\sqrt{2|\kappa^2|}\tanh\frac{\alpha\ell}{2}\right)}$$

$$= \left(1-\frac{1}{\alpha}\sqrt{\frac{2\omega\rho_0 C_\rho}{K}}\tanh\frac{\alpha\ell}{2}\right)^{-1}$$

Considering the denominator of (71)

$$\text{Denominator} = 1-\frac{16\pi}{\ell}A\sum_{\substack{m=1\\(m\ \text{odd})}}^{\infty}\frac{\ell^2}{m^2\pi^2}\frac{1}{\left(\kappa^2+\frac{m^2\pi^2}{\ell^2}\right)}\left[\frac{a^2}{2}-\frac{a}{\sqrt{\kappa^2+\frac{m^2\pi^2}{\ell^2}}}\frac{I_1(\kappa_m a)}{I_0(\kappa_m a)}\right]$$

$$= 1-\frac{16\ell^3}{\pi^3}A\sum_{\substack{m=1\\(m\ \text{odd})}}^{\infty}\frac{1}{m^2}\frac{1}{(m^2+x^2)}\left[\frac{a^2}{2}-\frac{\ell a}{\pi\sqrt{x^2+m^2}}\frac{I_1(\kappa_m a)}{I_0(\kappa_m a)}\right.$$

which may be split up since all series are absolutely convergent, giving

$$\text{Denominator} = 1 - 16\frac{\rho^3}{\pi^3}A\left\{\frac{a^2}{2x^2}\sum_{(m\ \text{odd})}^{\infty}\frac{1}{m^2} - \frac{a^2}{2x^2}\sum_{(m\ \text{odd})}^{\infty}\frac{1}{m^2+x^2} - \right.$$
$$\left. - \frac{\rho a}{\pi}\sum_{m=1}^{\infty}\frac{I_1(\kappa_m a)}{I_0(\kappa_m a)}\frac{1}{m^2(m^2+x^2)^{3/2}}\right\} \qquad 3.72$$

Summing the first two series:-

$$\text{Denominator} = 1 - 16\frac{\rho^3}{\pi^3}A\left\{\frac{a^2\pi^2}{16x^2} - \frac{a^2\pi}{8x^3}\tanh\frac{\pi x}{2}\right.$$
$$\left. - \frac{\rho a}{\pi}\sum_{m=1}^{\infty}\frac{I_1(\kappa_m a)}{I_0(\kappa_m a)}\frac{1}{m^2(m^2+x^2)^{3/2}}\right\} \qquad 3.73$$

The third series converges rapidly.

Equation 3.73 gives the exact form of the correction term. If the

same approximation with respect to chopping frequency is applied here as to the numerator, then we have that the third term is negligible compared with the first two. Leaving:-

$$\text{Denominator} = 1 - \frac{2\rho^3 a^2 A}{\pi^2 x^2}\left\{\frac{\pi}{2} - \frac{1}{x}\tanh\frac{x\pi}{2}\right\}$$

$$\text{Denominator} = 1 - 2AV_0\left[\frac{1}{2} - \frac{1}{\kappa\rho}\tanh\frac{\kappa\rho}{2}\right]$$

Approximating $\quad \frac{1}{\kappa\rho}\tanh\frac{\kappa\rho}{2} \simeq \frac{1}{2\rho}\sqrt{\frac{2K}{\omega\rho_0 C_\rho}}(1-i)$

$$\text{Denominator} = 1 - \frac{AV_0}{K^2}\left[1 - \frac{s}{\rho}(1-i)\right]$$

$$\left(\text{where } s = \sqrt{\frac{2K}{\omega\rho_0 C_\rho}}\right)$$

$$= 1 - \frac{P_0}{T_0 C_\rho \rho_0}\left[\left(1 - \frac{s}{\rho}\right) + i\frac{s}{\rho}\right]$$

$$= \frac{R}{C_\rho \rho}\left\{\left[\frac{C_\rho \rho}{R} - \rho + s\right] - is\right\}$$

where R = the gas constant for 1 gram,

$$= \frac{R}{C_\rho \rho}\left[\left(\frac{C_\rho \rho}{R} - \rho + s\right)^2 + s^2\right]^{\frac{1}{2}} e^{-i\psi'}$$

$$\text{where } \tan\psi' = \frac{S}{\left(\frac{C_p l}{R} - l + S\right)} \qquad 3.74a$$

Thus the complete approximate solution for I is

$$I = Q\pi a^2 \frac{\left[1+e^{-\alpha l}\right]}{\sqrt{\alpha^4+\kappa^2}} \frac{C_p l}{R} \frac{\left[\left(\sqrt{\frac{1}{2|\kappa^2|}} - \frac{1}{\alpha}\tanh\frac{\alpha l}{2}\right)^2 + \frac{1}{2}\frac{1}{|\kappa^2|}\right]^{\frac{1}{2}}}{\left[\left(\frac{C_p l}{R} - l + S\right)^2 + S^2\right]^{\frac{1}{2}}} e^{i(\theta'-\phi'+\psi')} \qquad 3.75$$

Hence from equation 3.44, the amplitude of the pressure variations in the spectrophone will be

$$p = \frac{P_0}{T_0} \frac{Q_t\left[1+e^{-\alpha l}\right]}{\sqrt{\alpha^4+\kappa^4}} \frac{C_p}{R} \frac{\left[\left(\sqrt{\frac{1}{2|\kappa^2|}} - \frac{1}{\alpha}\tanh\frac{\alpha l}{2}\right)^2 + \frac{1}{2}\frac{1}{|\kappa^2|}\right]}{\left[\left(\frac{C_p l}{R} - l + S\right)^2 + S^2\right]^{\frac{1}{2}}} e^{i(\omega t-\gamma+\theta'-\phi'+\psi')} \qquad 3.76$$

E Analysis of theoretical results

(i) Validity of assumptions

Before drawing any conclusions from the results of the previous sections it is first necessary to justify the various assumptions made.

a) The assumption made in obtaining equation 3.10 was

$$\frac{\eta\omega}{C^2} \ll 1 \quad \text{or} \quad \frac{\rho_1(\gamma) B_{01}(1+g)\omega}{C^2} \ll 1 \qquad 3.77$$

As shown in Part B (above), the value of $\rho_1(\gamma)B_{01}$ for typical experimental conditions is $\sim 10^{-2}$.

The experimental value of ω in the present work was never less than 10^3 so that for (77) to hold the value of C^2 should be $\gg 10$ sec^{-2}. This effectively means a relaxation time $\ll 5 \times 10^{-1}$ sec. For lower chopping frequencies the relaxation time can be correspondingly longer. In the present work (77) should hold under all experimental conditions employed.

b) In Parts C and D the assumption was made that $\frac{\omega}{\beta} \gg 1$, in order to simplify the general expressions for $\bar{\tau}$. β (the thermal diffusivity) is always < 10 in the present experiment so that this assumption should hold well for the chopping frequencies used.

c) The assumption was made in defining the system to be analysed, that the spectrophone walls were absolutely rigid. This assumption is modified on two counts. Firstly, the microphone diaphragm is obviously not rigid but has a finite impedance. Secondly, the gas inlet tube, if not completely sealed at the chamber wall, constitutes a finite impedance to any pressure generated in the cell.

The effect of non-rigid walls may be incorporated into the theory in the following way, assuming harmonic solutions for the excess temperature, pressure and density.

Instead of equation (35) we have

$$\frac{V_0 P}{P_0} = \int_{V_0} \frac{\Delta\rho\, dV}{\rho_0} + \int_{V_0} \frac{\nu\, dV}{T_0} \qquad 3.78$$

where $\int_{V_o} \Delta\rho \, dV$ is not now zero, due to the finite volume displacement.

If the chamber volume at any instant is $V = V_o + \Delta V$, where

$$\Delta V = \Delta V \, e^{i\omega t}$$

then from the conservation of mass in the spectrophone

$$\rho \Delta V = - \int_{V_o} \Delta\rho \, dV \qquad 3.78a$$

or approximately

$$\rho_o \Delta V = \int_{V_o} \Delta\rho \, dV$$

Thus 3.79

$$\frac{\rho V_o}{P_o} = \int_{V_o} \frac{v \, dV}{T_o} - \Delta V$$

3.79

Introducing the acoustic impedance as presented by the walls to the gas in the cell. (Z)

$$\frac{dV}{dt} = i\omega \Delta V = \frac{-P}{Z} \qquad 3.80$$

Therefore

$$\frac{P V_o}{P_o} = \int_{V_o} \frac{v \, dV}{T_o} - \frac{-P}{i\omega Z}$$

$$P = \frac{P_o}{V_o T_o} \int_{V_o} \frac{v \, dV}{\left(1 + \frac{P_o}{V_o i\omega Z}\right)} \qquad 3.81$$

which reduces to (44) if $Z \longrightarrow \infty$. The impedance due to the microphone diaphragm will be at frequencies well below the diaphragm resonance, that of a pure compliance. For the commercial Bruel and Kjaer condenser microphone it should be extremely high, with an equivalent volume of less than 0.2 cm.

The impedance of the gas inlet tube will depend upon its radius (b). (see, for example, Olson - 'Acoustic Engineering'[76]).

If $b > 10\sqrt{\frac{\eta}{\rho_0 \omega}}$ where η = coefficient of viscosity then neglecting radiation impedance it can be shown that

$$Z \simeq \sqrt{\frac{2\eta\rho_0\omega}{\pi b^3}} \cdot d + j\left(\frac{\rho_0 d\omega}{\pi b^2} + \sqrt{\frac{2\eta\rho_0\omega}{\pi b^3}} \cdot d\right) \qquad 3.82$$

where d = length of the tube. This is valid for tubes of about $0.1 \sim 1$ cm. radius. For very small tubes for which $b < \sqrt{\frac{\eta}{\rho_0 \omega}}$, other flow conditions exist, and

$$Z \simeq \frac{d}{\pi b^2}\left(\frac{8\eta}{b^2} + i\frac{4}{3}\omega\rho_0\right) \qquad 3.83$$

In the present spectrophone equation (3.83) should hold.

The spectrophone cavity and inlet tube could theoretically form a Helmholtz resonator of resonant frequency

$$f = \frac{c}{2\pi}\sqrt{\frac{\pi b^2}{d.V_0}} \qquad 3.84$$

(although this will be modified by the viscous damping). However if b is small, since the resistance $\propto \frac{1}{b^4}$ in (83) such a resonance will be

heavily damped, and the impedance due to the inlet tube, which is acoustically sealed in the present apparatus, almost infinite.

The geometric boundary conditions premised in Part A are well justified experimentally, except for thosepertaining to the incident radiation. The actual incident radiation amplitude at the window, does not closely approximate to a form $I_o e^{i\omega t}$ as assumed, where $I_o \neq f(r\phi)$. The system of mechanical chopping inevitably leads to i) a non-sinusoidal time variation at any point on the window, ii) a phase lag across the width of the window, resulting in a non-uniform intensity over the window surface at any instant of time. Effect (i) will mean that besides the fundamental component, harmonics will be generated in the spectrophone. Since the excited state population of molecules is always $\ll$ than the ground state population, the principle of superposition should hold for all frequency components and the tuned detecting system should extract the fundamental with little interference or loss of sensitivity. With regard to (ii), experimental tests (to be described in Chapter 4) show that non-uniformity of irradiation has no effect upon the experimental phase-shifts. This is to be expected for a spectrophone used within its proper chopping frequency range (as discussed in the next section), where the phase and amplitude of the pressure variations should be independent of the spatial distribution of the heat input.

(ii) Conclusions

As discussed in the previous section, the solutions obtained for the

varying pressure in the spectrophone, given by equations (54) and (76) should be valid for quite a wide range of chopping frequency. The lower frequency limit, i.e. $\frac{\omega}{\beta} \gg 1$ essentially means that the acoustic period must be much smaller than the characteristic time in which heat may be conducted to the walls from the interior of the gas. The higher frequency limit is set by the assumption of identical pressure in the chamber. For the spectrophone used in this research, the range of frequency for which the theory is valid is quite large, from about 20 - 1000 c/s.

Looking at (54) and (76) in detail, the most important factors from the viewpoint of vibrational relaxation time measurements, are the phase shifts between the heat input into the gas, from the internal modes, and the resulting pressure amplitude which is detected by the microphone. These "spectrophone" phase shifts are due to the translational energy redistribution process determined by the thermal and acoustic boundary conditions. In the case of (54) they are ϕ' and θ where

$$\tan\theta' = \frac{\omega}{\beta\alpha^2}$$

$$\tan\phi' = \frac{1}{\left(1 - \frac{1}{\alpha}\sqrt{\left(\frac{2\omega}{\beta}\right)}\tanh\alpha\ell\right)}$$

(76) has in addition ψ', where

$$\tan\psi' = \sqrt{\frac{2K}{\omega\rho_0 C_p}}\left[\frac{C_p\ell}{R} - \ell + \sqrt{\frac{2K}{\omega\rho_0 C_p}}\right]^{-1}$$

due to the inclusion of the compressional energy term. It will be seen that for high enough values of ω, for which the solutions (54) and (76) are themselves valid, the spectrophone phase shifts tend to whole multiples of $\frac{\pi}{4}$, viz.

$$\left.\begin{array}{l} \theta' \longrightarrow \text{a lead of } \frac{\pi}{4} \\ \phi' \longrightarrow \text{a lag of } \frac{\pi}{4} \end{array}\right\} \quad \theta' + \phi' \longrightarrow 0$$

$$\psi' \longrightarrow 0$$

so that the net spectrophone phase shift tends to zero.

Furthermore, provided that ω is large, say 10^3, θ', ϕ' and ψ' are relatively insensitive to changes in the other variables, such as C_p, ρ_0, α. Thus generally quite unrealistic changes in gas density, heat conductivity or integrated absorption coefficient are needed if the spectrophone phase shift is to change appreciably from zero. This is, of course, a relative matter and depends upon the resoltuion of the spectrophone and the magnitude of the relaxation time to be measured. In this experiment, the resolution of the apparatus is such that for all gases and gas mixtures used, for the chopping frequencies used, then the spectrophone phase shifts are effectively zero. This point is vital for the "calibrating gas" method of using the spectrophone, where it is essential for similarity to exist between the two gases, with respect to all non-relaxation phase shifts. The fact that for reasonable experimental conditions, the spectrophone phase shift tends to zero is

in complete agreement with Delany, Montan and other workers in their theoretical treatments.

A final point to make is that the phase shifts given by ϕ', θ' and ψ' will only be of use where the necessary resolution is such that such small phase changes need to be computed. They will not be used for conditions outside the range where these phase shifts are small, for in this case (54) and (76) will not be valid and the full expressions for $\overline{v}$ and p must be used.

CHAPTER 4

APPARATUS AND EXPERIMENTAL PROCEDURE

The apparatus was constructed on the same basic principles as that first developed by Delany. The purpose is to measure the phase difference between the acoustic signal obtained from the spectrophone and the incident infra-red radiation. This is achieved by having an auxiliary light beam modulated at the same time as the radiation and which via a photocell will give an electrical signal in phase with it. This signal is used as the reference channel in a conventional phasemeter. For descriptive purposes the apparatus may be divided into four parts; the spectrophone, gas handling system, optical system, and electronics.

(I) Spectrophone

The spectrophone cell was made from a block of aluminium. The gas inlet plate, window and microphone holders were constructed of copper and aluminium with P.T.F.E. insulation. The chamber is cylindrical in shape, of length 6 cm, and diameter 2.5 cm with optical windows at each end. The chamber has provision for two microphones to be set facing each other half way along the axis. This is to allow the investigation of the acoustic properties of the chamber by the reciprocity technique, and was an important feature of the original Delany spectrophone.

Initially condenser microphones were designed and constructed for use in the spectrophone. Figure 13 shows a diagram of the

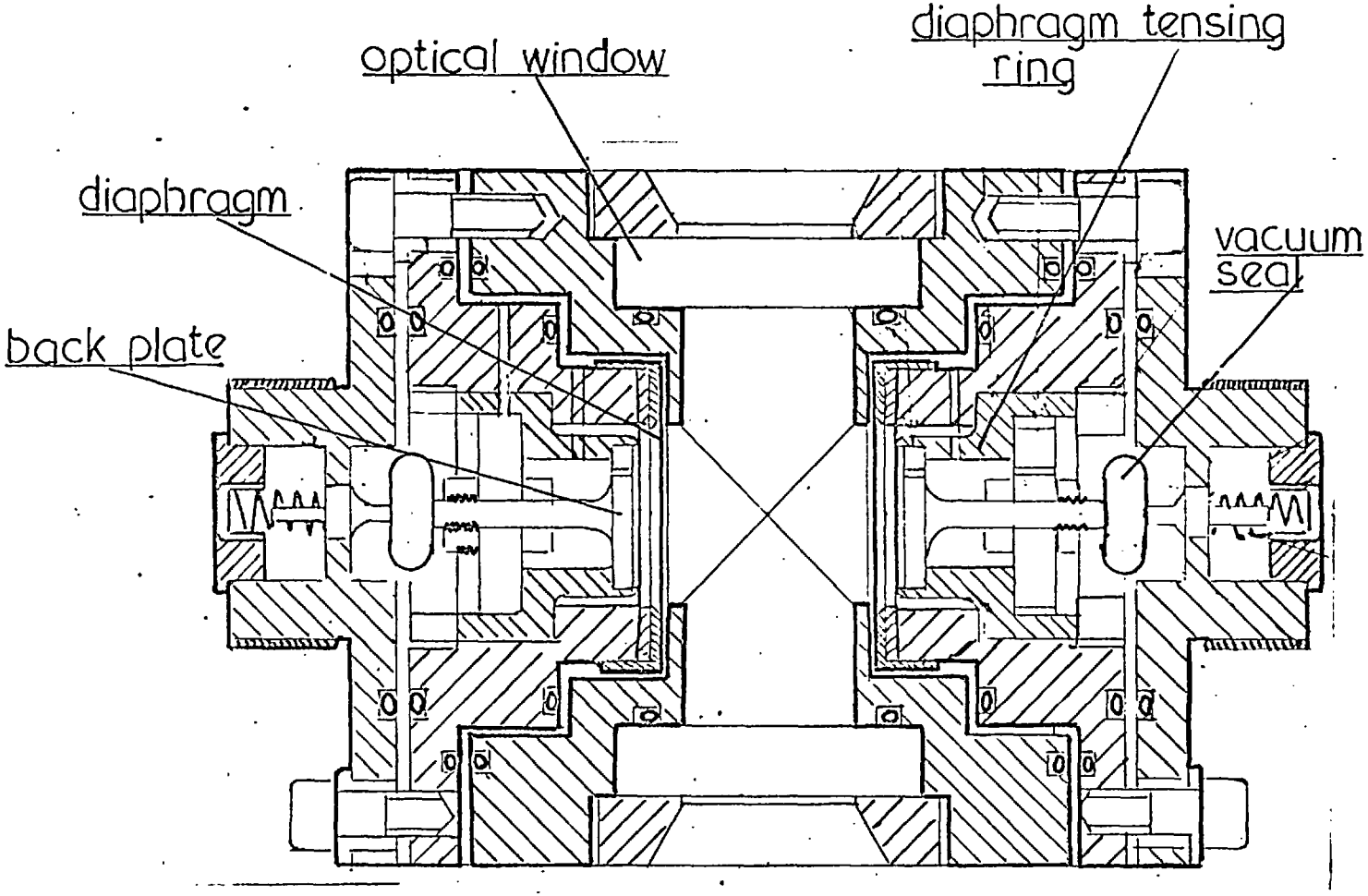

FIG 13 Plan of spectrophone fitted with special condenser microphones

spectrophone fitted with these microphones. The construction was of brass, copper and aluminium with metallized 25 gauge Melinex polyester film used for diaphragms. These were one inch in diameter, secured by a copper clamping ring and stretched by means of an accurately machined nylon tensing ring. By means of a finely threaded nut, the brass backplate could be moved relative to the diaphragm to an accuracy of .00025". The microphones were vacuum tight when fixed in the chamber and provision was made in the gas inlet plate for pressure equalization, as shown in Figure 14.

Later, it was decided to use Bruel and Kjaer condenser microphones (Type 4131) and these were fitted to the spectrophone in specially made holders. The microphones were rendered vacuum tight by means of a special coupler between the microphone cartridge and its cathode follower. This was found to lower the microphone sensitivity by one or two db, but had no other effect upon performance. Figure 14 shows a diagram of the spectrophone fitted with a B and K microphone. The microphone was sealed into the chamber behind the capsule pressure equalization vent. Figure 15a shows a photograph of the assembled spectrophone together with a B and K microphone and one of the laboratory built microphones. Figures 15b and 15c show photographs of the "home-made" condenser microphone assembly, and the B and K microphone and holder.

Gas was admitted into, and evacuated from the chamber through a special gas inlet plate attached to the top of the spectrophone, as shown in Figure 14. This incorporated a Wilson seal allowing the

FIG 14

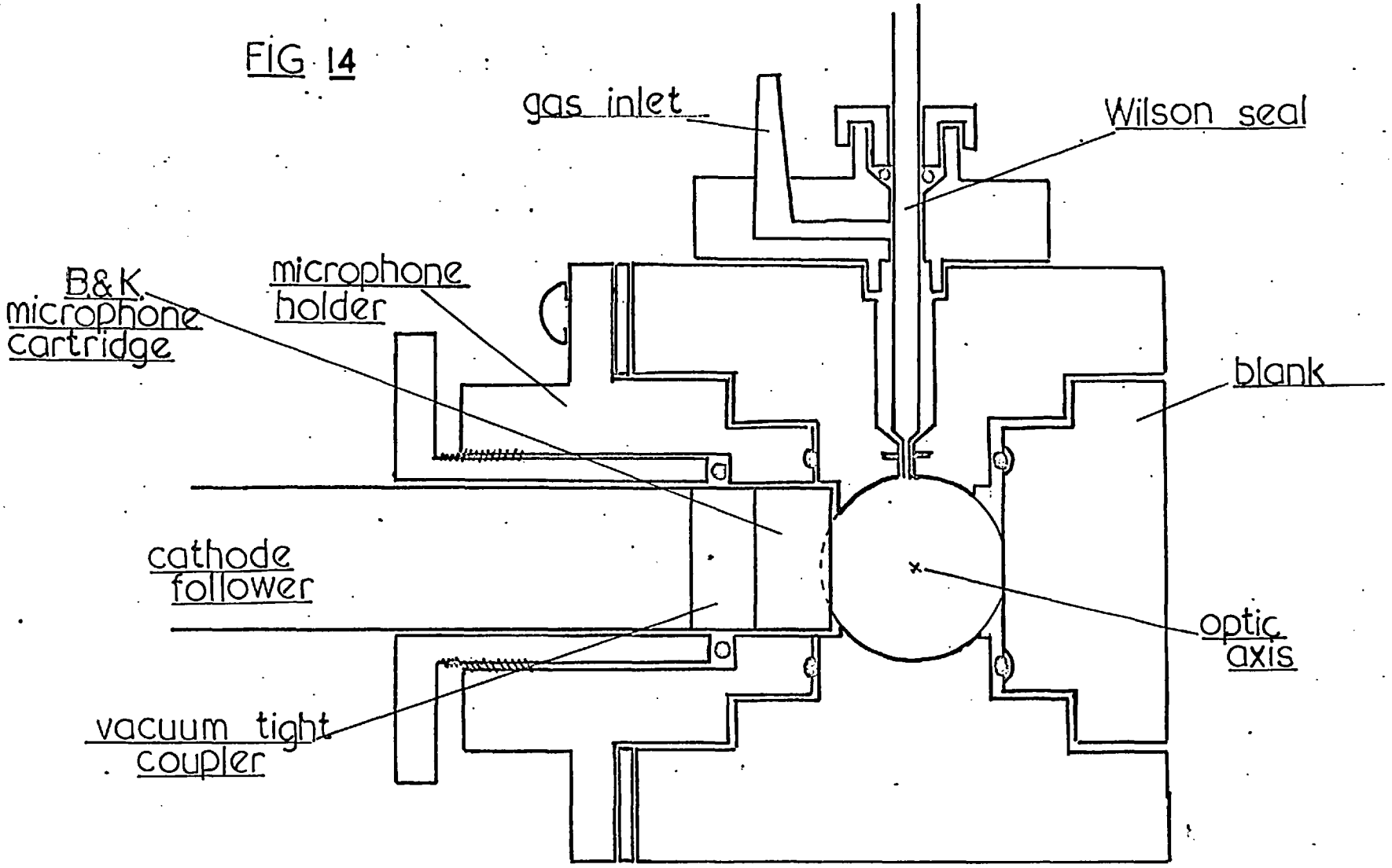

DIAGRAM OF SPECTROPHONE. (Fitted with BRUEL & KJAER microphone)

FIG 15 a

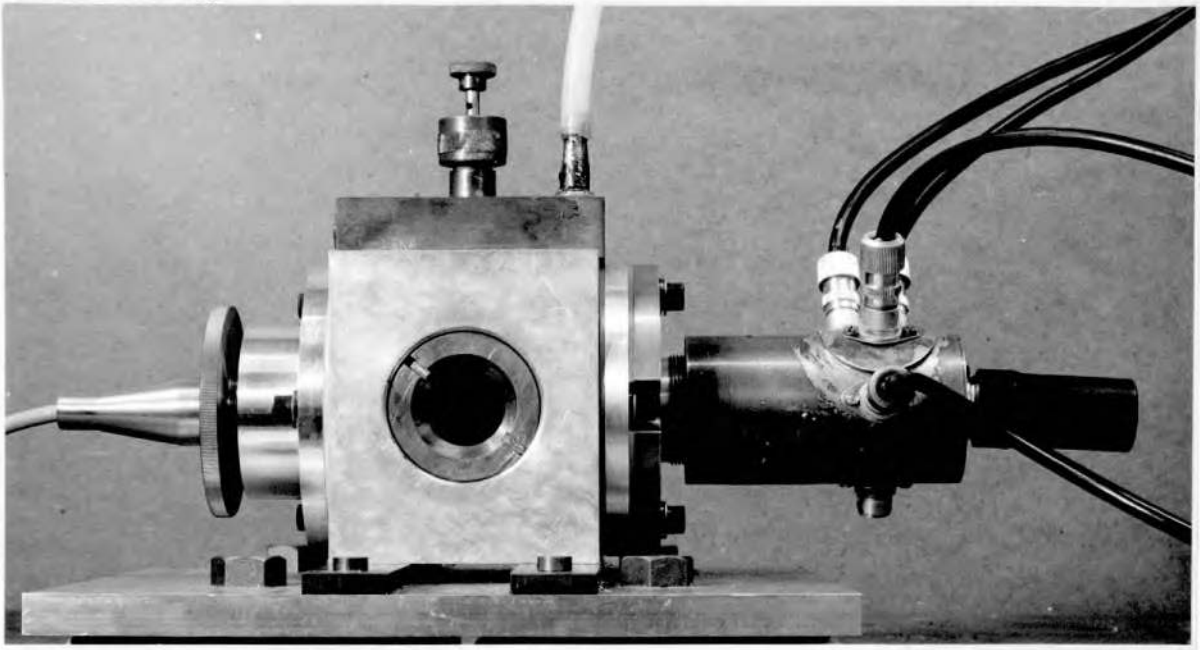

b

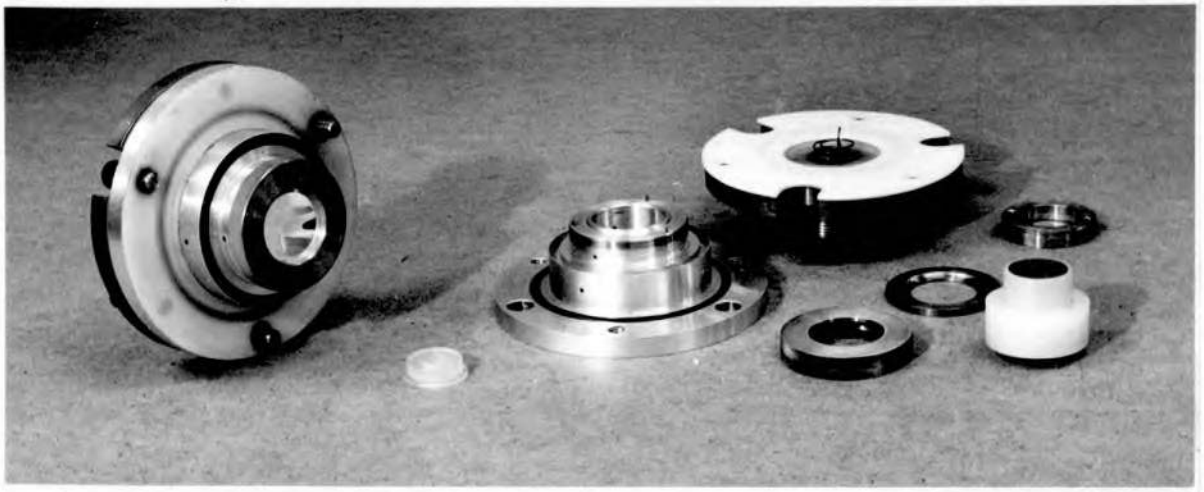

c

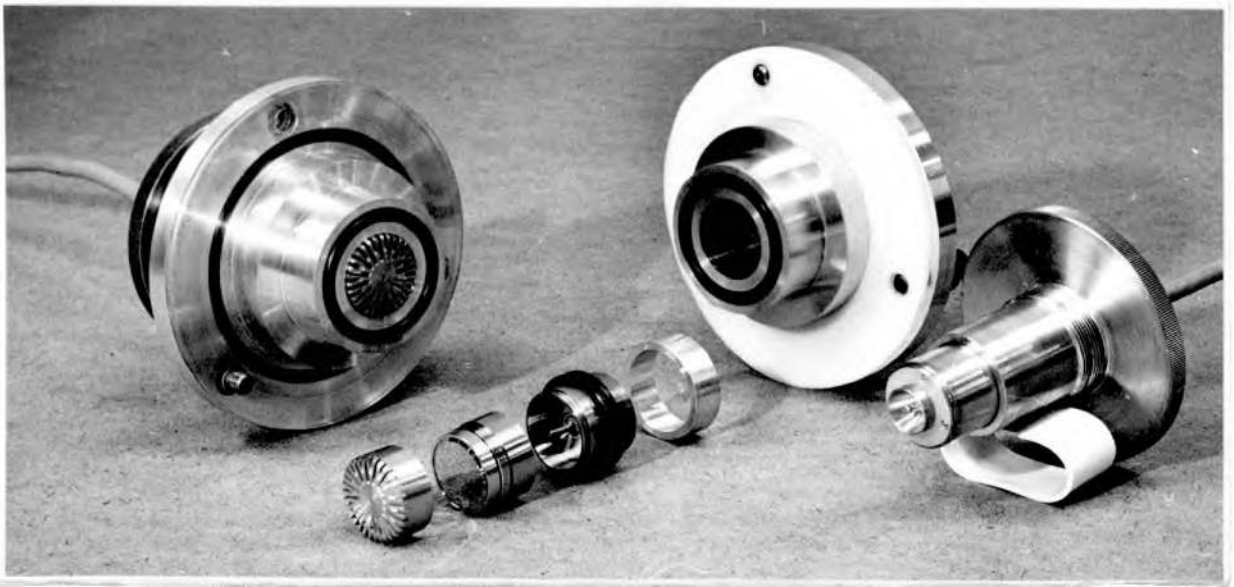

opening to the chamber (and in the case of the specially constructed microphones, the pressure equalization vents) to be acoustically sealed during the taking of measurements. The chamber was made vacuum tight at the windows, and microphones by use of high temperature viton 'O' rings.

The acoustic behaviour of the spectrophone was investigated by the reciprocity technique as described by Delany. Since phase is the primary quantity measured in the spectrophone, the phase response of the microphones was measured as well as the amplitude response. The B and K oscillator type 1012, with compressor controlled output, was used as a driving source in the calibrations.

Figure 16 shows the phase responses of a B and K microphone and the two specially made condenser microphones (designated 1 and 2) as a function of frequency, as measured in the spectrophone cell. The gas was air at atmospheric pressure. The resonances occurring at high frequency are probably due to chamber effects and help to fix practically the upper limiting frequency permissible in the spectrophone, as discussed in Chapter 3.

Figure 17 shows the relative signal amplitude obtained from the receiving microphone in the chamber as a function of frequency for the B and K microphone and laboratory built microphone 1 (curves A and B). The driving transducer in each case was microphone 2. As an example of the importance of acoustic considerations in spectrophone work, curve C shows the amplitude response of microphone 1, measured similarly to curve B except that the microphone pressure

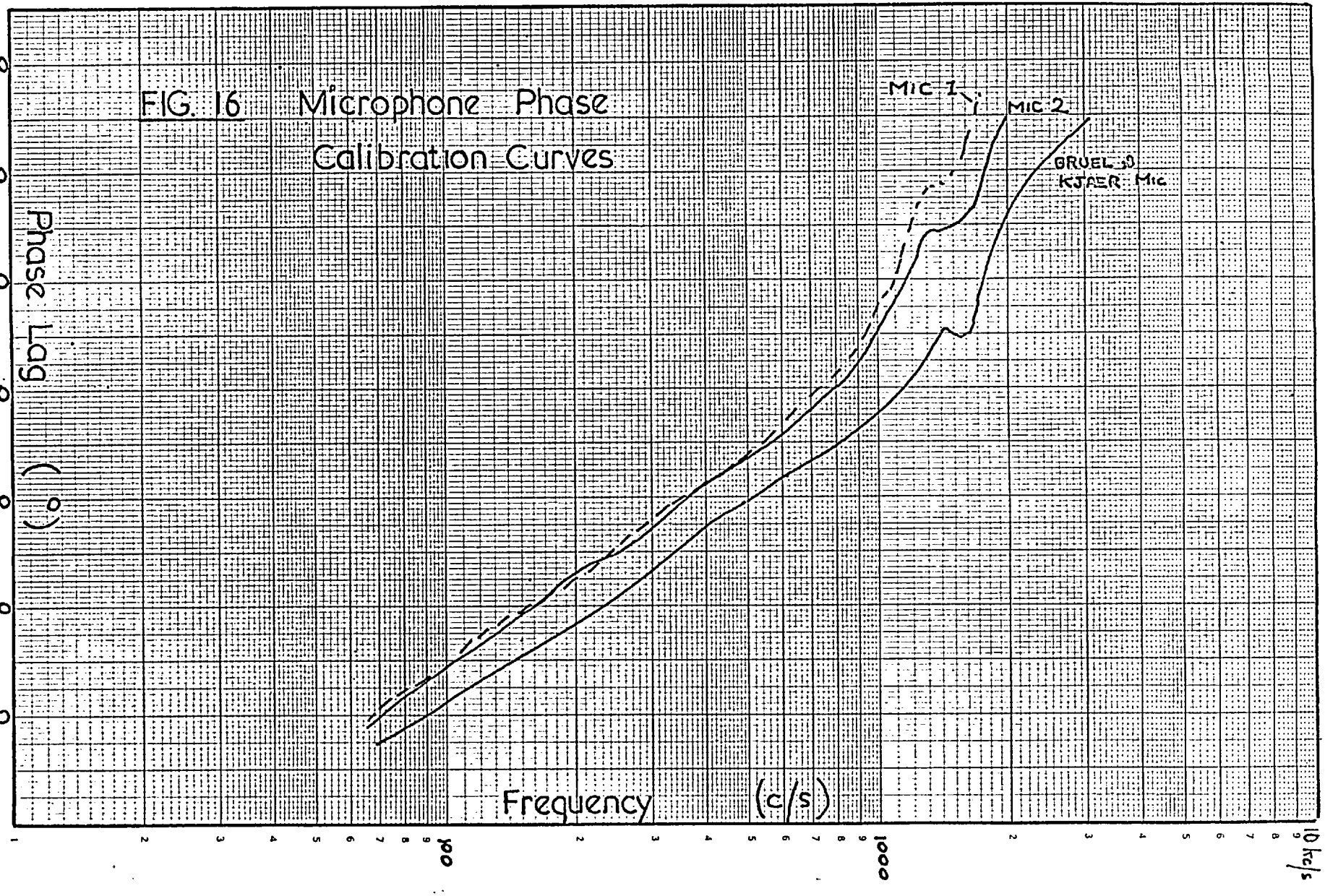
FIG. 16 Microphone Phase
Calibration Curves
MIC 1
MIC 2
BRUEL & KJAER Mic
Phase Lag (°)
60
50
40
30
20
10
0
Frequency (c/s)
100
1000
10 kc/s

equalization vents were not blocked. There are many extra resonances at low frequencies; these are probably due to Helmholtz resonator effects. Curve D shows the response of microphone 1 driven by microphone 2 in a small 8 cc. coupler.

The changes in phase response of the spectrophone to changes in ambient pressure and gas density were investigated. Figure 18 shows the phase response of the B and K microphone in the chamber for carbon dioxide, ethane, and helium, all at 480 torr pressure. The microphone phase lag decreases with the density of the gas, but for carbon dioxide and ethane, the main experimental and calibrating gases, there is only a one or two degree difference over the experimental range of the apparatus.

The phase response of the B and K microphone over the frequency range 50 - 1 Kc/s remained quite constant with variation in pressure down to about 80 torr when some fall in phase lag occurred. Carbon dioxide and ethane gave approximately the same fall-off, but with light gases such as helium the effect was greater.

By fitting a microphone in a special holder, into the optical window cavity, the effect of the position of the receiving microphone on the phase and amplitude response was checked. No difference was found below 1.4 k c/s, supporting the assumption of identical pressure in the cell. This assumption was further tested by checking the phase response of microphones in the correct and window positions using the optic-acoustic signal obtained from radiation entering the other window. The response remained unaffected by all changes in the angle of incidence or aperture of the radiation beam, except that the laboratory built

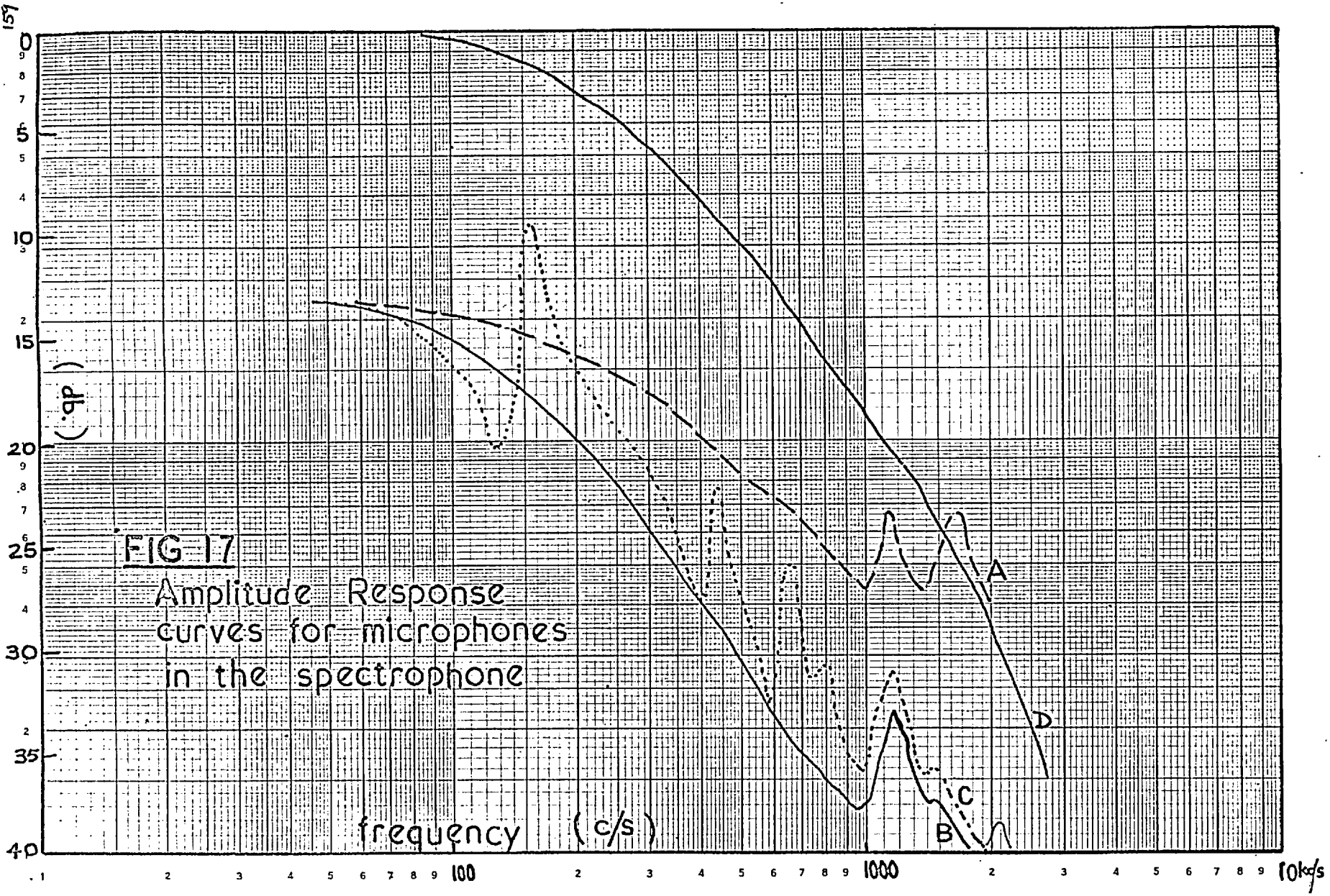

FIG 17

Amplitude Response curves for microphones in the spectrophone

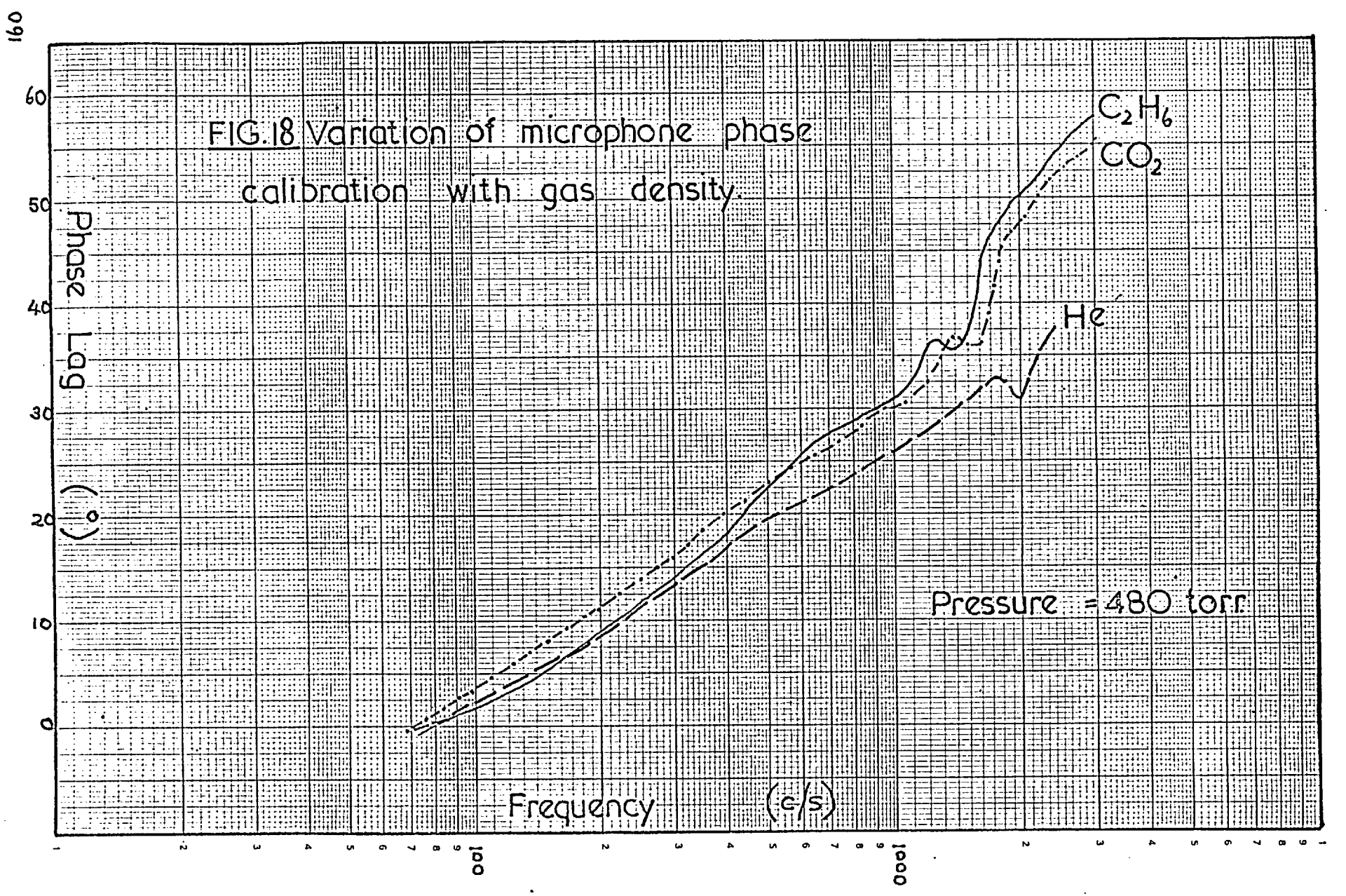
FIG. 18 Variation of microphone phase calibration with gas density.
Phase Lag (°)
Frequency (c/s)
C_2H_6
CO_2
He
Pressure = 480 torr
160
60
50
40
30
20
10
0
100
1000

microphones had an appreciable phase variation with the amplitude of the incoming radiation. For this main reason, together with their greater sensitivity to changes in chamber pressure and gas density, these microphones were rejected in favour of the B and K microphone.

(II) Gas handling apparatus

A schematic diagram of the gas handling system is shown in Figure 19. Pyrex glass was used for the connecting tubes, except for short lengths of nylon tubing connecting the system to the chamber and to the gas cylinders. The stainless steel mixing unit is totally enclosed and rotated by the force of an external magnet upon a bar of mild steel fixed to the bottom of the unit. The magnet is mounted upon the shaft of a variable speed motor. The oil diffusion pump was also made of glass and formed an integral part of the system. The glass stop-cocks were probably the least satisfactory part of the system, requiring frequent cleaning and re-greasing. Metal diaphragm valves would probably have proved superior.

A McLeod gauge, reading to 10^{-5} torr, was used to measure the pressure in the chamber, and a Pirani gauge reading to 10^{-4} torr, the pressure in the mixing and filling sections. The latter was also extremely useful for locating small leaks.

It is of first importance in vibrational relaxation measurements to obtain as clean and leak-free a system as possible, because of the strong effect of certain impurity molecules on the relaxation. Thus the spectrophone cell and parts were vacuum baked, before assembly, and as much as possible of the glass tubing heated when in position and under vacuum, to drive off occluded gases. The nylon tubing was

FIG. 19 Diagram of gas-handling system.

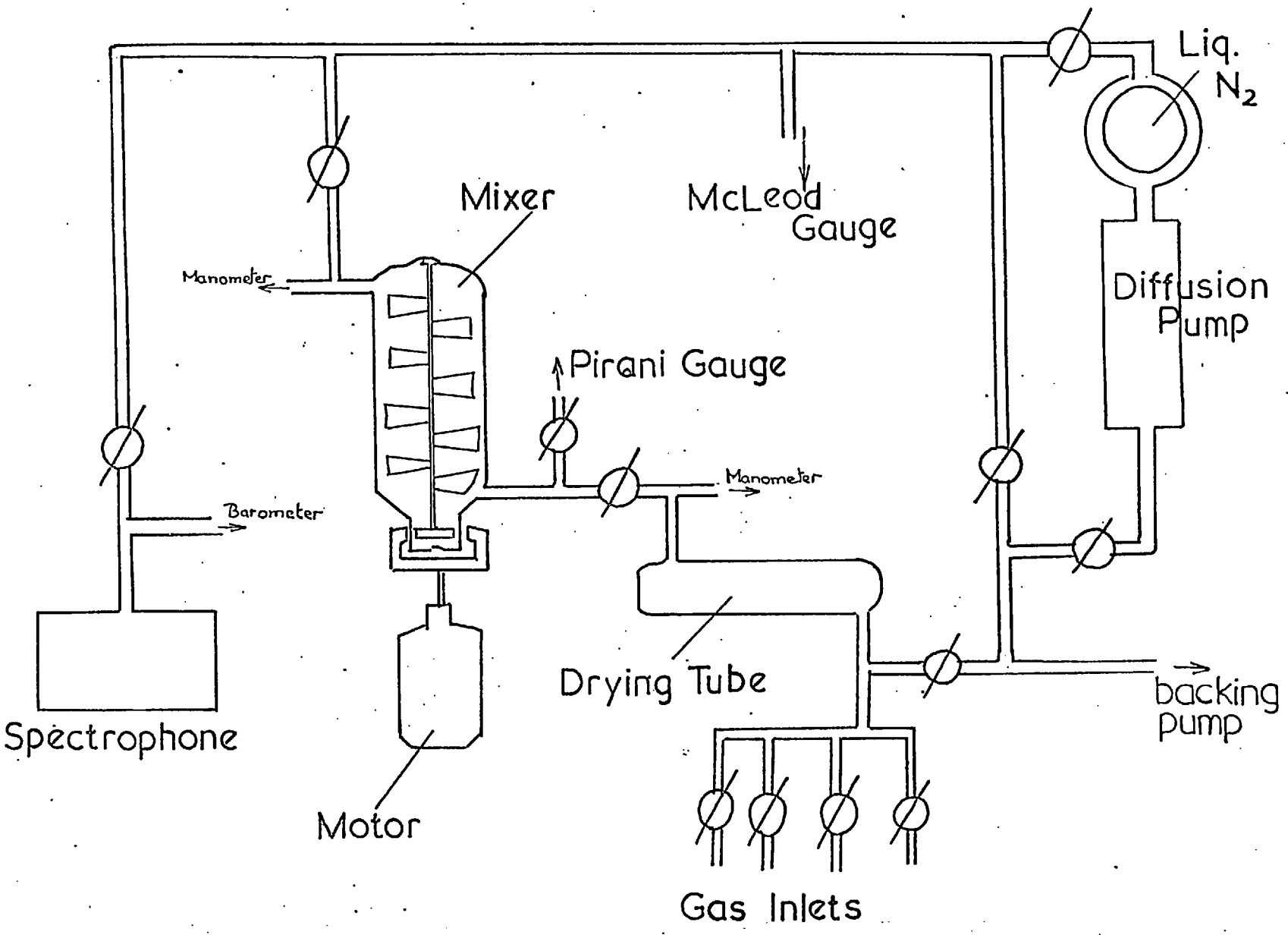

also vacuum baked at 100°C. In addition, it was found that with the B and K microphone fixed in the chamber it was possible to bake the evacuated spectrophone in situ at 100°C by means of a small aluminium box fitted with heating elements which could be lowered over the chamber. Under optimum conditions the whole apparatus could be pumped down to better than 10^{-5} torr. On shutting off the pump, the pressure in the spectrophone remained lower than 10^{-4} torr for about four minutes, and better than 10^{-3} for periods of over an hour. The pressure in the mixer and drying tube remained below 10^{-3} indefinitely.

During the filling of the apparatus with gas, the pressure in the chamber was measured by a mercury barometer and, in the filling and mixing sections, by mercury manometers.

Carbon dioxide and nitrous oxide were the gases investigated in the present work. The carbon dioxide was obtained from the Distiller's Company. It was of 'analytical' grade, with a specified residual gas impurity < 20 p.p.m. and water vapour impurity < 40 p.p.m. The nitrous oxide was obtained from the medical division of the British Oxygen Company. No detailed specification was available, although a supply of gas from the same source was found to contain 20 p.p.m CO_2 and an appreciable amount of water vapour. The calibrating gases were obtained from the Infra-red Development Company, and were of commercial grade. Argon was also obtained from the same company. This was called "100% Argon" and had a specified purity of 25 p.p.m. residual gas impurity (mainly nitrogen) and 8 p.p.m. H_2O. The other noble gases were obtained in glass bottles at N.T.P. from the British

Oxygen Company. Helium and neon were described as spectroscopically pure, with purity guaranteed to 99.99%, the chief residual impurity being nitrogen. The krypton was of a similar purity except for 0.1% xenon, whilst the xenon had 2% krypton impurity.

No further purification of the gases was attempted except for drying over phosphorous pentoxide.

(III) Optical System

The optical set-up used was extremely simple. The arrangement may be seen in Figure 20. The source of infra-red radiation was a Nernst filament mounted horizontally. The radiation was reflected from an aluminised concave mirror and brought to a focus at the modulating slits. The modulating system consisted of a fixed but adjustable horizontal slit placed just behind a rotating chopping disc. This was made of steel, 11 in. diameter, having forty accurately cut circular holes of 9/16 in. diameter equally spaced round the circumference at a distance of 5 in. from the centre. Thus radiation was modulated by a circular aperture moving across a fixed slit. By focussing the beam at a point between disc and slit, it was possible with this system to obtain an approximately sinusoidal radiation input to the spectrophone.

The reference light channel, arranged diametrically opposite the spectrophone channel, utilized a galvanometer light source. To prevent leakage of light between the two channels the adjustable slits were set in a solid plate completely separating the motor, chopper and light sources from the rest of the apparatus. The chopping disc was rotated by a $\frac{1}{4}$ h.p. d.c. motor, the disc being dynamically balanced to the motor shaft. The motor speed was controlled by a Servomex

Type M.C.43 servo-motor controller, by which means the chopping frequency could be held constant to $\pm$ 0.3 c/s at 1 kc/s, with negligible drift.

The spectral range of the radiation entering the spectrophone was limited by a suitable choice of chamber window and infra-red filter. The optical window materials used were caesium iodide (transparent to 60μ), rock salt (transparent to 15μ), and arsenic trisulphide glass (transparent to 8μ). Filters available were short wavelength indium antimonide and glass filters and long-pass interference filters. The latter were simply mounted behind the slit plate in cardboard holders.

(IV) Electronic apparatus

A block diagram of the electronic apparatus is shown in Figure 20. The reference signal from the photocell is amplified and passed through a filter set at the fundamental chopping frequency. This is necessary to obtain a clean enough signal for the reference input of the phasemeter. The optic-acoustic signal passes from the microphone cathode follower to a tuned amplifier again tuned at the fundamental frequency. For the B and K microphone, the B and K Wave Analyser Type 2105 was used on 25 db tuning. The phasemeter was a Solartron Resolved Component Indicator Type VP 250, giving in phase and quadrative R.M.S. voltages with respect to the reference voltage.

The waveform of the reference signal, and the frequency were monitored by an oscilloscope and frequency counter respectively. Tests showed that the phase of the reference channel remained quite constant over the normal time taken to complete a measurement, but

FIG 20 Block Diagram of Apparatus

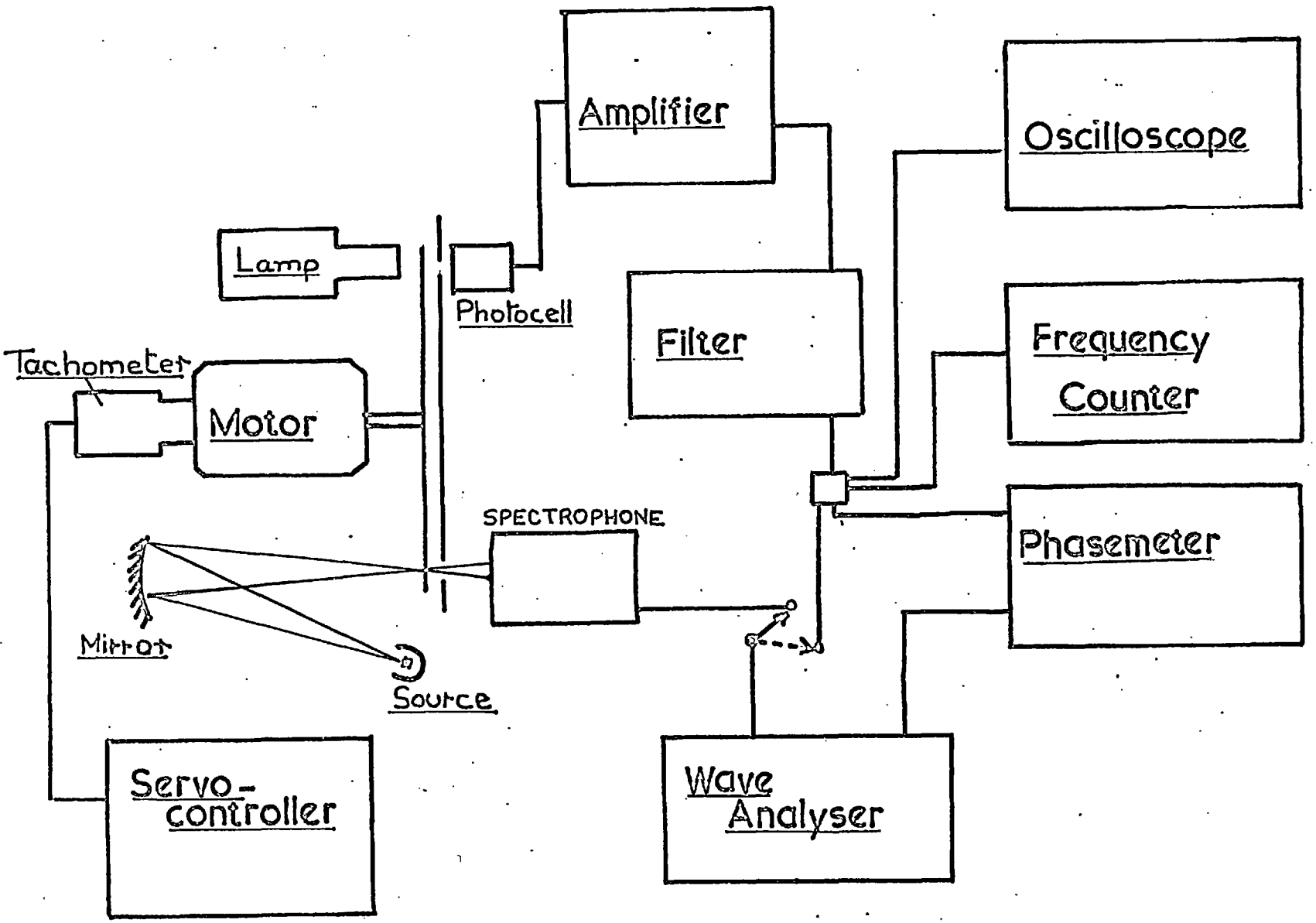

that the phase of the signal channel could vary randomly over several degrees in the same period due to small changes in frequency taking the wave analyser off tune. Hence it was necessary to measure the phase characteristic of the analyser, using the reference signal, immediately before and after each optic-acoustic phase measurement.

Precautions were taken to avoid vibrations from the chopping motor and backing pump, causing noise in the signal channel. The chopping motor was bolted to a large mass of several hundredweight standing on a bench separate from the rest of the apparatus. This bench stood upon foam rubber antivibration pads. The backing pump was positioned upon the laboratory floor, also on foam rubber, and connected to the apparatus via flexible P.V.C. tubing. The noise level (with the B and K microphone in the chamber) was below readable level on the 100 μvolt scale of the wave analyser when tuned to 800 c/s, and about 60 μv on broad band.

Figures 21 and 22 are photographs showing the apparatus from different viewpoints.

(V) Experimental Procedure

One microphone was used in the chamber during the taking of measurements, the other being replaced by an aluminium blank. Before admitting gas, the whole apparatus was pumped down to at least 5×10^{-5} torr. Gas was then admitted to the drying and mixing sections, still keeping the chamber under vacuum. The chamber was flushed with dried gas two or three times before finally filling to the desired pressure. Once the gas was in the spectrophone the phase reading

FIG 21a

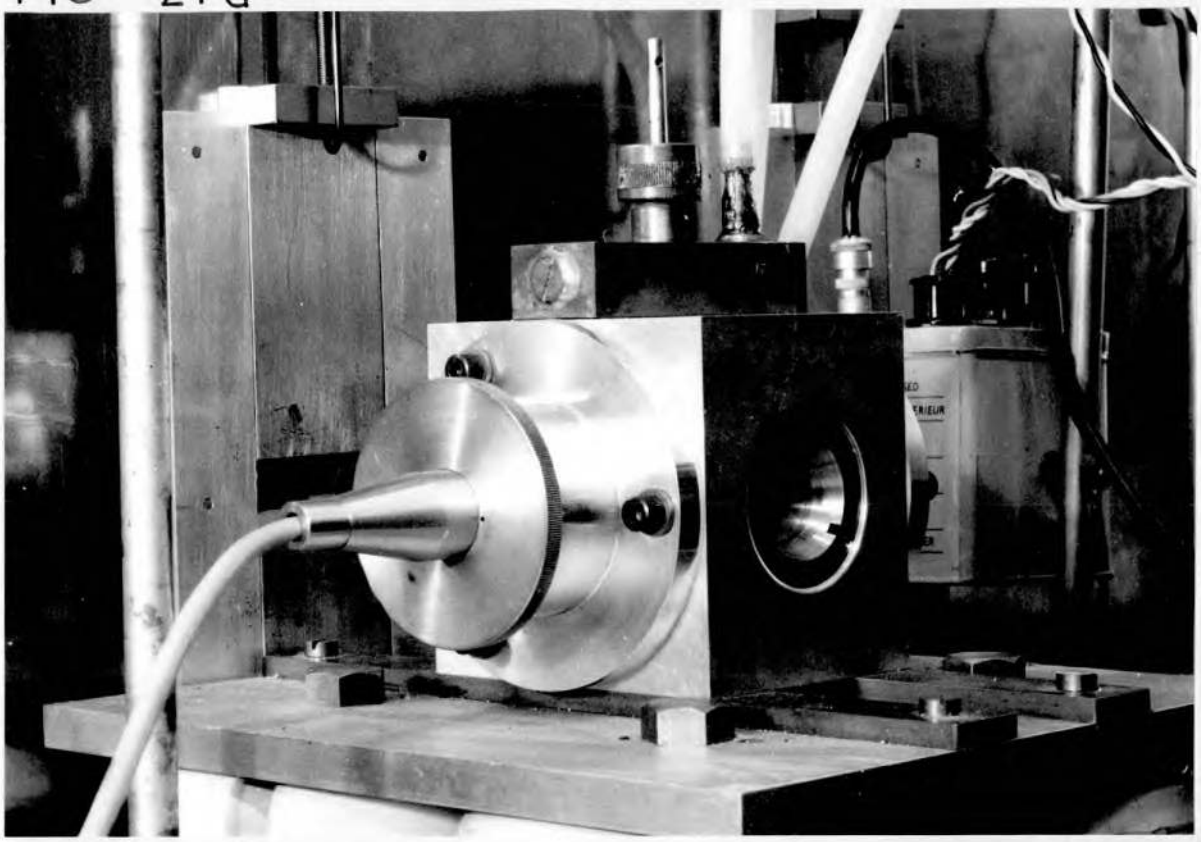

b

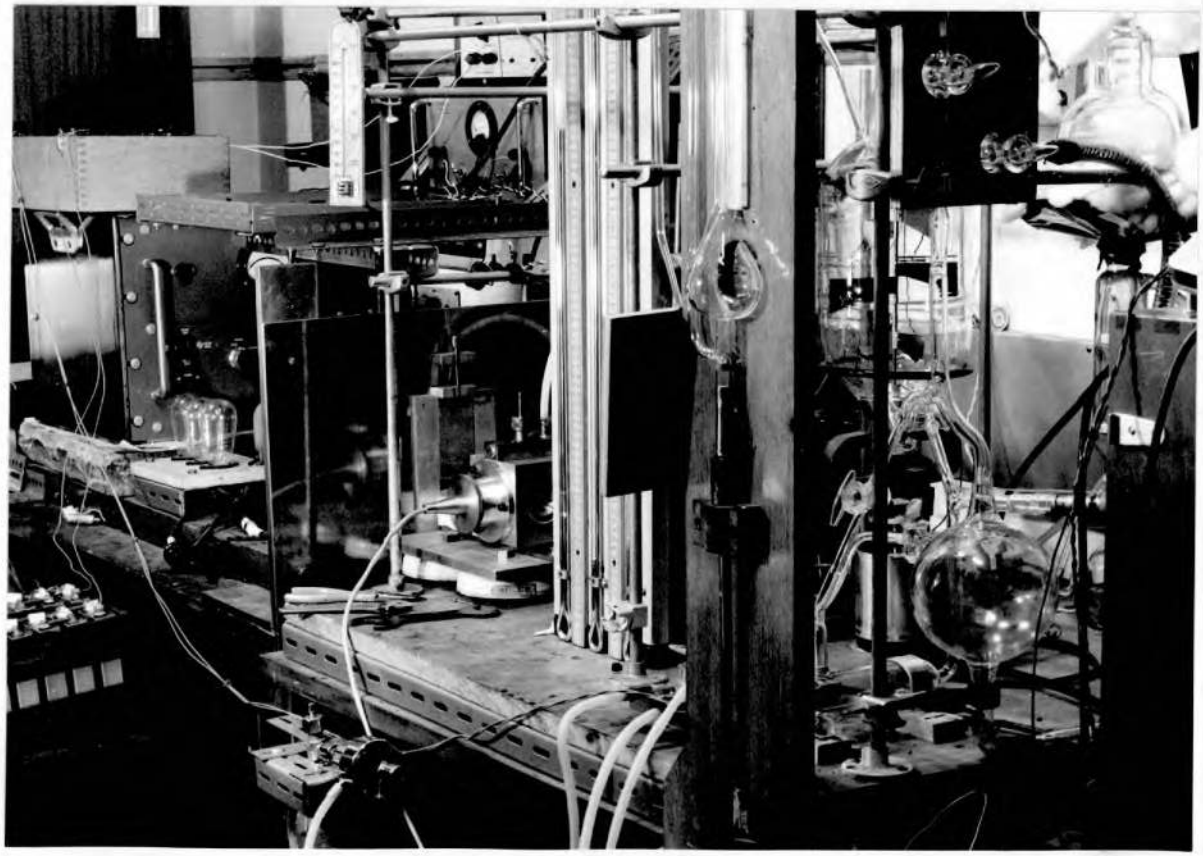

FIG 22

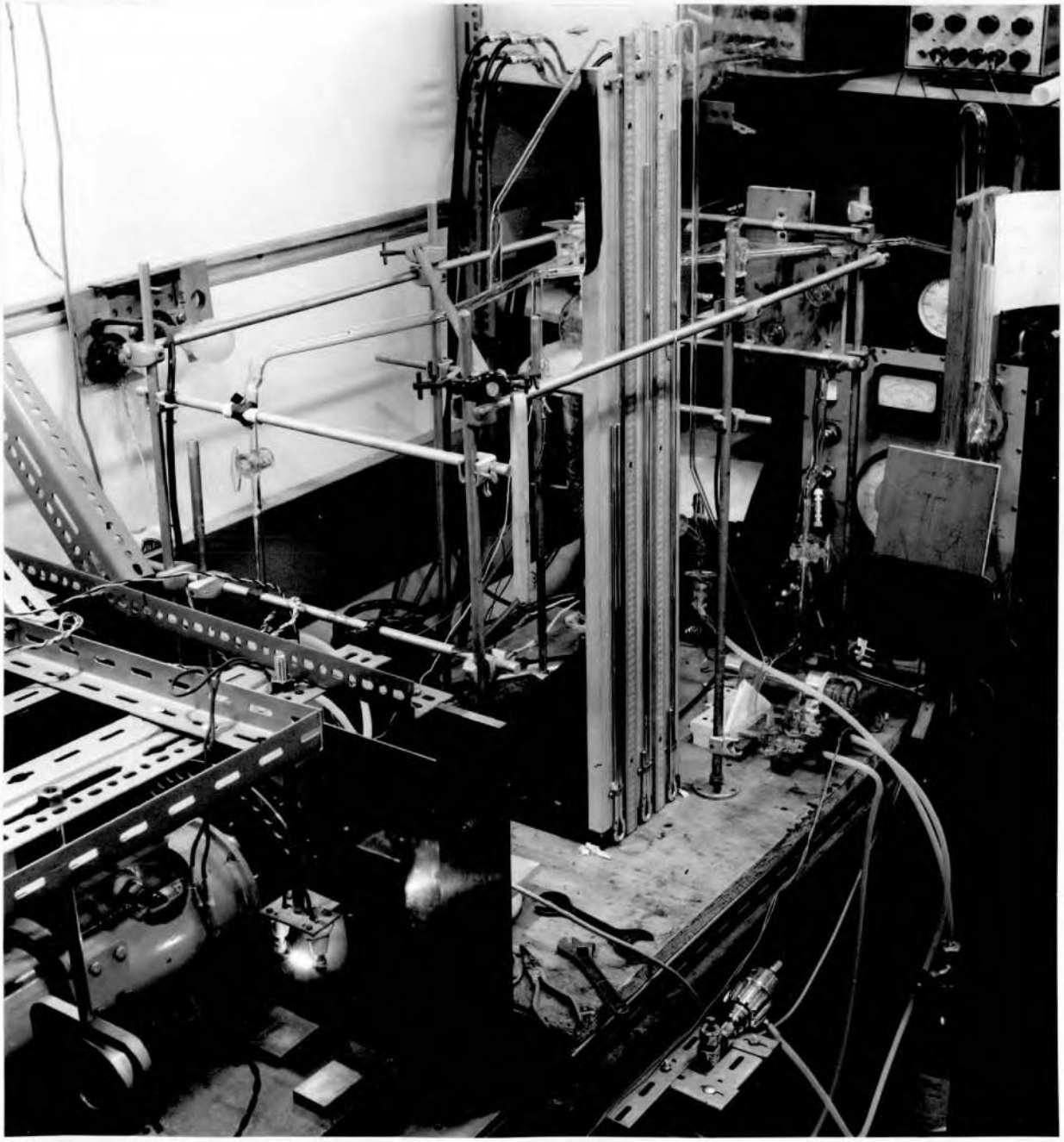

was taken as quickly as possible (~ 1 minute) and each charge of gas was only used for one measurement. The phase characteristic of the wave analyser was measured immediately before and after each reading. For mixtures the gases were stirred together vigorously for two minutes.

The experimentally measured phase shift ϕ between the reference channel and optic-acoustic signal consists of three parts. These are i) χ the relaxation phase lag, 11) ϕ_s the 'spectrophone' phase lag as given in equations 53a and 74 of Chapter 3, iii) ϕ_I the instrumental phase shift due to misalignment of the optical slits and phase shifts in the electronic apparatus and microphone. From the results of Chapter 3, ϕ_s should be negligible for chopping frequencies inbetween an upper and a lower limit. For the present apparatus these limits should be about 50 c/s and 1 kc/s. In order to eliminate the instrumental phase shifts, the calibrating gas technique was adopted. Instrumental phase shifts should be independent of spectrophone conditions for a given gas pressure and frequency. Furthermore they should be approximately constant or at least slow varying. The principle of the calibration, as first suggested by Professor Decius at Oregon, is to measure the instrumental phase shifts using a relaxing gas in the spectrophone, whose relaxation time is shorter than the smallest resolvable time of the apparatus. Thus for the calibrating gas, χ will be effectively zero, and providing $\phi_s = 0$, then $\phi_{exptl.} = \phi_I$. It is important to ensure that for both the gas under investigation and the calibrating gas, the spectrophone

phase shift $\phi_s = 0$ at the modulation frequency used. The present apparatus has a lower limit to measurable relaxation times of a few tenths of a microsecond at one atmosphere pressure. Thus ethane and its immediate homologues with well established relaxation times of the order of 10^{-8} sec. [9][77] and large integrated absorption coefficients, were considered suitable. Three of these gases, ethane, propane and n-butane were tried, and Figure 23 shows experimental phase shift ϕ versus pressure for each of these gases. The flatness of the plots and their close agreement strongly validates the method. For ethane, which was chiefly used, both upper and lower frequency limits for $\phi_s = 0$ are slightly higher than for both CO_2 and N_2O, but measurements made between 100 - 1 Kc/s should be satisfactory. The slight fall-off in ϕ at very low pressure is due to microphone response changes as pointed out in Section I. However, these were found to be approximately the same for both ethane and carbon dioxide and should not therefore cause appreciable error.

The experimental procedur e adopted therefore was to follow each carbon dioxide of nitrous oxide reading with a calibration reading at approximately the same pressure. Since traces of ethane were found to be very efficient at shortening the relaxation time of CO_2, care was taken thoroughly to pump down and flush out the apparatus before commencing the next reading. One further test made to confirm the validity of the calibration procedure was to observe the change in phase shift with time for a sample of gas left in the spectrophone. With CO_2, the phase lag decreased with time, some change usually being noticeable after a few minutes, followed by a slower decrease

FIG. 23 Calibrating gas test.

Experimental phase shift (ϕ) against pressure.

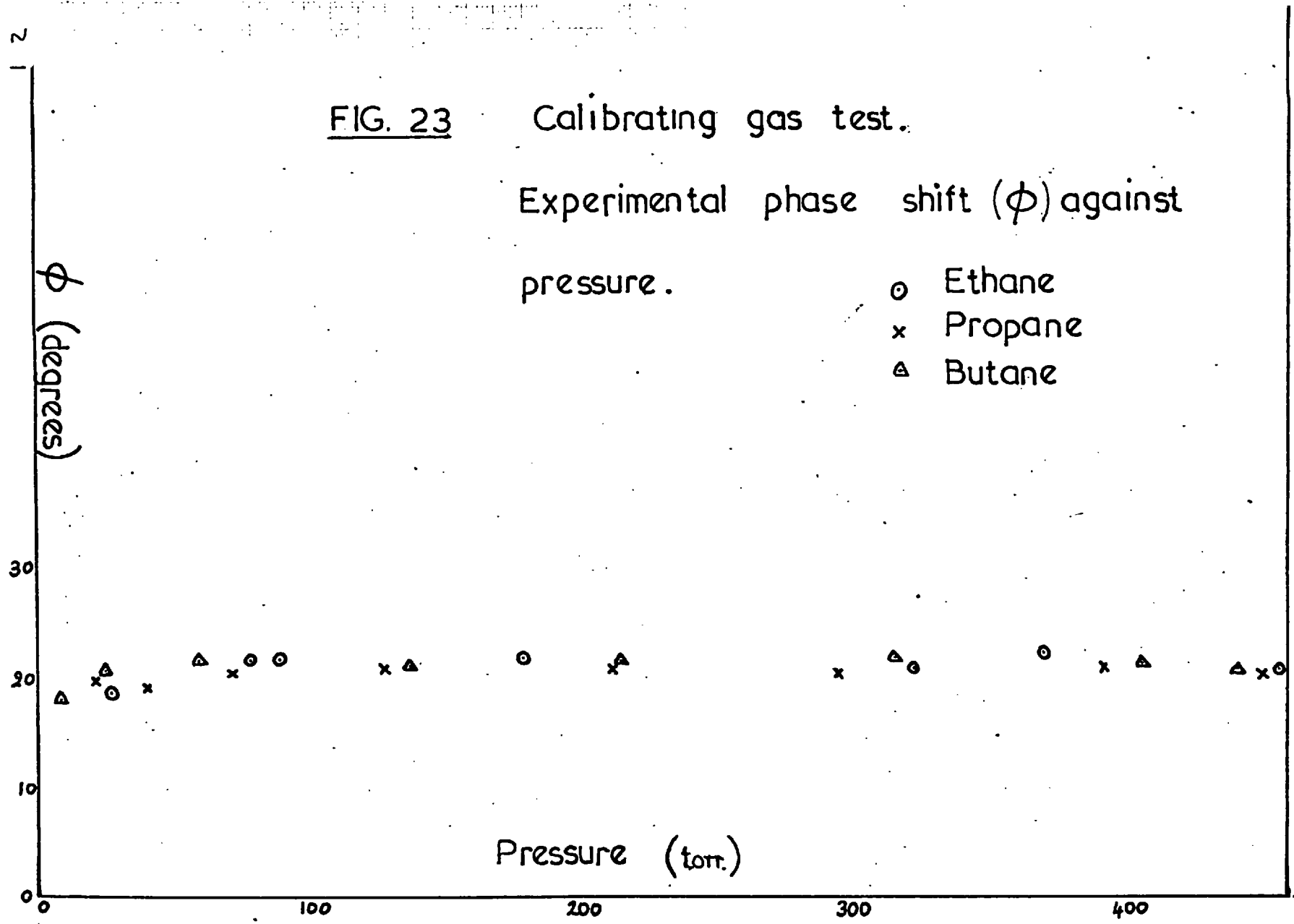

continuing over periods of hours. This was much greater at low pressures when the relaxation phase shift is large. For ethane, however, the phase shift did not alter, even at 10 torr pressure over a period of ten hours.

(VI) Sensitivity of apparatus and accuracy of measurements

The accuracy of the phase measurements depended upon the magnitude of the signals. Measurements on signals > 10 μvolts could be made to $\pm 1^{\circ}$ of phase. This included most calibration measurements and measurements on the 4.3 μ CO_2 and 4.5 μ N_2O bands made at pressure above ~ 70 torr. For measurements below this pressure on these bands and for measurements on the other, weaker bands, the probable error was larger, although often the results as a whole examined graphically showed a much smaller spread than thus indicated. It was found that the smallest optic-acoustic signal whose phase could be measured was 0.5 μv corresponding to a sound pressure level in the spectrophone of $\sim 10^{-4}$ dynes cm^{-2}.

As stated above, the range of frequencies useable in the present apparatus extends from about 100 c/s to 1 kc/s. At 800 c/s, which was the frequency most commonly used for measurements, one degree of relaxation phase lag corresponds to a relaxation time of about 3.5 μsec. Thus only vibrations whose relaxation time is significantly over about 7 μsec at the lowest practical pressure (determined by the absorption coefficient of the band) can be investigated quantitatively.

By means of the barometer and manometers, gas pressures could be measured to $\pm$ 1 mm of Hg. Mixtures were made by letting one gas into the mixer to the desired partial pressure, re-evacuating the

drying chamber and letting the second gas into this to approximately atmospheric pressure. This was always at least five times greater than the pressure of the first gas in the mixer. Then the tap between the mixer and the drying chamber was partially opened until the pressure in the mixer rose to the final required value. The accuracy of mixing ratio thus achieved depended upon the desired ratio, and the two gases concerned. If both gases were from cylinders, then the smaller component of the mixture was allowed in first, achieving a high pressure difference across the mixer-drying tube tap. However, the gases from bottles at N.T.P. (e.g. helium, xenon, etc.) had always to be let into the mixer first, so that it was difficult to obtain accurate mixtures containing a high concentration of these gases, especially for helium with its high effusion rate. The probable error in mixing ratio thus varied from about $\pm$ 2% in the majority of cases to about $\pm$(15 - 20) % in unfavourable cases.

CHAPTER 5

EXPERIMENTAL RESULTS

I Measurements on Pure Carbon Dioxide

(i) Range of measurements

Measurements of the relaxation phase lag were made over the pressure ranges 1 - 500 torr for the 4.3 μ CO_2 band and 30 - 500 torr for the 15 μ CO_2 band.

Measurements were made at a chopping frequency of 200, 500 and 800 c/s. No detectable difference between results (allowing for the change in ω) was found for all these frequencies and most measurements were made at 800 c/s.

Figure 24 shows a typical plot of experimental phase lag ϕ against pressure P for the 4.3 μ band. Figure 25 shows a similar plot for the 15 μ band. In both graphs the corresponding calibrating gas (ethane) plot is also shown. The relaxation phase lag ψ is obtained merely by subtracting the value of $\phi_{\text{calibration}}$ from ϕ_{CO_2} as described in Chapter 4.

About twenty different runs were made on each band over a period of several months. On several occasions smaller relaxation phase shifts were obtained (particularly for the 4.3 μ band at low pressures) than given in Figures 24 and 25. However, in all cases, this occurred when it was suspected that the impurity contamination in the system was too high, either due to a poor vacuum or recent surface contamination of the spectrophone during dismantling. It was found that flushing the spectrophone several times with carbon dioxide, restored the phase lag to nearly its normal value and that flushing was beneficial even when the vacuum in the chamber was initially good. The ethane

FIG. 24 Experimental phase lag (ϕ) versus pressure (P)

($4{\cdot}3\mu$ CO_2 band)

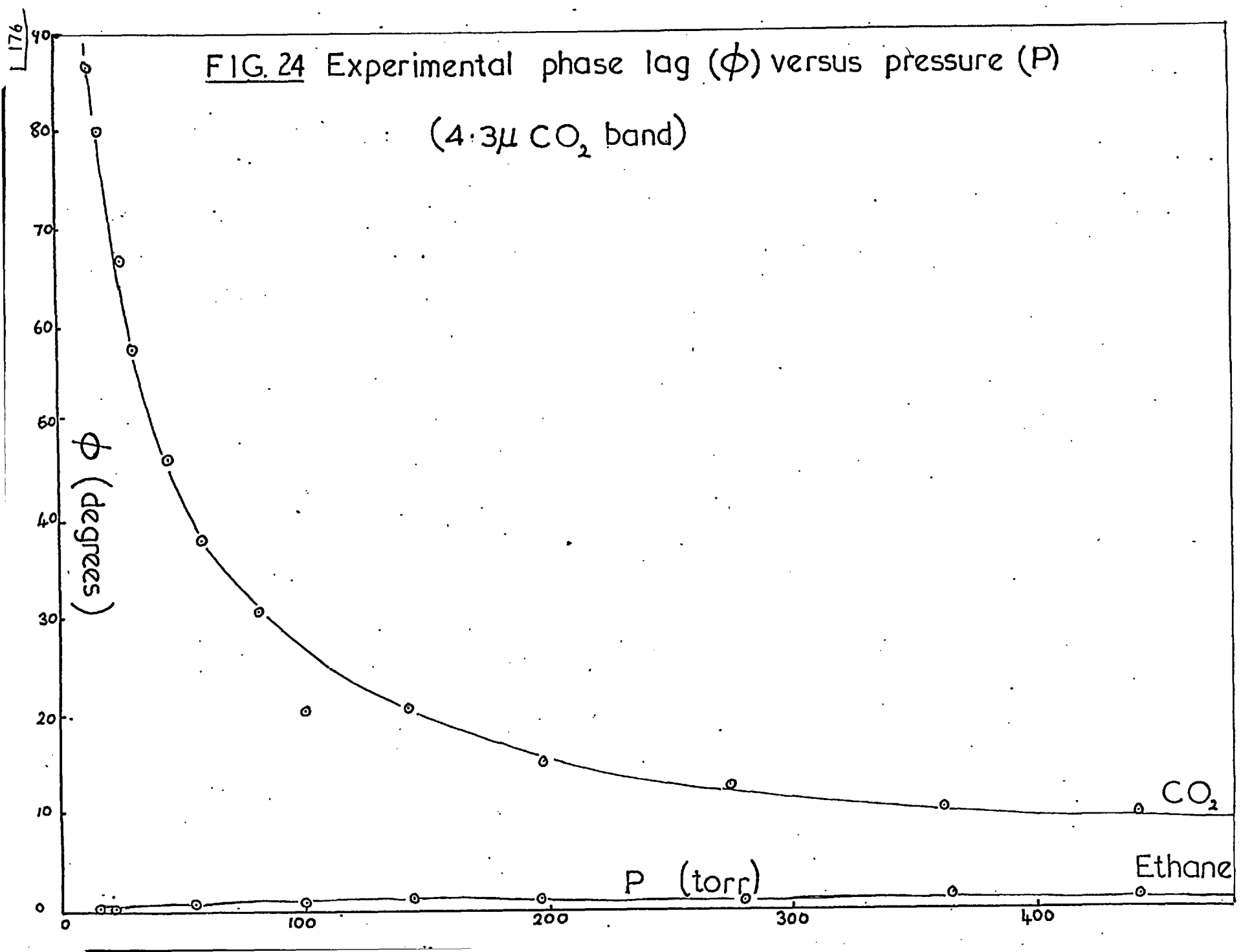

FIG. 25 Experimental phase lag ϕ versus pressure (P)

(15μ CO_2 band)

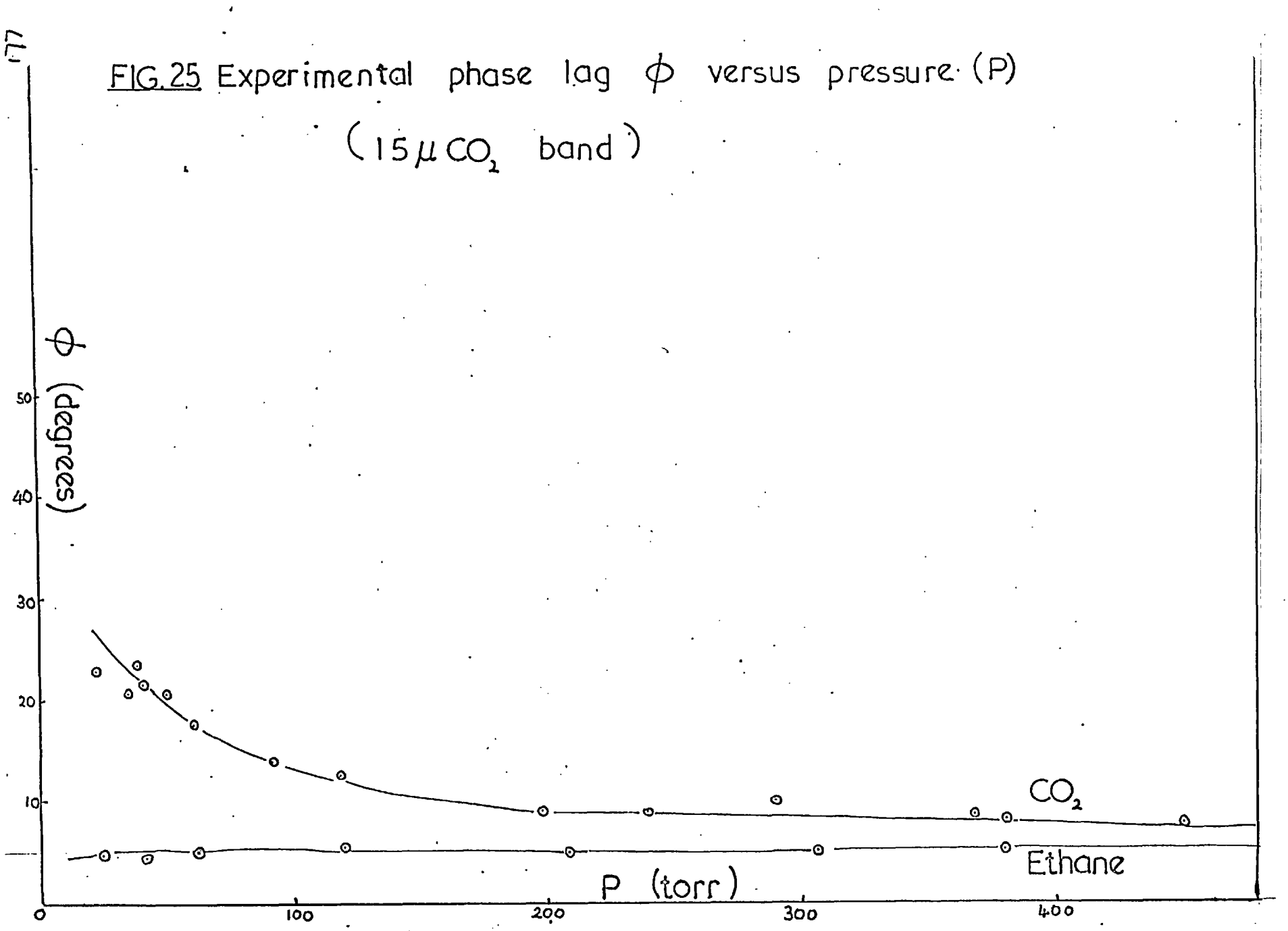

FIG. 26. Plot of $\tan\gamma$ against $(\text{pressure})^{-1}$ for 15μ CO_2 band.

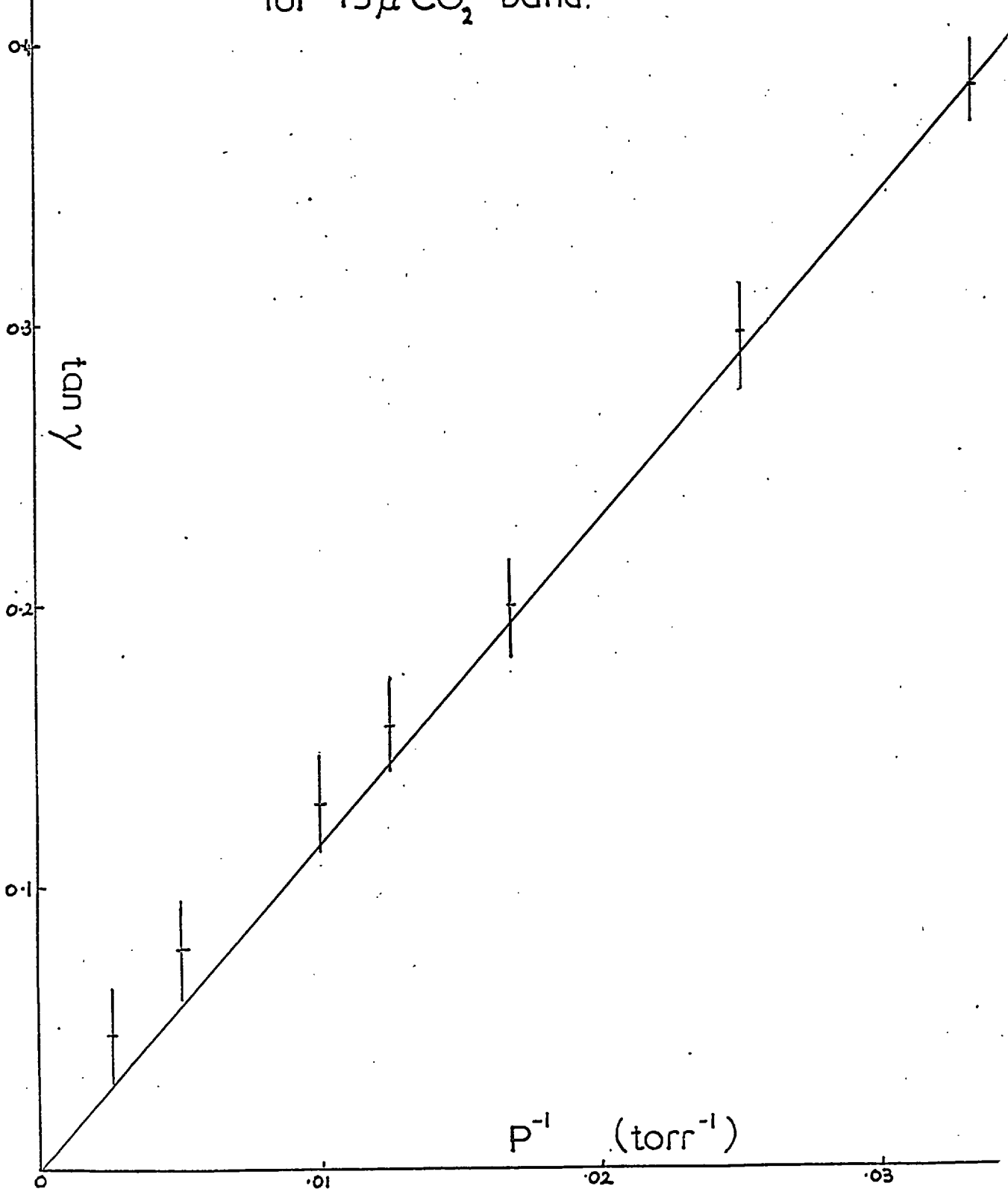

FIG. 27 Plot of $\tan\gamma$ versus $(\text{pressure})^{-1}$

$4 \cdot 3\mu$ band of CO_2

(single relaxation scheme)

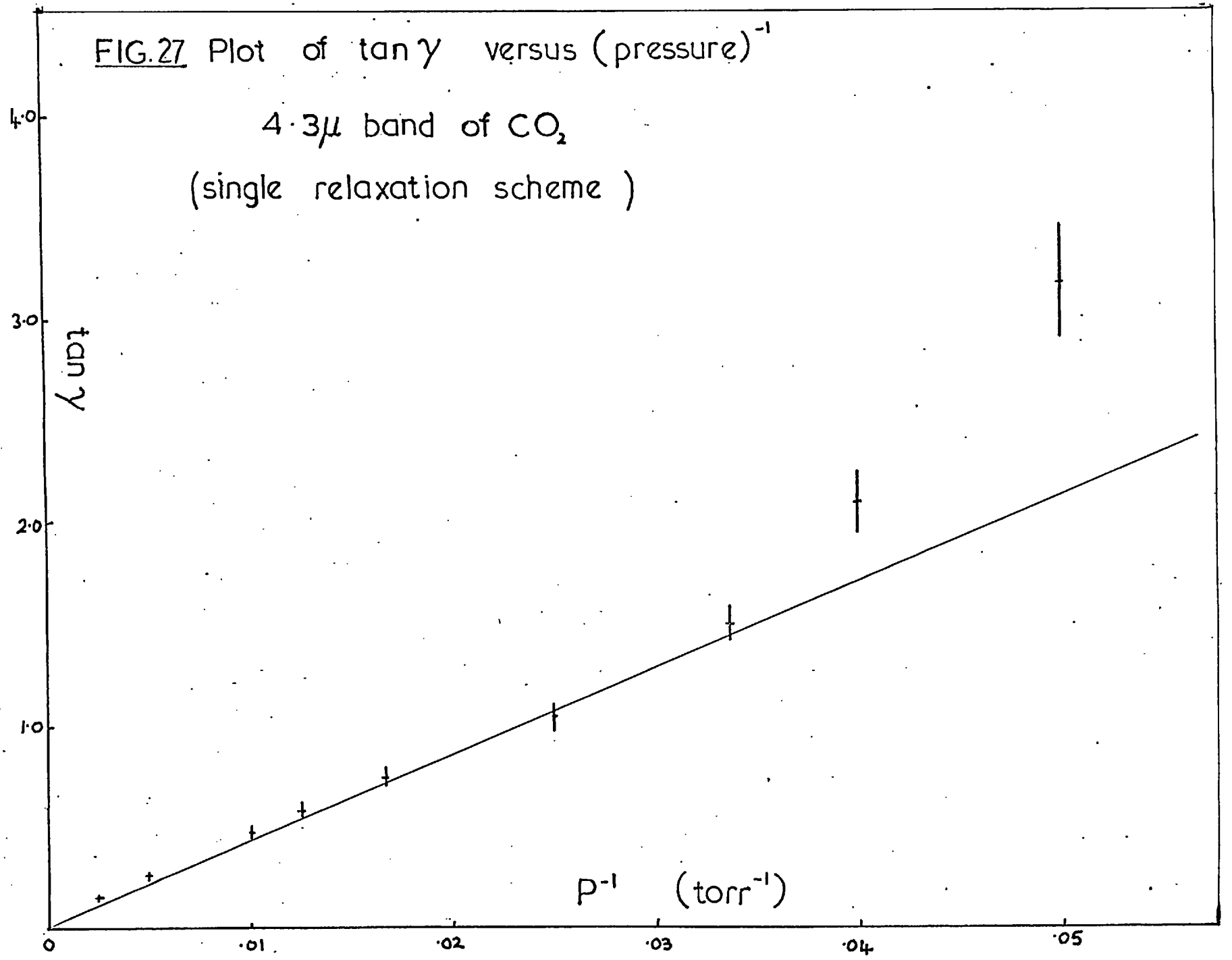

calibration was found to remain constant over the complete pressure range on all runs. Under optimum conditions, therefore, Figures 24 and 25 were found to be quite reproducible, although there was a large amount of scatter at the low pressure end of the 15μ band data.

(ii) Evaluation of relaxation times

The relaxation of the 15 μ bending vibration to the ground state should involve a single step energy exchange with translation. Thus $\tan \gamma = \omega \tau_2$ as given by equation 3.22 of Chapter 3. Tan γ should be proportional to 1/P and Figure 26 shows this relationship for the results for Figure 25, and similar runs. The relaxation time of the bending mode at 1 atmos. pressure is $\tau_2 = 3 \pm 2$ μsec. The probable error was determined from the limits to the possible slope of Figure 26, taking into account the variations in readings from run to run and the probable phase error of each reading.

As discussed in Chapter 1, from theoretical grounds one would expect the 4.3 μ asymmetric valence mode to relax by the complex process $h\nu_3 \rightarrow h\nu_2 + h\nu_1$, all the energy eventually reaching translation via the bending modes. Making reasonable approximations, the relaxation may be considered as a two step process $h\nu_3 \rightarrow 3h\nu_2 \rightarrow$ translation, in which two rate constants and hence two relaxation times are involved. This was the case treated in section (vii) of Chapter 3(B). There it was shown that the relaxation phase shift $\gamma \simeq \gamma_1 + \gamma_2$ where γ_1 and γ_2 are given by $\tan \gamma_1 = \omega \tau_3$, $\tan \gamma_2 = \omega \tau_2$. τ_2 will correspond to the relaxation time of the 15 μ band as calculated from Figure 26. τ_3 may be called the relaxation time of the ν_3 vibration for the complex relaxation scheme.

If the 4.3 μ band relaxes by direct energy exchange with translation,

then tan $\gamma = \omega\tau'_3$, where τ'_3 is the relaxation time for the single relaxation scheme. In this case tan γ should be proportional to 1/P as for the 15 μ band. As can be seen in Figure 27, where the experimental tan γ, obtained from Figure 24, is plotted against inverse pressure, the relationship is far from linear. The indicated value of τ'_3 at 1 atmos. is 13 $\pm$ 2 μsec.

To obtain τ_3, assuming a double relaxation, the values of γ_2 (obtained from Figure 25) are subtracted from the corresponding values of γ (obtained from Figure 24) at identical pressures to give γ_1. The plot of tan γ versus 1/P is shown in Figure 28. The value of τ_3 indicated is 8 μsec at one atmosphere. The probable error, obtained similarly to that of the 15 μ band, is $\pm$ 3 μsec.

II Measurements on Carbon Dioxide - Noble gas mixtures

(i) Range of measurements

Measurements were made with mixtures of CO_2 and the five inert gases, helium, neon, argon, krypton and xenon. Runs were made by varying the concentration of noble gas in the mixture while maintaining a constant total pressure. As discussed previously, the accuracy of the mixing ratio depended upon the gases, total pressure, and desired concentration, but were generally accurate to 1 or 2 per cent.

Nearly all measurements were made on the 4.3 μ band. This band is inaccessible to study by ultrasonic methods, and has most interest for optic-acoustic work, and furthermore the much lower sensitivity of the apparatus for measurements with the 15 μ band made investigations of mixtures with low CO_2 concentrations difficult, except at high pressures. However, measurements were made on argon-carbon

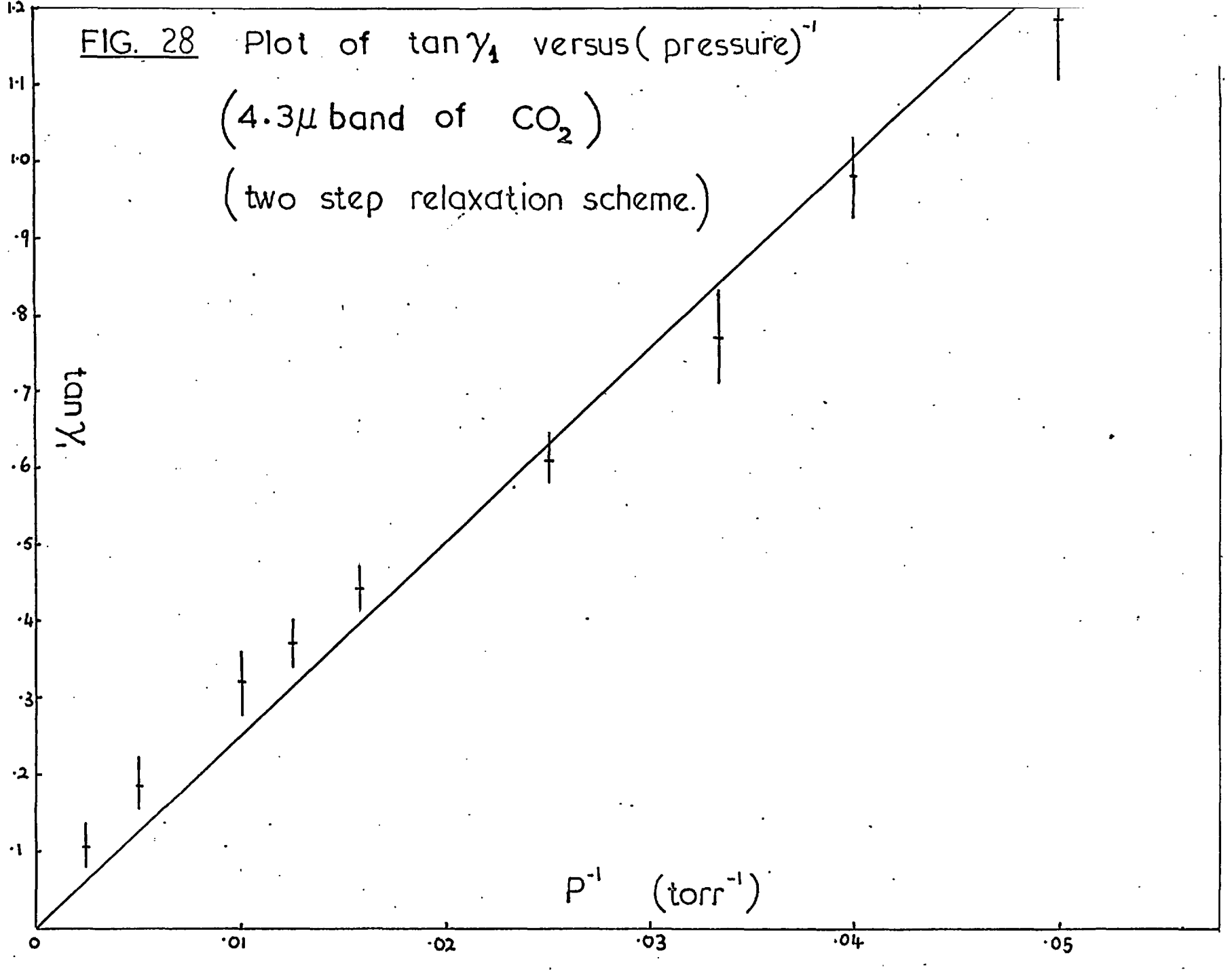
FIG. 28 Plot of tan γ_1 versus (pressure)$^{-1}$
(4.3μ band of CO_2)
(two step relaxation scheme.)
tan γ_1
1·2
1·1
1·0
·9
·8
·7
·6
·5
·4
·3
·2
·1
0
·01
·02
·03
·04
·05
P^{-1} (torr^{-1})

FIG. 29 Results for CO_2–He Mixtures ($4 \cdot 3\mu$ band)

Variation of Relaxation Phase Shift (γ)

with CO_2 concentration (x)

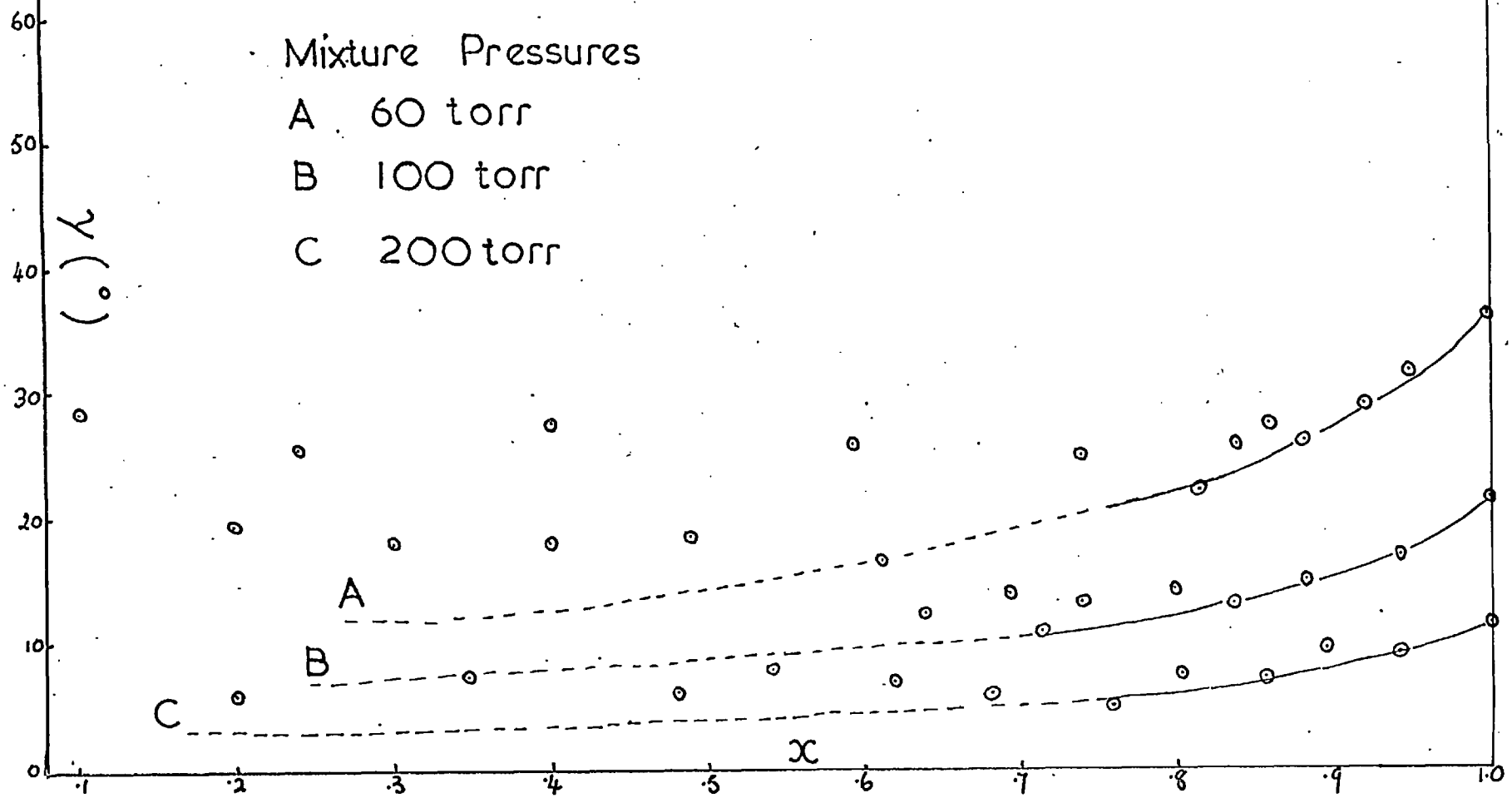

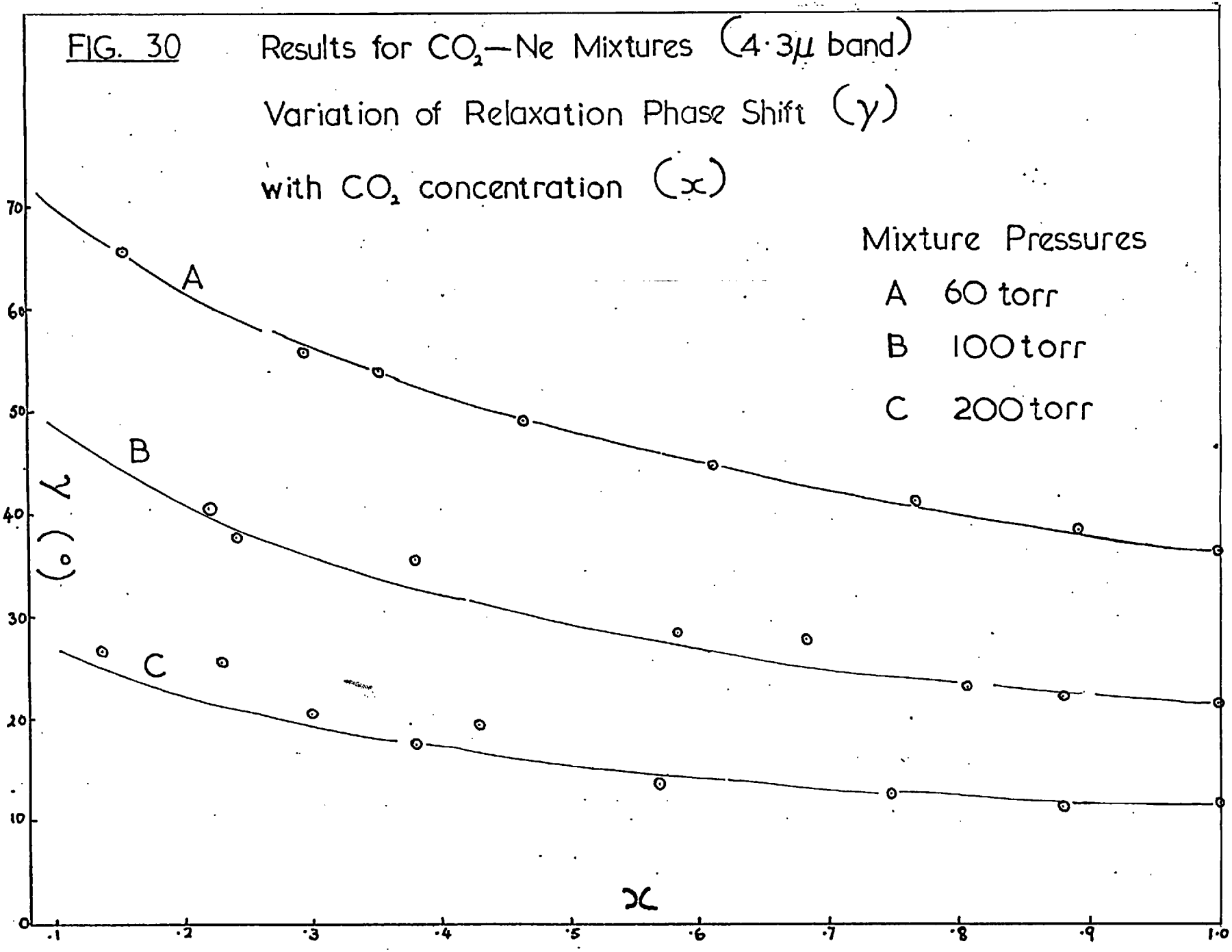
FIG. 30
Results for CO_2—Ne Mixtures (4·3μ band)
Variation of Relaxation Phase Shift (γ)
with CO_2 concentration (x)
Mixture Pressures
A 60 torr
B 100 torr
C 200 torr
A
B
C
γ (°)
x
70
60
50
40
30
20
10
0
·1
·2
·3
·4
·5
·6
·7
·8
·9
1·0

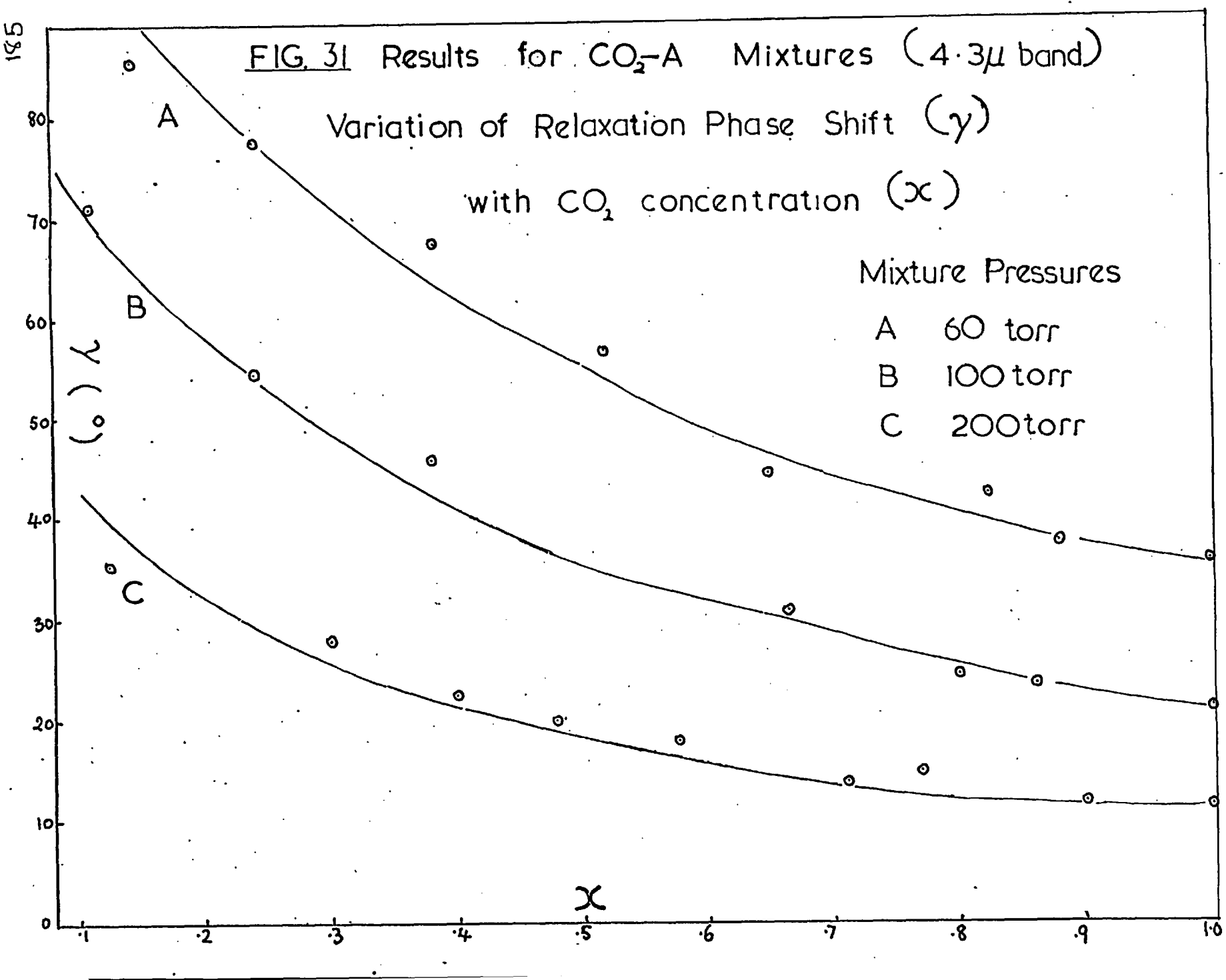
FIG. 31 Results for CO_2–A Mixtures (4·3μ band)
Variation of Relaxation Phase Shift (γ)
with CO_2 concentration (x)
Mixture Pressures
A 60 torr
B 100 torr
C 200 torr
A
B
C
γ (°)
x
0
10
20
30
40
50
60
70
80
·1
·2
·3
·4
·5
·6
·7
·8
·9
1·0

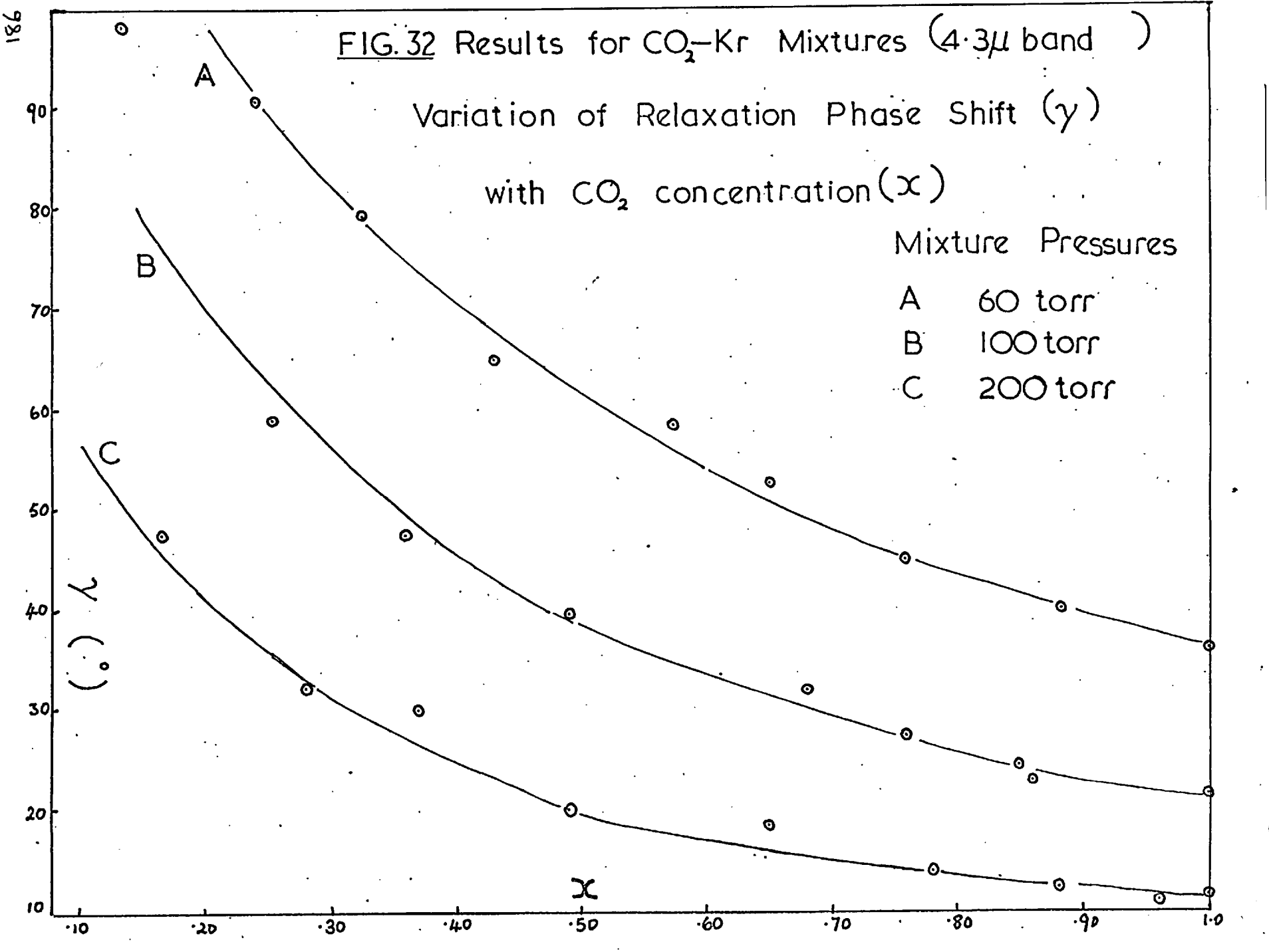
FIG. 32 Results for CO_2–Kr Mixtures (4·3μ band)
Variation of Relaxation Phase Shift (γ)
with CO_2 concentration (x)
Mixture Pressures
A 60 torr
B 100 torr
C 200 torr
A
B
C
γ (°)
x
90
80
70
60
50
40
30
20
10
·10
·20
·30
·40
·50
·60
·70
·80
·90
1·0

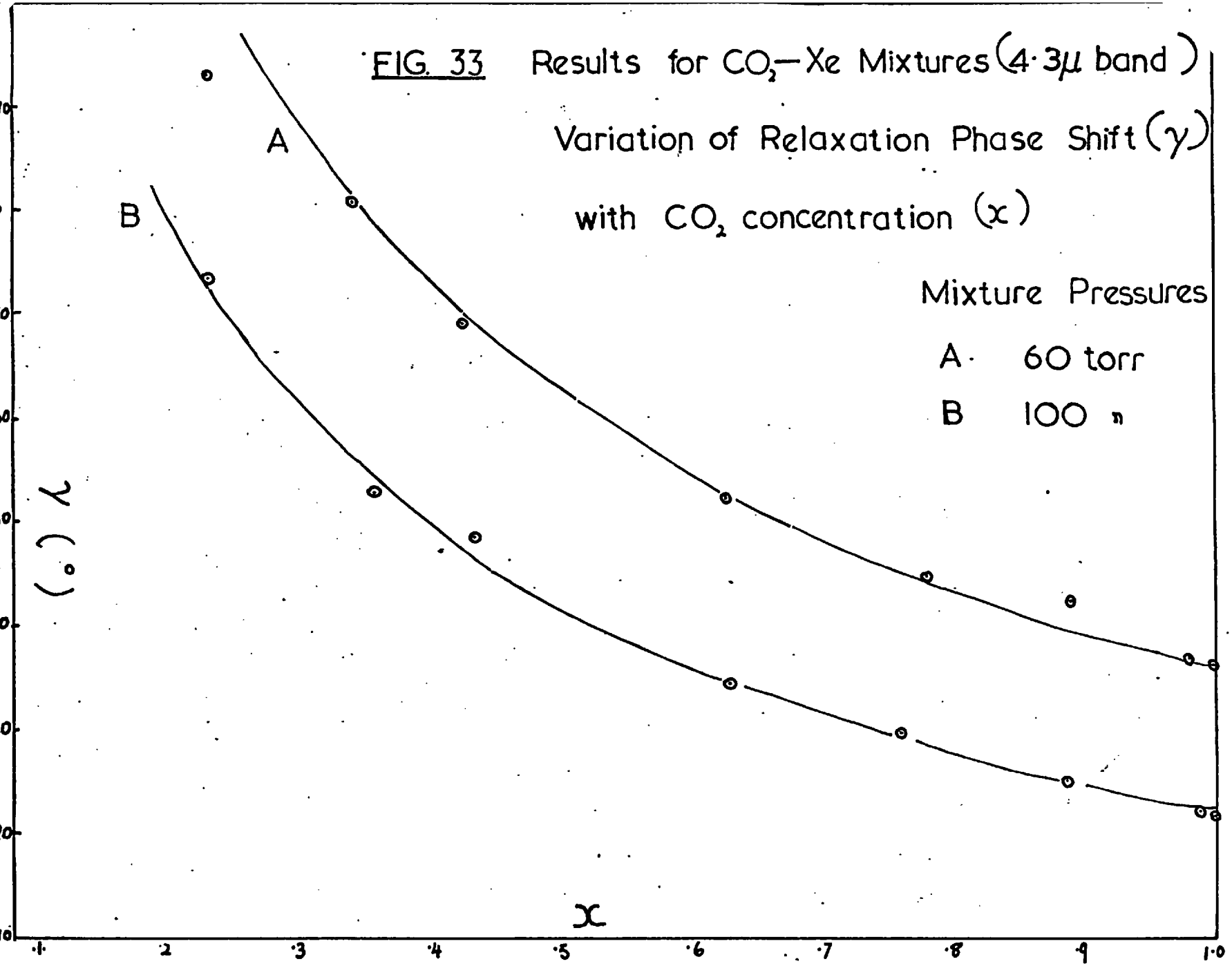
FIG. 33 Results for CO_2—Xe Mixtures (4·3μ band)
Variation of Relaxation Phase Shift (γ)
with CO_2 concentration (x)
Mixture Pressures
A 60 torr
B 100 "
A
B
γ (°)
x
90
80
70
60
50
40
30
20
10
·1
·2
·3
·4
·5
·6
·7
·8
·9
1·0

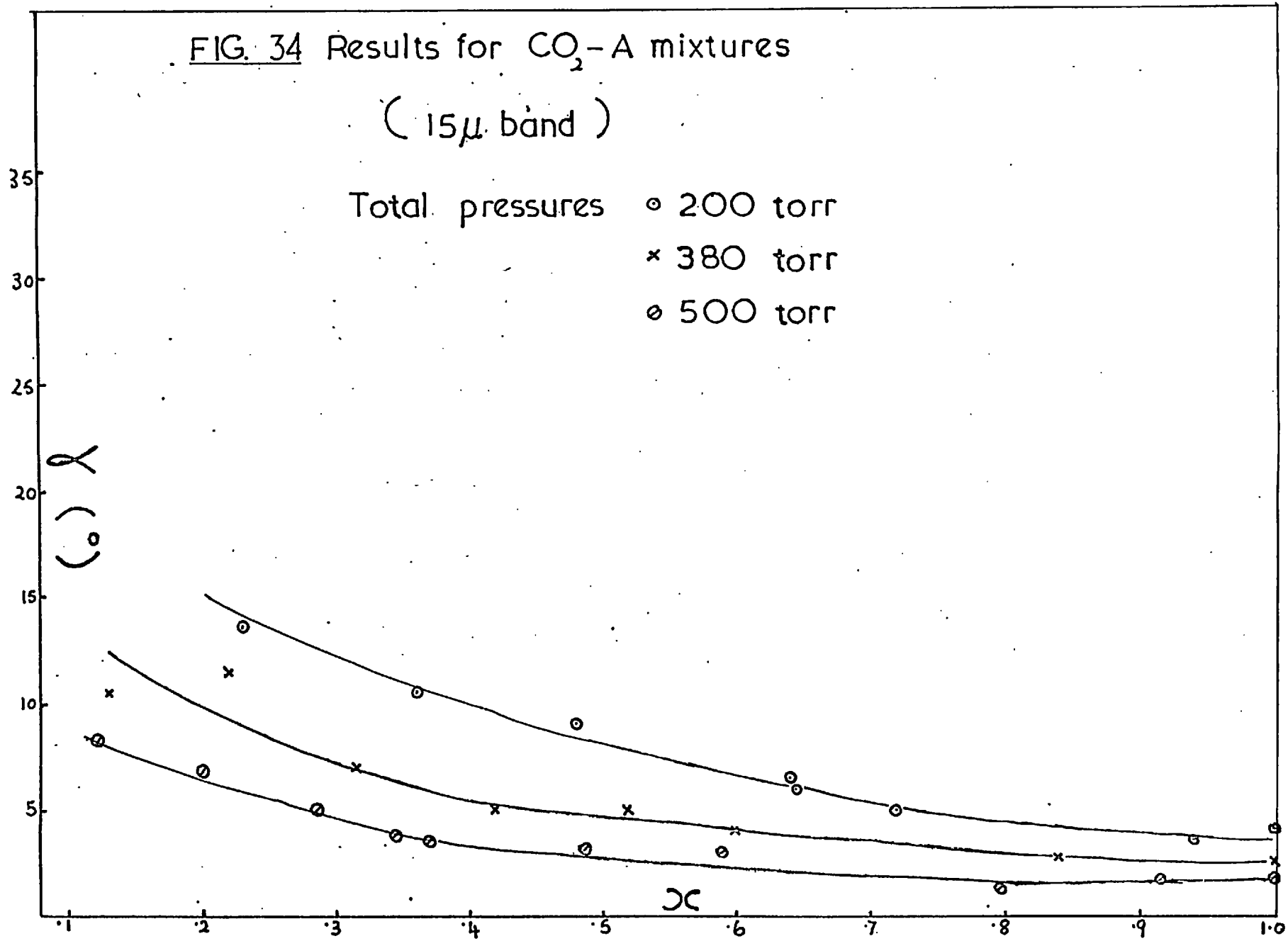
FIG. 34 Results for CO_2 – A mixtures
(15μ band)
Total pressures
⊙ 200 torr
× 380 torr
⊘ 500 torr
$\alpha_{(0)}$
x
35
30
25
20
15
10
5
·1
·2
·3
·4
·5
·6
·7
·8
·9
1·0

dioxide mixtures using the 15 μ band since sufficiently pure argon was available in large quantities.

For the 4.3 μ band runs were made at total pressures of 200, 100 and 60 torr, for all the noble gases except xenon, for which runs were made at 100 and 60 torr only. Figures 29, 30, 31, 32 and 33 show the experimental plots for these measurements. The instrumental phase shift, as given by the calibration gas, has been subtracted from each reading to give the relaxation phase lag. Figure 34 shows a similar plot for the runs on CO_2-argon mixtures using the 15 μ band.

The results for helium mixtures show that as the concentration of helium in the mixture increases the trend of the readings reverses towards a larger phase lag. This implies a minimum relaxation time for a certain mixing ratio, which cannot be explained theoretically. In addition, the results at high helium concentrations had poor reproducibility. As mentioned in Chapter 4, the accurate mixing of helium and carbon dioxide was difficult for high helium concentrations, which might account for this latter fact, but the upward trend of the phase lag would seem to suggest some non-relaxation spectrophone effect. Although the density and thermal conductivity of helium are an order of magnitude different from the values for CO_2, calculations show that the experimental chopping frequency of 800 c/s lies well within the upper and lower frequency limits for helium as defined in Chapter 3. The most likely cause of the anomaly is the effect of the change of density of the mixture upon the microphone phase response. As noted in Chapter 4, this does vary with density, especially at low pressure, and by far the largest variation in gas density occurs in the helium-carbon dioxide mixtures.

(ii) Analysis of results for CO_2 mixtures

A gas having a vibration which relaxes with a single relaxation time, when mixed with an inert diluent B, has an effective relaxation time τ_{eff}, for a concentration x of A, as given in Chapter 1, of

$$\frac{1}{\tau_{eff}} = \frac{x}{\tau_{AA}} + \frac{(1-x)}{\tau_{AB}} \qquad 5.1$$

where τ_{AA} and τ_{AB} are the relaxation times (at the same temperature and pressure as the mixture) of A molecules in pure A and in otherwise pure B respectively. In the spectrophone for a single relaxation process

$$\tau = \frac{\tan\gamma}{\omega}$$

and therefore

$$\frac{1}{\tan\gamma} = x\omega\left[\frac{1}{\tau_{AA}} - \frac{1}{\tau_{AB}}\right] + \frac{\omega}{\tau_{AB}} \qquad 5.2$$

A graph of $\frac{1}{\tan\gamma}$ against x will thus be a straight line whose intercept upon the $\frac{1}{\tan\gamma}$ axis will give the value of τ^{-1}_{AB}.

Figure 35 shows such plots for the 15 μ A-CO_2 mixture results of Figure 34. Values for τ_{AB} indicated, are 72 μsec at 500 torr, 99 μsec at 380 torr, and 173 μsec at 200 torr, with probable errors of $\pm$ 10 per cent, as determined from possible variation in graph slopes. These are 12, 11 and 12 times respectively the corresponding values found for pure carbon dioxide at these pressures.

FIG. 35 CO_2–A mixtures (15μ band)

Plots of $(\tan\gamma)^{-1}$ against (x).

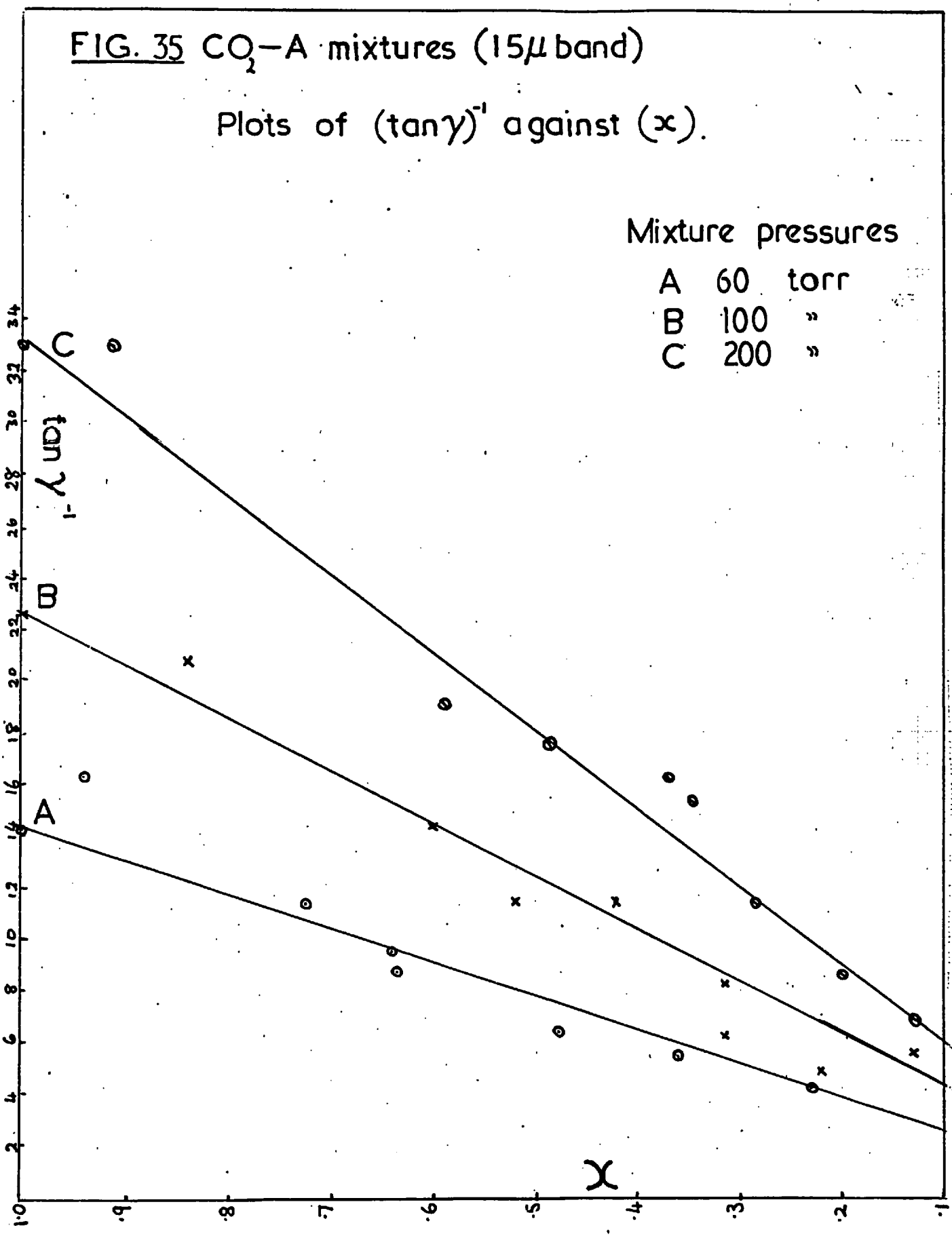

The analysis of the 4.3 μ results depends upon the relaxation scheme adopted for the band. For a single step relaxation, equation 5.2 will apply and Figures 36, 37, 38, 39 and 40 show $x - \frac{1}{\tan\gamma}$ plots for the results, shown in Figures 29 through 33. Because of the apparent anomaly in the rest of the readings, only the helium data with $x > 0.6$ was used to plot Figure 36, and also in the subsequent calculations. Table 5.1* gives the values of τ_{AB} and τ_{AB}/τ_{AA} calculated from the graphs.

For the two-step relaxation scheme for the 4.3 μ band, equation 5.1 should apply to both τ_3 and τ_2 since both steps in the energy transfer should be collision induced. Thus the total spectrophone phase lag $\gamma = \gamma_1 + \gamma_2$ will be given by

$$\tan\gamma = \tan(\gamma_1 + \gamma_2) =$$

$$= \frac{\omega(\tau_{2\,eff} + \tau_{3\,eff})}{(1 - \omega^2 \tau_{2\,eff}\,\tau_{3\,eff})}$$

$$= \omega\left[\frac{1}{\tau_{3\,eff}} + \frac{1}{\tau_{2\,eff}}\right] \Big/ \left[\frac{1}{\tau_{3\,eff}} \cdot \frac{1}{\tau_{2\,eff}} - \omega^2\right]$$

$$= \frac{\omega\left\{x\left[\left(\frac{1}{\tau_3^{AA}} - \frac{1}{\tau_3^{AB}}\right) + \left(\frac{1}{\tau_2^{AA}} - \frac{1}{\tau_2^{AB}}\right)\right] + \left(\frac{1}{\tau_3^{AB}} + \frac{1}{\tau_2^{AB}}\right)\right\}}{\left[x\left(\frac{1}{\tau_3^{AA}} - \frac{1}{\tau_3^{AB}}\right) + \frac{1}{\tau_3^{AB}}\right]\left[x\left(\frac{1}{\tau_2^{AA}} - \frac{1}{\tau_2^{AB}}\right) + \frac{1}{\tau_2^{AB}}\right] - \omega^2}$$

5.3

* Page 223

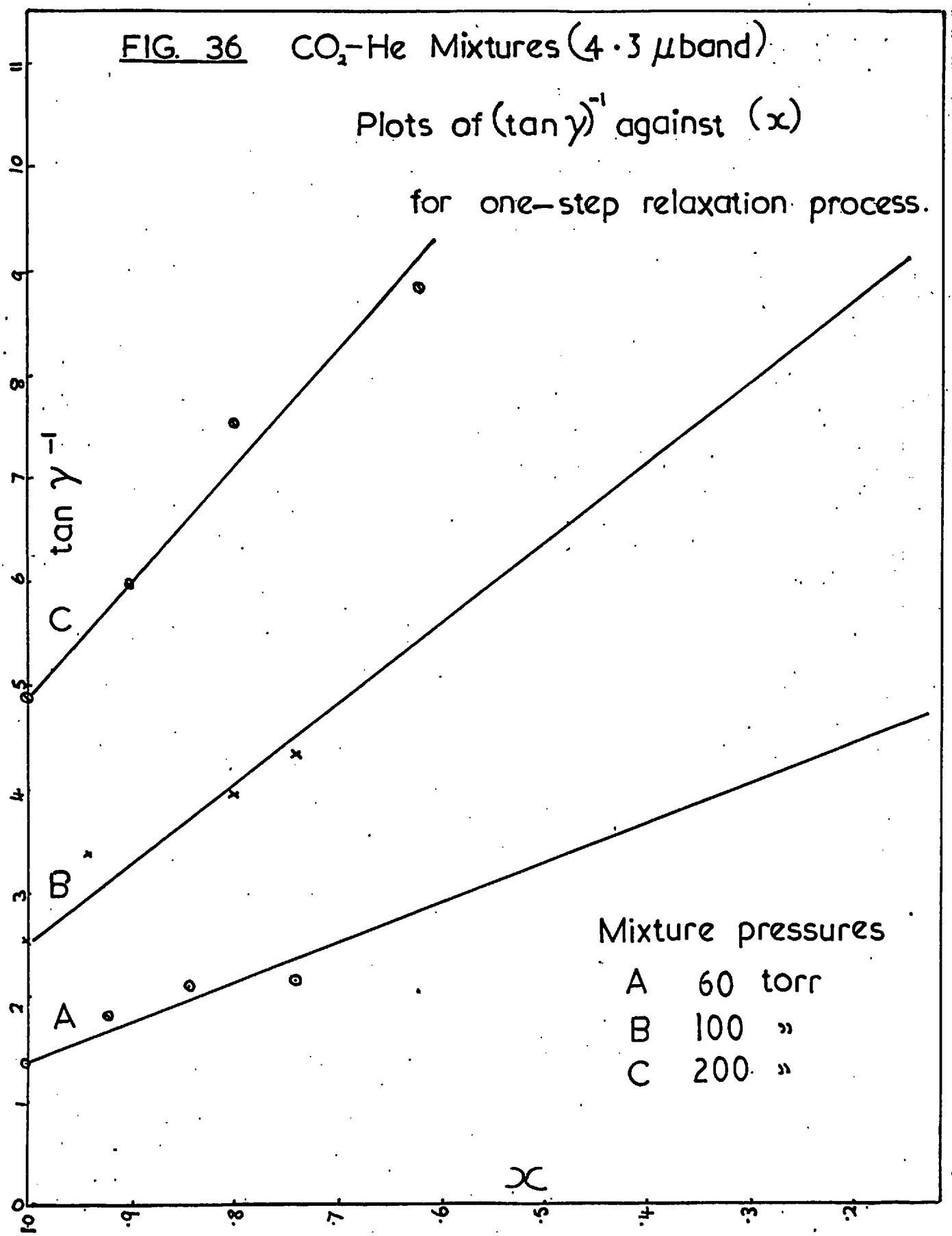
FIG. 36 CO_2–He Mixtures (4·3 μ band)
Plots of $(\tan\gamma)^{-1}$ against (x)
for one–step relaxation process.
$\tan\gamma^{-1}$
x
C
B
A
Mixture pressures
A 60 torr
B 100 "
C 200 "

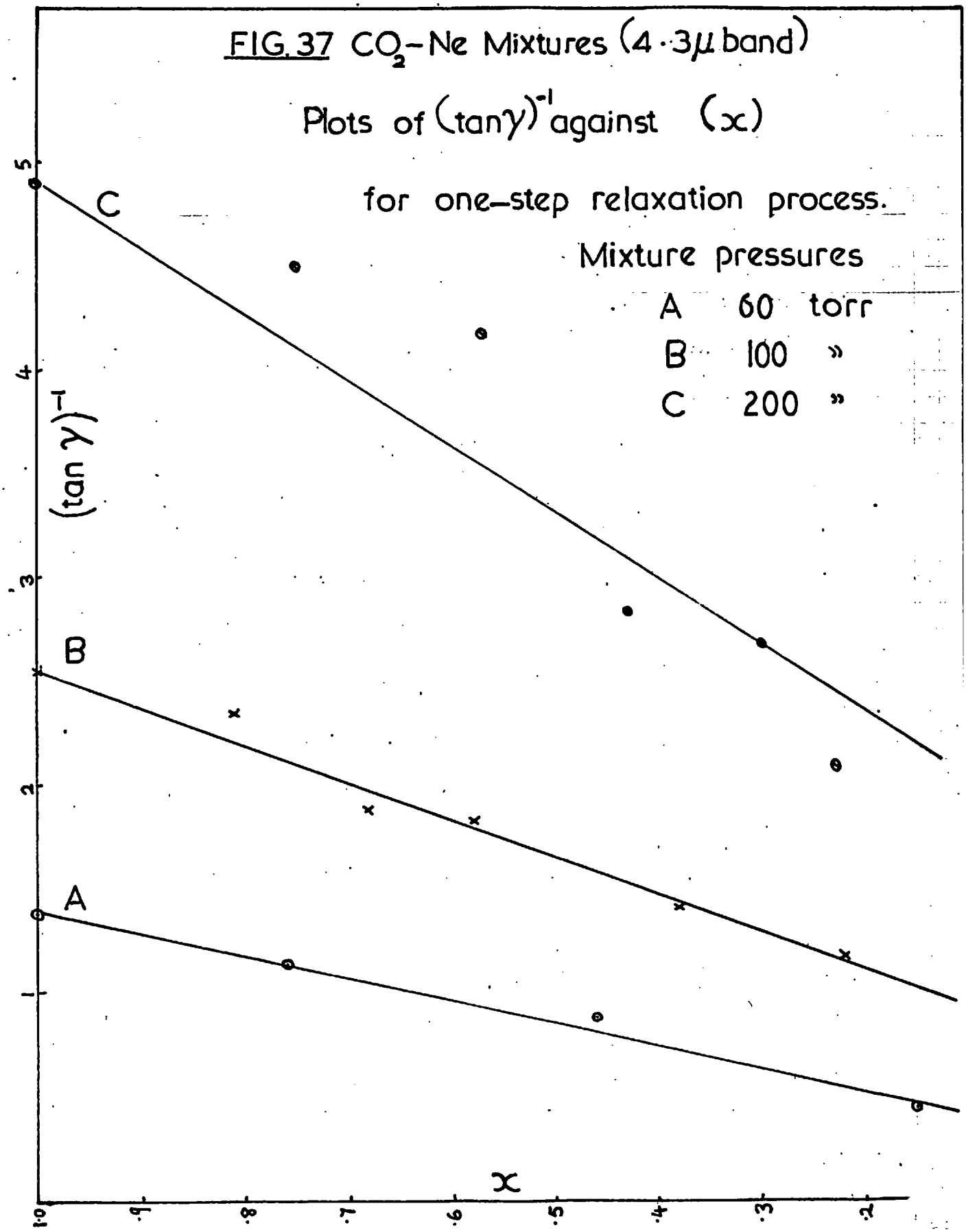
FIG. 37 CO_2–Ne Mixtures (4·3μ band)
Plots of $(\tan\gamma)^{-1}$ against (x)
for one-step relaxation process.
Mixture pressures
A 60 torr
B 100 »
C 200 »
C
B
A
$(\tan\gamma)^{-1}$
x
1·0
·9
·8
·7
·6
·5
·4
·3
·2
1
2
3
4
5

FIG. 38 CO_2–A Mixtures (4·3μband)

Plots of $(\tan\gamma)^{-1}$ against (x)

for one–step relaxation process.

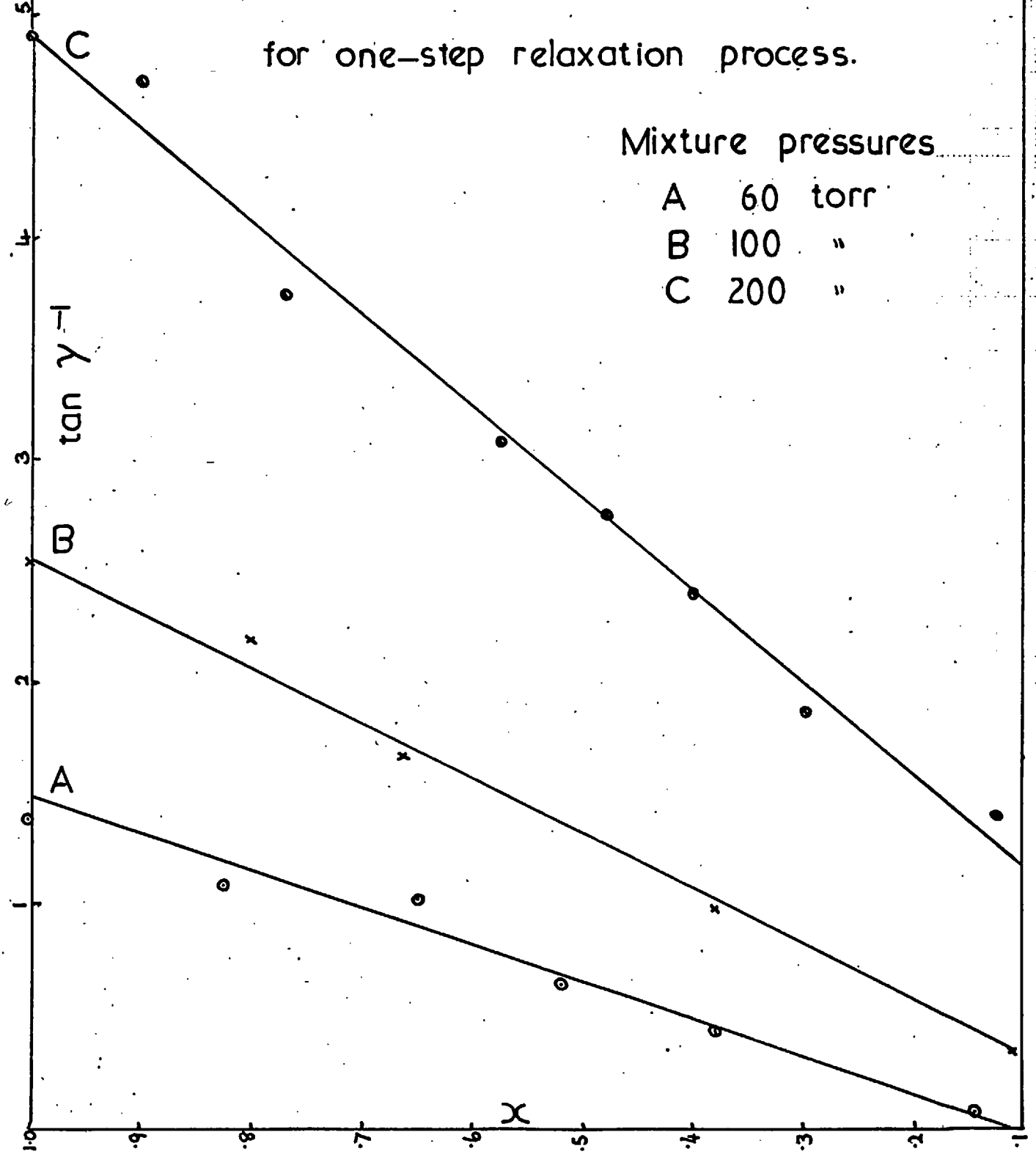

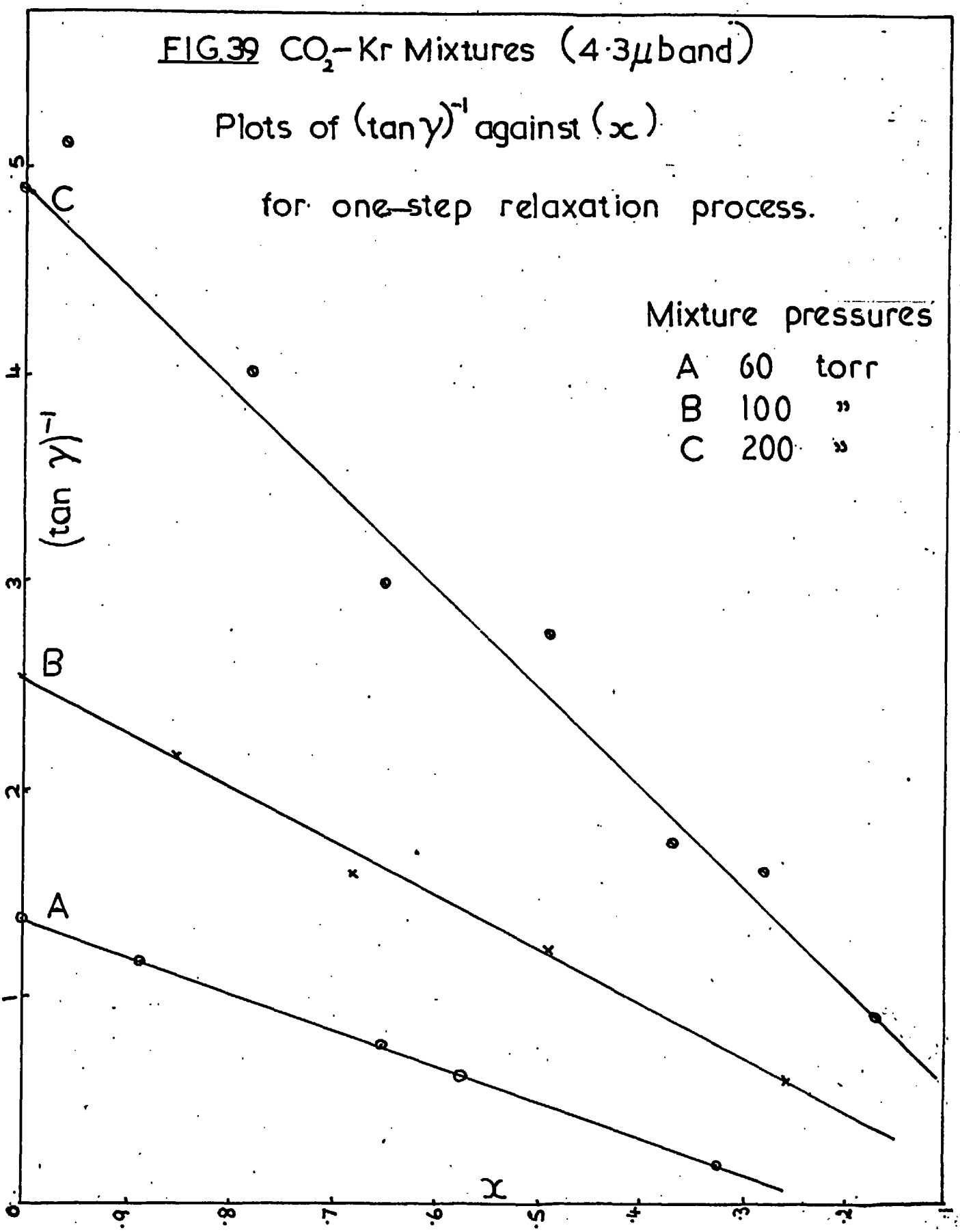
FIG.39 CO_2–Kr Mixtures (4·3μ band)
Plots of $(\tan\gamma)^{-1}$ against (x)
for one-step relaxation process.
Mixture pressures
A 60 torr
B 100 "
C 200 "
$(\tan\gamma)^{-1}$
x
A
B
C
0
1
2
3
4
5
·9
·8
·7
·6
·5
·4
·3
·2
·1

FIG.40 CO_2 – Xe Mixtures (4·3μ band)

Plots of $(\tan\gamma)^{-1}$ against (x)

for one-step relaxation process.

Mixture pressures

A 60 torr

B 100 "

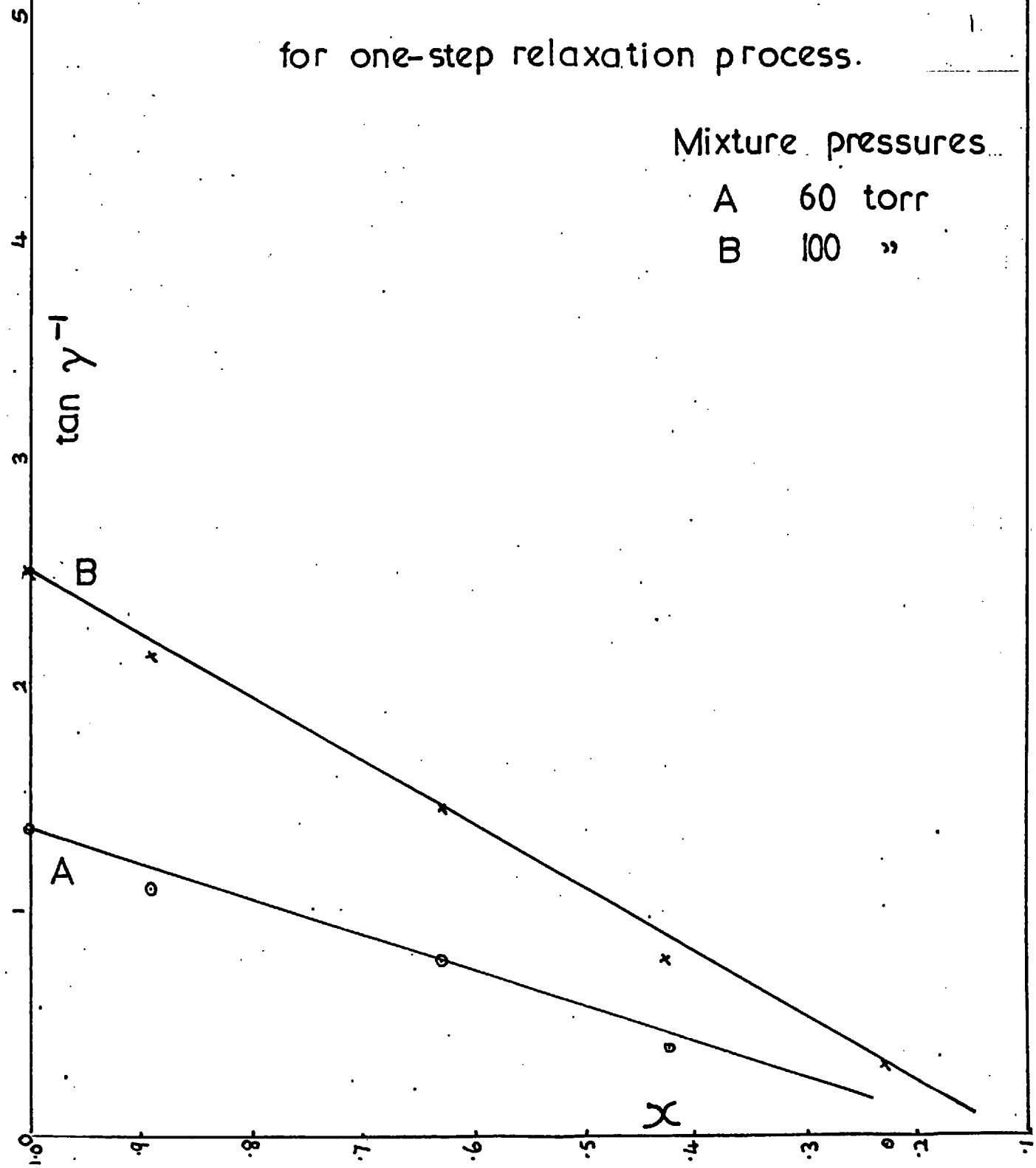

Figure 41 shows the difference between the variation of tan γ and 1/tan γ with x for the single and two-step relaxation schemes as represented by equations 5.2 and 5.3.

The exact form of tan γ as given by equation 5.3 is dependent upon the unknowns τ_3^{AB} and τ_2^{AB}, and the experimental results may be fitted by arbitrary pairs of values for these constants. Two different procedures have been adopted in investigating the applicability of equation 5.3 to the data. Equation 5.3 may be rewritten

$$\tan\gamma = \frac{\omega\left\{\frac{1}{\tau_3^{AA}}\left(x+g_3(1-x)\right)+\frac{1}{\tau_2^{AA}}\left(x+g_2(1-x)\right)\right\}}{\frac{1}{\tau_3^{AA}}\frac{1}{\tau_2^{AA}}\left[x+g_3(1-x)\right]\left[x+g_2(1-x)\right]-\omega^2} \qquad 5.4$$

where $g_3 = \tau_3^{AA}/\tau_3^{AB}$; $g_2 = \tau_2^{AA}/\tau_2^{AB}$.

If the ratio $\chi = \frac{g_3}{g_2}$ is given a certain value, then equation 5.4 may be fitted to the data and g_3 and g_2 determined. An approximate least squares fit of equation 5.4 to the experimental data, for $\chi = 1$, is shown by the solid curves in Figures 29 through 33. Table 5.2* shows the values of $g_3 = g_2$ thus obtained and the corresponding values of τ_3^{AB} and τ_2^{AB}.

A better method of evaluating g_2 and g_3 would be to determine g_2 in a separate series of experiments using the 15 μ band. As explained above, the present apparatus is unsuitable for such a study,

* Page 224.

FIG. 41 Theoretical variation of a, $\tan\gamma$ b, $\frac{1}{\tan\gamma}$ with concentration x, for single and two-step relaxation schemes

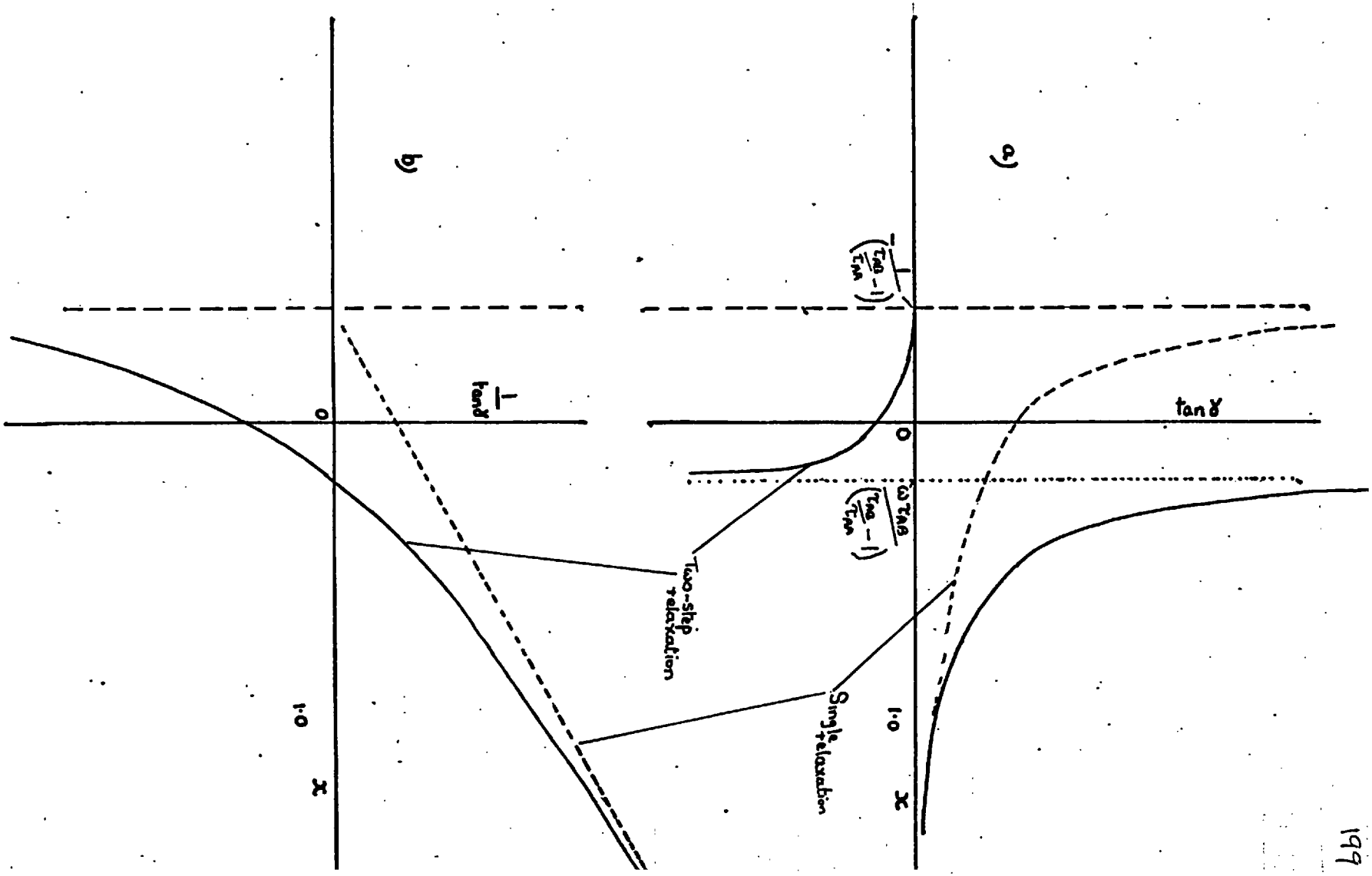

but ultrasonic measurements for the bending mode have recently been published by Cottrell et al.[78] giving the values of g_2 for $He-CO_2$ and $Ne-CO_2$ mixtures, while CO_2-A mixtures have been studied ultrasonically by Kneser et al.[79]. The reported values of g_2 were $g_2 = 14$ (CO_2-He), $g_2 = 0.5$ (CO_2-Ne) and $g_2 = 0.1$ (CO_2-A). This last result agrees well with the values quoted above for measurements with the present apparatus. Using these values of g_2, a least squares fit of equation 5.4 has been used to calculate g_3 for the experimental results on helium, neon and argon mixtures, and the results are given in Table 5.3.* These would seem to indicate that the inert gases are less inefficient in de-exciting the valence vibration than they are the bending vibration compared with carbon dioxide itself. Some doubt must be cast over the accuracy of the results for helium taken over a small range of mixture concentration. Assuming that both g_3 and g_2 depend regularly upon the reduced mass of the collision partners, then the helium, neon and argon results indicate by extrapolation (Figure 49) that for krypton and xenon the values of g_3 and g_2 are respectively 1/15 and 1/35 (CO_2-Kr), and 1/18 and 1/60 (CO_2-Xe). Figures 42 and 43 show how well equation 5.4 with these values for g_3 and g_2 fits the experimental data.

It is difficult to set a probable limit to the errors in the values of g_3 and g_2 as calculated in Tables 5.2 and 5.3 The individual phase readings should have an average accuracy of $\pm 2^\circ$, and an accuracy with respect to mixture concentration of better than $\pm .01$. However, even these small variations can have a considerable effect on the parameters of the best fit curves, especially for CO_2-Kr and CO_2-Xe mixtures. The largest variation in results appear in the values of g

*Page 225.

FIG. 42

CO_2-Kr mixtures (4·3μ band)

Fit of equation 5 to data

$g_2 = .029$

$g_3 = .067$

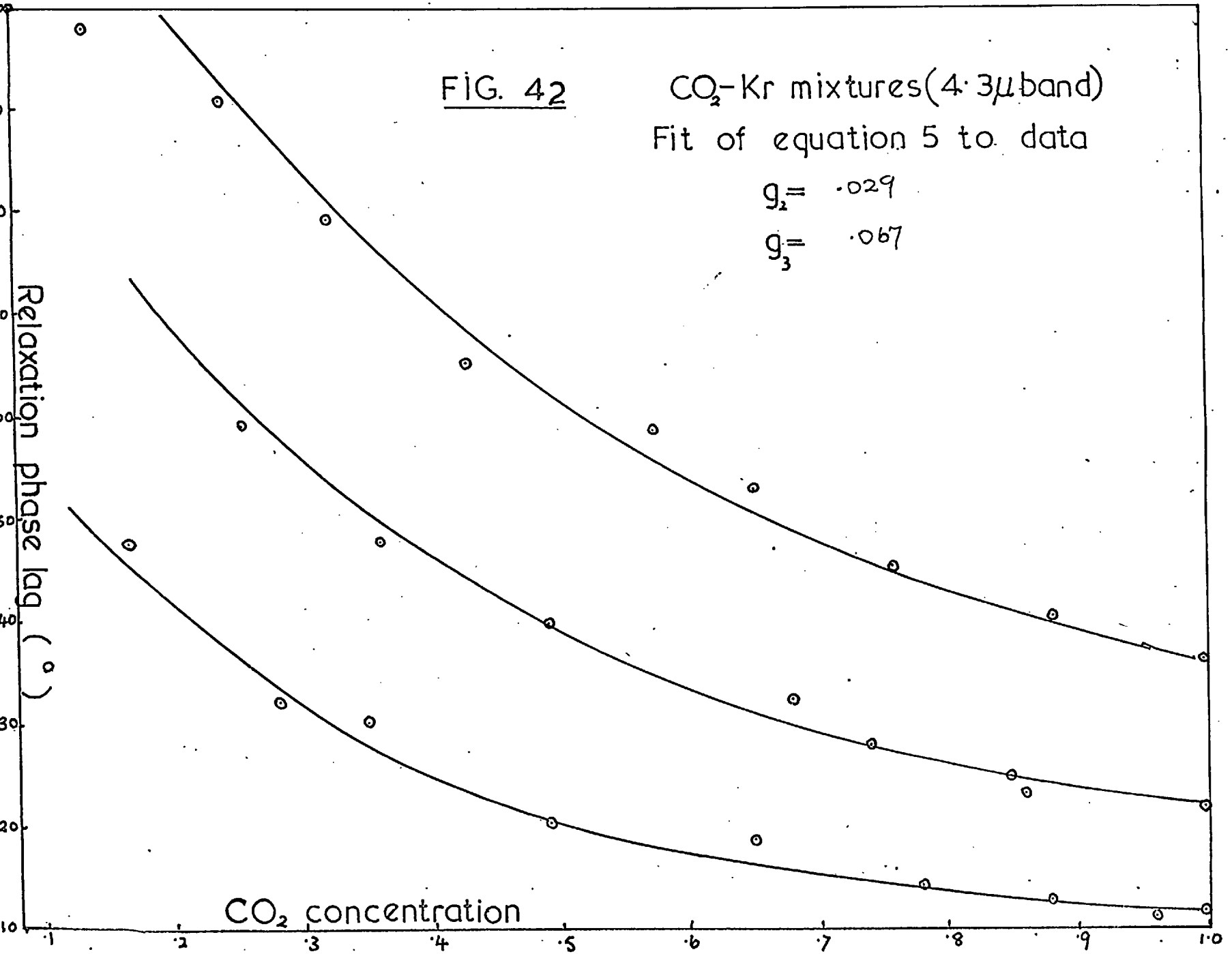

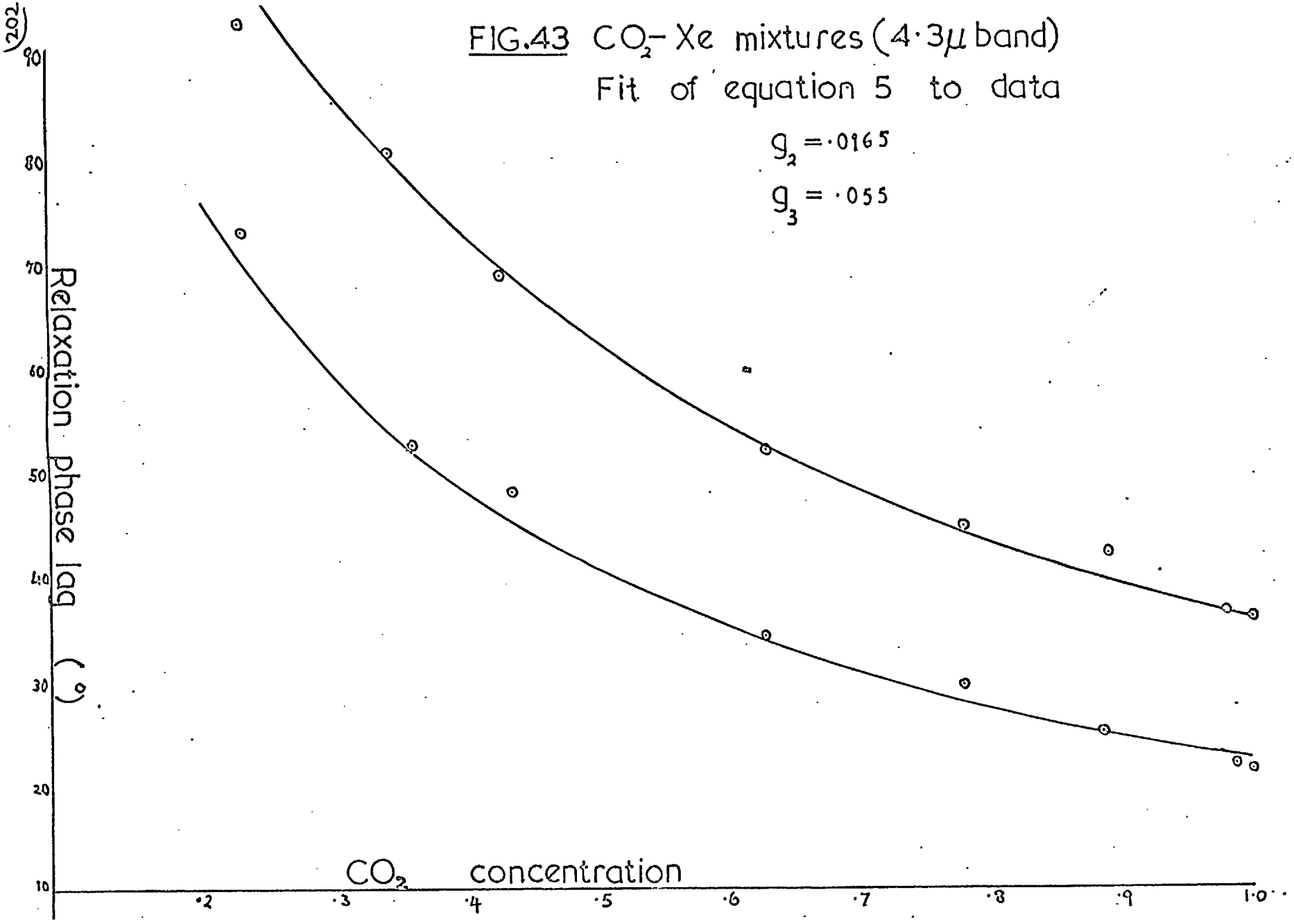
FIG.43 CO_2–Xe mixtures (4·3μ band)
Fit of equation 5 to data
$g_2 = \cdot 0165$
$g_3 = \cdot 055$
Relaxation phase lag (°)
90
80
70
60
50
40
30
20
10
CO_2 concentration
·2
·3
·4
·5
·6
·7
·8
·9
1·0

calculated for results at different pressures, and it is upon this which the error given in the tables is based.

III Miscellaneous measurements on carbon dioxide

Certain results, lying outside the main programme of data, are of interest in confirming the validity of the spectrophone method.

Figure 44 shows a plot of relaxation phase lag (for 4.3 μ band) against pressure for carbon dioxide diluted with, a) 2 per cent of hydrogen and b) 0.9 per cent ethane. Both hydrogen and ethane should be efficient at collisionally de-exciting the CO_2 vibrations and hence shortening the relaxation times, and have been found to be so experimentally in ultrasonic investigations. There is an uncertainty of $\pm$ 25 per cent in the concentrations of hydrogen and ethane in the mixtures. Higher concentrations of diluent could not be used because the relaxation time was shortened below the 1 μsec limit of the present apparatus. Thus quantitative determination of τ_{AB} was difficult. However, as can be seen by comparison with the pure CO_2 results, the relaxation phase shifts are greatly reduced, and taking the diluent concentrations as given above, the ratio $g = \tau_{AA}/\tau_{AB}$ comes out to be 925 in the case of ethane and 110 in the case of hydrogen.

In order to confirm the high de-exciting efficiency of water vapour on carbon dioxide, runs were made in which the carbon dioxide was not dried but allowed to stand over water for a considerable time before being passed into the spectrophone. Results were slightly variable, a typical plot is shown in Figure 45, together with the dry CO_2 curve for comparison. The relaxation time indicated is of the order of 2 μsec (single relaxation scheme). If the CO_2 is saturated with water

FIG.44.

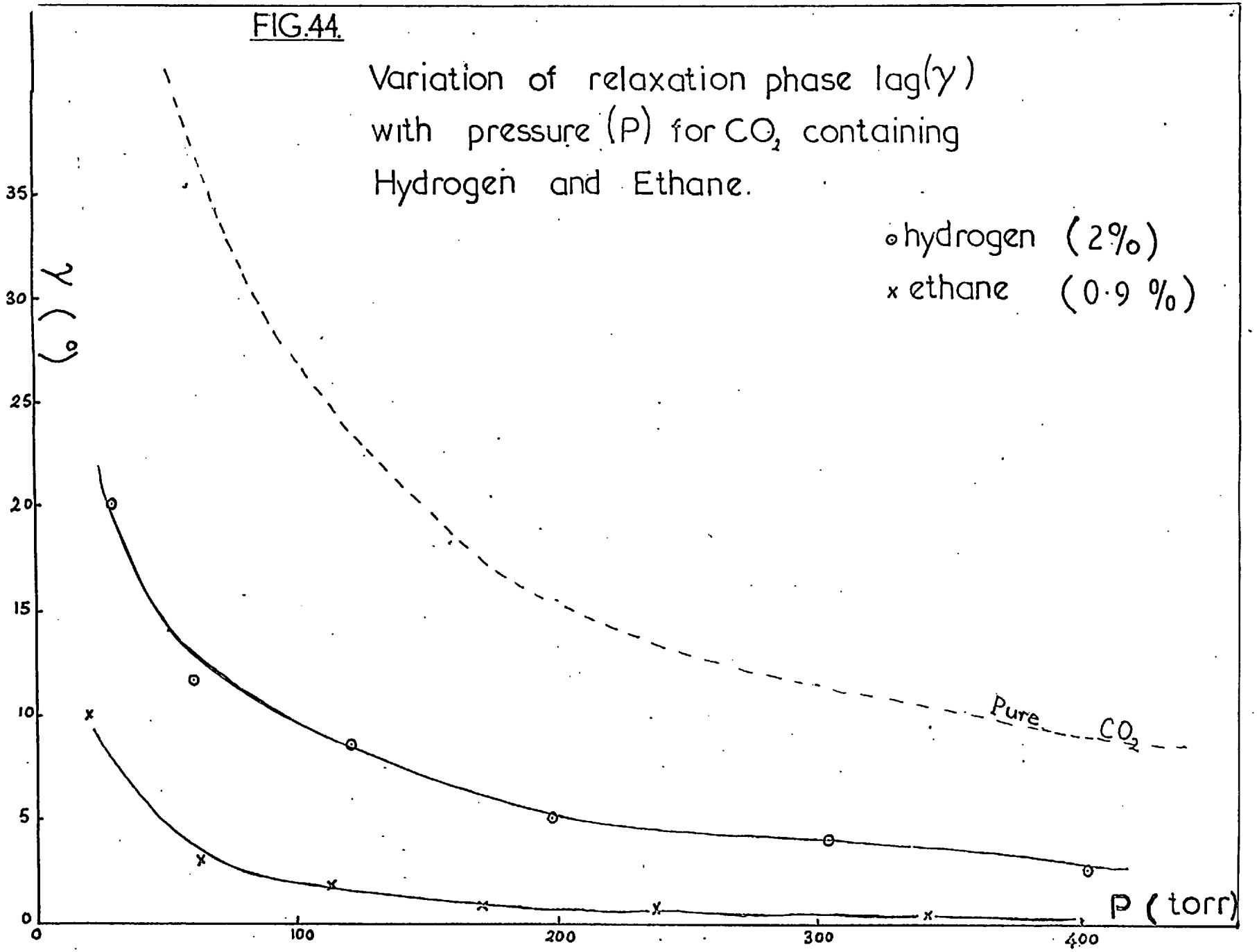
Variation of relaxation phase lag(γ) with pressure (P) for CO_2 containing Hydrogen and Ethane.
o hydrogen (2%)
x ethane (0·9 %)
γ (°)
Pure CO_2
P (torr)
0
5
10
15
20
25
30
35
0
100
200
300
400

FIG 45 Variation of relaxation phase lag (γ) with pressure (P) for CO_2 containing water vapour.

(4·3 μ band)

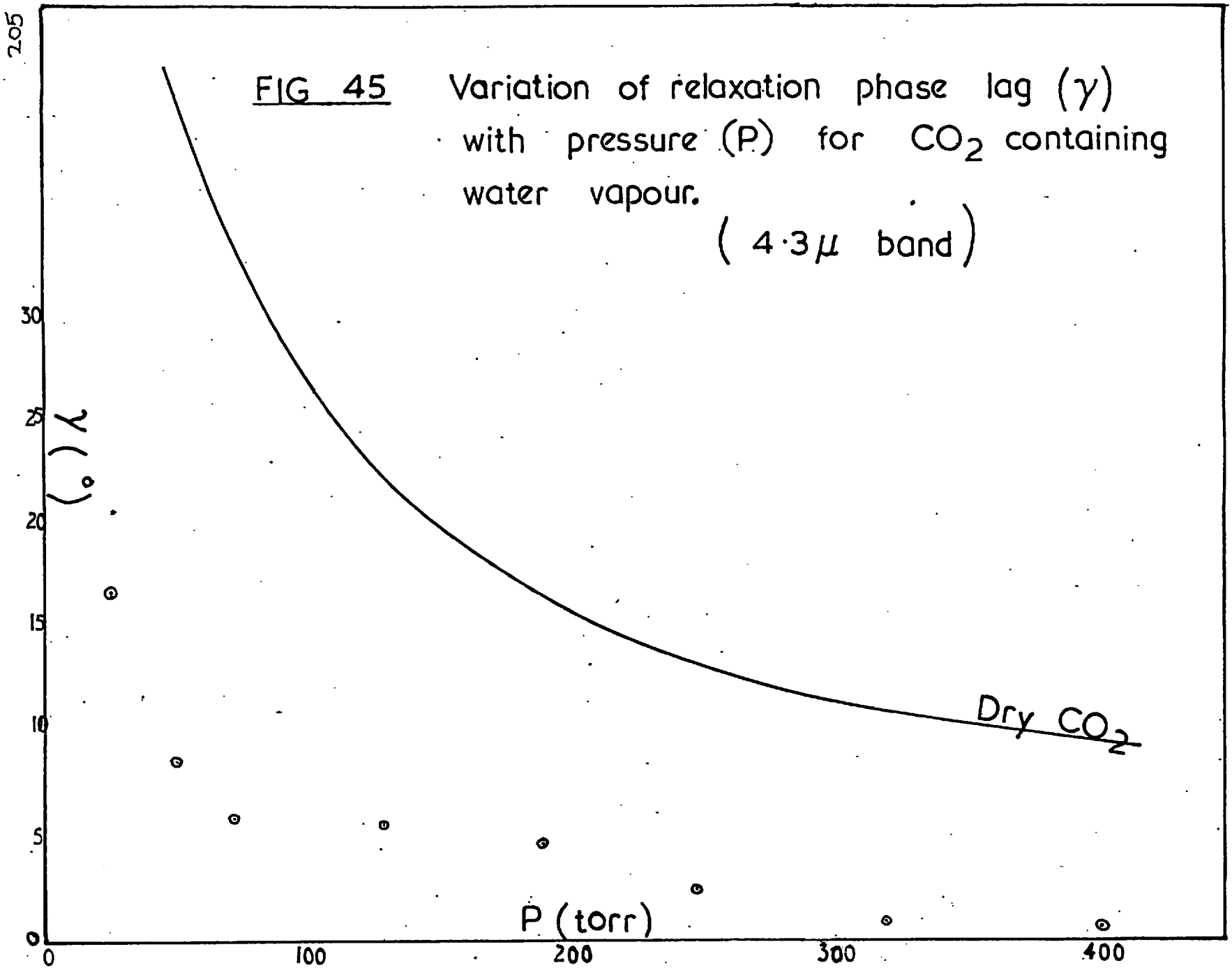

vapour this corresponds to a value of g of $\sim$ 2000.

IV Measurements on Nitrous Oxide

Measurements were made on the three infra-red active fundamental modes of nitrous oxide under similar conditions to those used for carbon dioxide. Typical plots of relaxation phase lag against pressure for these three bands are shown in Figure 46. The absorption coefficients of the 7.8 μ and 16 μ bands are quite small and the spectrophone has a low sensitivity for measurements on these bands. Consequently no quantitative values for relaxation time could be determined except for the 4.5 μ band. However, the results for the 7.8 μ and 16 μ bands do indicate relaxation times of less than 1 μsec at 1 atmos.

The 4.5 μ asymmetric stretch mode of N_2O may be treated in exactly the same way as the 4.3 μ mode of CO_2. Figure 47 shows $\tan \chi = 1/P$ plots according to both the single and two-step relaxation schemes. Since an independent determination of χ_2 for the 16 μ band could not be made with the present spectrophone, use was made of the value τ_2 = 0.95 μsec for this band obtained ultrasonically by Tempest et al. [80] for calculating the two-step relaxation time. The results of Figure 47 indicate a relaxation time of 3 $\pm$ 1 μsec for a single relaxation, and 2 $\pm$ 1 μsec for a two-step relaxation.

Figure 48 shows a plot of the variation of relaxation phase lag with concentration for nitrous oxide-argon mixtures (4.5 μ band). The relaxation time increases with argon concentration as with carbon dioxide. Values of $g = \tau_{AA}/\tau_{AB}$ indicated by the data are 0.15 for a one-step relaxation scheme, and 0.2 for a two-step relaxation scheme (assuming $\chi = 1$).

FIG. 46 Relaxation phase shift (γ) against pressure (P) for nitrous oxide

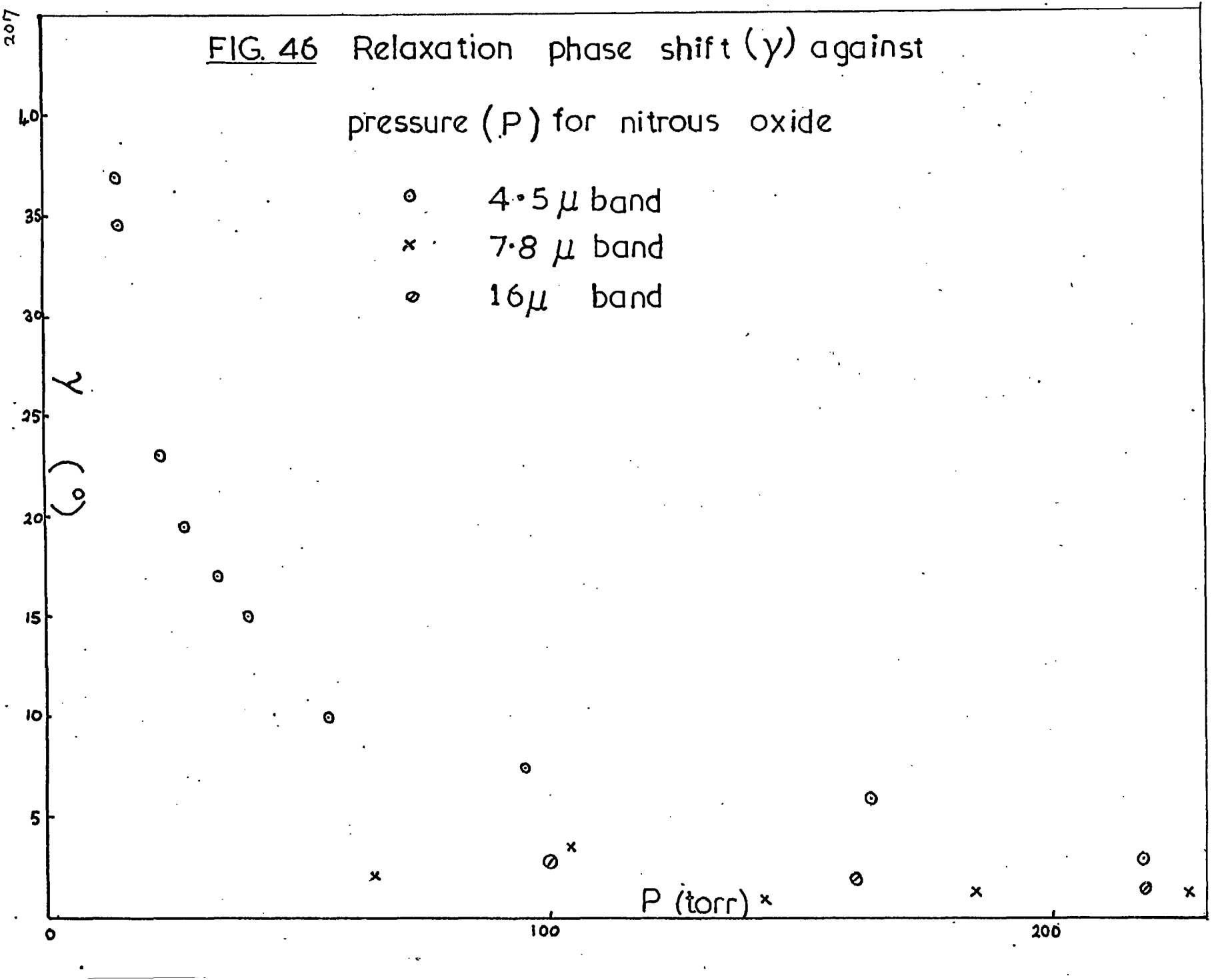

FIG. 47 Plots of $\tan\gamma$ versus $(\text{pressure})^{-1}$

for A, single step relaxation process

B, two-step relaxation process

(4·5μ band of nitrous oxide)

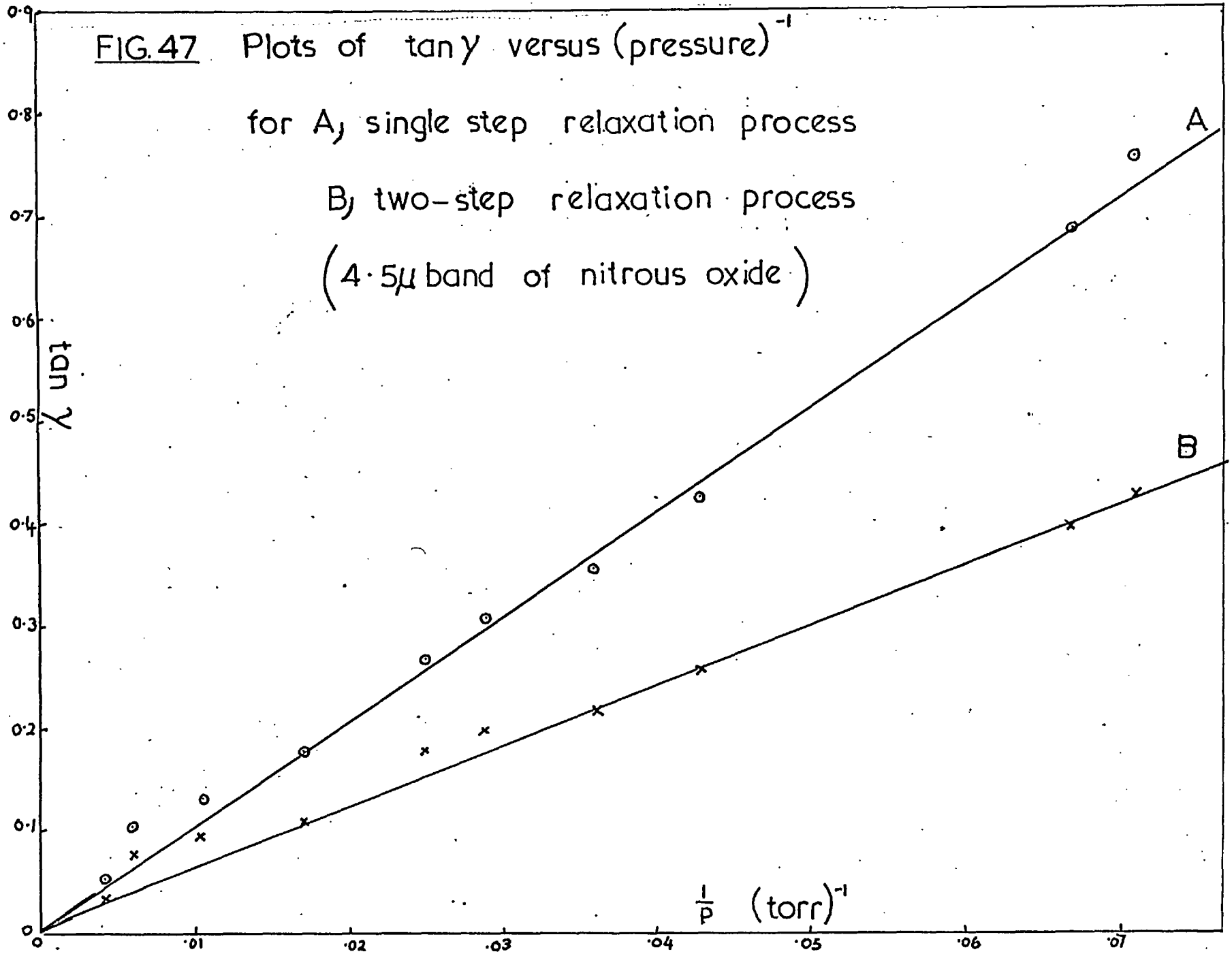

FIG. 48 Results for N_2O–A mixtures (4·5μ band)

Relaxation phase lag (γ)

versus N_2O concentration (x)

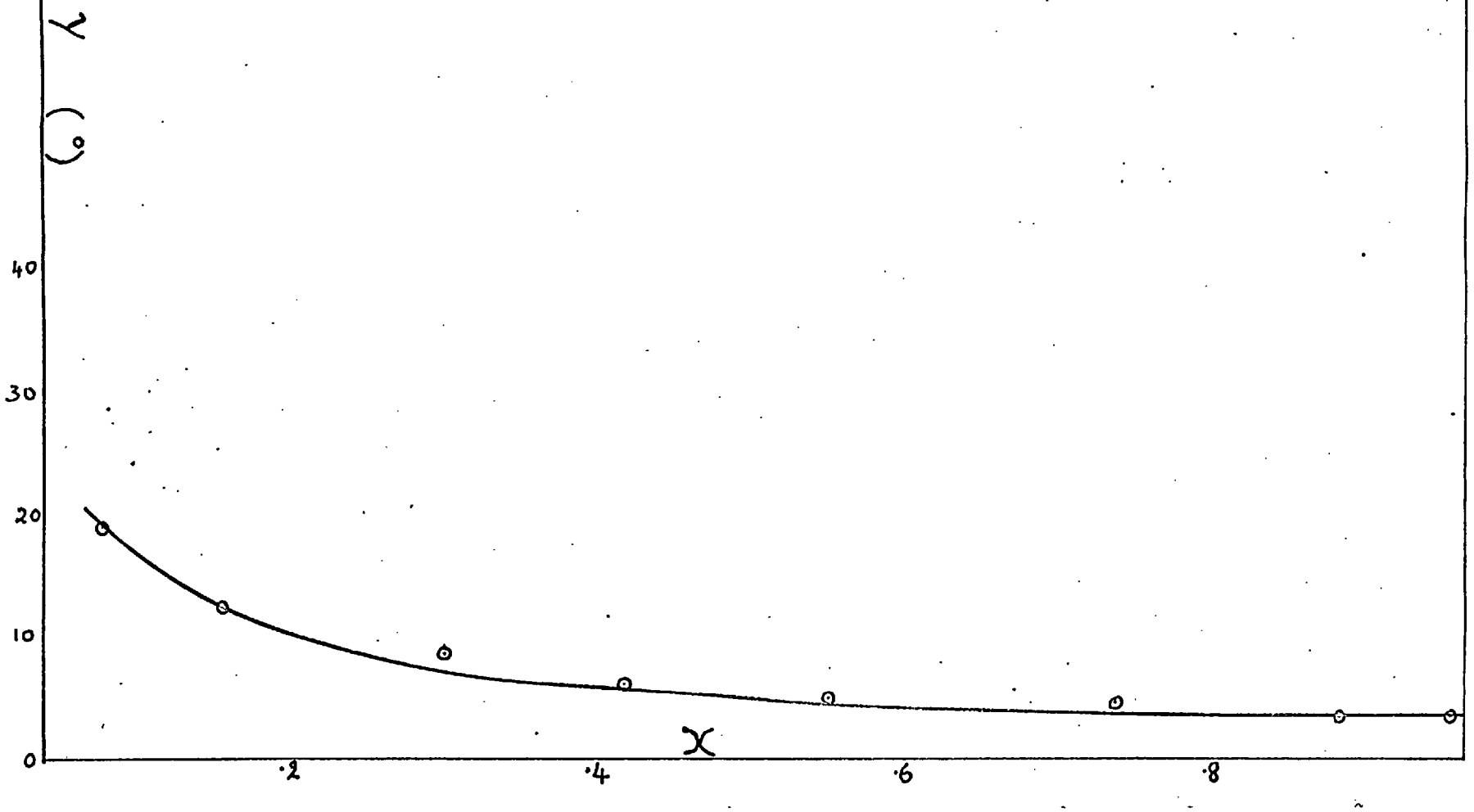

V Discussion of results and comparison with previous work

In any measurement of relaxation time, the question of gas purity is of first importance. Besides physical considerations of the apparatus and the experimental procedures undertaken to ensure a clean system, discussed in Chapter 4, the experimental results themselves should provide evidence of the degree of impurity contamination in the system. Two types of impurity may be distinguished. The first, which may be called "spectrophone impurity" is due to contamination by degassing from the walls of the chamber and connecting tubes or through leaks, after the gas has entered the apparatus and before a measurement may be taken. This contamination should be mainly a function of the time the gas is in the apparatus, and its effect should thus be relatively large in measurements made at low pressure or taking a considerable time to perform. The second type of impurity is that inherent in the supply of the gas before it is admitted into the apparatus. Such impurity, if not removed, will mean that even with perfectly clean apparatus the incorrect relaxation time will be measured. If the impurity is thoroughly mixed with the experimental gas, then a homogeneous mixture having its own definite relaxation time (at a given pressure and temperature) results. From the manufacturers' specifications, the amount of inherent impurity in all the experimental gases used in the present research should be very small, and this is supported by the experimental results with the possible exception of nitrous oxide. Together with the tests described in Chapter 4, the results also indicate that spectrophone impurity was small. Within the limits of experimental error the tan γ - 1/P plots are satisfactory straight lines although showing some signs of

proportionally longer relaxation times at high pressures. However, there is an alternative explanation of this trend. For most of the graphs, the best straight line through the data cuts the tan γ axis a small distance above the origin. This would seem to indicate a discrepancy between the true zero of γ and that given by the calibrating gas, probably due to a small difference in the microphone phase response for the two gases. This in no way invalidates the calibrating gas technique, which was essential to monitor the frequent changes in the instrumental phase shift. Providing that the phase difference is independent of pressure, as the results indicate, then this effect will merely mean a reduction of a few per cent in the calculated relaxation times.

For the inert gas mixtures, the results at 60 torr pressure do tend to give smaller τ_{AB} than the corresponding values given by the 200 torr data, but the differences are small except for xenon.

The value obtained for the relaxation time of the 15 μ bending mode of carbon dioxide (τ_2), namely 3 ± 2 μsec, is about half the value reported in the most recent ultrasonic interferometric measurements, references (81), (32) and (83). As stated in Section I, the sensitivity of the apparatus for measurements with this band was rather low. Readings were difficult to obtain at the low pressure end, below 100 torr, where the output of the microphone fell below 1 microvolt. As the readings in Figure 26 tend to indicate a longer relaxation time at higher pressures, it is possible that inaccuracies in the low pressure readings have led to too small a value for τ_2, although as discussed above this is not the most probable cause of the effect, especially as

the graph shows the mean of several measurements. The only other spectrophone measurement of τ_2, that of Slobodskaya [57] gave a value of 1.8 μsec. Calculations based upon the S.S.H. theory [7], give a value of τ_2 of 2 μsec, which is in closer agreement with the spectrophone results than those obtained ultrasonically, although it is doubtful if the theoretical value can be calculated to this accuracy.

The only results which may be directly compared with the present results on the 4.3 μ band of carbon dioxide are previous spectrophone results. Delany [68], working in this laboratory, obtained a value of 11 μsec, and although not filtering his radiation, this should be essentially due to the strongly absorbing ν_3 vibration. Slobodskaya obtained a value of 7 μsec. Both these values were calculated on the basis of a single relaxation process for which the present value is 13 μsec. Later results by Slobodskaya [84] gave a lower value for τ_3 of 3 μsec, although there is a strong indication that the CO_2 used was contaminated with water vapour.

The only other experimental evidence available on the relaxation of the ν_3 mode is that of high temperature shock tube studies. Gaydon and Hurle [85] have interpreted their line reversal temperature measurements as giving a relaxation time for this mode of about 45 μsec at 2500°K, implying a relaxation time at room temperatures of the order of seconds. The interpretation of the line reversal data is, on their own admission, very uncertain. Borrell and Hornig [86] have specifically examined the ν_3 modes of CO_2 and N_2O in a shock tube, using a fluorescence method. For CO_2 they obtained a value of τ_3 of 7 μsec at 600°K. This implies a relaxation time at room temperatures of about 40 μsec. This is in much closer agreement with the spectrophone results, although it does mean if correct, that the latter have been

considerably shortened by impurity. However, Borrell and Hornig state for the 15 μ CO_2 band, a value for τ_2 of 3 μsec at 600°K, which implies a value of over 20 μsec at room temperatures. Since this is considerably longer than both spectrophone and ultrasonic values, it is possible that there is a systematic error in the method used to calculate the relaxation time from the shock-tube data. Borrell and Hornig suggest the two-step relaxation process as explaining their results. This interpretation is supported by the present results. The theoretical value of τ_3, as worked out by Herzfeld, using the S.S.H. theory, is about 15 μsec for the two step-relaxation process, in excellent agreement with the experimental value, whereas a single-step relaxation requires a relaxation time several orders of magnitude larger. Comparing Figures 27 and 28, it can be seen that the data does favour the two-stage relaxation scheme.

There are no previous measurements with which to compare the results on inert gas mixtures using the 4.3 μ band. Delany's result that $g_3 > 1$ for CO_2-A mixtures appears incorrect. The inefficiency of the inert gases in de-exciting the CO_2 bending vibration (τ_2) is well established from ultrasonic measurements [78][79] and is well supported by the CO_2-A mixtures investigated in this research. The present mixture results strongly favour a two-step relaxation scheme for the 4.3 μ mode. As shown in Table 5.1, low pressure runs with argon, krypton and xenon mixtures give relaxation phase lags $> \frac{\pi}{2}$, which is impossible for a single relaxation process.

Assuming the two-step process to hold, the difficulty is to decide on the value of χ. Table 5.3 shows that the variation of g_3 with collision reduced mass does not seem to be as large as that of g_2.

However, the helium results must be considered with some caution, since it is impossible to determine to what extent the non-relaxation phase shift affecting these results influences the readings, even at low helium concentrations. For neon and argon, the values of χ are 0.6 and 1.3 respectively, and as the probable error in these measurements is $\pm$ 20 per cent, these two results hardly contradict the simple interpretation of $\chi = 1$. On the other hand, values of g_3 and g_2 for $Kr-CO_2$ and $Xe-CO_2$ mixtures obtained from Table 5.3 by extrapolation (i.e. by assuming a regular collision reduced-mass dependence for P_{10} in each stage of the relaxation) do fit the experimental data for these mixtures well as shown in Figures 42 and 43.

Theoretically, it is difficult to decide what the relative values of g_3 and g_2 should be. Other things being equal, one might expect $\chi < 1$, for in the de-excitation of ν_3 via $\nu_1 + \nu_2$, the multiplicity of decay paths is reduced in a CO_2-noble gas molecule collision compared with a CO_2-CO_2 collision. In the latter, the ν_1 and ν_2 modes of the second CO_2 molecule are available to take up the ν_3 energy. This multiplicity factor is about 4. However, the present data does not support this hypothesis. The asymmetric valence mode is quite different from the bending mode, involving a quite different motion of the oxygen atoms in the CO_2 molecule. Thus one might expect for a particular collision (i.e. taking into consideration orientation factors, etc.) a quite different perturbation upon the vibrating system, and hence a different dependence of the transition probability upon the collision parameters.

In Figure 49, values of $\log_{10} \frac{P_{10}^{AB}}{P_{10}^{AA}}$, obtained from values of g_2

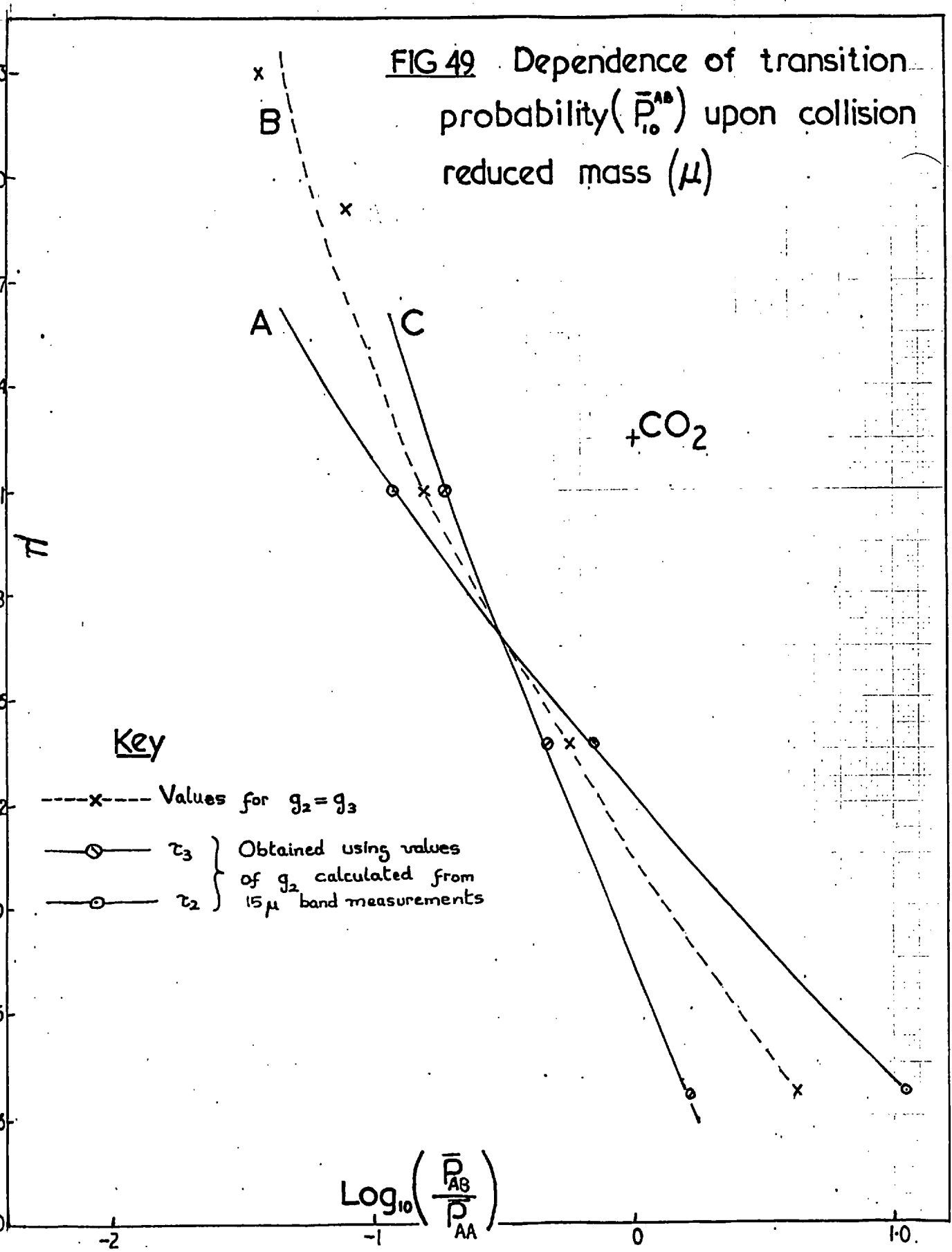
FIG 49 Dependence of transition probability($\bar{P}_{10}^{AB}$) upon collision reduced mass (μ)
B
A
C
+CO2
T
Key
Values for $g_2 = g_3$
τ_3
τ_2
Obtained using values of g_2 calculated from 15μ band measurements
$\text{Log}_{10}\left(\frac{\bar{P}_{AB}}{\bar{P}_{AA}}\right)$
33
30
27
24
21
18
15
12
9
6
3
0
-2
-1
0
1·0

and g_3 (both for $g_2 = g_3$ (graph B), and for those values obtained by using the experimental results for He-CO_2, Ne-CO_2 and A-CO_2 mixtures on the 15 μ band (graphs A and C)), are plotted against the collision reduced mass μ. The near linearity of these plots suggests that the reduced mass dependence of $\bar{P}_{10}^{AB}$ is mainly determined by an exponential factor. From graphs A and C the values of g_2 and g_3 for CO_2-Kr and CO_2-Xe mixtures were estimated for use in Figures 42 and 43. The results suggest that there are regular reduced mass dependencies for both steps of the 4.3 μ relaxation with respect to the inert gases as collision partners, and that these are basically similar. The difference in slope between plots A and B will be due to variation between the modes in other factors determining the transition probabilities.

The S.S.H. theory and similar approximate treatments of vibrational relaxation yield expressions for $\bar{P}_{10}$ involving a collision reduced mass factor of - $\mu^{\frac{1}{3}}$ in the exponent, plus ad additional mass dependent pre-exponential factor (see, for example, equation 1.15). This latter factor is difficult to obtain expect in the case of diatomic molecules, but should be in the form of μ^2 x a factor mainly depending upon the masses of the carbon and oxygen atoms. Thus taking the pre-exponential mass dependent factor to be of the form μ^2 only, theory predicts a mass dependence of

$$P_{10}^{AB} = A\,\mu^2 \exp(-B\mu^{\frac{1}{3}}) \qquad 5.5$$

Since B will be $\gtrsim$ 10 for both steps of the CO_2 relaxation, the exponential factor will be the dominant term, as expected from the results of Figure 49. In order to test whether equation 5.5 is applicable to the present data, Figure 50 shows plots of $\mu^{\frac{1}{3}}$ against

FIG 50. Fitting experimental data to equation 5.5

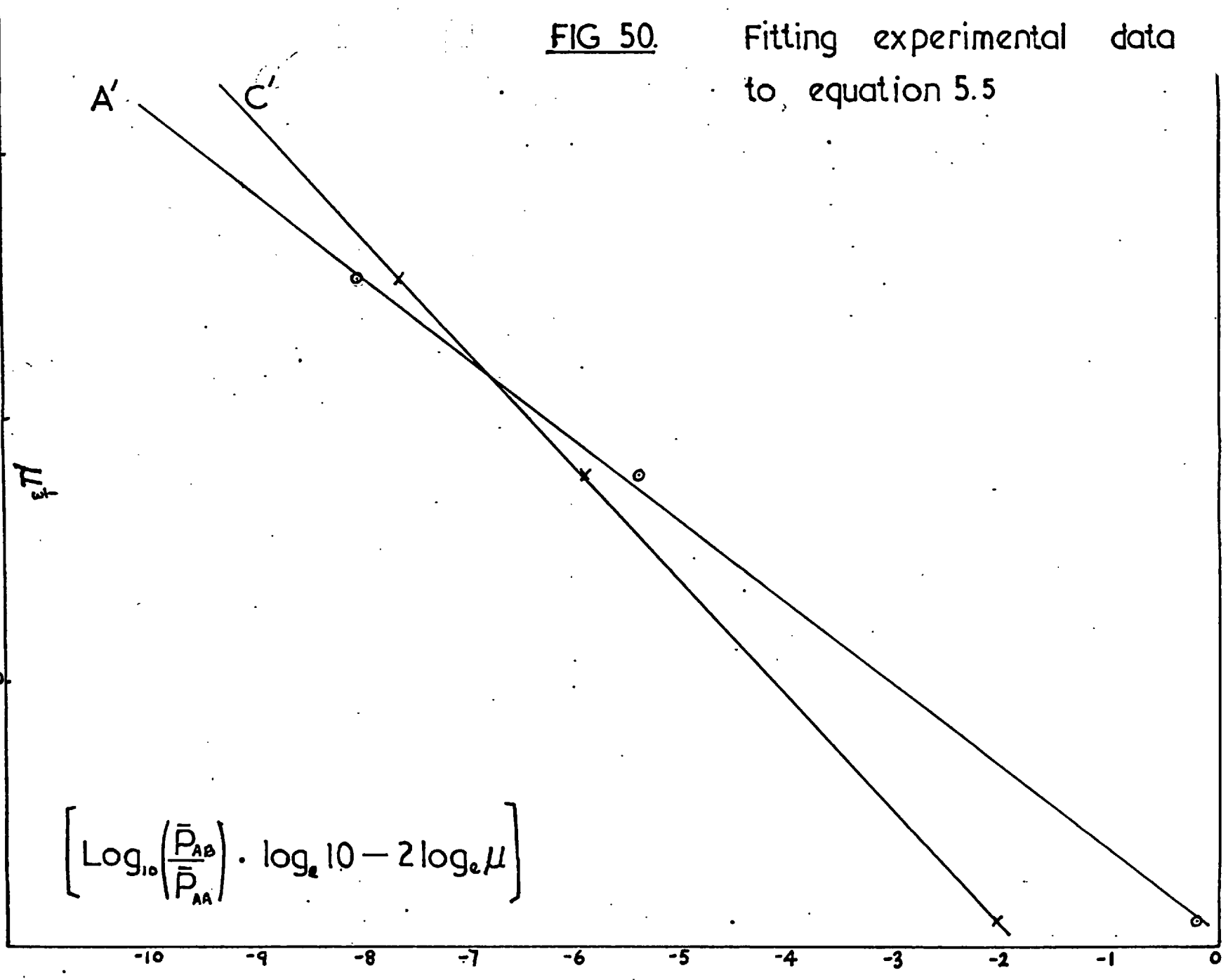

$\left\{ \log_{10} \left(\frac{P_{10}^{AB}}{P_{10}^{AA}} \right) \times \log_e 10 - 2 \log_e \mu \right\}$ for the data corresponding to plots A and C of Figure 49. There appears to be good agreement with the limited data. The slopes of plots A' and C' are according to theory

$$- B = - \frac{3}{2} \frac{(16 \pi^4 \Delta E^2)^{\frac{1}{3}}}{(\alpha^2 h^2 kT)}$$

where ΔE is the energy to be exchanged with translation and α is the intermolecular force range parameter. Assuming the validity of the two-step relaxation scheme for the 4.3 μ CO_2 vibration, i.e. E = 500k for the first-step (graph C') and E = 960k for the second (graph A'), the graphs yield respectively values of α of 5.2×10^8 cm^{-1} and 5.7×10^8 cm^{-1}. Another fact which emerges from Figure 49, is that carbon dioxide self-collisions do not follow the same collision-reduced mass dependence of transition probability as the mixtures. This is not surprising, considering that self-collisions involve two triatomic molecules, as contrasted with the simpler atom-molecule collisions in the mixtures. The latter might be expected to form a consistent group, in which the relative transition probabilities follow a simple reduced mass dependence, as predicted in approximate tneories like the S. S. H. The relative transition probabilities of, say, CO_2 - CO_2 and CO_2 -A collisions, on the other hand, would seem to depend upon some other factor.

This leads to the problem of why the inert gas molecules as a group are so inefficient at inducing vibrational transitions in carbon

dioxide compared with the CO_2 molecules themselves and other molecules of comparable mass. Cottrell and Day [78] have suggested that the inert gas-CO_2 intermolecular potential must be unusually 'soft', leading to a low transition probability by Ehrenfest's principle. Another possibility, recently put forward, is that vibrational-rotational energy transfer may be important in the de-excitation process. In this case, the removal of half the rotational states and possibly important rotational orientation factors would explain the inefficiency of the nearly spherical inert gas molecules. The removal of a particularly favou .rable orientation factor might also be important in a vibration-translation energy transfer process.

There have been no previous measurements on mixtures of carbon dioxide with hydrogen, ethane or water vapour using the 4.3 μ band. Gaydon and Hurle [85] found that water vapour considerably shortened the relaxation time of ν_3 in their shock-tube measurements. CO_2-H_2 and CO_2-H_2O mixtures have been extensively studied in ultrasonic absorption and dispersion measurements (see, for example, reference (9)). Values for g_2 range from 100 - 500 for CO_2-H_2 at room temperatures, and from 600 - 5000 for CO_2-H_2O. The values found for g'_3 in the present work (110 for CO_2-H_2 and 2000 for CO_2-H_2O) lie within this range, showing that the hydrogen and water molecules must be efficient de-exciters of both stages of the ν_3 relaxation. Measurements of g_2 for mixtures of carbon dioxide with light hydro-carbons indicate that ethane should also be an efficient de-exciter of the CO_2 vibrations and this is confirmed by the present results. These measurements although only semi-quantitative, give confidence in the overall performance of the apparatus.

Several previous ultrasonic measurements of the relaxation time of the 16 μ bending vibration of nitrous oxide have been made. Most recent measurements [80][87] give a value for ν_2 of about 0.8 - 1.0 μsec. The 7.8 μ valence vibration should have approximately the same relaxation time (Chapter 1, Part III) and these values of less than 1 usec are qualitatively confirmed in the present work. With respect to the 4.5 μ band, Gauthier and Marcoux [88] have measured by means of an infra-red fluorescence method at low pressures, obtaining a result corresponding to a relaxation time of $\sim 10^{-4}$ sec at 1 atmosphere. Borrell and Hornig in their shock-tube obtained a value of 11 μsec at 600°C. Both these results are in considerable disagreement with the present work and if correct, must imply that the nitrous oxide used in the spectrophone contained some impurity. However, as noted above, there is a possibility that the relaxation time was over-estimated in the shock tube measurements. The results for N_2O-A mixtures imply that the inert gases are also inefficient at de-exciting the nitrous oxide vibrations. Being a molecule of similar type to carbon dioxide, the two cases may well be closely analogous.

VI Conclusions

The present results overall give confidence in the validity of vibrational relaxation time measurements made with a Delany-type spectrophone. At the same time they confirm that great care must be taken in the design of the apparatus to avoid cavity and Helmholtz resonance effects, and phase shifts due to varying transducer response. The neglect of these precautions could possibly have affected the work of some earlier experimenters.

The results strongly indicate that the asymmetric valence vibrations of carbon dioxide and nitrous oxide relax by a two-stage process via the bending modes. The relaxation time of the first stage, i.e. essentially the energy transfer $v_3 \longrightarrow v_2$, is longer by a factor of about two, than that of the second stage, which is effectively the relaxation of the bending mode.

Results for carbon dioxide-inert gas mixtures show that the inert gases are relatively inefficient at collisionally de-exciting carbon dioxide vibrations, compared with the self-collisions. The effect would seem to occur both in the relaxation of the valence and bending modes. As a group, the inert gases give a collision reduced mass dependence to the carbon dioxide relaxation similar to that predicted by current theories of vibrational-translational energy transfer. Carbon dioxide itself does not fit into this dependence. Results also indicate that the inert gases are probably equally inefficient at de-exciting nitrous oxide.

Further spectrophone measurements made over a wide range of chopping frequencies would help to confirm the two-stage nature of the valence mode relaxation. A series of measurements upon nitrous oxide-inert gas mixtures would (by comparison with the present results on carbon dioxide) provide further evidence on the apparent similarity of the two molecules with respect to relaxation. Useful information might be obtained from similar measurements on other simple characteristic types of polyatomic molecule.

The future development of the spectrophone technique would seem to depend upon the extension of the range of measurable relaxation times. An instrument capable of accurate measurements of the order of 10^{-7}

or even 10^{-8} sec. would be an extremely useful tool for helping to fill remaining gaps in the understanding of vibrational relaxation processes, such as the importance of rotational-vibrational energy transfer, and the explanation of the behaviour of certain anomalous systems. Also the spectrophone, thus developed, would facilitate a deeper investigation of the exact pattern of energy transfer in many complex relaxations involving polyatomic molecules. Such detailed analyses are important in the study of many spectroscopic and chemical phenomena, besides providing basic information on intramolecular and intermolecular forces.

TABLE 5.1

CO_2 - Noble gas mixtures (4.3 μ band)

Values of τ_{AB} and τ_{AB}/τ_{AA} for the single relaxation scheme

Inert diluent	Mixture Pressure (torr)	τ_{AB} (μs)	τ_{AB}/τ_{AA}
Helium	200	13 ± 2	0.27
	100	20 ± 3	0.23
	60	40 ± 6	0.264
Neon	200	128 ± 20	2.74
	100	260 ± 30	3.7
	60	640 ± 60	4.3
Argon	200	335 ± 50	7.1
	100	2770 ± 1000	39
	60	Negative	-
Krypton	200	1040 ± 400	22
	100	Negative	-
	60	"	-
Xenon	100	"	-
	60	"	-

TABLE 5.2

CO_2 - Inert gas mixture (4.3 μ band)

Values of g found by fitting equation (3) to data with $\chi = 1$

Inert gas	Total pressure (torr)	g	Average g
Helium	200	3.6	
	100	7.6	5.0 ± 1.8
	60	3.6	
Neon	200	0.44	
	100	D.39	0.4 ± .05
	60	0.465	
Argon	200	0.117	
	100	0.135	0.13 ± .009
	60	0.137	
Krypton	200	0.035	
	100	0.086	0.067± .029
	60	0.06	
Xenon	100	0.02	0.033± .011
	60	0.042	

TABLE 5.3

CO_2 - Noble gas mixture (4.3 μ band)

Calculation of g_3 using published values of g_2

Diluent	g_2	Mixture Pressure (torr)	Calculated value of χ	Average value g_3
Helium	14	200 100 60	.11 .188 .105	1.9 ± .5
Neon	0.5	200 100 60	.53 .61 .76	0.315 ± .16
Argon	0.1	200 100 60	1.08 1.17 1.6	.142 ± .025

References

1. Herzfeld, K. and Rice, F.O. Phys.Rev. 31, 691 (1928)

2. Kneser, H.O. Ann. Phys. 11, 761 (1931)

3. Landau, L. and Teller, E. Phys. Zeit. Sowjetunion, 10 , 34 (1936)

4. Herzfeld, K. and Litovitz, T. "The absorption and dispersion of ultrasonic waves" Academic Press (1959)

5. Bauer, H.J. "Physical Acoustics" Vol. IIA, p.48, Academic Press (1965)

6. Hirschfelder, J., Curtiss, C., and Bird, R. "Molecular Theory of Gases and Liquids" Wiley, New York (1954)

7. Herzfeld, K. "Dispersion and Absorption of Sound in Molecular Processes" Inter. School of Physics "enrico Fomi" course 27, Academic Press (1962)

8. Takayanagi, K. Progr. Theoret. Phys. (Suppl.) No. 25 (1963)

9. Cottrell, T.L. and McCoubry, J.C. "Molecular Energy Transfer in Gases" Butterworths, London (1958)

10. Lavercombe, B.J. M.Sc. dissertation "Molecular excitations in fluids" London University (1962)

11. Zener, C., Phys. Rev. 38, 277 (1931)

12. Jackson, J.M. and Mott, N.F. Proc. Roy. Soc. 137A, 703 (1932)

13. Zener, C. Proc. Camb. Phil. Soc. 29, 136 (1933)

14. Millikan, R.C. and White, D.R. J.chem. Phys. 39B, 3209 (1963)

15. Schwartz, R., Slawsky, Z., and Herzfeld, K. J.chem. Phys. 20, 1591 (1952)

16. Cottrell, T.L. and Ream, N. Trans. Faraday Soc. 51, 159, 1453 (1955)

17. Dickens, P.G. and Ripamonti, A. Trans. Faraday Soc. 57A, 735 (1961)

18. Tanczos, F. J.chem. Phys. 25, 439 (1956)

19. Parker, J.G. Phys. Fluids 2, 449 (1959)

20. Dickens, P.G. and Linnet, J. Proc. Roy. Soc. 243A, 84 (1954)

21. Widom, B. Disc. Faraday Soc. 33, 37 (1962)

22. Landau, L. Physik. Z. Sowjetunion 1, 81 (1932) 2, 46 (1932)

23. Landau, L. and Liftshitz, I. "Quantum Mechanics" p. 180, London (1958)

24. Widom, B. and Shin, H. Bull. Amer. Phys. Soc. 8, 532 (1963)

25. Shin, H.K. J.chem. Phys. 41B, 2864 (1964)

26. Benson, S. and Barend, G. J.chem. Phys. 37B, 1386 (1962) 40A, 1289 (1964)

27. Salkoff, M. and Bauer, E. J.chem. Phys. 29, 26 (1958)

28. Bartlett, M. and Moyal, J. Proc.Camb. Phil. Soc. 45, 545 (1949)

29. Curtiss, C. and Adler, F. J.chem. Phys. 21, 1199, 2045 (1953)

30. Cottrell, T.L. and Matheson A J. Trans. Faraday Soc. 58B, 2336 (1962) 59A, 824 (1963)

31. Nikitin, E.E. Disc. Faraday Soc. 33 (1962)

32. Rapp, D. J.chem. Phys. 40B, 2813 (1964)

33. Widom, B. and Bauer, S.H. J.chem. Phys. 21, 1670 (1953)

34. Herzfeld, K. Disc. Faraday Soc. 33 (1962)

35. Nikitin, E.E. Dokl. Akad. Nauk. SSSR 132, 395 (1960)

36. Witteman, W.J. Philips Research Repts. Suppl. No. 2 (1963)

37. Laidler, K.J. and Gil, L. Proc. Roy. Soc. 250A, 121, 251A, 66 (1959)

38. Holmes, R., Smith, F.A. and Tempest, W. Proc. Roy. Soc. 81, 311 (1963)

39. Pielmeier, W.H. and Telfair, D. Rev. Sci. Inst. 13, 122 (1940)

40. Stewart, J.L. Rev. Sci. Instrum. 17, 59 (1946)

41. Hubbard, J.C. Phys. Rev. 35, 1442, (1926) 36, 1668 (1930) 38, 1011 (1931)

42. Knudsen, V.O. and Fricke, E. J.A.S.A. 10, 89 (1938)

43. Gaydon, A.G. and Hurle, I.R. "The shock tube in high-temperature chemical physics" Chapman and Hall, London (1963)

44. Hornig, D. and Cowan, G.R. J.chem. Phys. 18, 1008 (1950) 61, 856 (1957)

45. Gaydon, A.G., Clouston, J.G. and Glass, I. Proc. Roy. Soc. A. 248, 429 (1958)

46. Kantrowitz, A. J.chem. Phys. 14, 150 (1946)

47. Millikan, R.C. Phys. Rev. Letters 8, 253 (1962)

48. Rossler, F. Z.Phys. 96, 251 (1935)

49. Callear, A.B. and Smith, I.W.M. Trans. Faraday Soc. 59, 1720 (1963)

50. Stevens, B. Chem. Rev. 57, 439 (1957)

51. Dwyer, R.J. J.chem. Phys. 7, 40 (1939)

52. White, J.U. J.chem. Phys. 8, 79 (1940)

53. Libscomb, F.J., Norrish, R.G. and Thrush, B.A. Proc. Roy. Soc. A233, 455 (1956)

54. Callear, A.B. Applied Optics, 2, 145 (1965)

55. Gorélik, G. Dokl. Akad. Nauk. SSSR, 54, 779 (1946)

56. Tyndall, J. Proc. Roy. Soc. 31, 307 (1881)

57. Slobodskaya, P.V. Izvest. Akad. Nauk. SSSR, 21, 656 (1948)

58. Jacox, M.E. and Bauer, S.H. J.phys. Chem. 61, 833 (1957)

59. Woodmansee, W. and Decius, J.C. J.chem. Phys. 36, 1831 (1962)

60. Delany, M.E. Science Progress, 47, 459 (1959)

61. Cottrell, T.L. Trans. Faraday Soc. 46, 1025 (1950)

62. Moore, C.B. J.chem. Phys. 43, 2979 (1965)

63. Montan, D.N. Ph.D. thesis, Oregon State University (1959)

64. Arnold, H.D. and Crandall, I.B. Phys. Rev. 10, 22 (1917)

65. Ballantine, S. J.A.S.A. 3, 319 (1932)

66. Landau, L. and Lifshitz, I. "Fluid Mechanics" London (1958) p.183 et seq.

67. Jones, W.D. Ph.D. thesis, Oregon State University (1957)

68. Delany, M.E. Ph.D. thesis, London University (1958)

69. Stephanov, B.I. and Girin, O.P. J.E.T.P. (SSSR) 20, 947 (1950)

70. Stull, V.R., Wyatt, P.J. and Piass, G.N. Appl. Opt. 3, 243 (1964)

71. Millikan, R.C. Paper presented at Chemical Soc. Symposium "Molecular Relaxation Processes" Aberystwyth (1965)

72. Penner, S.S. "Quantitative Molecular Spectroscopy" Pergamon (1959)

73. Dennison, D.M. Rev. Mod. Phys. 3, 280 (1931)

74. Burch, D.E. and Williams D., and Gryvnak, D. Appl. Opt. 1, 759 (1962)

75. Burch, D.E. and Williams, D. Appl. Opt. 1, 473 (1962)

76. Olson, H.F. "Acoustical Engineering" Van Norstrand (1957)

77. Lambert, J.D. and Salter, R. Proc. Roy. Soc. 253A, 277 (1959)

78. Cottrell, T.L. and Day, M.A. Paper presented at Chemical Soc. Symposium, "Molecular Relaxation Processes" Aberystwyth (1965)

79. Kneser, H.O. and Roesler, H. Acoust. 9, 224 (1959)

80. Tempest, W., Holmes, R. and Parbrook, H.D., Acoust. 10, 155 (1960)

81. Angona, F.A. J.A.S.A. 25, 1116 (1953)

82. Shields, F.D. J.A.S.A. 31, 248 (1959)

83. Blythe, A., Cottrell, T.L. and Day, M.A. Acoust. 16, 118 (1965)

84. Slobodskaya, P.V. "Soviet Physics" Doklady 3, 624 (1958)

85. Hurle, I.R. and Gaydon, A.G. Nature, 188, 1858 (1959)

86. Borrell, P. and Hornig, D. Paper presented at Chemical Soc. Symposium "Molecular Relaxation Processes", Aberystwyth (1965)

87. Wight, H.M. J.A.S.A. 28, 459 (1956)

88. Gauthier, G. and Marcaux, J. Canad. J. Phys. 39, 1130 (1961)

LIST OF SYMBOLS USED

A Einsteim coefficient for spontaneous emission of radiation.

$A(\bar{\nu})$ Absorptivity. The fraction of radiation intensity absorbed/unit optical density at wave number $\bar{\nu}$.

A (Chapter 3D) $\equiv \frac{i\omega}{K}\frac{P_0}{T_0 V_0}$

a Radius of spectrophone cell.

B (Chapter 3 C,D) $\equiv \left\{ Q_1 \frac{m\pi}{l} \left(\alpha^2 + \left(\frac{m\pi}{l}\right)^2\right)^{-1} \left[1 - (-\delta)^m e^{-\alpha l}\right] \right\}$

B_{01} Einstein coefficients of induced absorption of radiation.

B_{10} Einstein coefficients of induced emission

b Spectrophone inlet tube radius.

C Specific heat (at constant volume unless specified by subscript.)

Cv Specific heat at constant volume.

Cp Specific heat at constant pressure.

Ce Contribution to specific heat from translational degrees of freedom.

C_i " " " " internal

C_o Limiting value of relaxing specific heat. $\omega \to 0 \; (= Ce + Ci)$

C_∞ $\omega \to \infty \; (= Ce)$.

C (Chapter 3 B.) $\equiv \left\{ f_{10} + f_{01} + A + (B_{01} + B_{10}) \beta(\nu) f(z) \right\}$

c (Chapter 2 I.), velocity of sound.

c Velocity of light.

D $\equiv \left\{ f_{01} + \beta(\nu) B_{01} f(z) \right\}$

d Length of spectrophone inlet tube.

E Internal energy (usually / unit volume).

E_0 Internal energy for equilibrium with the translational temperature.

F (Chapter 3 D) $\equiv \left\{ U \int_{V_0} v \, dV + B \right\}$

f_{10} Rate constants for collisional de-excitation in two-state gas.

f_{01} " " " " excitation " " " "

f_f Rate constant for fluorescence.

f(z) Function describing fall off of radiation absorbed along the axis of the cell.

Go (Chapter 3 C) $\equiv \frac{Q_0 \alpha}{\alpha^2 + \sigma^2} \left[(-1)^m e^{-\alpha l} - 1 \right]$

G (Chapter 3 C) $\equiv \frac{Q_1 \alpha}{\alpha^2 + \sigma^2} \left[(-1)^m e^{-\alpha l} - 1 \right]$

g_2 g_1 Degeneracy weighting factors for ground and excited states.

δ $= g_1 / g_0$

g (Chapter 5) ratio of $\tau_n^{AA} / \tau_n^{AB}$ for the 'n' vibration of a molecule.

H Relaxation heat input /sec /unit volume to the gas in the spectrophone.

H_0 Constant components of H.

H_1 Time varying

h Planck's constant, $(6.62 \times 10^{-27}$ erg.sec.)

I Symbol for various integrals; (Chapter 3 D) $\equiv \int_{V_0} v \, dV$.

In(x) Modified Bessel function of the first kind.

I_ν Radiation intensity at frequency ν.

i $\sqrt{-1}$

Jn(x) Bessel function of the first kind.

j Rotational state quantum number.

K Coefficient of thermal conductivity

Ko(x) Modified Bessel function of the second kind.

k Boltzmann's constant, $(1.38 \times 10^{-16}$ erg/deg.)

l length of spectrophone cell.

M Molecular weight.

m Reduced mass of de-exciting molecule.

N_0 Total number of molecules/ c.c. in ground state.

N_1 " " " " first excited "

N_2 (Chapter 3 B.(vii)). Number of molecules/ c.c. excited in ν_2 vibration.

N_3 (") " " " " " " ν_3 "

P_0 Ambient pressure.

P Equivalent pressure :In mixtures , used spectroscopically to signify that for line broadening considerations, self collisions are more efficient than those with diluent. For CO_2 $P = (P_0 + 0.3x)$, where x is partial pressure of CO , is often used.

$P_{\bar{\nu}}$ Spectral absorption coefficient at wave number $\bar{\nu}$.

P_{10} Probability of vibrational de-excitation/collision.

$\bar{P}_{10}$ Average probability of vibrational de-excitation /collision.

p Time varying pressure amplitude due to optic-acoustic effect.

Q_0 H_0 / K

Q_1 H_1 / K

Q' (Chapter 3 C D) $\equiv \left\{ \frac{Q_0}{y} + Q_1 \left(\frac{y \cos\gamma + \omega \sin\gamma}{\omega^2 + y^2} \right) \right\}$

q' Compressional heat input / unit volume to gas in spectrophone.

q_m $(\sigma^2 + y/\beta)^{1/2}$

R Molar gas constant.

r Intermolecular distance.

r Distance parameter in Lennard-Jones, Morse potentials.

r (Chapter 3) Radial distance from axis of spectrophone

S Integrated absorption coefficient.

$S_{jj'}$ Integrated absorption coefficient for single rotational line in a vibration -rotation band.

s (Chapter 3 D) $\equiv \sqrt{\frac{2K}{\omega \rho_0 C_p}}$.

T Absolute temperature.

T_0 Ambient spectrophono temperature.

$T(\bar{\nu})$ Transmissivity. Fraction of radiation intensity transmitted / unit optical density at wavenumber .

t Time.

U (Chapter 3 D) $\equiv \frac{i\omega}{\sigma K} \frac{P_0}{V_0 T_0} (1 - (-1)^m)$

u (Chapter 3) $= (\nu'' + B/q_m^2)$

u (Chapter 3) $\equiv \alpha l / \pi$

V Volume

Vo Volume of spectrophone cell.

v Time varying temperature amplitude in spectrophone.

$\bar{v}$ Spatially averaged time varying temperature amplitude in spectrophone.

$v' \equiv \int_0^\infty v e^{-yt} dt$

$v'' = \int_0^l v' \sin \frac{m\pi}{l} z \, dz$.

W Energy absorbed in spectrophono/ unit area /optical path length X.

w $\equiv \pi / \rho$.

X Optical path length (density) (in atmos.-cm).

x Concentration (mol. fraction).

x Internal coordinate of molecule. (Chapter 3).

x (Chapter 3 C, D) $\equiv i\omega / \beta w^2$

y Laplace transform for time. (Chapter 3,C)

Z Acoustic impedance.

Z (Chapter I) Number of collisions /molecule / sec.

Z_0 (Chapter I) 'Steric' factor.

$Z_{10} \equiv (\bar{P}_{10})^{-1}$

z Axial coordinate in spectrophone.

α Molecular potential range parameter.

α (Chapter 2).Sound absorption coefficient.

α Integrated absorption coefficient for vibrational band.

α Constant determining fall off of radiation absorbed along the cell axis.

β Thermal diffusivity.

χ $\gamma_3/\gamma_2 \equiv \tau_3^{AA}/\tau_3^{AB} \div \tau_2^{AA}/\tau_2^{AB}$.

δ (Chapter 3 B) $\equiv \beta(\omega) . B_{01} f(z) / D$.

$\mathcal{E}$ Energy parameter in Lennard-Jones and Morse potential.

γ (Chapter 3 B) $\equiv \beta(\omega) (B_{01} + B_{10}) f(z) / C$

η Coefficient of viscosity .

γ Relaxation phase shift.

γ Ratio of specific heats of gas.

$\kappa^2 \equiv i\omega\rho_0 C_p / K$

$\kappa_m^2 \equiv (\kappa^2 + \sigma^2)$

λ Complex laplace transform variable.

λ Wavelength of sound.

μ Collision reduced mass.

μ $(\sigma^2 + \lambda/\beta)^{1/2}$

ν Vibrational frequency.

$\bar{\nu}$ Wave number.

ω Angular chopping frequency.

ϕ Experimental phase shift.

ϕ_1 Instrumental phase shift.

ϕ_s Spectrophone phase shift.

$\phi' = \tan^{-1}\left\{ \left[1 - \frac{1}{\alpha}\sqrt{2\omega/\beta} \tanh \frac{\alpha l}{\sqrt{2}} \right]^{-1} \right\}$

$\gamma' = \tan^{-1}\left\{ s \left(\frac{C\rho l}{R} - 1 + s \right)^{-1} \right\}$.

ρ Density.

ρ_0 Ambient density in spectrophone .

$\Delta\rho$ Varying amplitude of density in spectrophone.

$\rho(\nu)$ Radiation density at frequency ν.

σ $\equiv \frac{m\pi}{l}$.

$= k\nu/k$

θ' (Chapter I B) $\equiv \frac{16\pi^4 \mu \nu^2}{\alpha^2 k}$

$\theta' = \tan^{-1}\left\{ \omega / \beta\eta^2 \right\}$

τ Relaxation time.

τ^{AA} Relaxation time for self-collions.

τ^{AB} Relaxation time for relaxing molecules A in diluent B.

τ_R Radiational lifetime.

ξ Sound particle displacement.

φ Azimuthal coordinate in spectrophone coordinate system.

ζ Real number defined in contour integration of v.